



**SPATIAL AND TEMPORAL CORRELATION
OF SURFACE TEMPERATURE AND WIND
OBSERVATIONS**

by

CAPT ANTHONY J. WARREN

and

CAPT JOHN A. RUPP

NOVEMBER 1991

**APPROVED FOR PUBLIC RELEASE;
DISTRIBUTION IS UNLIMITED**

USAF DTIC QUALITY INSPECTED 3
**ENVIRONMENTAL TECHNICAL
APPLICATIONS CENTER**

Scott Air Force Base, Illinois, 62225-5438

19970205 061




REVIEW AND APPROVAL STATEMENT

USAFETAC/PR--91/016, *Spatial and Temporal Correlation of Surface Temperature and Wind Observations*, November 1991, has been reviewed and is approved for public release. There is no objection to unlimited distribution of this document to the public at large, or by the Defense Technical Information Center (DTIC) to the National Technical Information Service (NTIS).


PATRICK J. BREITLING
Chief Scientist

FOR THE COMMANDER


WALTER S. BURGMAN
Scientific and Technical Information
Program Manager
29 November 1991

A NOTE TO OUR CUSTOMERS--

The authors and editors of this publication welcome feedback, both positive and negative. We value your opinion. Please let us know what you like and do not like about our products. Also, please let us know if your address has changed, or if you wish to receive more or fewer copies of AWS and USAFETAC technical documents in primary distribution. If you need more copies of this document, or if you know of someone else who might be interested in this or other AWS/USAFETAC publications, let us know that, too. Call, write, or FAX:

USAFETAC/LDE,
Scott AFB, IL 62225-5458

DSN 576-6648 Commercial 618 256-6648 FAX 3772

REPORT DOCUMENTATION PAGE

2. Report Date: November 1991
3. Report Type: Project report
4. Title: Spatial and Temporal Correlation of Surface Temperature and Wind Observations
6. Authors: Capts Anthony J. Warren and John A. Rupp
7. Performing Organization Name and Address: USAF Environmental Technical Applications Center (USAFETAC/DNY), Scott AFB, IL 62225-5438
8. Performing Organization Report Number: USAFETAC/PR--91/016
12. Distribution/Availability Statement: Approved for public release; distribution is unlimited.
13. Abstract: Nearly all weather support products depend on the fundamental accuracy of the basic weather observation, and observational accuracy depends, at least in part, on frequency and spacing. In many parts of the world, surface observations are only taken at 3-hour intervals. Weather station spacing is irregular, and there may be less than one reporting station every 200 km. When a weather observation is needed at a specific time and place (as in climatological analysis), it is usually necessary to interpolate by using the data closest to that time from the nearest available weather station. There are errors inherent in this procedure, and users of such data normally require estimates of those errors. This study provides these error estimates as functions of time and distance for surface weather observations of temperature, wind speed, and wind direction. After the methodology is explained, results are provided in appendices as probability data in a series of charts that show percentiles of cumulative distribution of changes in temperature, wind speed, and wind direction as functions of distance or time.
14. Subject Terms: CLIMATOLOGY, WEATHER, WEATHER OBSERVATIONS, WEATHER STATIONS, SPATIAL DISTRIBUTION, RESOLUTION, SURFACE TEMPERATURE, WIND, WIND SPEED, WIND DIRECTION, MODELS, CORRELATIONS, TEMPORAL CORRELATIONS, SPATIAL CORRELATIONS, ERRORS
15. Number of Pages: 141
17. Security Classification of Report: Unclassified
18. Security Classification of this Page: Unclassified
19. Security Classification of Abstract: Unclassified
20. Limitation of Abstract: UL

Standard Form 298

PREFACE

This report documents work done to complete USAFETAC Project #910108, which was in response to a support assistance request from the HQ Air Weather Service Product Improvement Division (AWS/XTX). USAFETAC was asked to estimate spatial and temporal errors inherent in interpolating weather observations. Error estimates were to be stratified by time of day, season, and geographical region. The results were to be used in assessing limitations on the accuracy of weather observations.

Nearly all weather support products depend on the fundamental accuracy of the basic weather observation. Observational accuracy depends, at least in part, on frequency and spacing. In many parts of the world, surface observations are only taken at 3-hour intervals. Weather station spacing is irregular, and there may be less than one reporting station every 200 km.

When a weather observation is needed at a specific time and place (as in climatological analysis), it is usually necessary to interpolate by using the data closest to that time from the nearest available weather station. There are errors inherent to this procedure, and users of such data normally require estimates of those errors. This study provides these error estimates as functions of time and distance for surface weather observations of temperature, wind speed, and wind direction. After the methodology is explained, results are provided in appendices as probability data in a series of charts that show percentiles of cumulative distribution of changes in temperature, wind speed, and wind direction as functions of distance or time.

The authors wish to acknowledge Lt Col Roger C. Whiton (USAFETAC/DN) and Mr Charles R. Coffin (USAFETAC/DNY) for their contributions to this work. A special acknowledgment is extended to Mr Albert R. Boehm of Hughes STX Corporation (under contract to the Phillips Laboratory's Geophysics Directorate) for recommending the approach used in this study and for providing several helpful suggestions.

CONTENTS

	Page
Chapter 1 INTRODUCTION	
1.1 Purpose	1
1.2 Approach	1
1.3 Method	1
1.4 Output Format	1
Chapter 2 STATISTICAL MODEL	
2.1 Introduction	2
2.1.1 Exception for Coastal Climates	2
2.2 Normal Distributions	2
2.3 Derivation	2
2.4 Wind Speed and Direction	4
2.4.1 Variable Transformations	4
2.4.2 Sample Calculations	4
2.5 Temporal Correlation	5
2.6 Correlation Coefficients	5
2.6.1 Sensitivity to the Correlation Coefficient	5
2.6.2 Meaning of the Correlation	5
2.7 Statistical Parameters	6
2.8 Station Selection	6
Chapter 3 VERIFICATION OF ASSUMPTIONS	
3.1 Test for Normality	7
3.1.1 Skewness	7
3.1.2 Kurtosis	7
3.1.3 Interpretation of Skewness and Kurtosis	7
3.2 Test on Temperature	8
3.3 Test on Wind Components	8
3.4 Multivariate Normal Distributions	10
Chapter 4 COASTAL ENVIRONMENT	
4.1 Climate	12
4.2 Mesoscale Correlation Structure	12
4.3 Larger-Scale Correlation Structure	13
4.4 Changes in Mean Temperature	13
4.5 Distribution of Mean Temperature	13
4.6 Distribution of the u - and v -Components of Wind	14
4.7 Conclusion	15
Chapter 5 DISCUSSION OF RESULTS	
5.1 Results	16
5.2 Interpretation	16
5.2.1 Example in the Temporal Case	16
5.2.2 Example in the Spatial Case	16
5.2.3 Additional Example	16
5.2.4 Plots with Little Variability	16
5.3 Final Point	17

BIBLIOGRAPHY	18
GLOSSARY	19
APPENDIX A Spatial Correlation of Temperature	A-1
APPENDIX B Spatial Correlation of Wind Direction	B-1
APPENDIX C Spatial Correlation of Wind Speed	C-1
APPENDIX D Temporal Correlation of Temperature	D-1
APPENDIX E Temporal Correlation of Wind Direction	E-1
APPENDIX F Temporal Correlation of Wind Speed	F-1

FIGURES

	Page
Figure 1. Graphic depiction of a normal probability density function and the probabilities described by equations 1 and 2.	3
Figure 2. Comparison of the observed and simulated cumulative distribution functions for the 3-hour change in temperature for Topeka at winter-sunrise.	11
Figure 3. Comparison of the observed and simulated cumulative distribution functions for the 3-hour change in wind direction for Topeka at winter-sunrise.	11
Figure 4. Comparison of the observed and simulated cumulative distribution functions for the 3-hour change in wind speed for Topeka at winter-sunrise.	11
Figure 5. Comparison of the observed and simulated cumulative distribution functions of the difference in temperature between Topeka and Ft Riley at winter-sunrise.	11
Figure 6. Comparison of the observed and simulated cumulative distribution functions of the difference in wind direction between Topeka and Ft Riley at winter-sunrise.	12
Figure 7. Comparison of the observed and simulated cumulative distribution functions of the difference in wind speed between Topeka and Ft Riley at winter-sunrise.	12
Figure 8. Map of Patrick AFB WINDS sensors.	13
Figure 9. Correlation of temperature among the Patrick AFB WINDS locations as a function of distance. Also shown is the expected correlation using the model of Bertoni and Lund.	14
Figure 10. Correlation of temperature between Patrick AFB and neighboring synoptic stations.	14
Figure 11. Mean maximum temperature throughout Florida in January.	15
Figure 12. Mean minimum temperature throughout Florida in January.	15
Figure 13. Mean maximum temperature throughout Florida in July.	15
Figure 14. Mean minimum temperature throughout Florida in July.	15
Figure 15. Modeled change in mean temperature as a function of distance inland during summer at noon.	16
Figure 16. Modeled change in mean temperature as a function of distance inland during summer at sunrise.	16
Figure 17. Modeled change in mean temperature as a function of distance inland during winter at noon.	16
Figure 18. Modeled change in mean temperature as a function of distance inland during winter at sunrise.	16

TABLES

	Page
Table 1. The corresponding change in wind direction (degrees) for the stated values of u_1, v_1, u_2, v_2 (knots).	5
Table 2. Stations used as representative of the climates selected in this study.	6
Table 3. Skewness and kurtosis values for temperature distributions at Topeka	8
Table 4. Skewness and kurtosis values for the u -component of the surface wind at Topeka	9
Table 5. Skewness and kurtosis values for the v -component of the surface wind at Topeka	10

1. INTRODUCTION

1.1 Purpose. Nearly all weather support depends on the fundamental accuracy of the weather observation. Observational accuracy depends, at least in part, on frequency and spacing. In many parts of the world, surface observations are only taken at 3-hour intervals. Weather station spacing is irregular and there may be less than one reporting station every 200 km. Therefore, when a weather observation is needed at a specific time and place (as in climatological analysis), it is usually necessary to use data closest to that time from the nearest available weather station. There are errors inherent in this approach, and users of the observational database usually require estimates of those errors. The purpose of this study is to provide such estimates as functions of time and distance for surface weather observations of temperature, wind speed, and wind direction.

1.2 Approach. The spatial and temporal correlation of surface observations is a function of many variables, including distance, direction, climate, geography, season, time of day. Although there are no limits on the types of stratification possible, this study focuses primarily on *distance* and its temporal counterpart, *observation age*. The probability that a temperature at a distance x from a given location (or a time t from a given time) falls within a specified range will be computed. These probabilities will be stratified by climatological region, season, and time. The six climatological regions considered are: *continental*, *arctic*, *desert*, *maritime*, *tropical*, and *coastal*. The three time periods considered are: *midnight*, *sunrise*, and *local noon*.

1.3 Method. In this study, we computed probabilities for "generic" climates rather than for specific regions or stations. The irregular spacing of weather stations, differences in topography, and differences in instrument exposure often make using actual data difficult. Additional considerations are required to determine if, and to what extent, the observed spatial decorrelation is a result of effects common to similar climates, or if it is a result of local effects. To make this determination, we used a statistical technique to evaluate the spatial and temporal correlation of surface observations.

1.4 Output Format. The probability data is provided on a series of charts that show percentiles of the cumulative distributions of changes in temperature, wind speed, or wind direction as functions of distance or time.

2. STATISTICAL MODEL

2.1 Introduction. The evaluation of changes in temperature or wind variables as a function of distance or time is complicated by the irregular spacing of weather stations. In any given region, station spacing is roughly on the order of one per 100 km, which provides a limited sampling. Although there are databases with finer grid spacing, resolution will always be limited by station spacing, a fact that makes it hard to analyze the accuracy of the data. In addition, no geographical region is truly homogeneous; all regions have, to varying degrees, local features that affect weather observations. Although it's difficult to filter out these microscale and mesoscale effects, especially for winds, we devised a statistical model to evaluate changes in temperature, wind speed, and wind direction with distance. We selected a representative station for each climatological region. Topeka, Kansas, for example, was selected to represent the continental climate. In this model, it was assumed that all points surrounding Topeka have exactly the same climate; for each model climate, the mean and standard deviation of temperature and the u - and v -components of the wind were then computed. We assumed that these variables are normally distributed, and confirmed this assumption with tests on the skewness and kurtosis of the actual distributions.

2.1.1 Exception for Coastal Climates. We cannot make the assumption of homogeneity in coastal areas because of discontinuities resulting from the sea-breeze front, which is largely responsible for observed changes in temperature, wind speed, and wind direction. We analyzed the coastal climate separately--see Chapter 4.

2.2 Normal Distributions. The assumption that temperatures follow a normal distribution and that the u - and v -components of the wind follow a bivariate normal distribution are made frequently (Boehm, 1976; Buell, 1972; Thiebaut and Pedder, 1987). In this study, we assumed that the joint distribution of temperature between two points (either in space or in time) is *bivariate* normal; we also assumed that the joint distribution of u - and v -components of wind between two different points is *quadrivariate* normal. The fact that the marginal distributions are normal is a necessary (but not sufficient) condition that the joint probabilities are also normal (Smith, 1976); even so, this assumption is often made. Univariate normal distributions are based on two parameters: the mean and standard deviation. The bivariate normal distribution has two means, two standard deviations, and a fifth parameter, which is the *cross-correlation coefficient*. Correlations for the quadrivariate normal distribution are more complex and are expressed by a 4x4 correlation matrix (see Smith, 1976, for further discussion).

2.3 Derivation. Values of fluid dynamical variables such as temperature and wind speed do not occur randomly; instead, they exhibit a spatial and temporal coherence caused by stresses within the viscous fluid. One would expect, for example, that temperature T_0 a very small distance away from temperature T at a central point would be strongly related to the temperature at the central point. In other words, the two temperature measurements should be strongly positively correlated and the probability of a large temperature difference $|T - T_0|$ between the two points should be small. Correspondingly, the temperature a substantial distance away from the central point will be less strongly related to the temperature at the central point; the two temperatures are generally less strongly positively correlated, and the probability of a large temperature difference between the two is correspondingly larger. The key point is that the correlation ρ between T and T_0 is, in general, a function of the distance r between the two points; i.e., $\rho = \rho(r)$. The temperature is normally distributed, and differences between temperatures are also normally distributed. The two variables are jointly related by the bivariate normal distribution, with one random variate being T , the other being T_0 , and the correlation between them being $\rho(r)$. If the temperature at a given point is T_0 , the probability that a temperature T at a distance r from the central point exceeds $T_0 + \Delta T$ is given by (Boehm, 1976):

$$P(T > T_0 + \Delta T | T_0) = 1 - \Phi \left[\frac{\ddot{y}_+ - \rho(r)\ddot{p}}{\sqrt{1 - \rho(r)^2}} \right] \quad (1)$$

where \ddot{p} is the equivalent normal deviate (END) of T_0 ; \ddot{y}_+ is the END of $T_0 + \Delta T$; and $\Phi(Q)$ is the (univariate) normal cumulative probability of obtaining an END of less than Q (see Figure 1). (For a discussion of the concept of equivalent normal deviates, see Whiton and Berecek, 1982.)

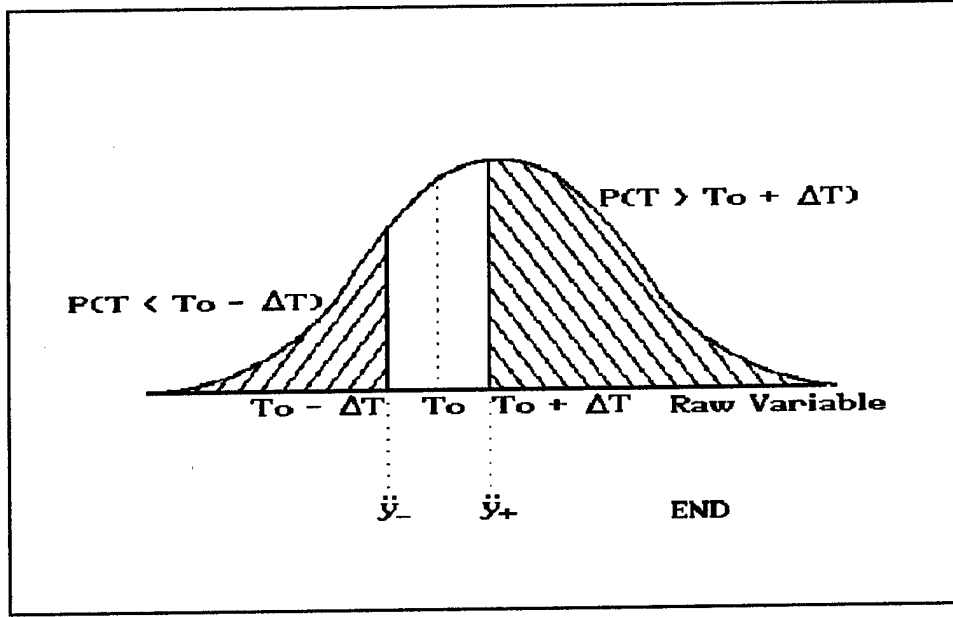


Figure 1. Graphic depiction of a normal probability density function and the probabilities described by Equations 1 and 2.

It must be emphasized that we have explicitly stated that the temperature at the central point, T_0 , has been held constant. Various values of T , r , and ΔT are inserted into the equation. Next we compute the conditional probability of obtaining a temperature less than $T_0 - \Delta T$:

$$P(T < T_0 - \Delta T | T_0) = \Phi \left[\frac{\ddot{y}_- - \rho(r)\ddot{p}}{\sqrt{1 - \rho(r)^2}} \right] \quad (2)$$

where \ddot{y}_- is the END of $T_0 - \Delta T$. Adding these cumulative values and then subtracting this sum from 1, yields the conditional probability that the temperature falls within a range of $2\Delta T$ about T_0 :

$$P(|T - T_0| < 2\Delta T | T_0) = 1 - [P(T > T_0 + \Delta T | T_0) + P(T < T_0 - \Delta T | T_0)] \quad (3)$$

To find the unconditional probability that the difference in temperatures between the two points is less than the value $2\Delta T$, integrate overall values of temperature at the central point (T_0):

$$P(|T - T_0| < 2\Delta T) = \int_{-\infty}^{+\infty} P(|T - T_0| < 2\Delta T | T_0) P(T_0) dT_0 \quad (4)$$

In these equations we account for the effect of distance through the correlation coefficient $\rho = \rho(r)$. It is immaterial how one subdivides the interval of temperature; it is the *total size* of the interval that matters. We can define a new interval $\Delta T' = 2\Delta T$, for which equations 3 and 4 will be valid.

2.4 Wind Speed and Direction. Computations of the changes in these variables with distance (or time) are complicated by the required variable transformation. Distributions of wind speed (V) and wind direction (θ) are far from normal. We must therefore transform V - θ components to u - v components. It is reasonable to assume that the joint distribution of u and v is bivariate normal (Smith, 1976). Computations of the mean and standard deviations of u and v and the cross correlation parameter ρ will let us specify the probability density function (PDF), $p(u, v)$. The joint probability of u and v between two points will be assumed to follow the quadrivariate normal distribution. There are two basic types of correlation coefficients in this type of distribution. The first is the *autocorrelation* which defines the correlation between the two u (or two v) components at two different points (either in space or time). The second type is the *cross-correlation coefficient*, which defines the correlation between the u and v components. This is a simplification, since the correlation structure in the quadrivariate normal distribution is a 4x4 matrix. However, following the technique in Smith (1976), all elements of this matrix can be obtained by specifying the two auto-correlations: ρ_{uu} and ρ_{vv} , and the cross-correlation ρ_{uv} . This technique ignores the so called "cross-lag coefficients," which are usually small and difficult to estimate from real data.

2.4.1 Variable Transformations. Once the PDFs for the components of the wind vector have been determined, transformations are necessary to compute the corresponding PDFs for wind direction and speed. Conceptually, this can be carried out using a "checkerboard" approach, in which finite increments of u are shown along the rows and finite intervals of v along the columns. The entry in each checkerboard, then, is the probability of the joint occurrence of the given u and v intervals.

2.4.2 Sample Calculation. To show how this technique works, consider a portion of the checkerboard as shown in Table 1. Values of u and v are depicted in intervals of 0.2 knots. Suppose the probability of ($u_1=1.0, v_1=0.8, u_2=1.2, v_2=1.0$) is computed to be 0.02. The change in wind direction represented by these values (from Table 1) is 11.5° . We use this information to compute the cumulative distribution function (CDF) of the change in wind direction. The value $P(u_1 = 1.0, v_1 = 0.8, u_2 = 1.2, v_2 = 1.0) = 0.02$ contributes a value 0.02 to the CDF for the value $P(\Delta\theta < 11.5^\circ)$. A summation is then made for all possible entries, and the complete CDF, independent of the initial wind direction is obtained. The probability that the change in wind direction $\Delta\theta$ is less than a threshold value $\Delta\theta_0$ is given mathematically by:

$$P(\Delta\theta < \Delta\theta_0) = \sum_{i=1}^M \sum_{j=1}^N \sum_{k=1}^M \sum_{l=1}^N P(u_{1i}, v_{1j}, u_{2k}, v_{2l} | \Delta\theta' \leq \Delta\theta_0) \quad (5)$$

where there are M increments of u and N increments of v . The change in wind direction between (u_1, v_1) and (u_2, v_2) is represented by $\Delta\theta'$. A similar computation is carried through for wind speeds. This highly iterative process is accomplished quickly on the USAFETAC mainframe computer, an IBM 3090.

Table 1. The corresponding change in wind direction (degrees) for the stated values of u_1, u_2, v_1, v_2 (knots).

$u_1 = 1.0 \quad v_1 = 0.8$				
	u_2			
	<u>1.0</u>	<u>1.2</u>	<u>1.4</u>	<u>1.6</u>
v_2				
1.0	6.3	1.1	3.1	6.7
1.2	11.5	6.3	1.9	1.8
1.4	15.8	10.7	6.3	2.5
1.6	19.3	14.5	10.2	6.3

2.5 Temporal Correlation. A technique similar to that described in Section 2.3 is used to compute the temporal correlations. The same distributions are assumed to apply. For the spatial correlations, we assumed that the mean and standard deviation of the variables of interest were the same at both points. For the temporal case, these distributions parameters are functions of *time*. The statistics are computed based on ± 3 hours of the mean. The actual data used to compute the statistical parameters are all obtained from stations that report hourly. Thus, the mean and standard deviation for each of the hours of interest are computed.

2.6 Correlation Coefficients. The spatial correlation of temperature as a function of distance was obtained from Bertoni and Lund (1964); it represents the average of many hundreds of pairs of stations in Europe. Bertoni and Lund obtained a functional relationship of correlation (ρ_s) with distance (r):

$$\rho_s(r) = \exp\left(-\frac{r}{r_s}\right) \quad (6)$$

where r_s is the scale distance, equal to 1,000 km. The spatial correlation of u - and v -components were obtained from Buell (1972), who suggested the model:

$$\rho_s(r) = \exp(-r^2/r_s^2) \quad (7)$$

where the scale distance r_s is 250 km. Cross-correlations and temporal correlations were all computed from observations from each of the representative stations--see Section 2.8. The differences in the corresponding scale distance reveal that the wind component spatial correlations decrease faster with distance than with temperature.

2.6.1 Sensitivity to Correlation Coefficient. Clearly, our assumptions of a universal spatial correlation structure are significant. Studies of the changes in this structure with various geographical regions, or as a function of season, have not been made; however, high precision of the correlation coefficient is not required, as will be shown by the following analysis.

2.6.2 Meaning of the Correlation Coefficient. For any normal distribution, 68% of all observations lie within one standard deviation (σ) of the mean. Similarly, 50% of all observations lie within 0.675σ of the mean. For two distributions with the same mean and the same standard deviation, the correlation coefficient is a measure of the reduction in the variance in one distribution when the value of the other variable is known.

For example, consider a temperature distribution with a mean of 90° F and a standard deviation of 6° F. We will assume that this distribution describes the temperature at two points, A and B. If the temperature at point A is 90° F and the autocorrelation (ρ) is 0.8, the standard deviation of the conditional distribution (σ_c) of temperature at point B is given by (Smith, 1976):

$$\sigma_c = \sigma \sqrt{1 - \rho^2} \quad (8)$$

or, in this example, 3.6° F. An approximation of the range where 50% of the temperatures at point B lie is then 2.2° F. If the autocorrelation were as low as 0.6 the range would be 3.2° F. Thus, a significant change in correlation (0.8 versus 0.6) results in only a 1° F change in the estimate of the 50th percentile of temperature differences.

2.7 Statistical Parameters. Although this example shows this problem's limited sensitivity to the correlation coefficient, it also highlights the much larger sensitivity of the final results to the standard deviation. A 20% increase in standard deviation results in a corresponding 20% increase in the range of temperatures expected. Less obvious in this example, is the sensitivity of the *means* of the two distributions. For example, when evaluating the change in temperature over a period of 2 hours, the mean temperature at each hour may be significantly different. Thus, even when correlations are high and standard deviations are low, if the change in the mean temperature is 3° F, the most likely difference will be at least 3° F. For most of the spatial calculations, this effect was not important because we assumed the means were constant. For temporal calculations, however, the effect was significant.

2.8 Station Selection. Six stations were selected for this study, one for each of the climatological regions introduced in Section 1.2. All were in the U.S., primarily because of the availability of *hourly* weather observations (at many overseas locations, weather observations are available only every 3 hours--this makes determination of temporal correlation nearly impossible). The U.S. stations were also more likely to be reliable--errors in the measurement of temperature, wind speed, and wind direction (especially biased errors) are extremely difficult to detect. A list of the stations selected is shown in Table 2.

Table 2. Stations used as representative of the climates selected in this study.

<u>Climate</u>	<u>Station</u>	<u>Block Station #</u>	<u>Latitude</u>	<u>Longitude</u>	<u>Elev(m)</u>
Continental	Forbes Field KS	724565	38° 57' N	95° 40' W	329
Arctic	Eielson AFB AK	702650	64° 40' N	147° 06' W	167
Tropical	Howard AFB PN	788060	8° 55' N	79° 36' W	16
Maritime	Hickam AFB HI	911803	21° 19' N	157° 44' W	4
Desert	Nellis AFB NV	723865	36° 14' N	115° 02' W	570
Coastal	Patrick AFB FL	747950	28° 14' N	80° 36' W	3

Observations from these stations were used to compute the mean and standard deviations of temperature, the *u* and *v* wind components, the wind component cross-correlations, and the serial correlations for temperature and wind components.

3. VERIFICATION OF ASSUMPTIONS

3.1 Test for Normality. A fundamental assumption of the model is that temperature and the u - and v -components of wind are all normally distributed. To test for this assumption, we used a technique by D'Agostino et al. (1990), which uses observed skewness and kurtosis to determine whether or not the normal distribution can be considered an approximation to the observed distribution. The chi-square and similar tests are much stricter; they consider the observed distribution non-normal if any type of statistically significant difference is observed.

3.1.1 Skewness. Skewness is a measure of the symmetry of the distribution. It is represented mathematically as b_1 and defined as:

$$b_1 = \frac{m_3}{m_2\sqrt{m_2}} \quad (9)$$

where

$$m_3 = \frac{1}{n} \sum_{i=1}^n (x_i - \bar{x})^3 \quad (10)$$

and

$$m_2 = \frac{1}{n} \sum_{i=1}^n (x_i - \bar{x})^2 \quad (11)$$

In these equations, x_i represents the individual observations, \bar{x} is the mean value, and n is the number of observations. A skewness of zero represents a symmetrical distribution.

3.1.2 Kurtosis. Although kurtosis is difficult to define, it basically discriminates between "peaked" and "flat-topped" distributions. It is assigned the symbol b_2 and defined as:

$$b_2 = \frac{m_4}{m_2} - 3 \quad (12)$$

where

$$m_4 = \frac{1}{n} \sum_{i=1}^n (x_i - \bar{x})^4 \quad (13)$$

3.1.3 Interpretation of Skewness and Kurtosis. By definition, a *normal* distribution has neither skewness nor kurtosis; i.e., $b_1 = 0$ and $b_2 = 0$. When the skewness is non-zero, the mean and the median do not coincide. When the kurtosis is positive, the distribution is flat and the number of observations that occur within one standard deviation of the mean is too small for a normal distribution. Conversely, a negative kurtosis reveals that too many observations occur within one standard deviation of the mean. For a normal distribution to be considered a reasonable approximation to an observed distribution, both the skewness and

kurtosis values must be reasonably close to zero. The criteria presented by D'Agostino et al. (1990) to test for normality are:

$$|b_1| < 4 \sqrt{\frac{6}{n}} \quad (14)$$

and

$$|b_2| < 4 \sqrt{\frac{24}{n}} \quad (15)$$

When both conditions are met, the observed distribution can be reasonably approximated as normal.

3.2 Tests on Temperature. Skewness and kurtosis values were computed for observations of temperature at Topeka for the four seasons and three time periods used in this study; the results are shown in Table 3. Also listed are the skewness and kurtosis thresholds (THSH) for testing normality. Skewness was detected at two time periods: spring-noon and summer-noon, but kurtosis was detected only at summer-noon. For these time periods, the assumption of normality is not supported. The data for summer noon revealed much larger values of skewness and kurtosis than for the other time groups. However, it generally justifies the assumption that temperature is normally distributed.

Table 3. Skewness and kurtosis values for temperature distributions at Topeka. Also listed are the number of observations (N) and thresholds for assuming a normal distribution.

<u>Season</u>	<u>Time</u>	<u>Skew</u>	<u>Kurt</u>	<u>N</u>	<u>Skew Thsh</u>	<u>Kurt Thsh</u>	<u>Criteria Met?</u>
WINTER	Midnight	-0.22	-0.22	725	0.36	0.73	Y
	Sunrise	-0.24	-0.51	835	0.34	0.68	Y
	Noon	0.06	-0.42	833	0.34	0.68	Y
SPRING	Midnight	0.13	-0.42	690	0.37	0.75	Y
	Sunrise	-0.17	-0.46	809	0.34	0.69	Y
	Noon	-0.53	0.53	810	0.34	0.69	N
SUMMER	Midnight	-0.26	0.03	688	0.37	0.75	Y
	Sunrise	-0.21	-0.37	811	0.34	0.69	Y
	Noon	-0.92	1.76	811	0.34	0.69	N
AUTUMN	Midnight	-0.02	-0.59	713	0.37	0.73	Y
	Sunrise	-0.03	-0.42	835	0.34	0.68	Y
	Noon	0.01	-0.39	836	0.34	0.68	Y

3.3 Tests on Wind Components. Similar tests were carried out to evaluate the assumption of normality for the u - and v -components of wind. These results are shown in Tables 4 and 5, respectively. It's clear that there are times when the assumption of normality is not justified. In fact, the test fails for the u -component during all four seasons at midnight. The large positive values of kurtosis indicate a peaked distribution; too many observations are clustered around the mean. This results from the fact that calm winds occur with higher frequency at night. Calm (and light) winds create additional problems. The transformation between u - v coordinates and V - θ coordinates can become unstable with light winds. A small change in u or v can result in large changes in θ . **EXAMPLE:** The components ($u = 1.0, v = 0.5$) corresponds to ($\theta = 243^\circ, V = 1.1$). A slight increase in the v -component to 1.5 knots results in a wind direction of 213° and a wind speed of 1.8 knots; a 1-knot change in one of the components resulted in a 30° change in wind direction.

To solve these problems, the statistics were recomputed to exclude wind speeds below 3 knots. This reduced kurtosis values, but generally not below the threshold values. It also resulted in an increase in kurtosis values for the v -components. For example, the kurtosis of the u -component at winter-midnight decreased from 2.14 to 1.36. However, the kurtosis of the v -component changed from 0.12 to -0.42. The assumption of normality is clearly a problem for modeling light winds. Since light winds are not of much interest in this study, computed statistics exclude conditions when winds were less than 3 knots. It is clear that the results of this study *do not* apply when winds are light.

Table 4. Values of skewness and kurtosis for the u -component of surface wind at Topeka. Also listed are the number of observations (N) and thresholds for assuming a normal distribution.

<u>Season</u>	<u>Time</u>	<u>Skew</u>	<u>Kurt</u>	<u>N</u>	<u>Skew Thsh</u>	<u>Kurt Thsh</u>	<u>Criteria Met?</u>
WINTER	Midnight	0.26	2.14	723	0.36	0.73	N
	Spring	-0.01	0.36	836	0.34	0.68	Y
	Noon	0.27	0.46	836	0.34	0.68	Y
SPRING	Midnight	0.18	1.45	690	0.37	0.75	Y
	Spring	0.13	0.15	810	0.34	0.69	Y
	Noon	0.16	0.20	810	0.34	0.69	Y
SUMMER	Midnight	-0.26	2.83	713	0.37	0.73	N
	Spring	-0.15	0.41	836	0.34	0.68	Y
	Noon	0.35	1.58	837	0.34	0.68	N
AUTUMN	Midnight	0.31	2.65	713	0.37	0.73	N
	Spring	0.19	0.65	837	0.34	0.68	Y
	Noon	0.52	1.14	837	0.34	0.68	N

Table 5. Values of the skewness and kurtosis of the v-component of wind at Topeka. Also listed are the number of observations (N) and thesholds for assuming a normal distribution.

<u>Season</u>	<u>Time</u>	<u>Skew</u>	<u>Kurt</u>	<u>N</u>	<u>Skew Thsh</u>	<u>Kurt Thsh</u>	<u>Criteria Met?</u>
WINTER	Midnight	0.00	0.12	723	0.36	0.73	Y
	Sunrise	-0.01	-0.40	836	0.34	0.68	Y
	Noon	0.10	-0.55	836	0.34	0.68	Y
SPRING	Midnight	0.12	0.47	690	0.37	0.75	Y
	Sunrise	0.19	-0.81	810	0.34	0.69	N
	Noon	0.30	-0.68	810	0.34	0.69	Y
SUMMER	Midnight	0.27	0.82	713	0.37	0.73	N
	Sunrise	-0.14	-0.27	836	0.34	0.68	Y
	Noon	-0.14	-0.50	837	0.34	0.68	Y
AUTUMN	Midnight	0.23	0.73	713	0.37	0.73	Y
	Sunrise	-0.05	-0.55	837	0.34	0.68	Y
	Noon	0.01	-0.66	837	0.34	0.68	Y

3.4 Multivariate Normal Distributions. To validate the assumptions that the temperature and u - and v -components of wind at two points are distributed according to a multivariate normal distribution, sample model distributions and an empirically computed distribution were compared. Figure 2 shows a comparison of the cumulative distributions of the 3-hour change in temperature during the winter-sunrise period at Topeka with the 3-hour change from the statistical model. The winter-sunrise period was selected because it had the largest amount of variability of all 12 time periods studied. Figure 3 shows the 3-hour change in wind direction at the same time period, and Figure 4 shows the 3-hour change in wind speed. Similar graphics (Figures 5-7) were prepared for the spatial correlation.

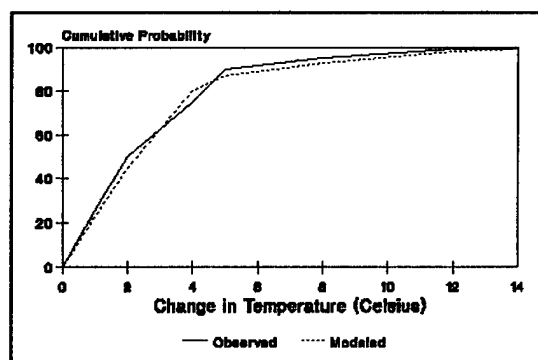


Figure 2. Comparison of the observed and simulated cumulative distribution functions for the 3-hour change in temperature for Topeka at winter-sunrise.

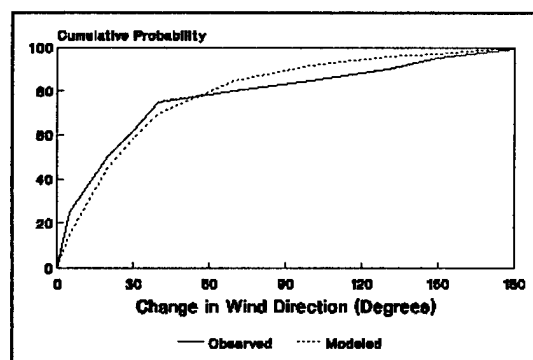


Figure 3. Comparison of the observed and simulated cumulative distribution functions for the 3-hour change in wind direction for Topeka at winter-sunrise.

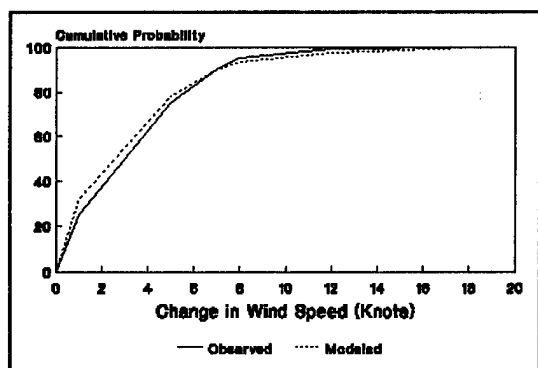


Figure 4. Comparison of the observed and simulated cumulative distribution functions for the 3-hour change in wind speed for Topeka, at winter-sunrise.

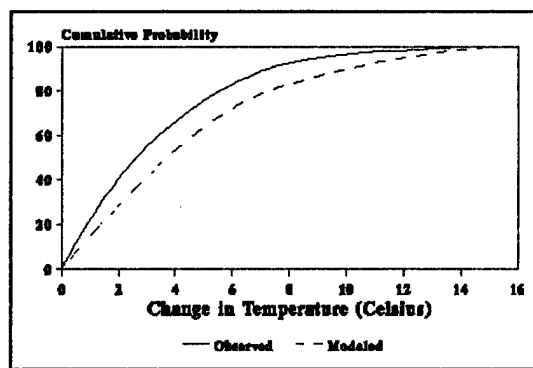


Figure 5. Comparison of the observed and simulated cumulative distribution functions of the difference in temperature between Topeka and Ft Riley at winter-sunrise.

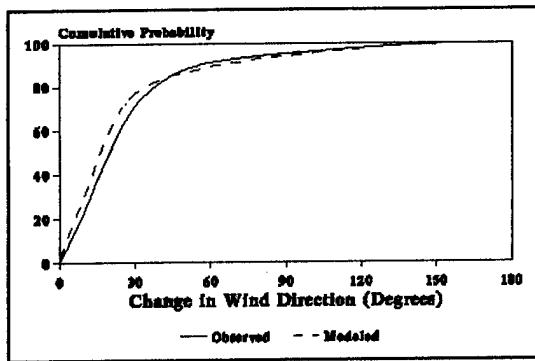


Figure 6. Comparison of the observed and simulated cumulative distribution functions for the *difference in wind direction* between Topeka and Ft Riley at winter-sunrise.

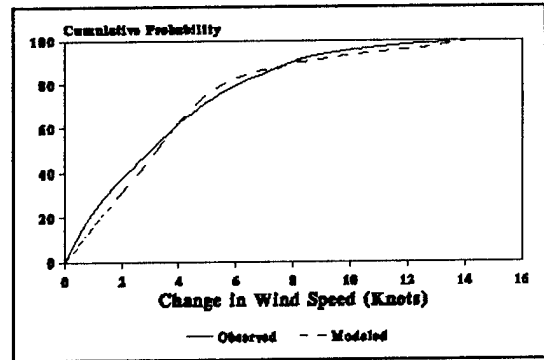


Figure 7. Comparison of the observed and simulated cumulative distribution functions for the *difference in wind speed* between Topeka and Ft Riley at winter-sunrise.

The changes in temperature, wind direction, and wind speed between Topeka and Fort Riley (60 nm west of Topeka) were computed and compared against the statistical model; there was good agreement. Model estimates of the percentile values through about the 75th percentile are very close to the observed values. However, estimates above the 75th percentile begin to deviate, due mainly to the fact that we are now using values in the tails of the modeled distributions. Departures from normality are most notable in these tails, and small errors are amplified. This effect is further enhanced by the small slope in the curve beyond about the 75th percentile. EXAMPLE: The model estimate of the 99th percentile of the 3-hour change in temperature is 14.3 and the actual value is 11.9. This may seem to be a large error, but the model estimate for the corresponding percentile to 11.9 is 98.5. In this region, small changes in percentile result in large changes in temperature. We do not believe that this effect is significant. Estimates of values even out to the 95th percentile are reasonable.

4. COASTAL ENVIRONMENT

4.1 Climate. The assumption of large-scale climatic homogeneity is clearly not true in coastal environments because the effect of the sea-breeze front provides a sharp discontinuity in air mass over relatively short distances. The movement of this front adds additional variability to coastal climates. We will attempt to consider the change in climate with distance to evaluate changes in temperature, wind speed, and wind direction with distance.

4.2 Mesoscale Correlation Structure. Since large temperature changes occur over relatively short distances, we need to be familiar with the correlation structure in the mesoscale. To obtain this information, we used the Weather Information Network Display System (WINDS) dataset from Cape Canaveral, Florida. The WINDS network consists of 28 sensors that measure temperature, wind direction, and speed. The largest distance between any two sensors is 30 km. Figure 8 is a map of sensor locations. Temperature and wind data are available for various levels, but for this study we considered only the lowest (10-meter) level. Next, we tried to find a relationship of temperature correlation with distance. A matrix of temperature correlations was computed for all possible pairs of stations. This can be depicted as:

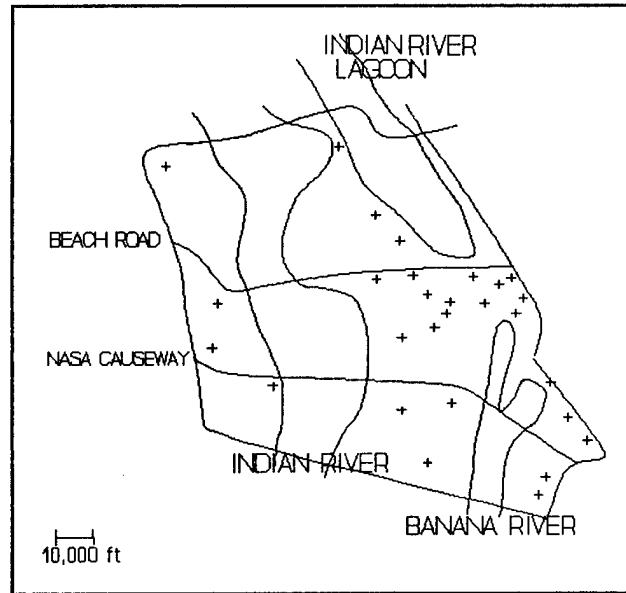


Figure 8. Map of Patrick AFB WINDS sensors.

$$\tilde{\rho} = \begin{bmatrix} 1 & \rho_{12} & \rho_{13} & \rho_{14} & \rho_{15} \\ . & 1 & \rho_{23} & \rho_{24} & \rho_{25} \\ . & . & 1 & \rho_{34} & \rho_{35} \\ . & . & . & 1 & \rho_{45} \\ . & . & . & . & 1 \end{bmatrix} \quad (16)$$

where $\tilde{\rho}$ is the matrix of correlation coefficients. The members of the matrix represent the correlation between two locations. For example, the correlation between locations 3 and 5 is given by ρ_{35} . Only the terms above the diagonal need to be computed, since this matrix is symmetric about the diagonal ($\rho_{14} = \rho_{41}$, etc.). Corresponding to each correlation, (e.g., ρ_{35}), is a distance, (e.g., r_{35}), between the two sensors. This was carried out for all the WINDS stations. The correlations are based on hourly temperature observations. Figure 9 is a plot of these correlations of temperature obtained from the WINDS dataset as a function of distance. Also shown is the expected correlation structure using the model of Bertoni and Lund (1964)--see equation 6. A functional relationship between correlation and distance is not observed in the mesoscale.

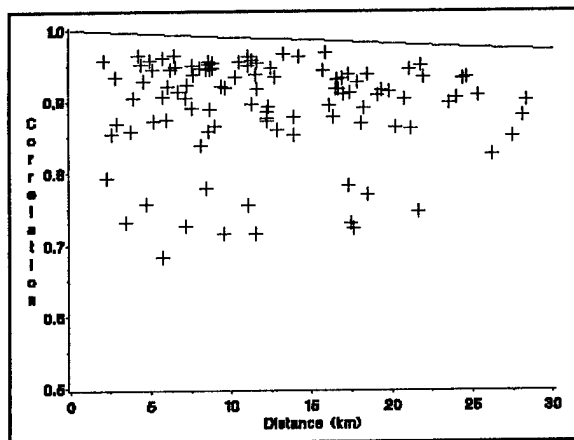


Figure 9. Correlation of temperature among Patrick AFB WINDS locations as a function of distance. Also shown is the expected correlation using the model of Bertoni and Lund.

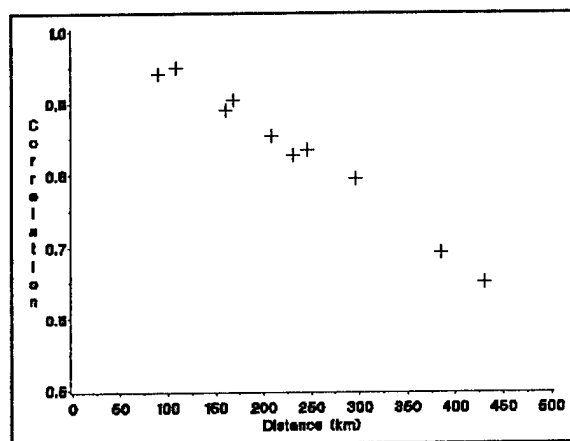


Figure 10. Correlation of temperature between Patrick AFB and neighboring synoptic stations.

A regression fit of these points resulted in a line independent of distance, suggesting that distance alone does not describe the decorrelation of temperature observations at the mesoscale. Differences caused by orographic controls and the sea breeze appear to be much more significant than distance once the separation becomes less than critical. We propose that this critical distance be used to define the mesoscale. Similar behavior is observed in the wind data. Other information is required to compute the correlation coefficient within the mesoscale. Tabor and Motte (1988) found that a detailed terrain dataset was sufficient to extrapolate wind speed and direction. This suggests that a mesoscale analysis of weather variables independent of a specific location is not practical.

4.3 Larger-Scale Correlation Structure. To supplement the mesoscale network, we used synoptic scale stations to determine whether the correlation models described in equations 6 and 7 also applied in coastal environments. The results of this study, which showed that the models were indeed valid, are shown in Figure 10. The scale distance in this plot (about 1,300 km) is slightly larger than the value (1,000 km) given in Section 2.7. This larger scale distance was used in carrying out the calculations for the coastal environment. The wind structure showed similar behavior, but the data from the limited number of stations was not as smooth. Therefore, we used the same scale distance as described in Section 2.7 (250 km) for the wind calculations.

4.4 Changes in Mean Temperature. As shown in Figures 11-14, the north-south and east-west temperature gradients are both significant. Figure 11 shows January mean maximum temperatures throughout Florida; Figure 12, mean minimums. Figure 13 shows July mean maximum temperatures; Figure 14, mean minimums. These figures show the effects of the ocean, which are much more pronounced in winter than in summer. Maximum temperatures during the day are warmer inland, but at night the warmest temperatures are along the coast. There was little change in the standard deviation of the temperature distributions at any given hour as a function of distance. These figures are based on data in Bradley (1978).

4.5 Distribution of Mean Temperature. Figures 11-14 show the observed change in mean temperature as a function of distance inland. Again, the assumption of a uniform mean (made for the other climates) clearly does not apply. We therefore assume the mean to be a function of *distance*; an assumption of a constant standard deviation is reasonable. We will modify our statistical model by including a relationship for the change in mean temperature as a function of distance in coastal climates.

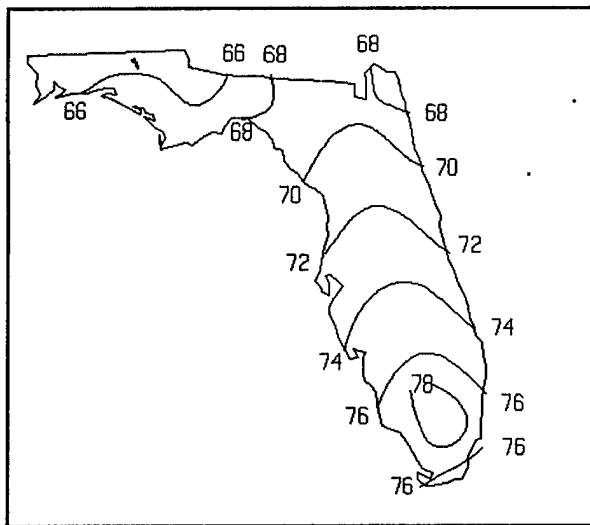


Figure 11. Mean maximum temperature throughout Florida in January.

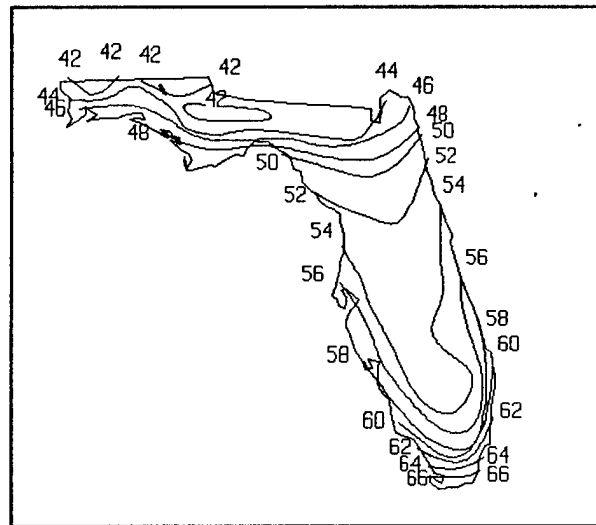


Figure 12. Mean minimum temperature throughout Florida in January.

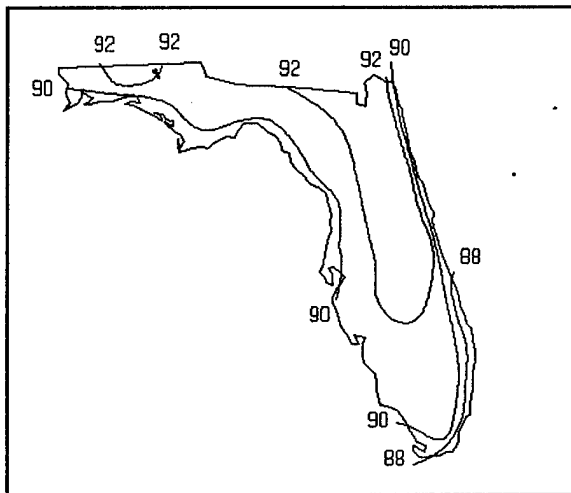


Figure 13. Mean maximum temperature throughout Florida in July.

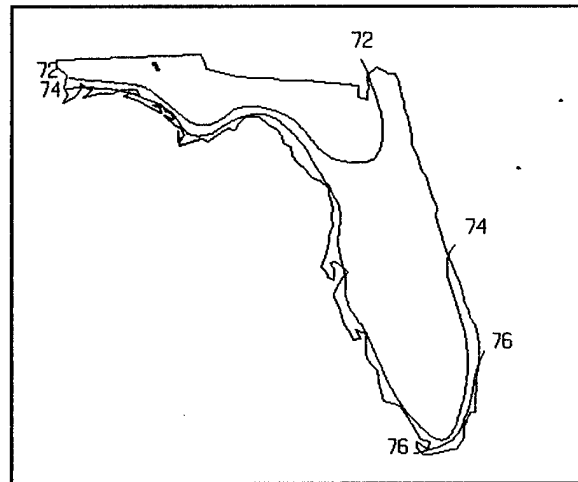


Figure 14. Mean minimum temperature throughout Florida in July.

Figure 15 shows the modeled change in mean summer maximum temperature as one moves inland. We assumed a constant slope out to a distance of 80 km, and a constant value beyond that. The data in Figure 15, based on the maximum temperature plots, was applied to calculations for changes in temperature at noon. Figure 16 is similar, but based on *minimum* temperatures; this model was applied to calculations made for sunrise. We assumed a constant mean for midnight, estimating that this was about the midpoint between maximum and minimum temperatures. Figures 17 and 18 depict the corrections applied for winter. For spring and autumn, averages of the corrections presented for winter and summer were used.

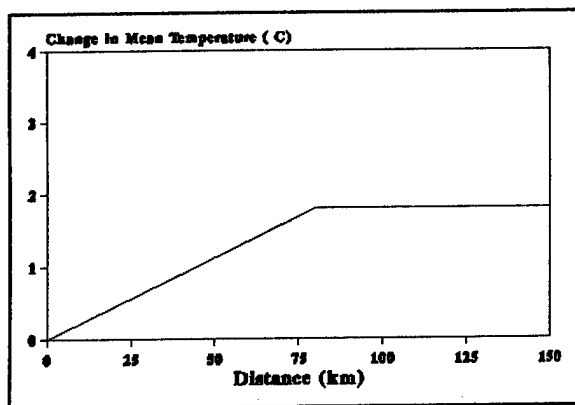


Figure 15. Modeled change in mean temperature as a function of distance inland during summer at noon.

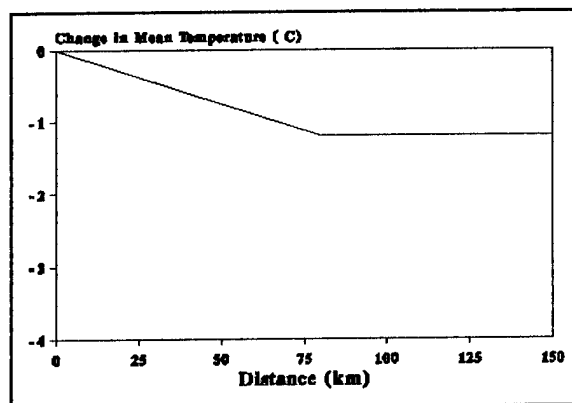


Figure 16. Modeled change in mean temperature as a function of distance inland during summer at sunrise.

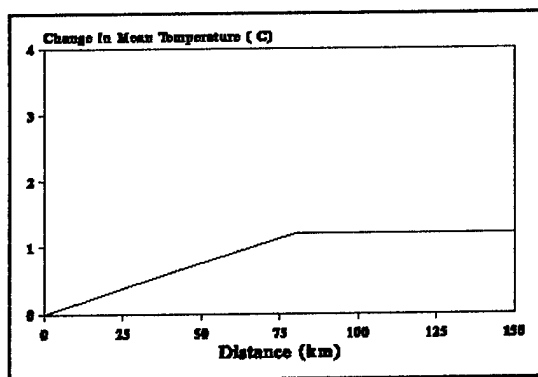


Figure 17. Modeled change in mean temperature as a function of distance inland during winter at noon.

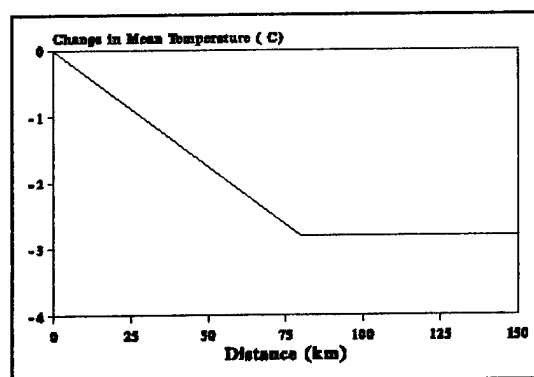


Figure 18. Modeled change in mean temperature as a function of distance inland during winter at sunrise.

4.6 Distribution of the u - and v -Components of Wind. Our analysis of mean u - and v -components as a function of distance did not show a pattern similar to temperature. Since there was no functional change in the mean wind components as a function of distance, we have assumed constant values for these variables.

4.7 Conclusion. The statistical model that describes the relationship of temperature (or wind direction or wind speed) cannot be used to describe mesoscale relationships. At scales less than some critical distance, correlation becomes independent of distance and dependent on the local orographic controls as they interact with the atmosphere to produce mesoscale effects. To describe mesoscale relationships, a mesoscale model must be used. The results of such a model is restricted to the particular location being studied. A generic approach to mesoscale analysis (not tied to any particular location) is not practical.

5. MODEL OUTPUT

5.1 Results. Model output is given as figures in Appendices A-F. For each climate, there are 18 figures per weather element. Each page depicts one of three time periods (local midnight, sunrise, and local noon), for each of the four seasons. Seasonal statistics were based on a representative month (winter = January; spring = April; summer = July; autumn = October). Appendices A-C give *spatial* results (A-temperature, B-wind direction, C-wind speed). Appendices D-F give *temporal* results (D-temperature, E-wind direction, F-wind speed). Altogether, there are 432 graphs (four per page; 18 pages per appendix; six appendices). Although the charts are labeled as correlations, there are no true correlation statistics in the graphs.

5.2 Interpretation. The horizontal axis in the graphs depicting temporal results gives the change in time from -3 hours to +3 hours. The vertical axis gives the change in each variable of interest (temperature, wind direction, or wind speed). For the spatial correlations, the horizontal axis lists the change in distance from 0 to 250 km; the vertical axis is the same. There are four graphs on each page. The climatological region and time period are constant, but each graph depicts a different season. On each graph, five curves are plotted: from bottom to top, they are the 25th, 50th, 75th, 90th, and 95th percentiles of y-axis values.

5.2.1 Example in the Temporal Case. Refer to the first page in Appendix D, and to the upper left-hand plot (the temporal correlation of temperature for continental climates at winter/midnight). The estimates for the percentiles of the synoptic-scale change in temperature from 3 hours before midnight to midnight are: 25th percentile-- -0.5°C ; 50th percentile-- -1.0°C ; 75th percentile-- -2.0°C ; 90th percentile-- -2.9°C ; and 95th percentile-- -4.5°C . In other words, at continental winter midnight, considering synoptic-scale processes alone, there is only a 10% risk of encountering a 3-hour temperature change greater than 2.9°C and only a 5% risk of a change greater than 4.5°C . If that risk is unacceptably high, an observing interval more frequent than once every 3 hours is recommended.

5.2.2 Example in the Spatial Case. Consider Appendix A, which shows continental winter midnight temperature differences as a function of the distance between two observing stations. Within 50 km, considering synoptic-scale processes alone, there is about an 18% risk of encountering a temperature difference of 3°C , whereas at 75 km there is a 25% risk of a temperature difference that large, and at 100 km there is a 50-50 chance of encountering such a difference. If a system under design requires that a field of temperatures be observed and that 90% of the observations must be within an error of 3°C (not considering mesoscale features), then the observing network must be spaced no wider than about 37 km. At continental summer midnight, the same performance can be achieved with a network spacing of 175 km.

5.2.3 Additional Example. If at continental winter midnight it is necessary to estimate the temperature at a point where there is no weather station by using data from a point 200 km away, then the median error, considering synoptic-scale processes alone is 3°C , and 90% of such errors will be within 7°C . At continental summer midnight, the median error in using a station 200-km distant is well within instrument observing error, and 90% of such errors are within 3°C .

5.2.4 Plots with Little Variability. In some of the charts, the lines are very close together. This is particularly true for plots of the maritime climate, in which the differences between any of the percentiles are small. The top curve always represents estimates of the 95th percentile.

5.3 Final Point. Although this study was limited to the spatial and temporal correlation of only three surface weather variables, the technique can be applied to other variables, both surface and upper-air. It is especially suited for upper-air variables where mesoscale effects are less significant. Smith (1976) used this technique to interpolate wind observations vertically, suggesting that a study on the vertical correlation of other weather variables might also be possible.

BIBLIOGRAPHY

- Bertoni, E.A. and I.A. Lund, *Winter Space Correlation of Pressure, Temperature, and Density to 16 Km*, AFCRL-64-1020, Air Force Cambridge Research Laboratories, Hanscom AFB, MA, 1964.
- Boehm, A.R, *Transnormalized Regression Probabilities*, AWS-TR-75-229, Air Weather Service, Scott AFB, IL, 1976.
- Bradley, J.T., *Climate of the States: Florida*, Gale Research Company, Detroit, 1978.
- Buell, C.E., "Variability of Wind with Distance and Time on Isobaric Surfaces," *J. Appl. Meteorol.*, vol 11, pp.1085-1091, 1972.
- D'Agostino, R.B., A. Belanger, and R.B. D'Agostino, Jr., "A Suggestion for Using Powerful and Informative Tests of Normality," *The American Statistician*, vol 44, pp. 316-321, 1990.
- Smith, O.E., *Vector Wind and Vector Wind Shear Models 0 to 27 Km Altitude for Cape Kennedy, Florida, and Vandenberg AFB, California*, NASA TM X-73319, George C. Marshall Space Flight Center, Marshall Space Flight Center, AL, 1976.
- Tabor, P.A. and D.L. Motte, *Optimal Placement of Meteorological Surface Sensors for Reconstruction of Wind Fields with Emphasis on Data Denied and Avoidance Areas*, paper presented at the Ninth Annual EOSAEL/TWI Conference, Las Cruces, NM, 1988.
- Thiebaux H.J., and M.A. Peddler, *Spatial Objective Analysis with Applications in Atmospheric Science*, Academic Press, San Diego, 1987.

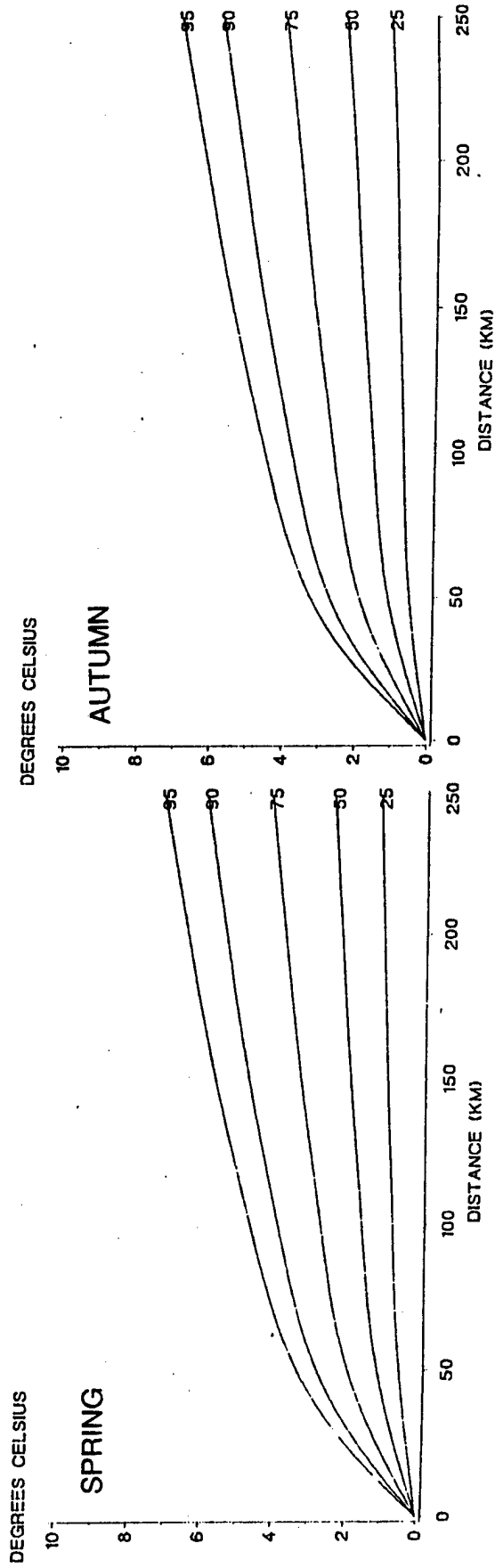
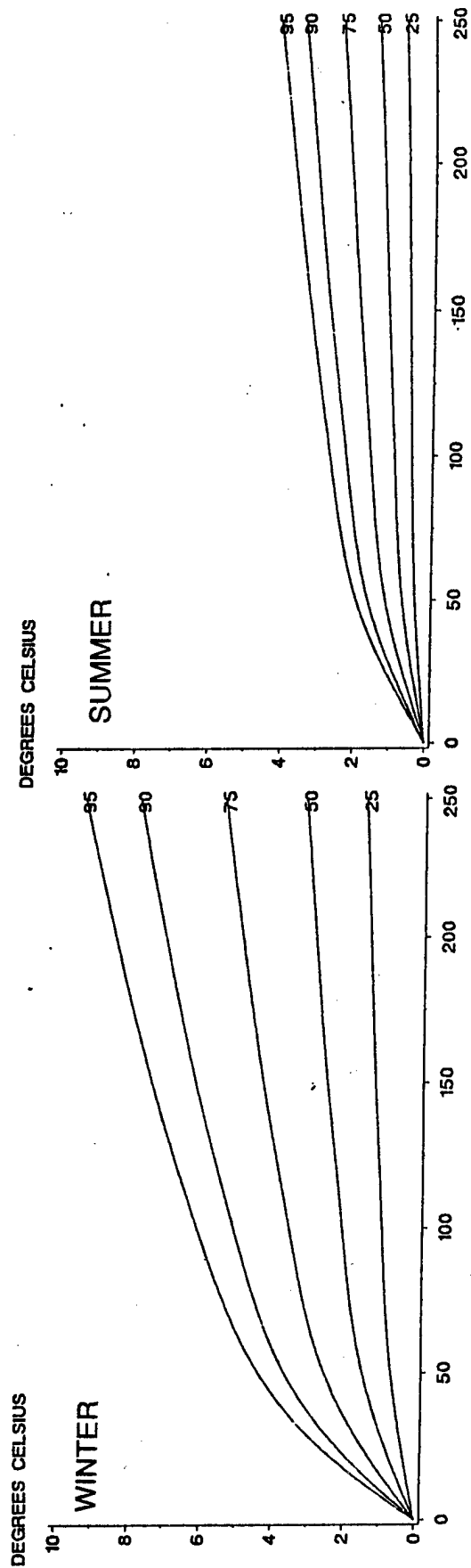
GLOSSARY

CDF	cumulative distribution function
END	equivalent normal deviate
km	kilometer
NM	nautical mile
PD	probability distribution function
Thsh	Threshold
USAFETAC	United States Air Force Environmental Technical Applications Center
WINDS	Weather Information Network Display System

APPENDIX A

SPATIAL CORRELATION OF TEMPERATURE

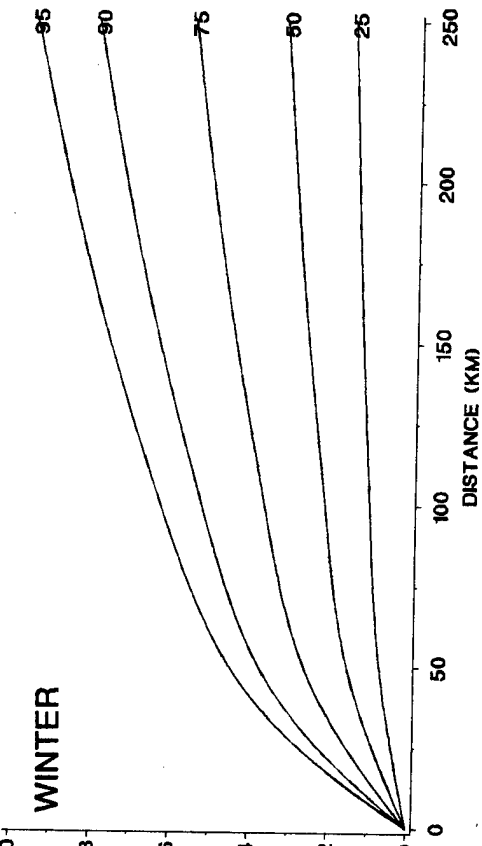
- A-1 Spatial correlation of temperature, continental climate, midnight.
- A-2 Spatial correlation of temperature, continental climate, sunrise.
- A-3 Spatial correlation of temperature, continental climate, noon.
- A-4 Spatial correlation of temperature, arctic climate, midnight.
- A-5 Spatial correlation of temperature, arctic climate, sunrise.
- A-6 Spatial correlation of temperature, arctic climate, noon.
- A-7 Spatial correlation of temperature, desert climate, midnight.
- A-8 Spatial correlation of temperature, desert climate, sunrise.
- A-9 Spatial correlation of temperature, desert climate, noon.
- A-10 Spatial correlation of temperature, maritime climate, midnight.
- A-11 Spatial correlation of temperature, maritime climate, sunrise.
- A-12 Spatial correlation of temperature, maritime climate, noon.
- A-13 Spatial correlation of temperature, tropical climate, midnight.
- A-14 Spatial correlation of temperature, tropical climate, sunrise.
- A-15 Spatial correlation of temperature, tropical climate, noon.
- A-16 Spatial correlation of temperature, coastal climate, midnight.
- A-17 Spatial correlation of temperature, coastal climate, sunrise.
- A-18 Spatial correlation of temperature, coastal climate, noon.



A-1 Spatial correlation of temperature, continental climate, midnight.

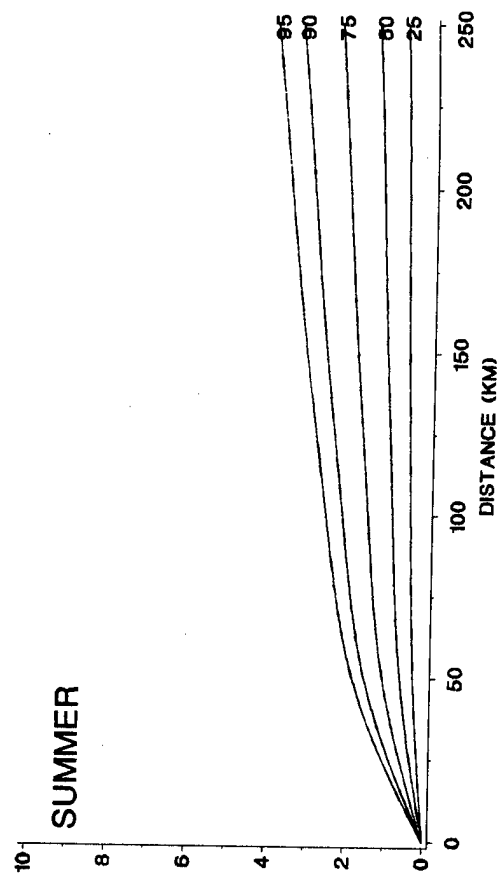
DEGREES CELSIUS

WINTER



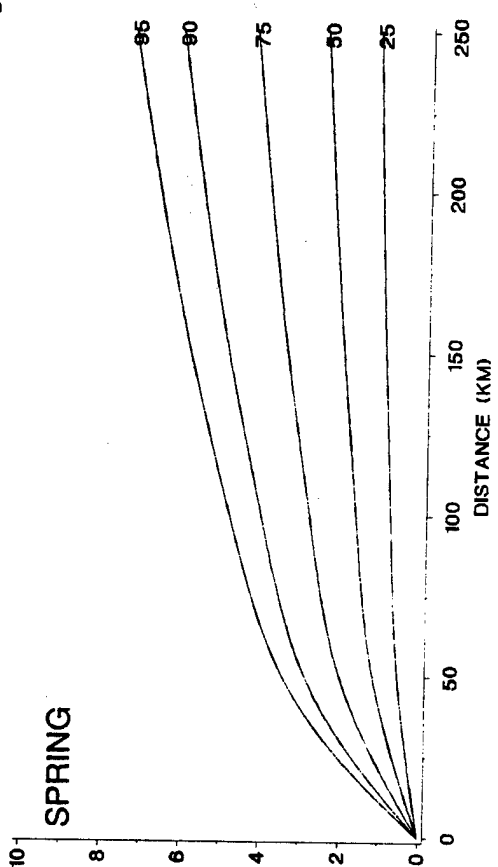
DEGREES CELSIUS

SUMMER



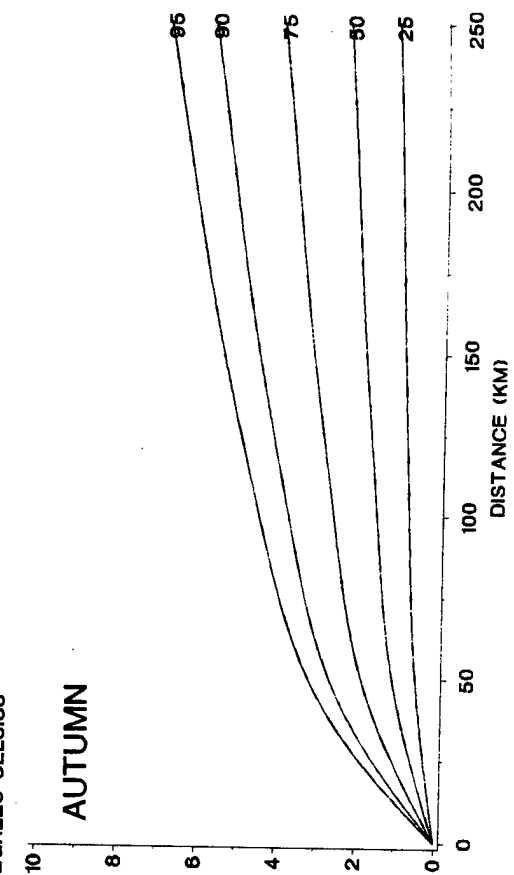
DEGREES CELSIUS

SPRING

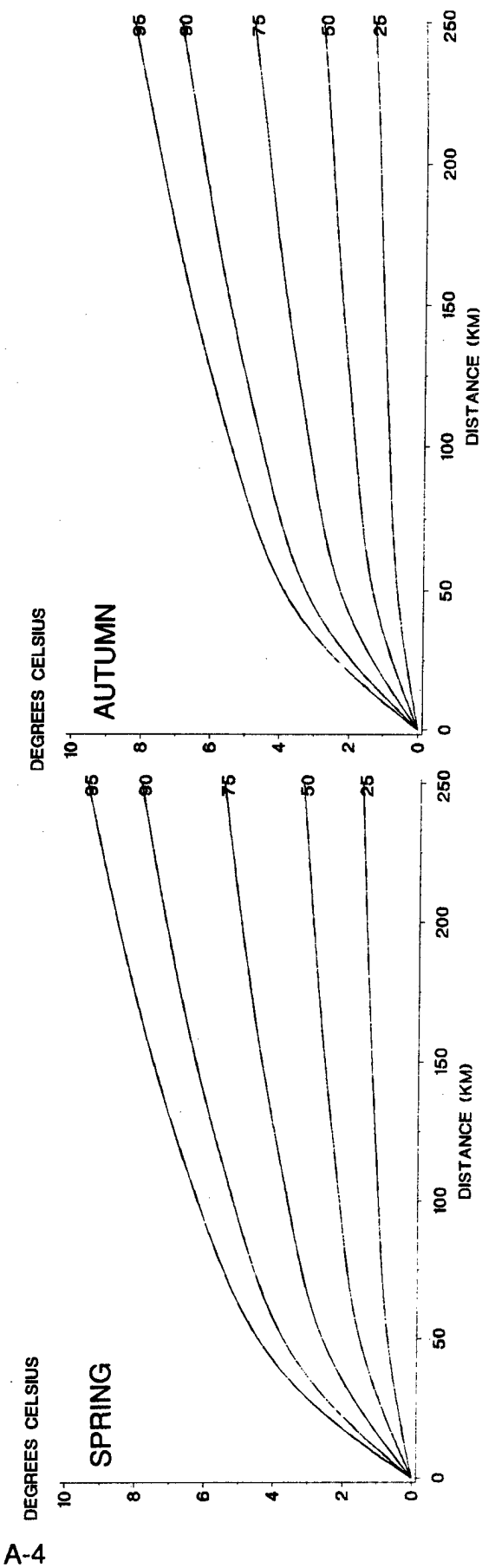
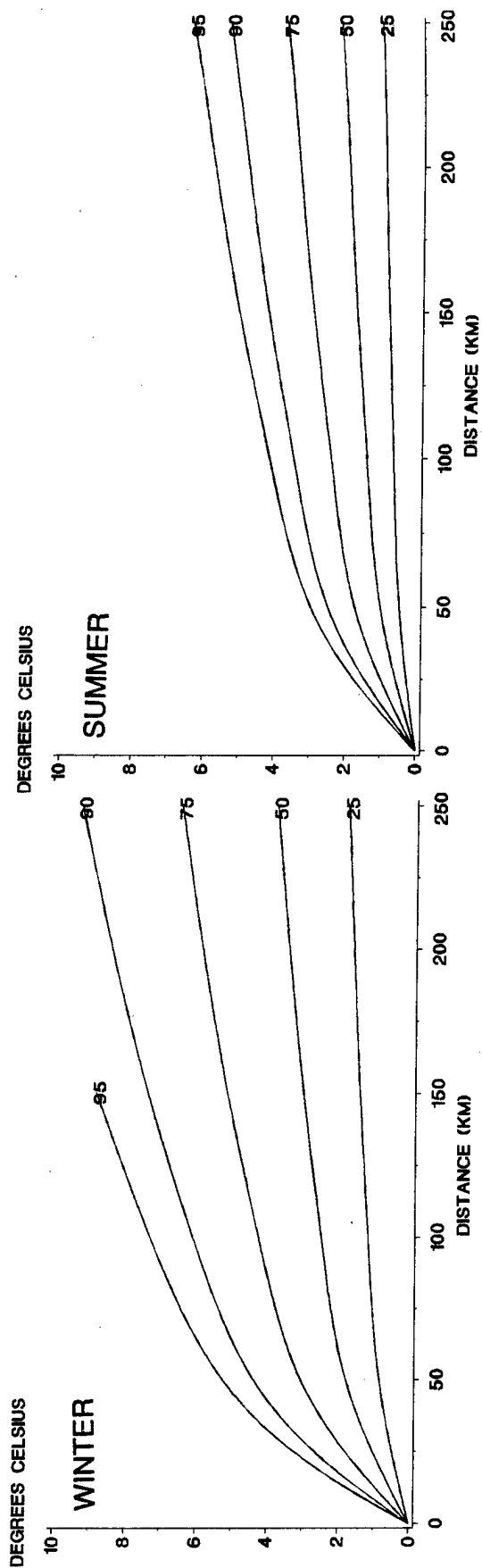


DEGREES CELSIUS

AUTUMN



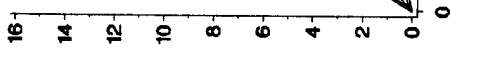
A-2 Spatial correlation of temperature, continental climate, sunrise.



A-3 Spatial correlation of temperature, continental climate, noon.

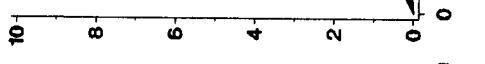
DEGREES CELSIUS

WINTER



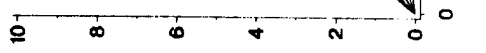
DEGREES CELSIUS

SUMMER



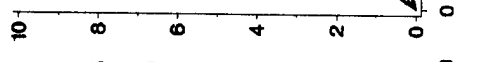
DEGREES CELSIUS

SPRING

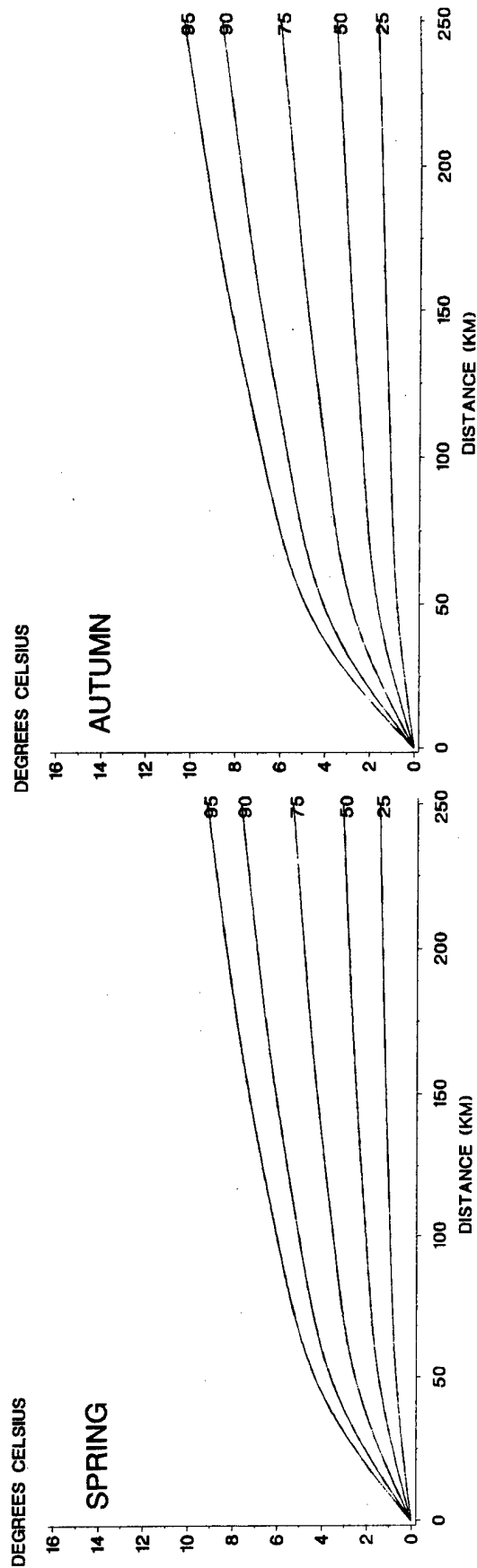
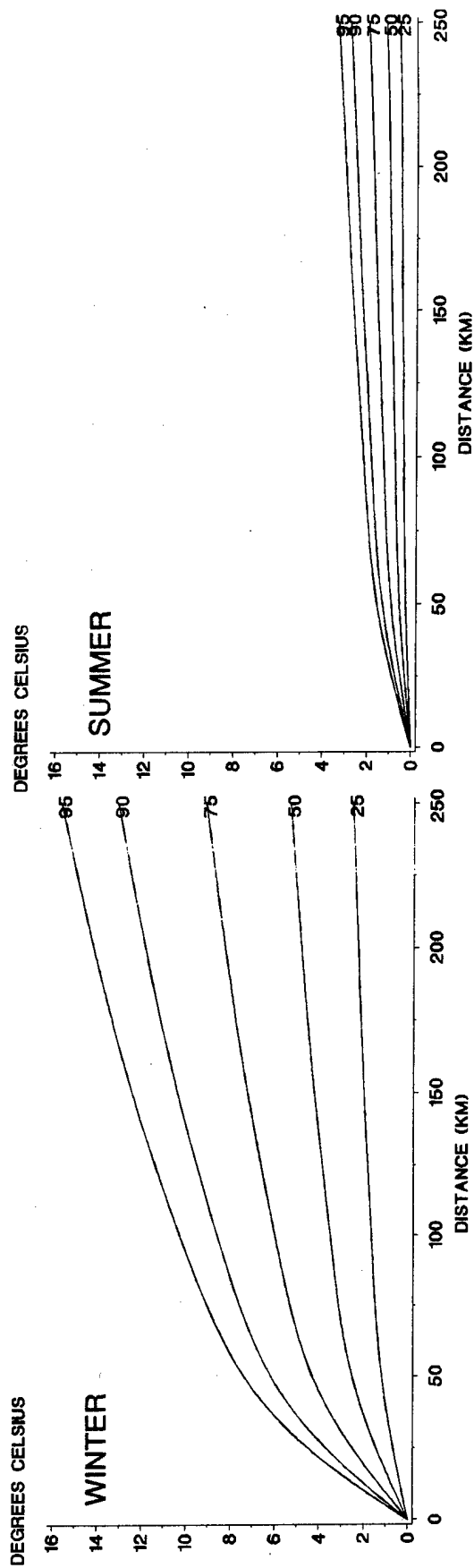


DEGREES CELSIUS

AUTUMN



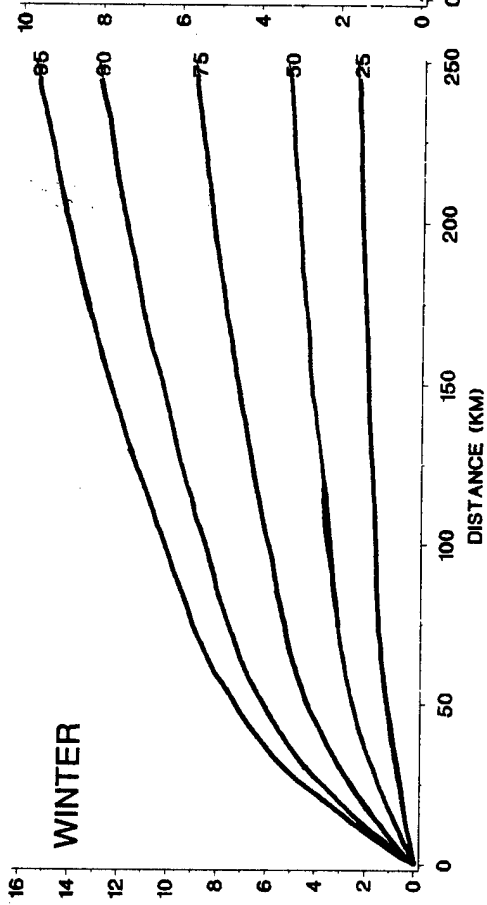
A-4 Spatial correlation of temperature, arctic climate, midnight.



A-5 Spatial correlation of temperature, arctic climate, sunrise.

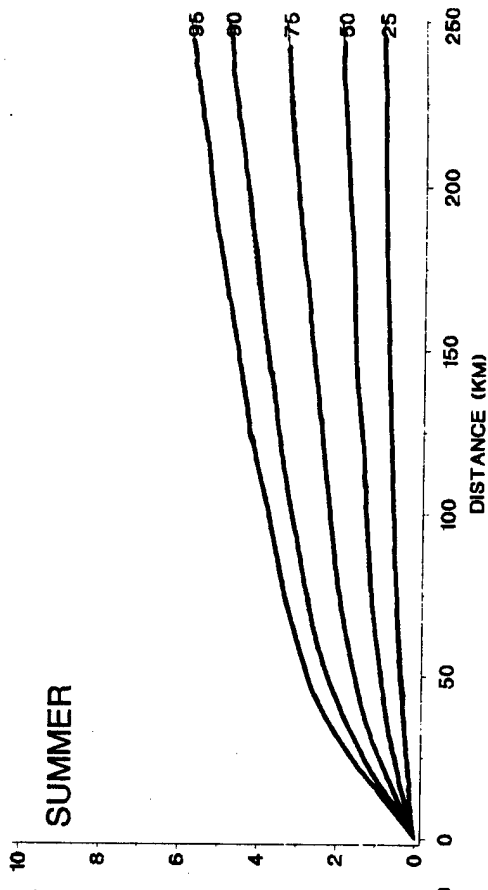
DEGREES CELSIUS

WINTER



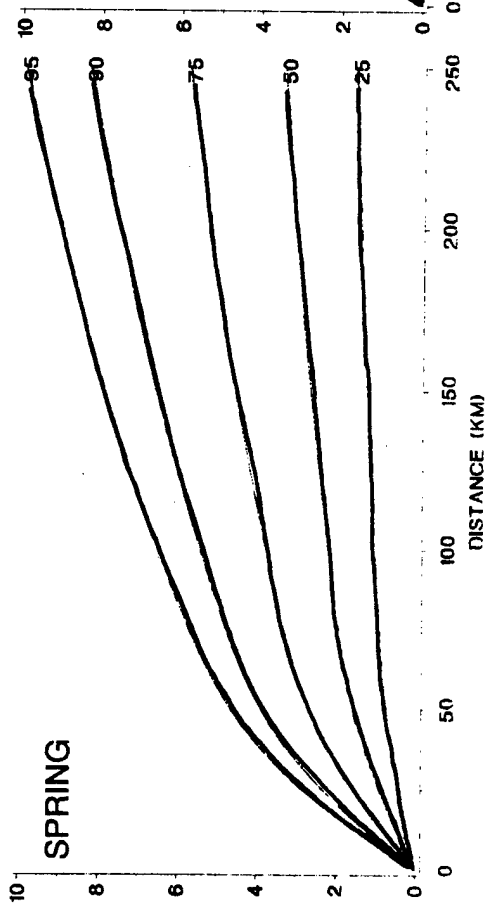
DEGREES CELSIUS

SUMMER



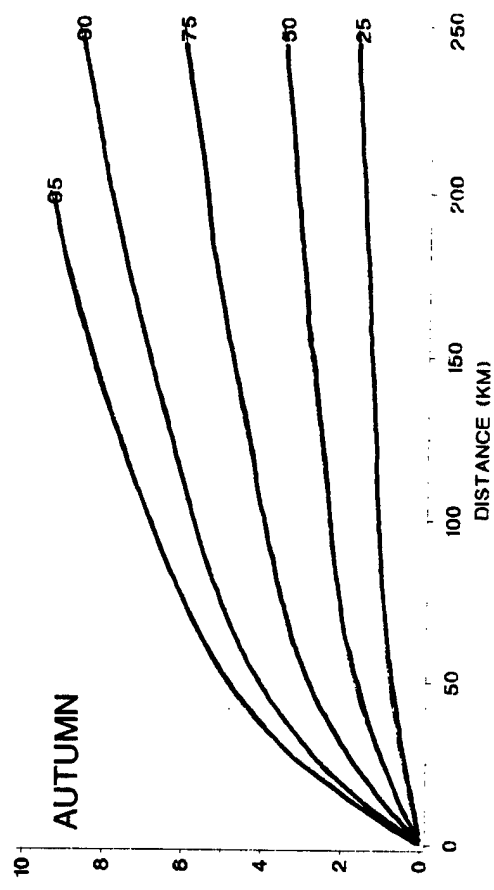
DEGREES CELSIUS

SPRING



DEGREES CELSIUS

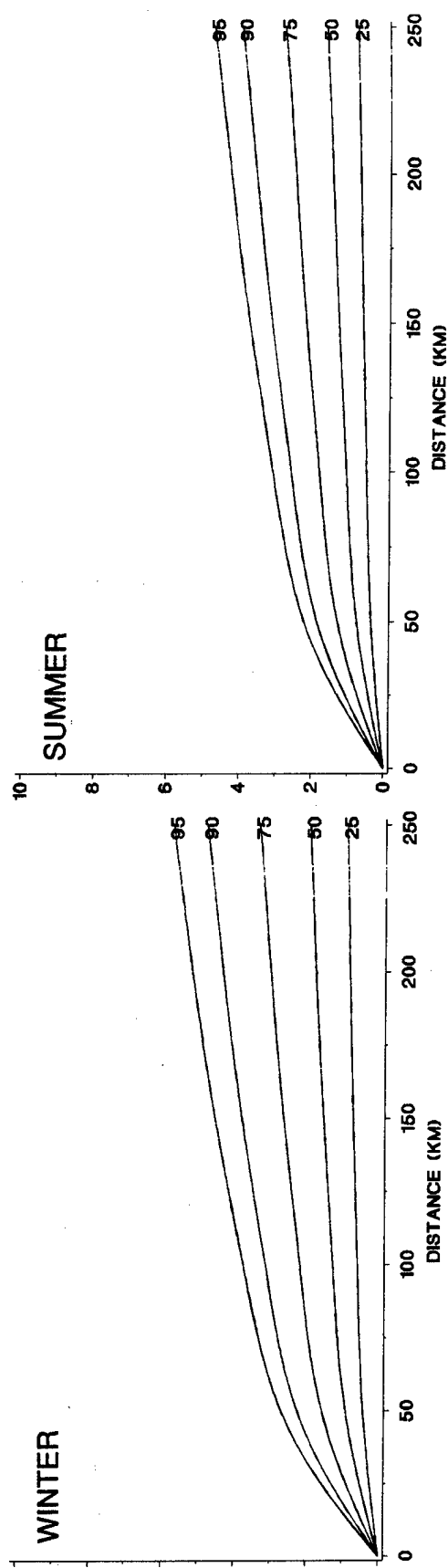
AUTUMN



A-6 Spatial correlation of temperature, arctic climate, noon.

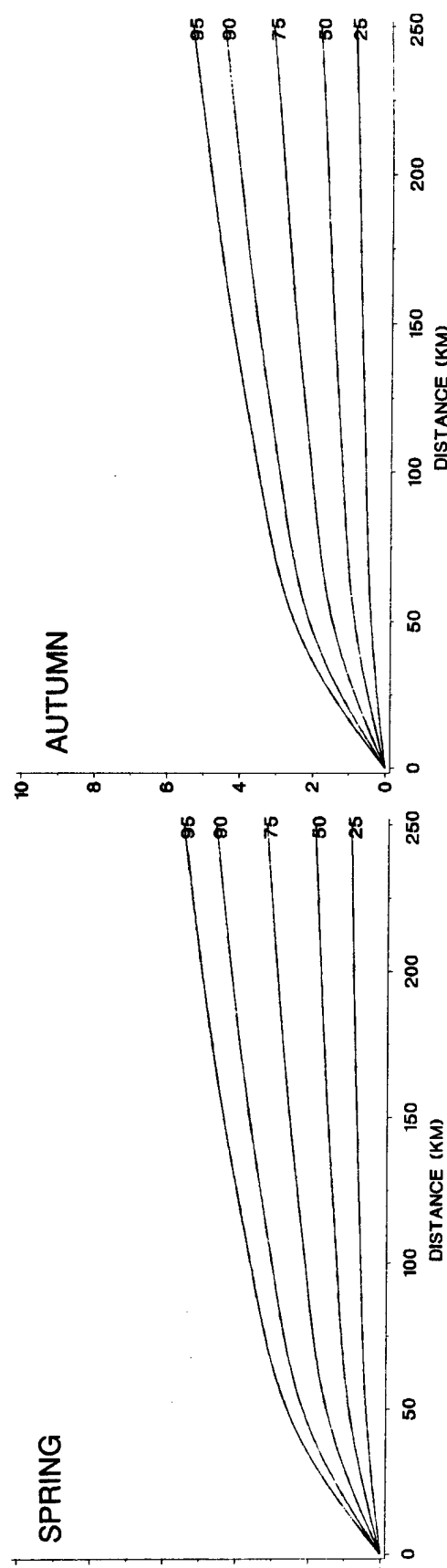
DEGREES CELSIUS

WINTER



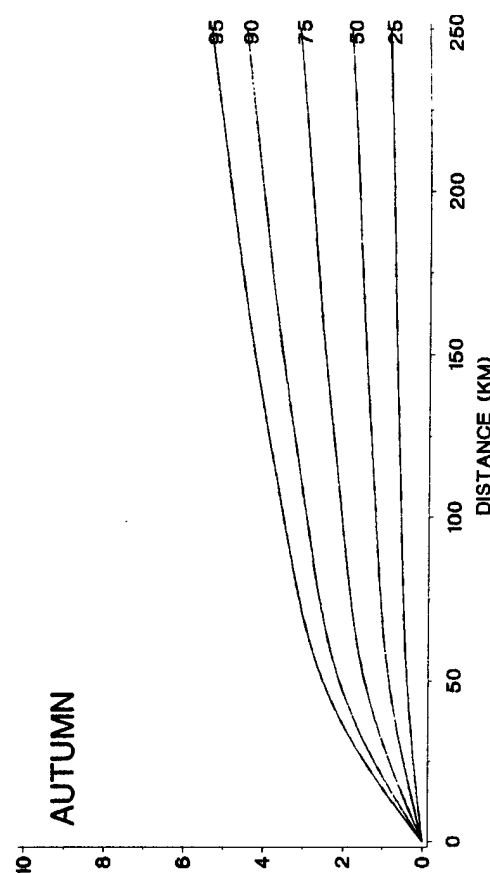
DEGREES CELSIUS

SPRING



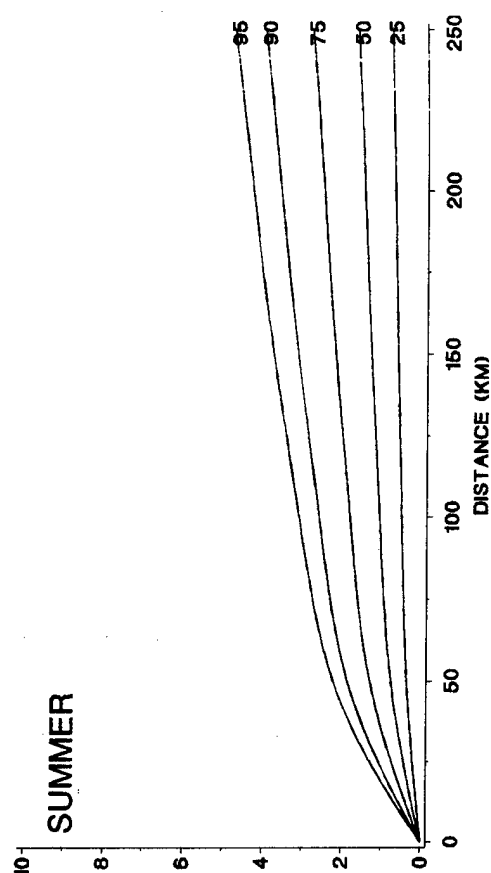
DEGREES CELSIUS

AUTUMN



DEGREES CELSIUS

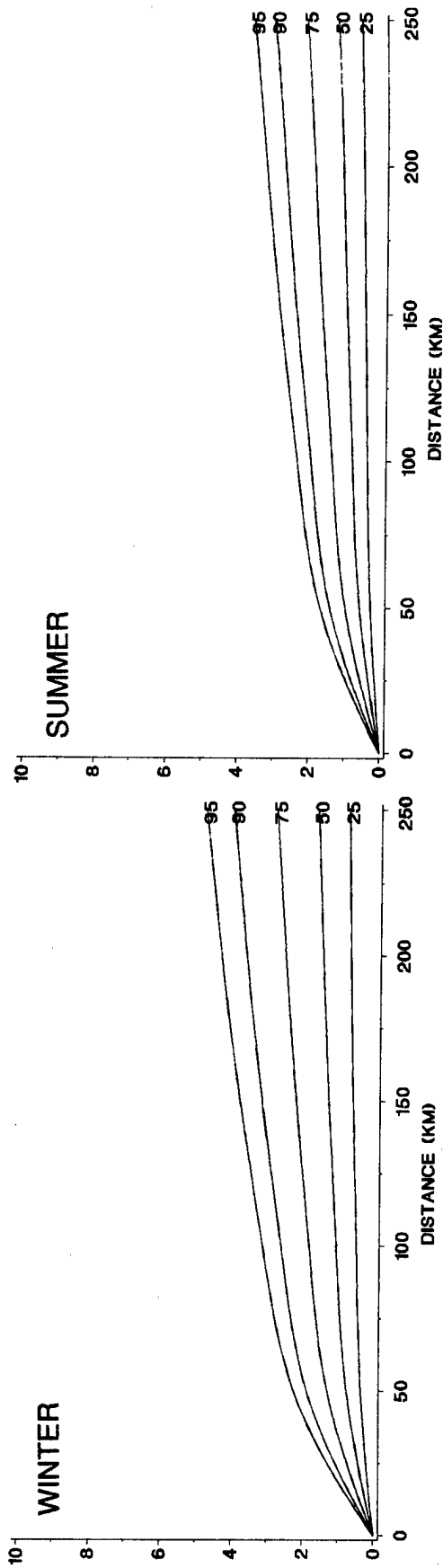
SUMMER



A-7 Spatial correlation of temperature, desert climate, midnight.

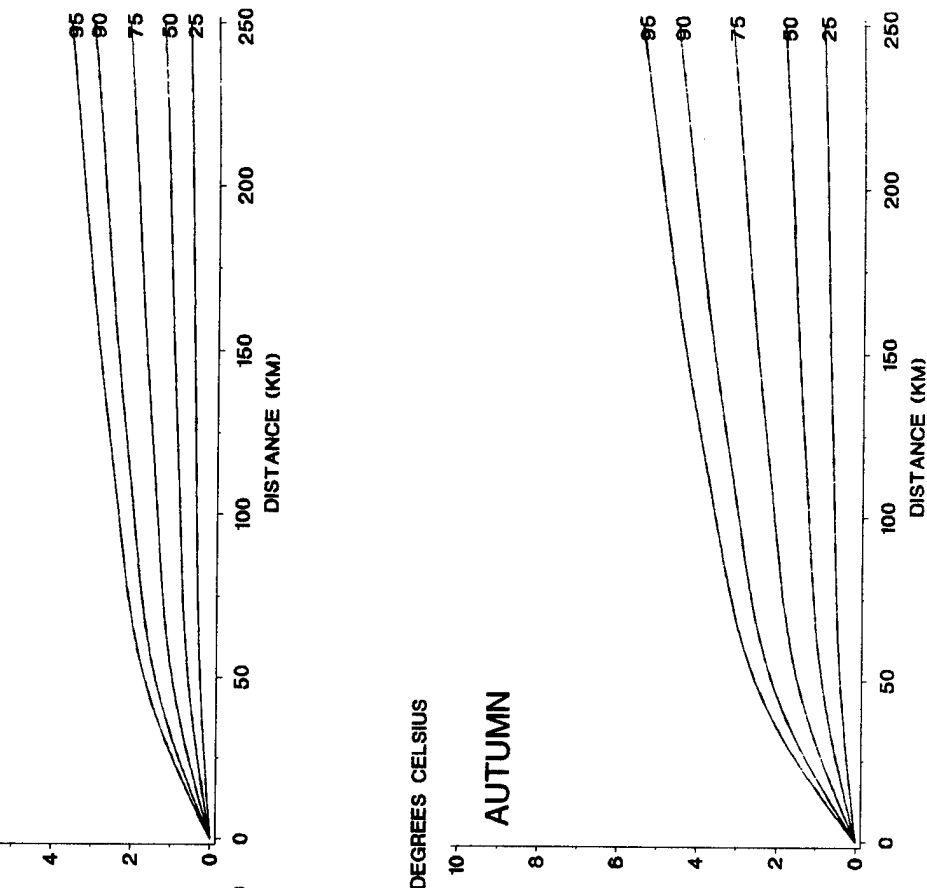
DEGREES CELSIUS

WINTER



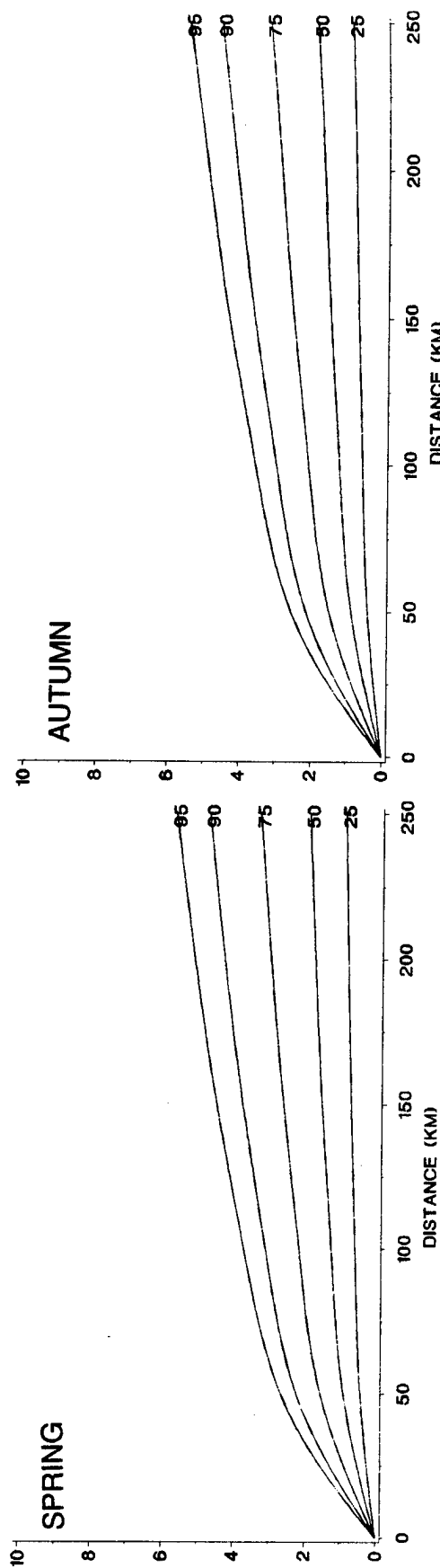
DEGREES CELSIUS

SUMMER



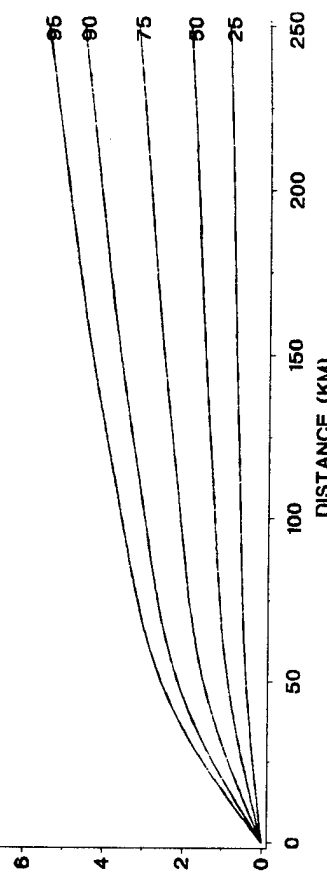
DEGREES CELSIUS

SPRING

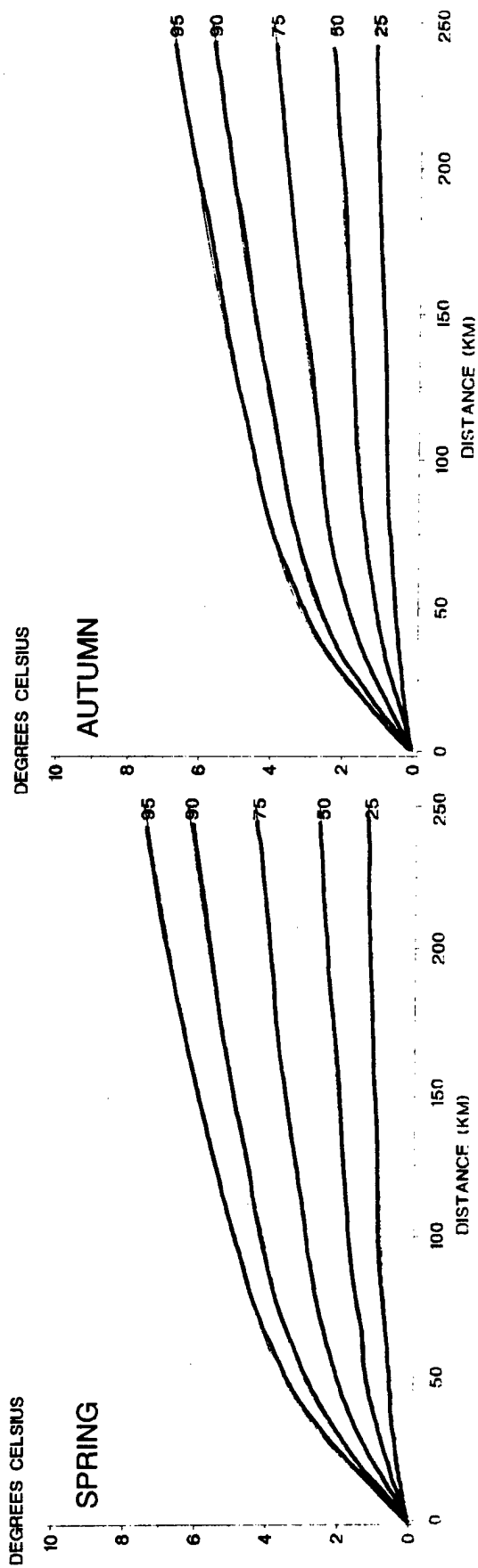
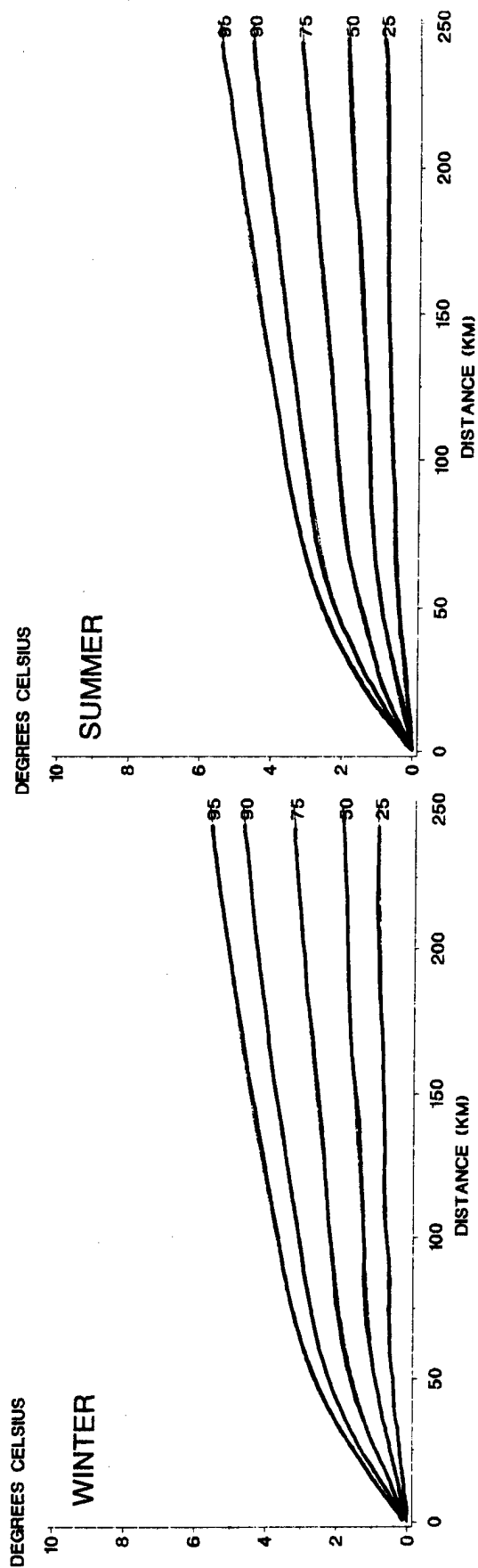


DEGREES CELSIUS

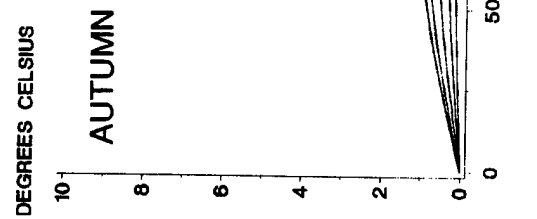
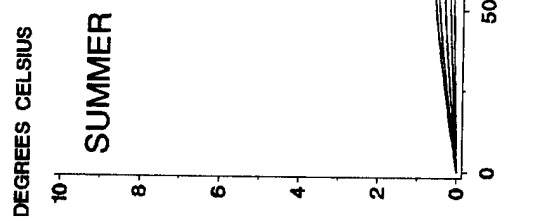
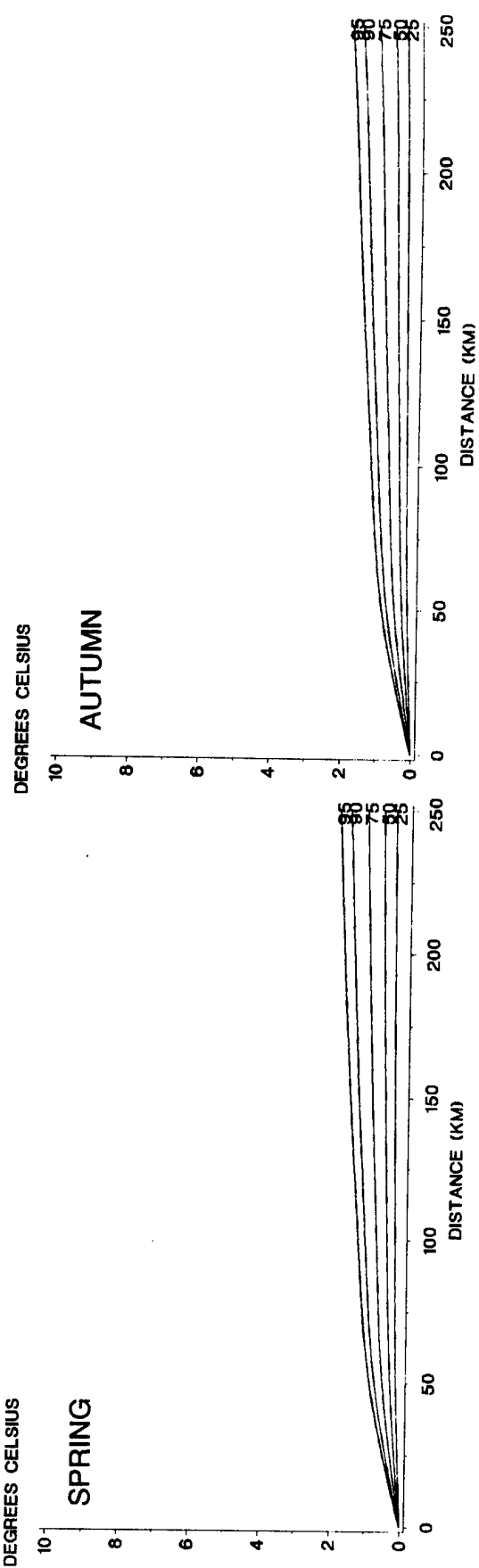
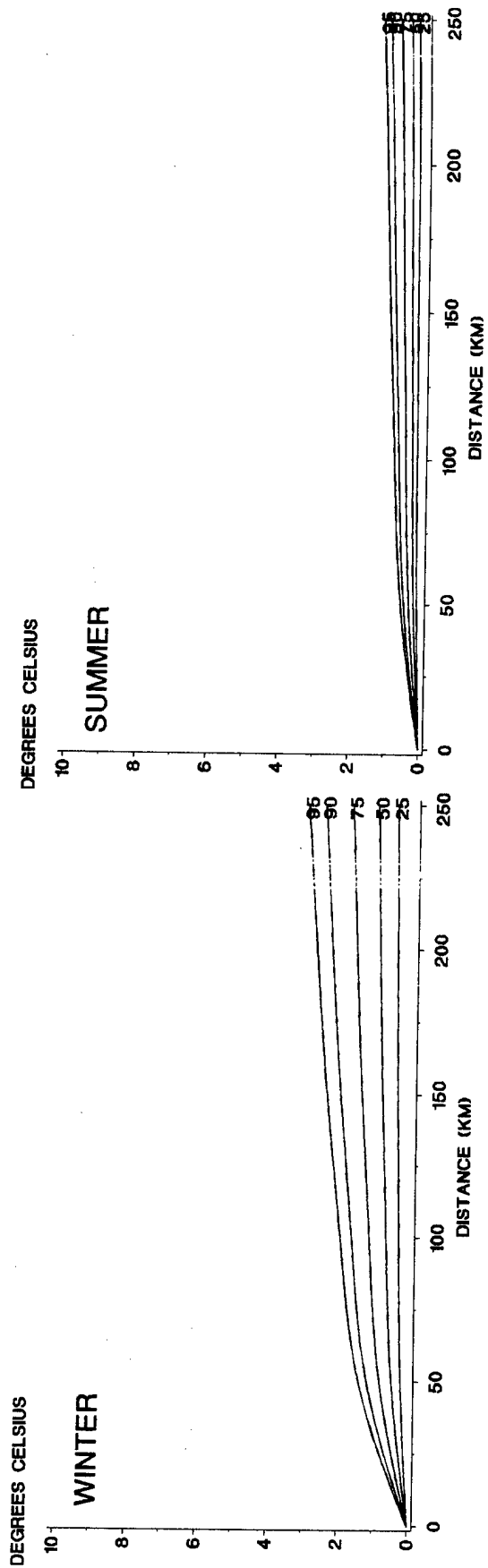
AUTUMN



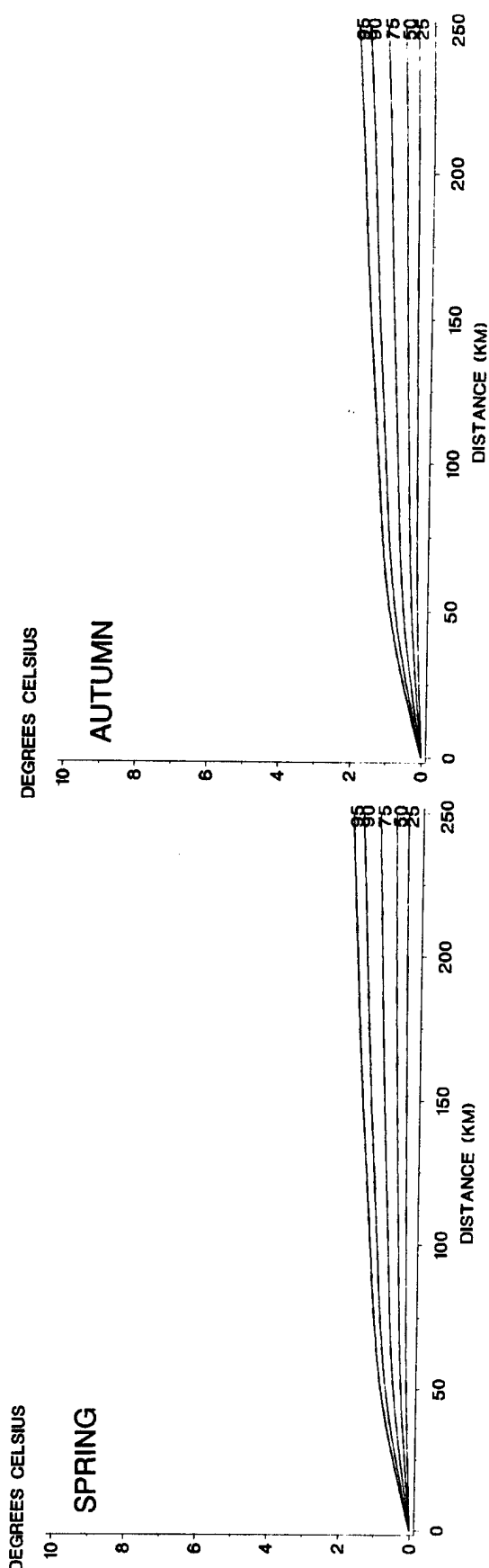
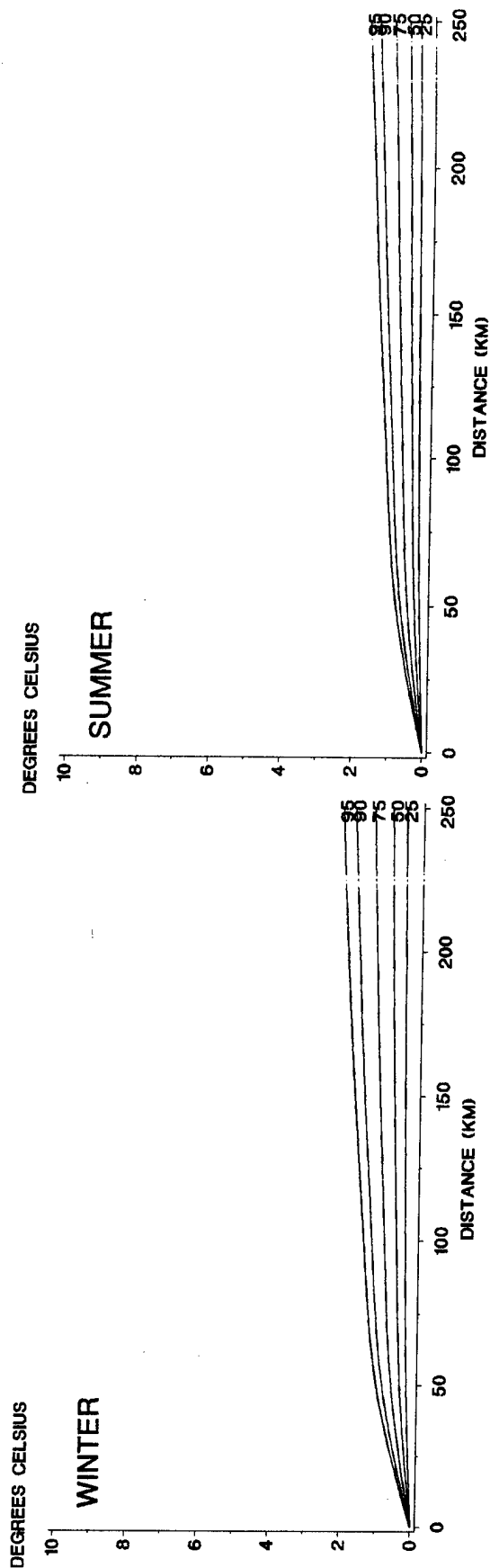
A-8 Spatial correlation of temperature, desert climate, sunrise.



A-9 Spatial correlation of temperature, desert climate, noon.



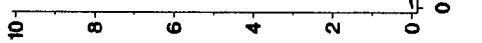
A-10 Spatial correlation of temperature, maritime climate, midnight.



A-11 Spatial correlation of temperature, maritime climate, sunrise.

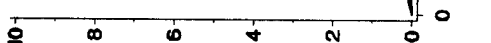
DEGREES CELSIUS

WINTER



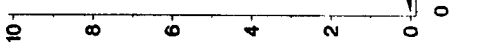
DEGREES CELSIUS

SUMMER



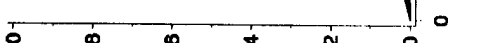
DEGREES CELSIUS

SPRING

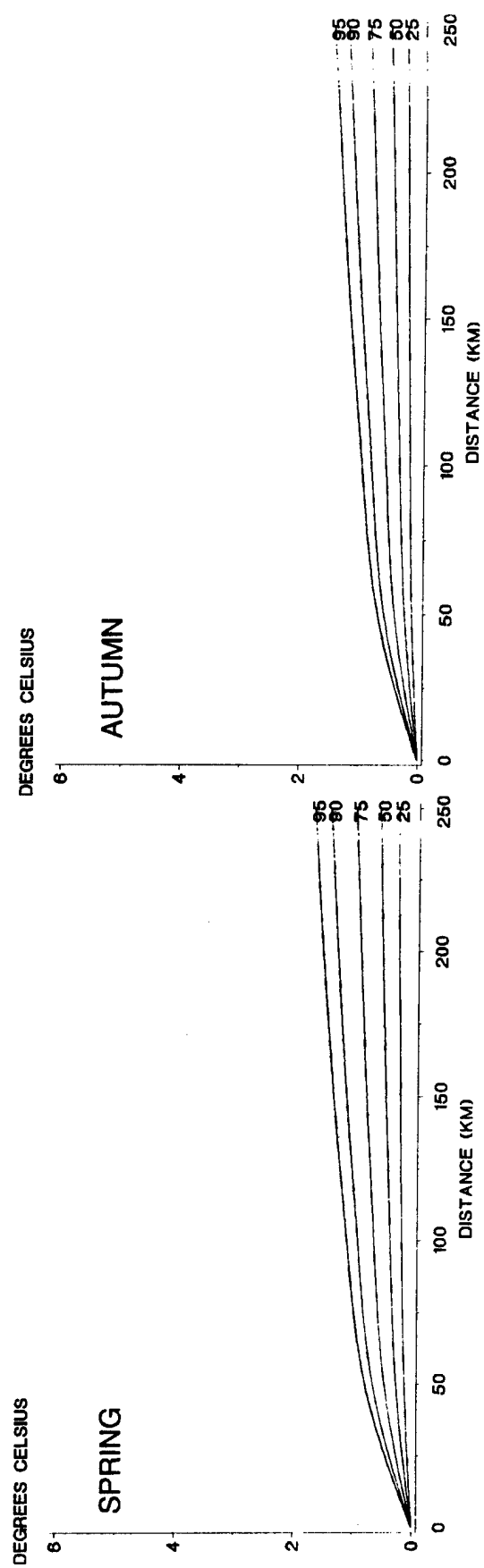
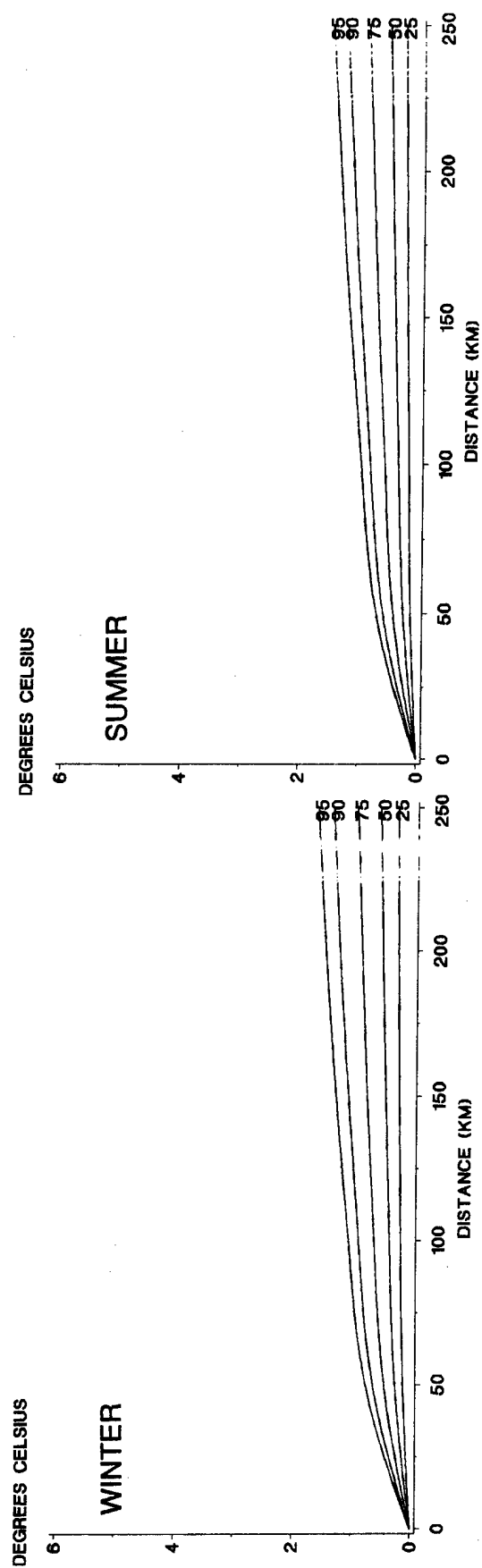


DEGREES CELSIUS

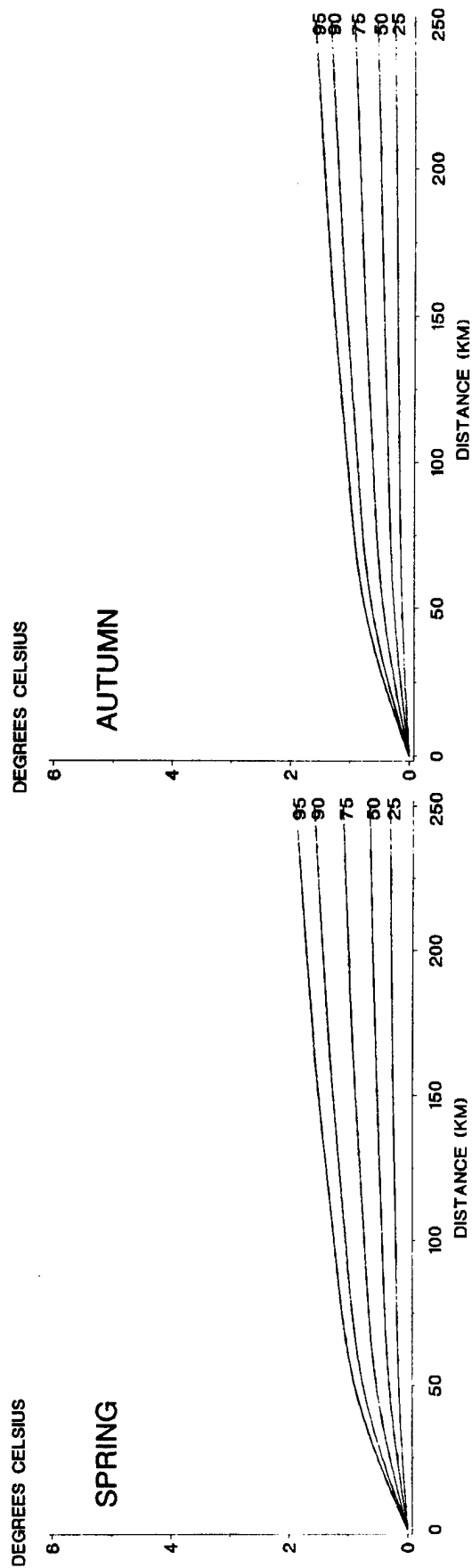
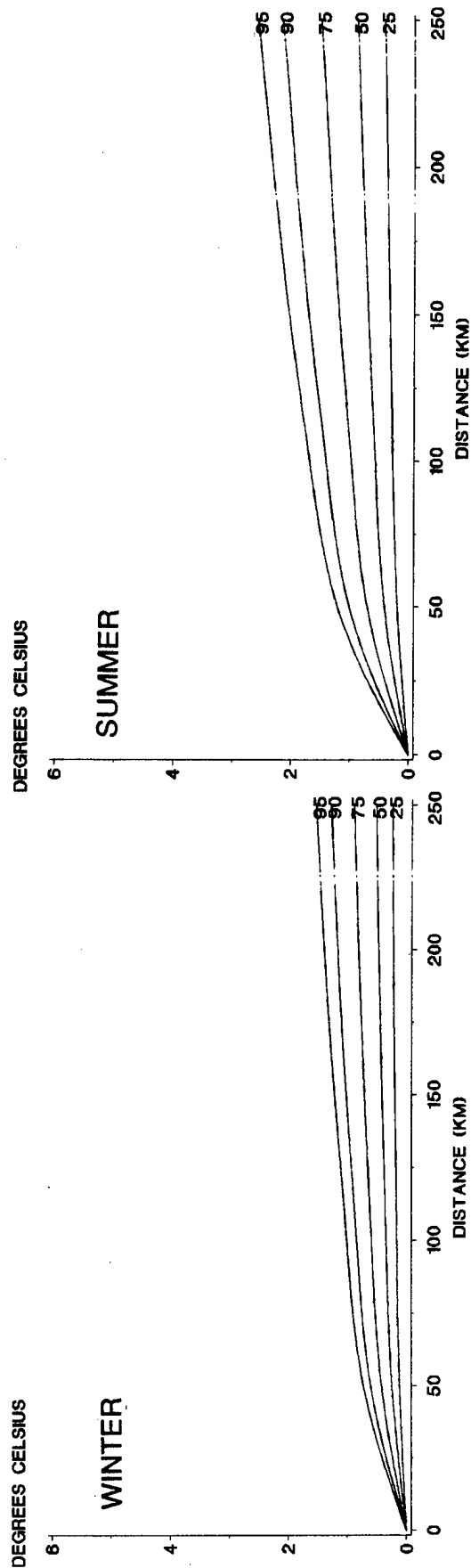
AUTUMN



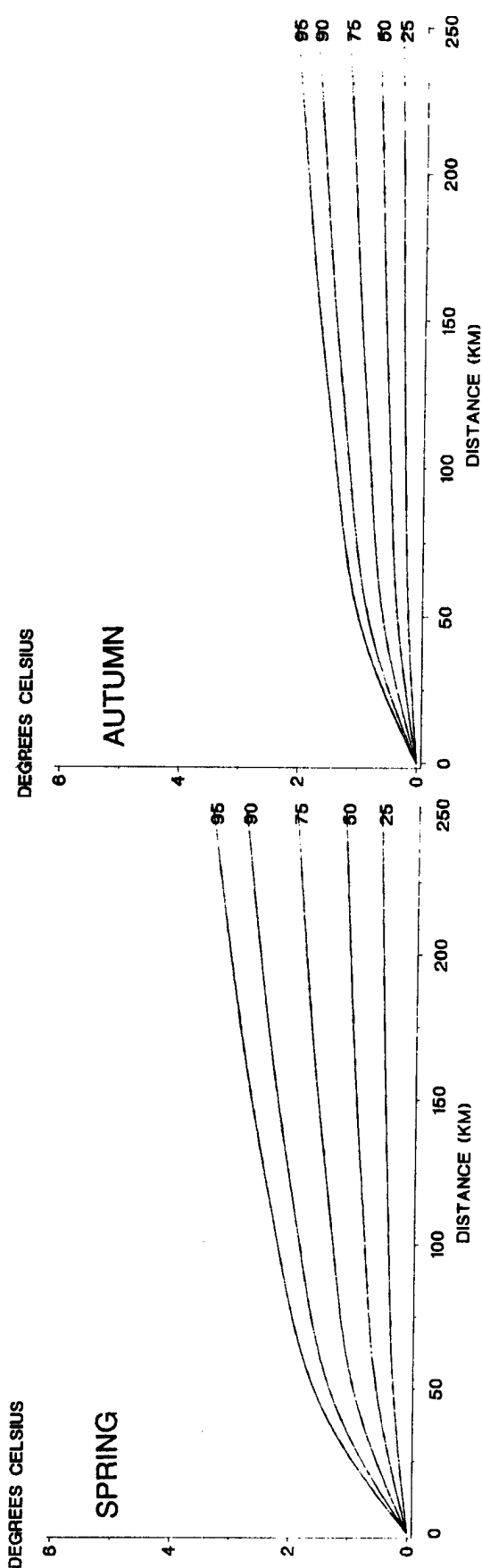
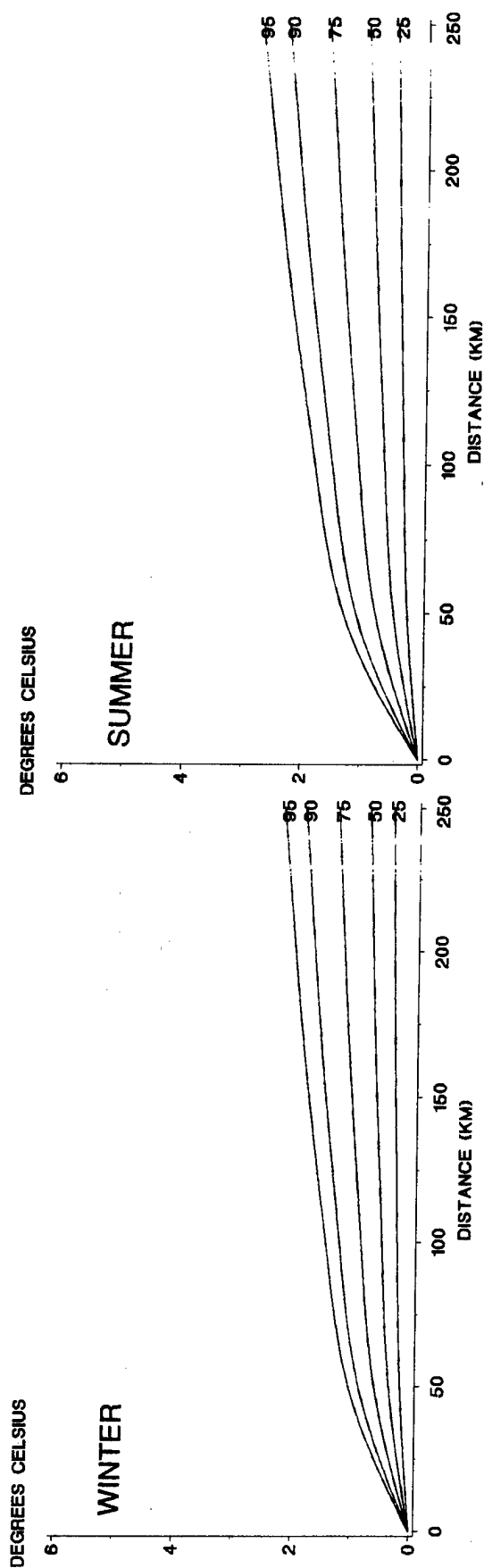
A-12 Spatial correlation of temperature, maritime climate, noon.



A-13 Spatial correlation of temperature, tropical climate, midnight.



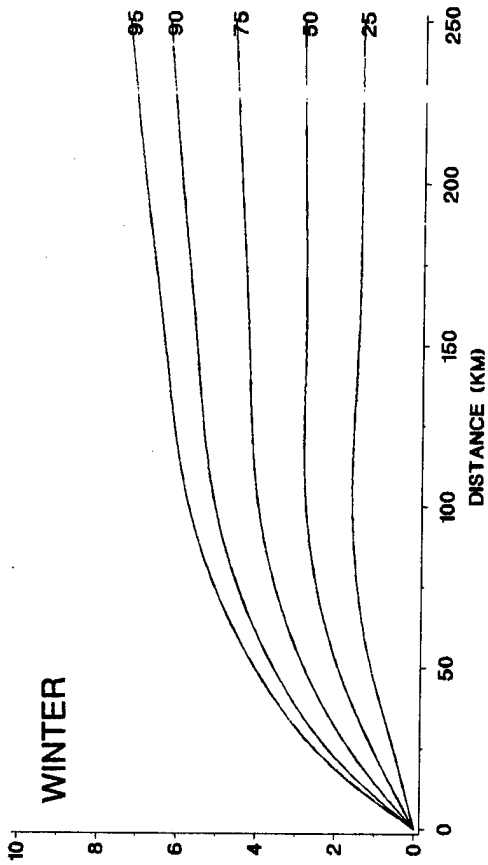
A-14 Spatial correlation of temperature, tropical climate, sunrise.



A-15 Spatial correlation of temperature, tropical climate, noon.

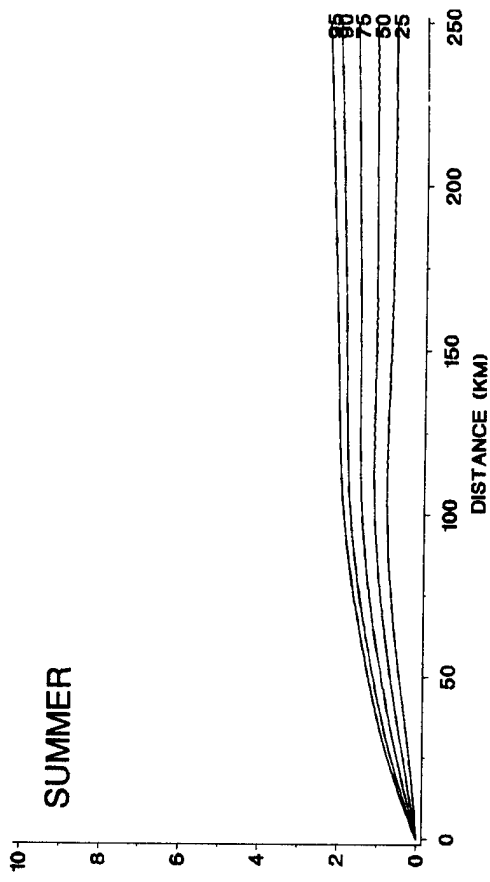
DEGREES CELSIUS

WINTER



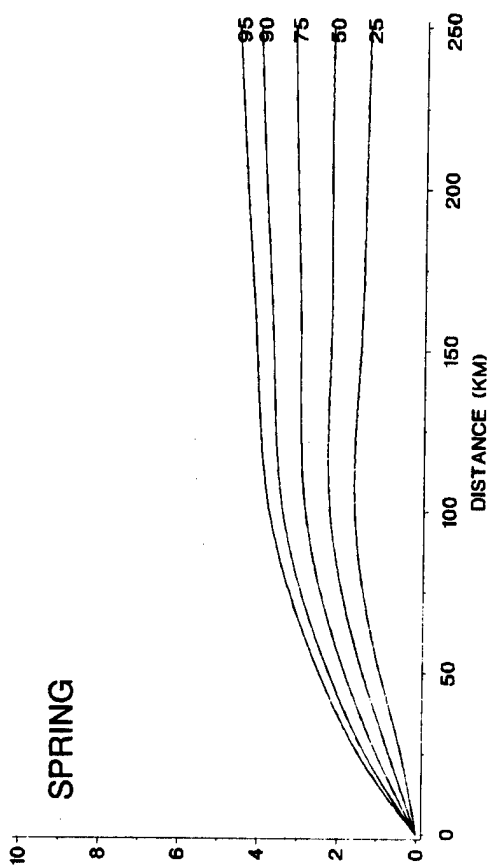
DEGREES CELSIUS

SUMMER



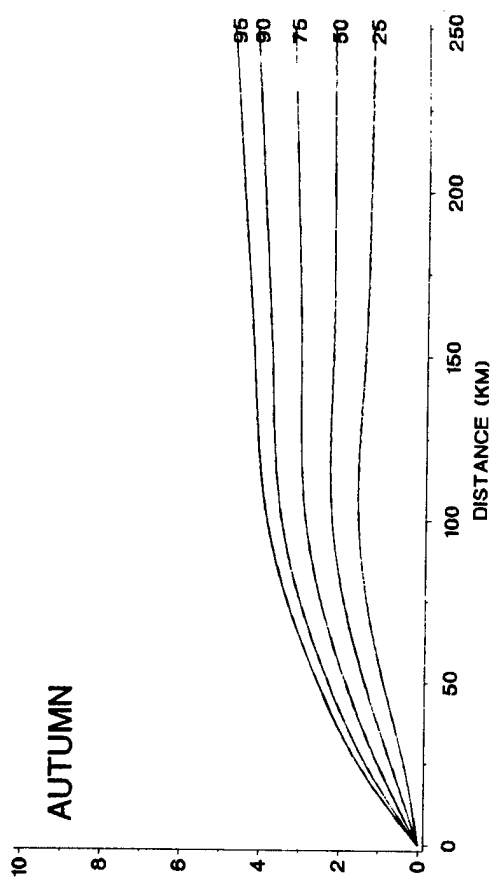
DEGREES CELSIUS

SPRING



DEGREES CELSIUS

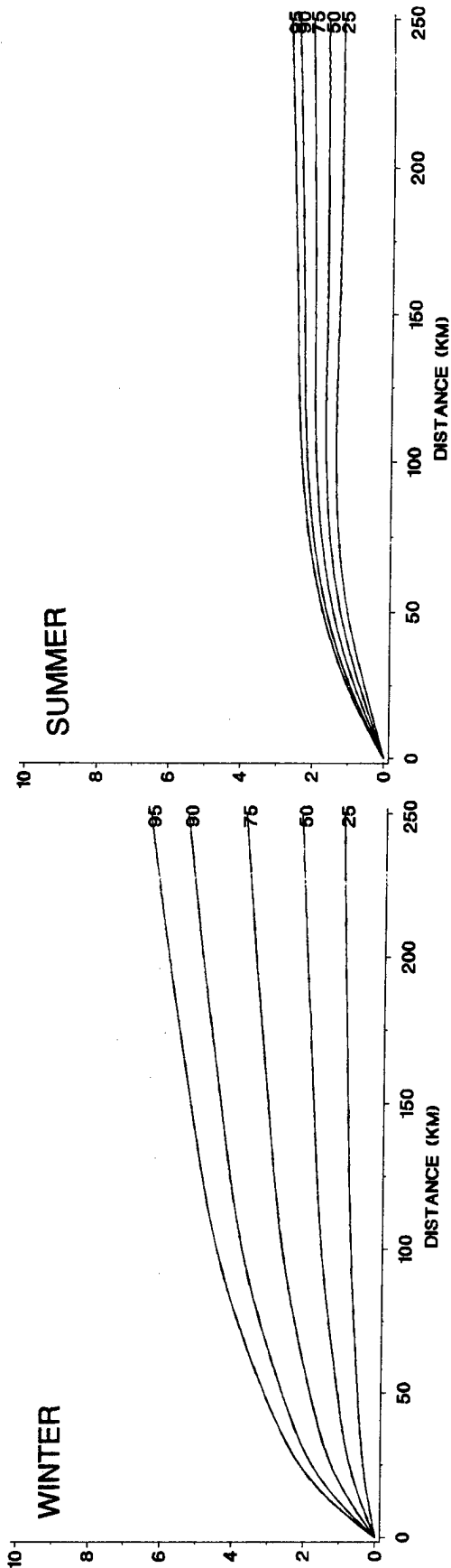
AUTUMN



A-16 Spatial correlation of temperature, coastal climate, midnight.

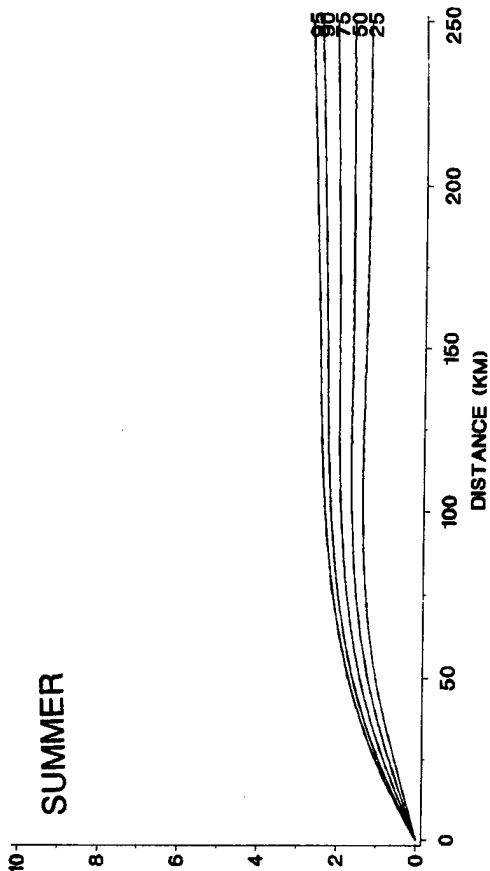
DEGREES CELSIUS

WINTER



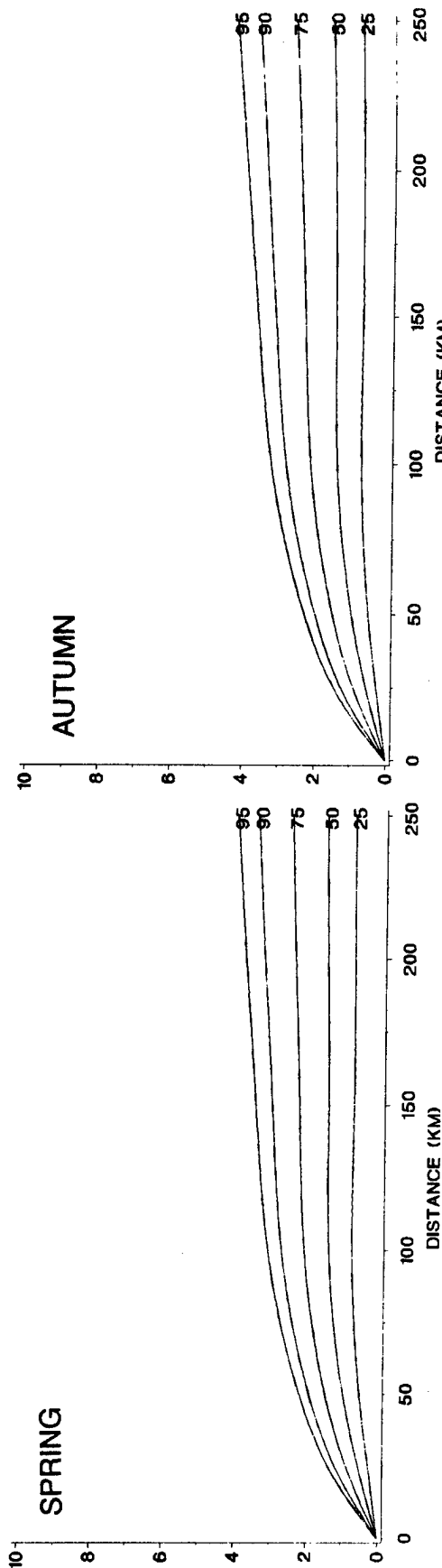
DEGREES CELSIUS

SUMMER



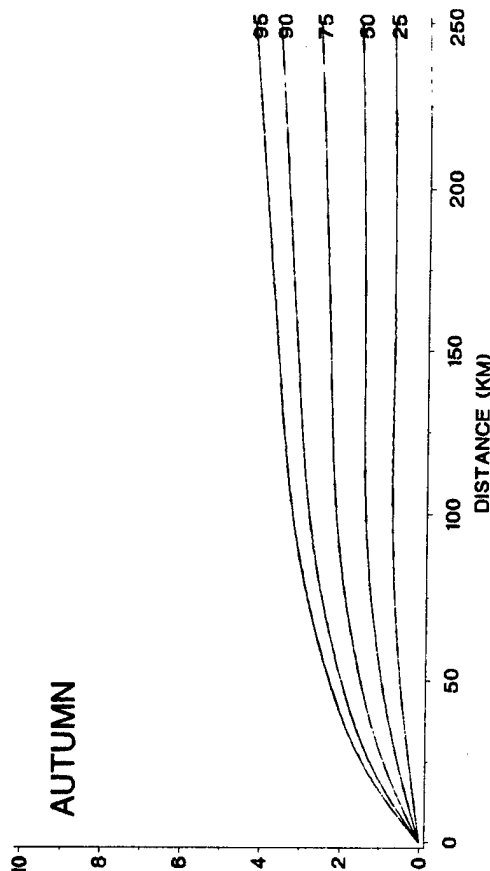
DEGREES CELSIUS

SPRING



DEGREES CELSIUS

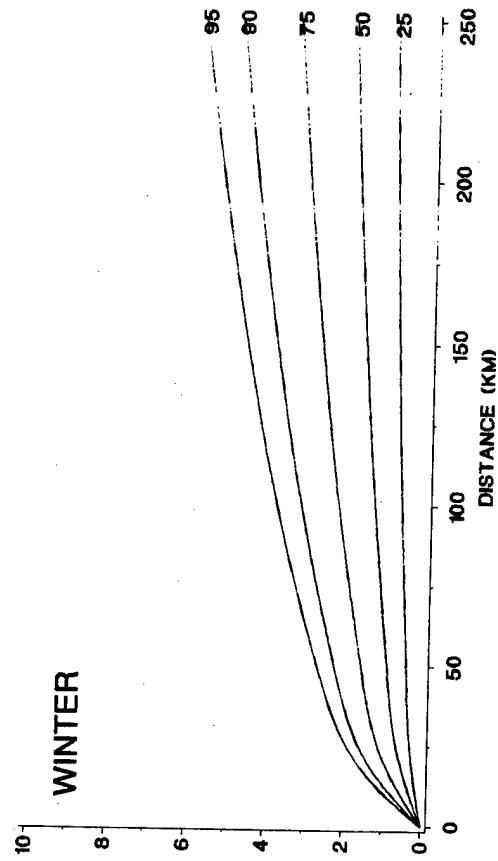
AUTUMN



A-17 Spatial correlation of temperature, coastal climate, sunrise.

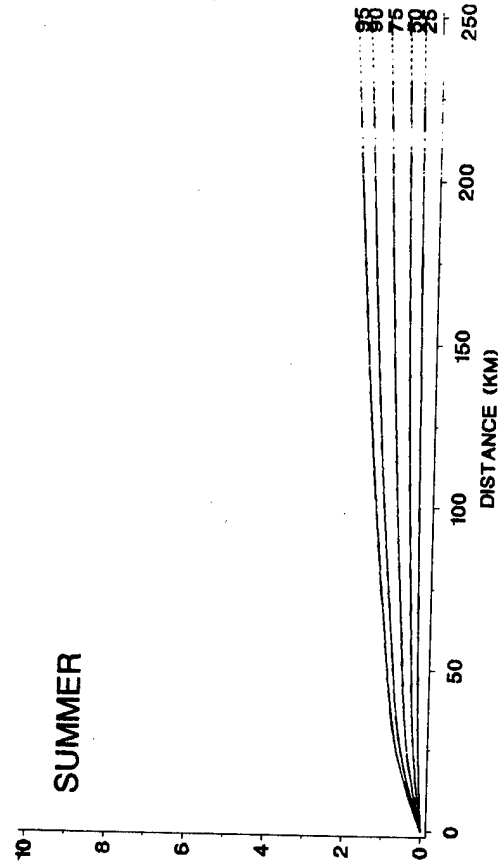
DEGREES CELSIUS

WINTER



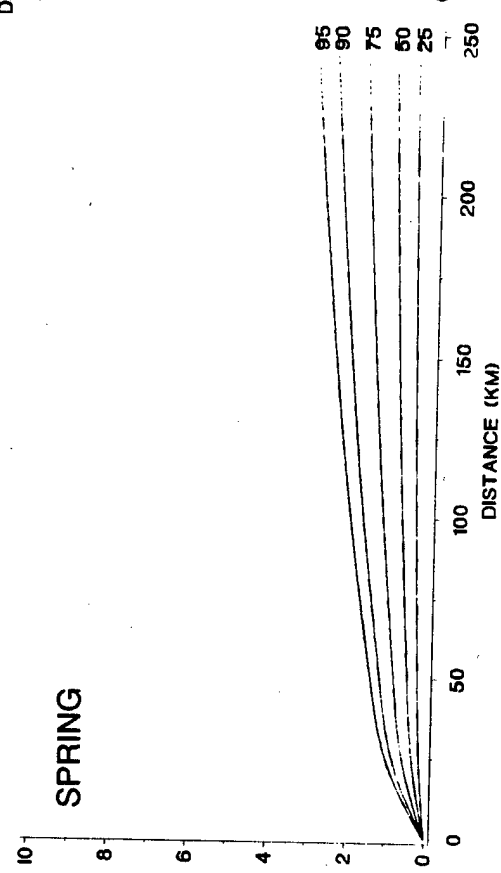
DEGREES CELSIUS

SUMMER



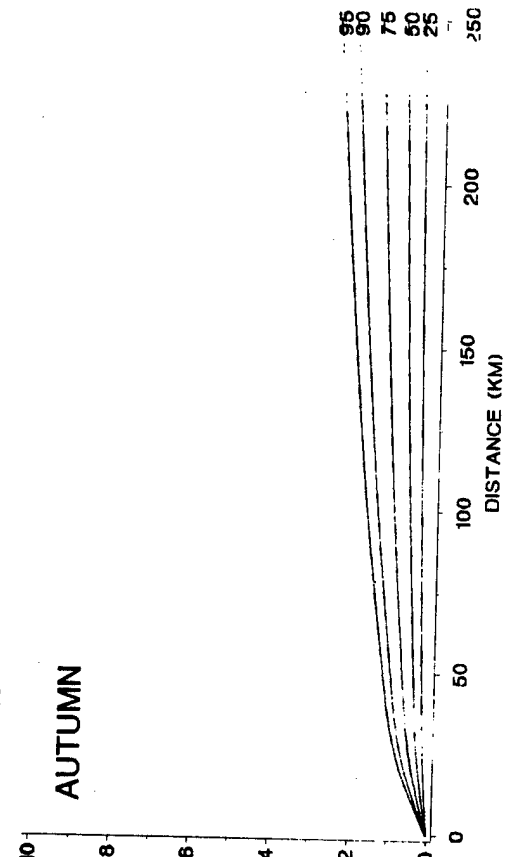
DEGREES CELSIUS

SPRING



DEGREES CELSIUS

AUTUMN

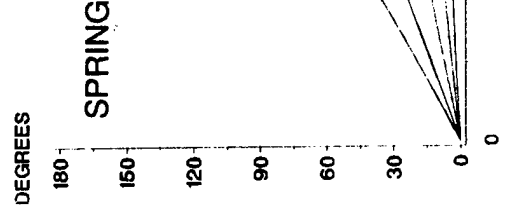
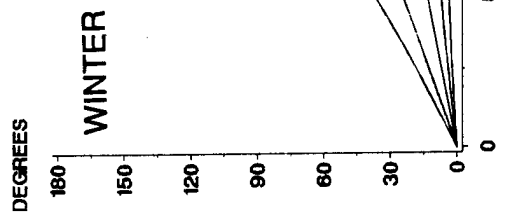
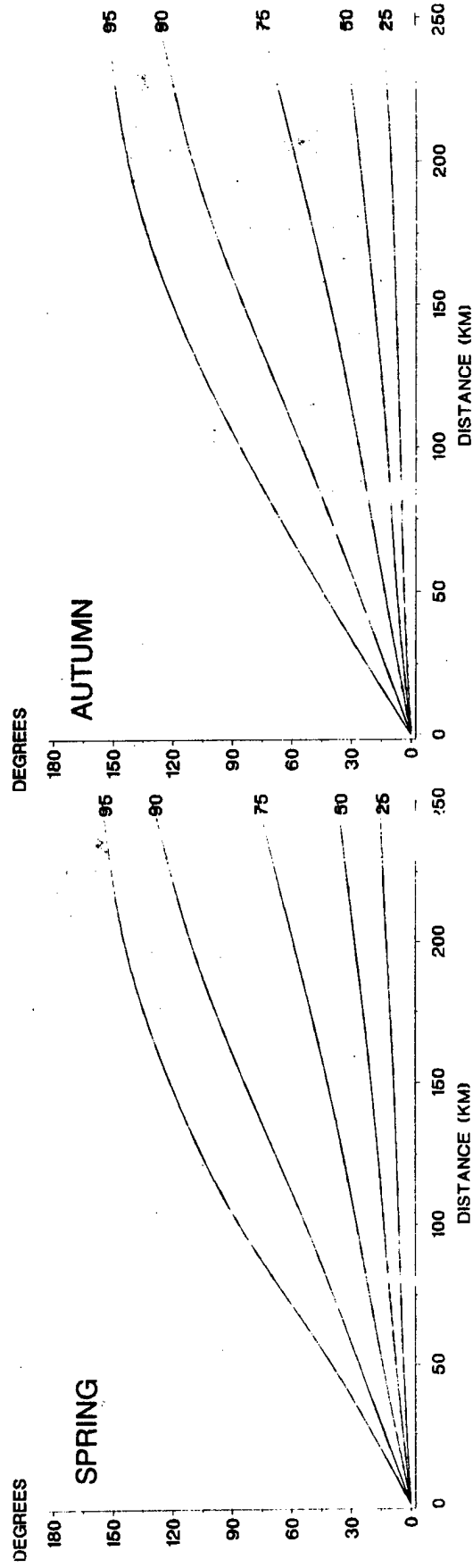
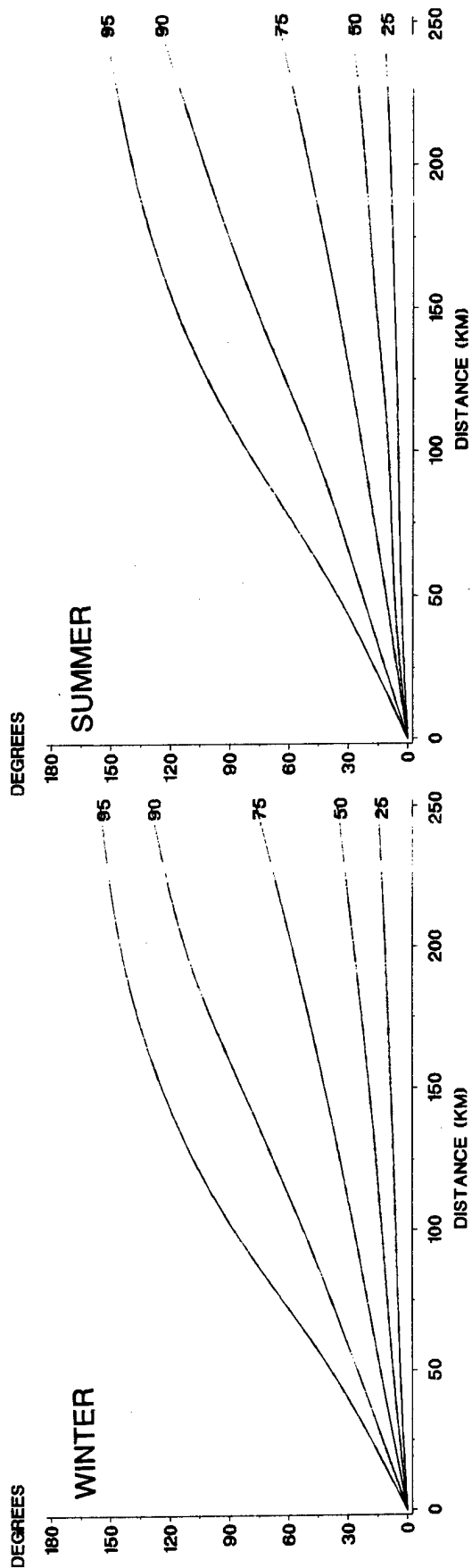


A-18 Spatial correlation of temperature, coastal climate, noon.

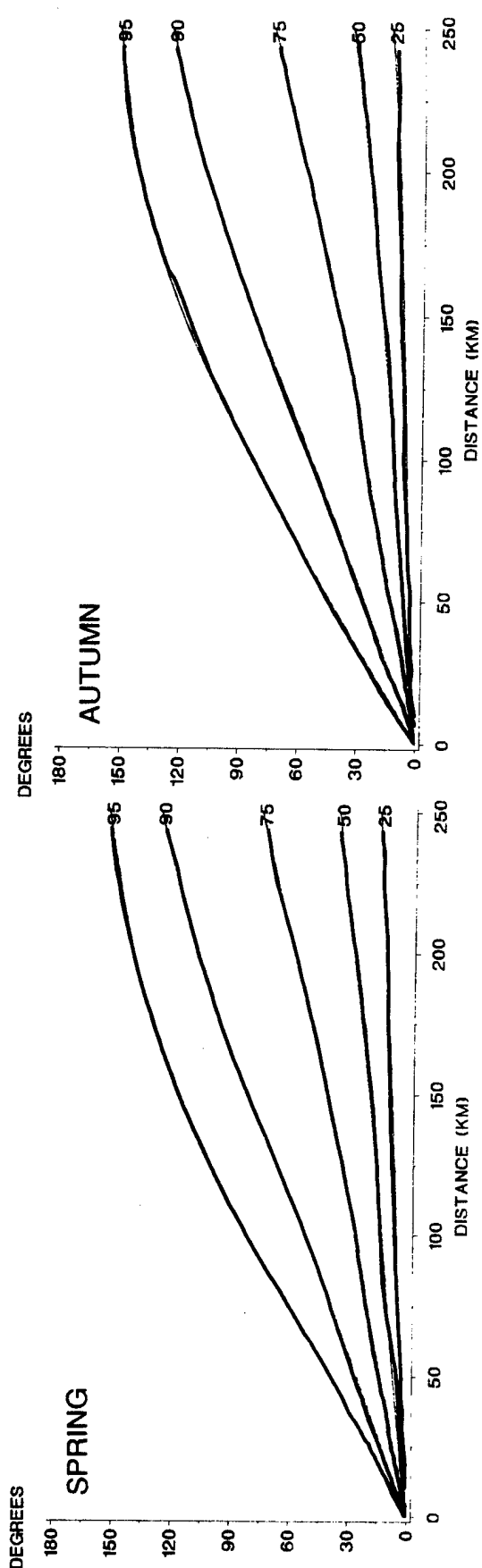
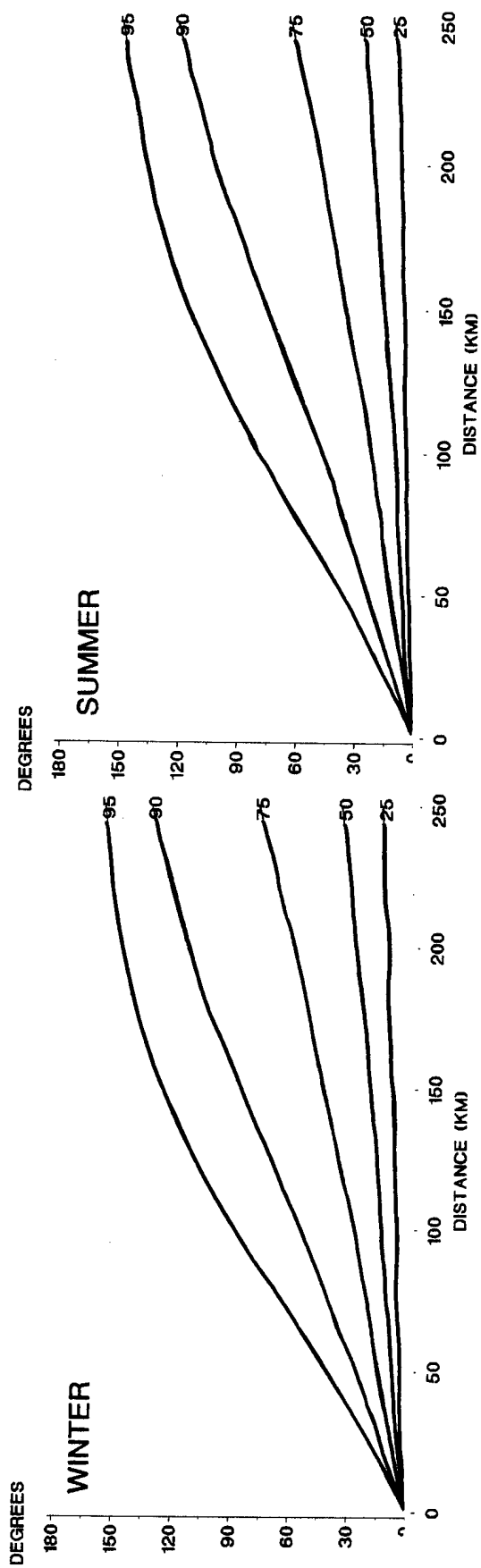
APPENDIX B

SPATIAL CORRELATION OF WIND DIRECTION

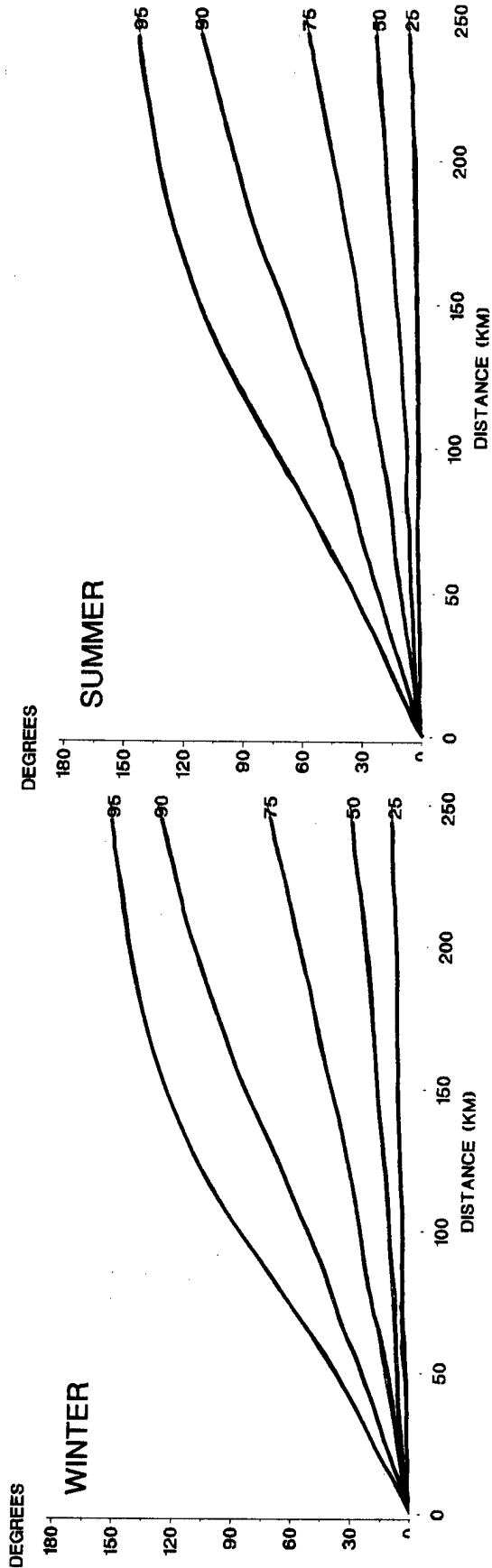
- B-1 Spatial correlation of wind direction, continental climate, midnight.
- B-2 Spatial correlation of wind direction, continental climate, sunrise.
- B-3 Spatial correlation of wind direction, continental climate, noon.
- B-4 Spatial correlation of wind direction, arctic climate, midnight.
- B-5 Spatial correlation of wind direction, arctic climate, sunrise.
- B-6 Spatial correlation of wind direction, arctic climate, noon.
- B-7 Spatial correlation of wind direction, desert climate, midnight.
- B-8 Spatial correlation of wind direction, desert climate, sunrise.
- B-9 Spatial correlation of wind direction, desert climate, noon.
- B-10 Spatial correlation of wind direction, maritime climate, midnight.
- B-11 Spatial correlation of wind direction, maritime climate, sunrise.
- B-12 Spatial correlation of wind direction, maritime climate, noon.
- B-13 Spatial correlation of wind direction, tropical climate, midnight.
- B-14 Spatial correlation of wind direction, tropical climate, sunrise.
- B-15 Spatial correlation of wind direction, tropical climate, noon.
- B-16 Spatial correlation of wind direction, coastal climate, midnight.
- B-17 Spatial correlation of wind direction, coastal climate, sunrise.
- B-18 Spatial correlation of wind direction, coastal climate, noon.



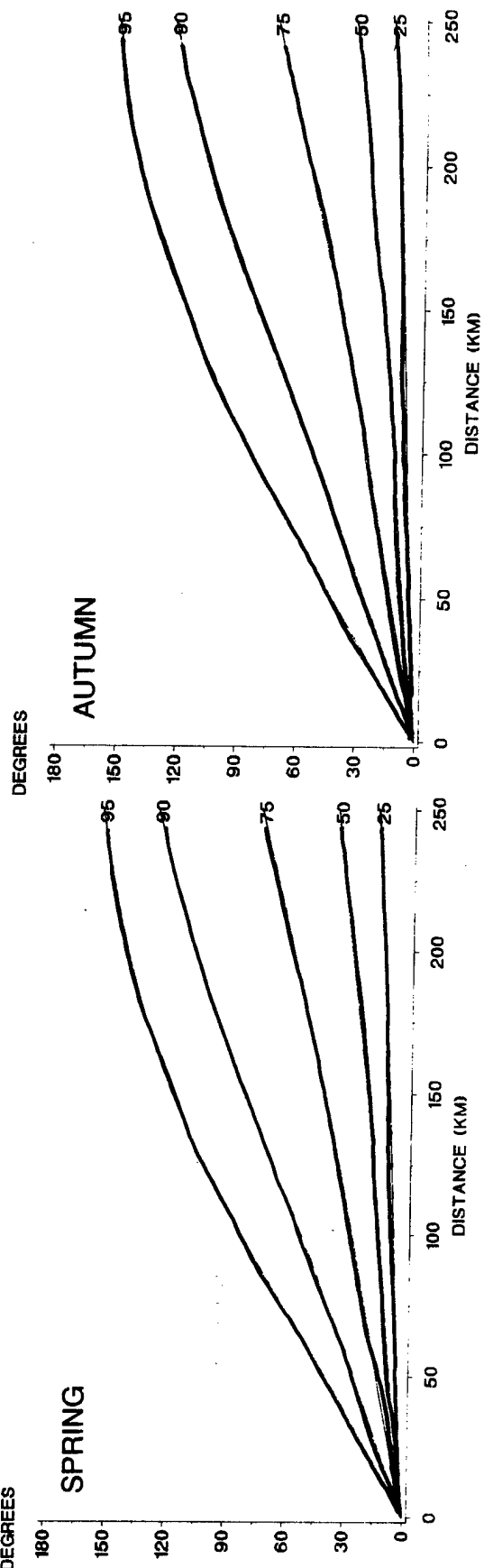
B-1 Spatial correlation of wind direction, continental climate, midnight.



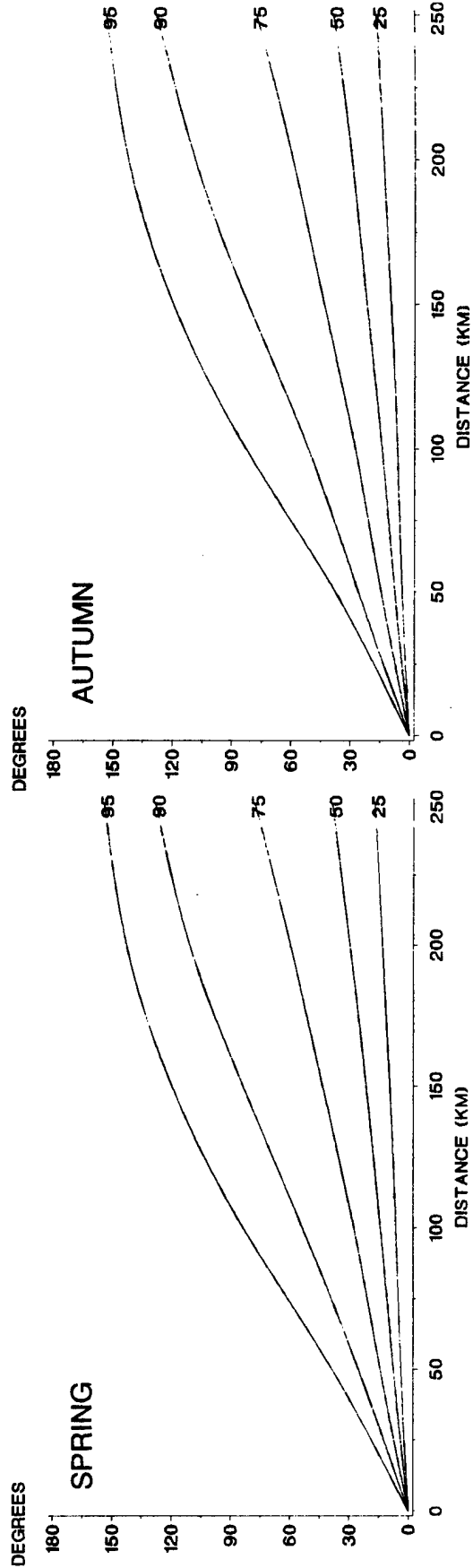
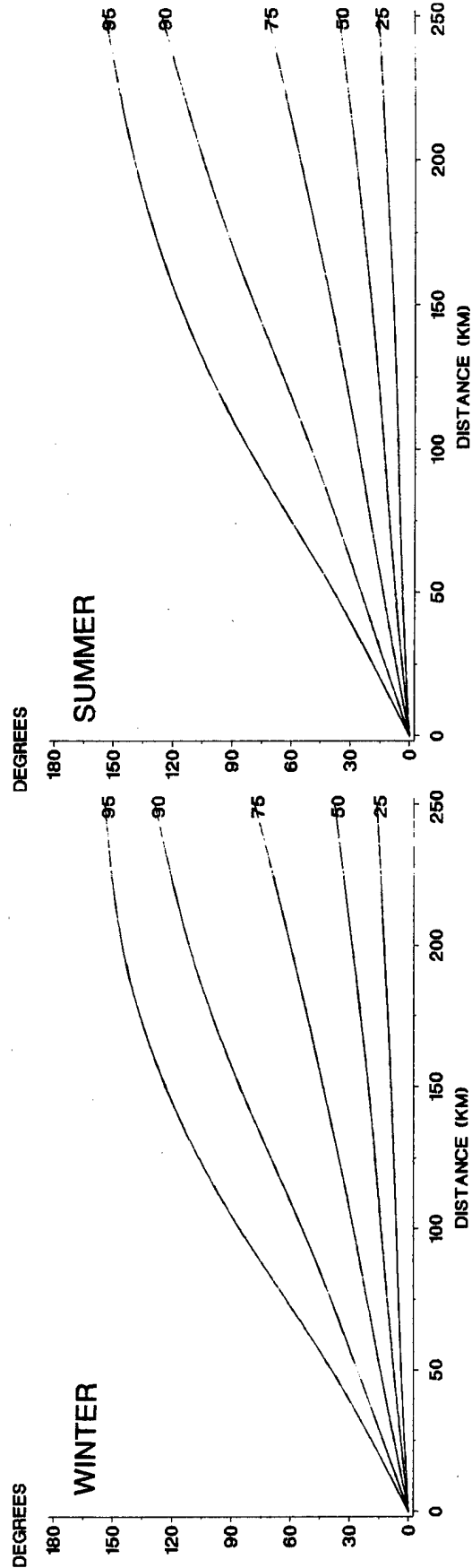
B-2 Spatial correlation of wind direction, continental climate, sunrise.



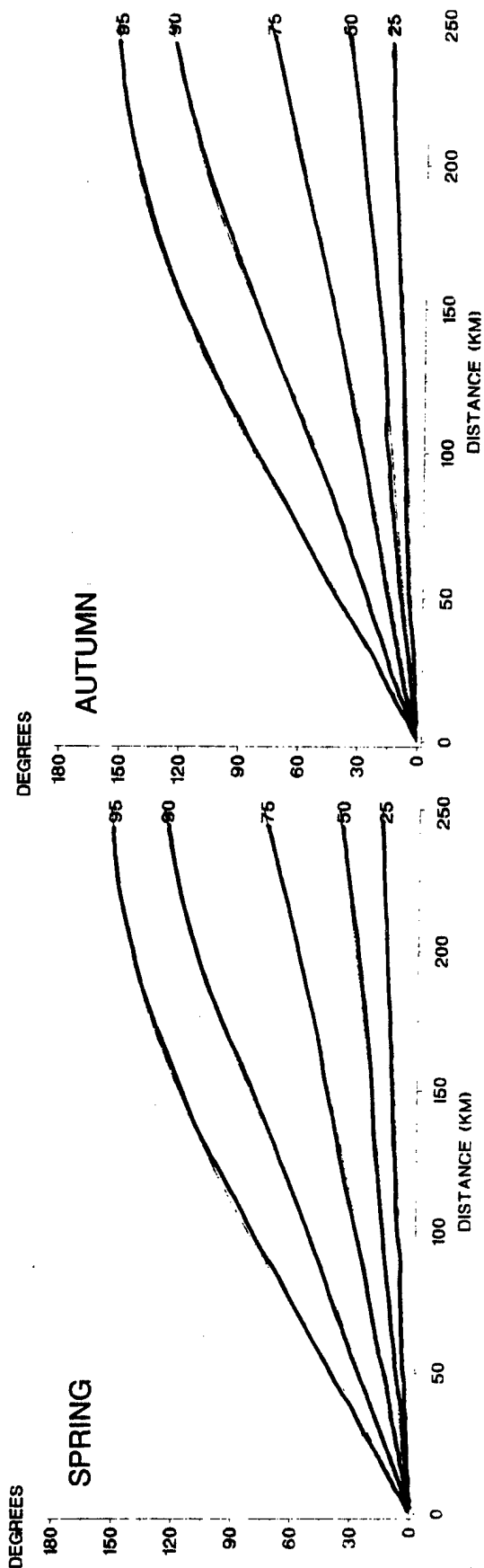
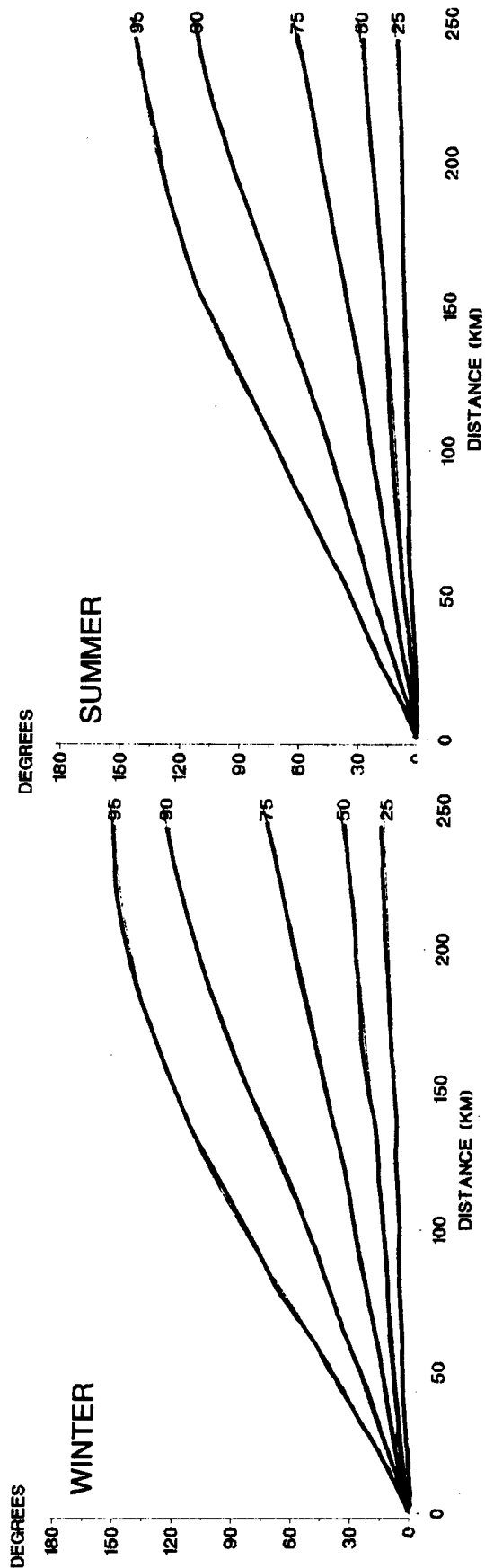
B-4



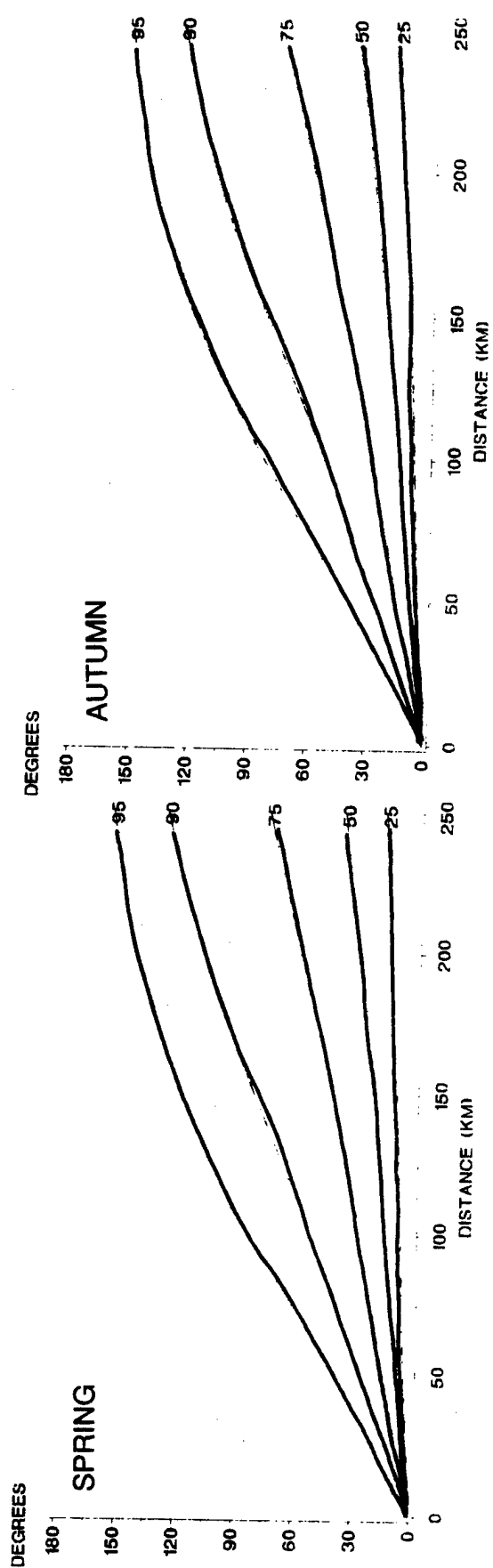
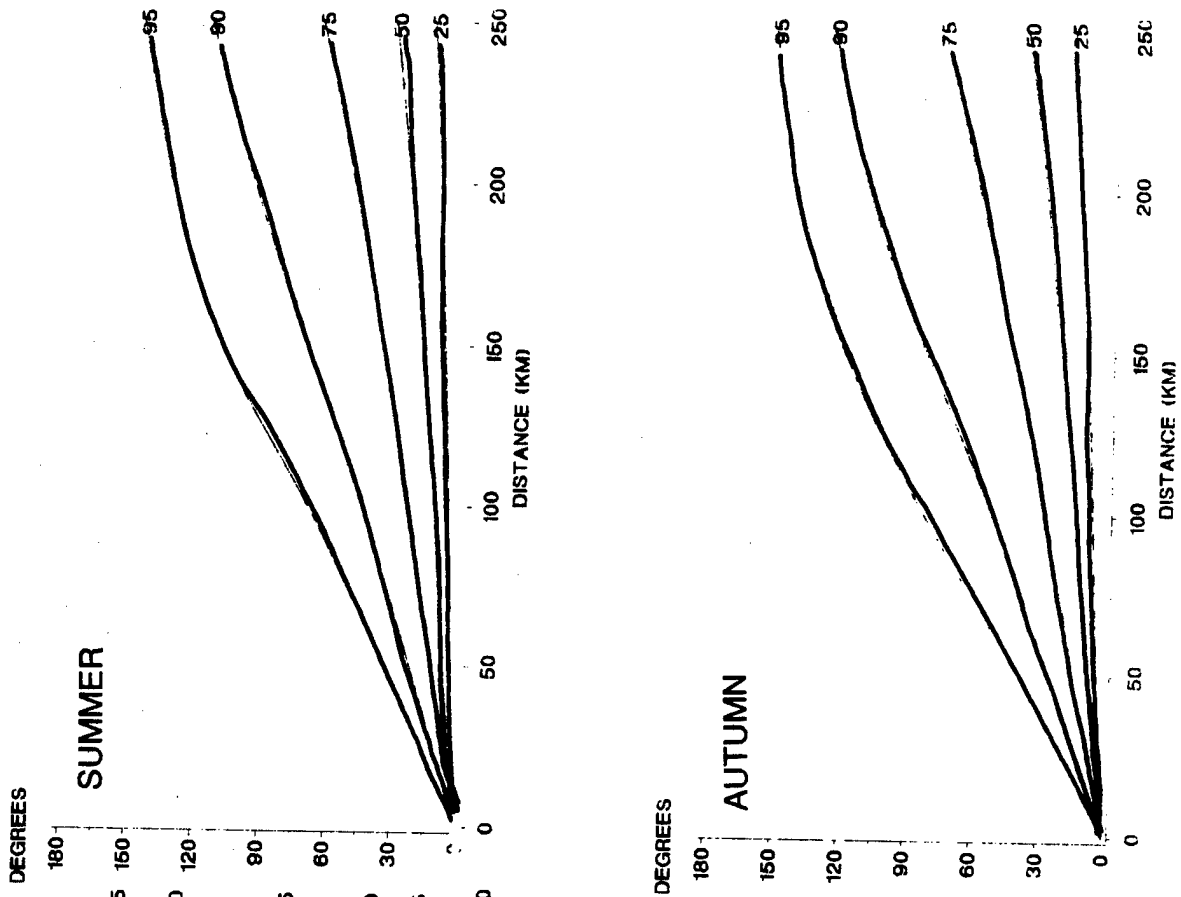
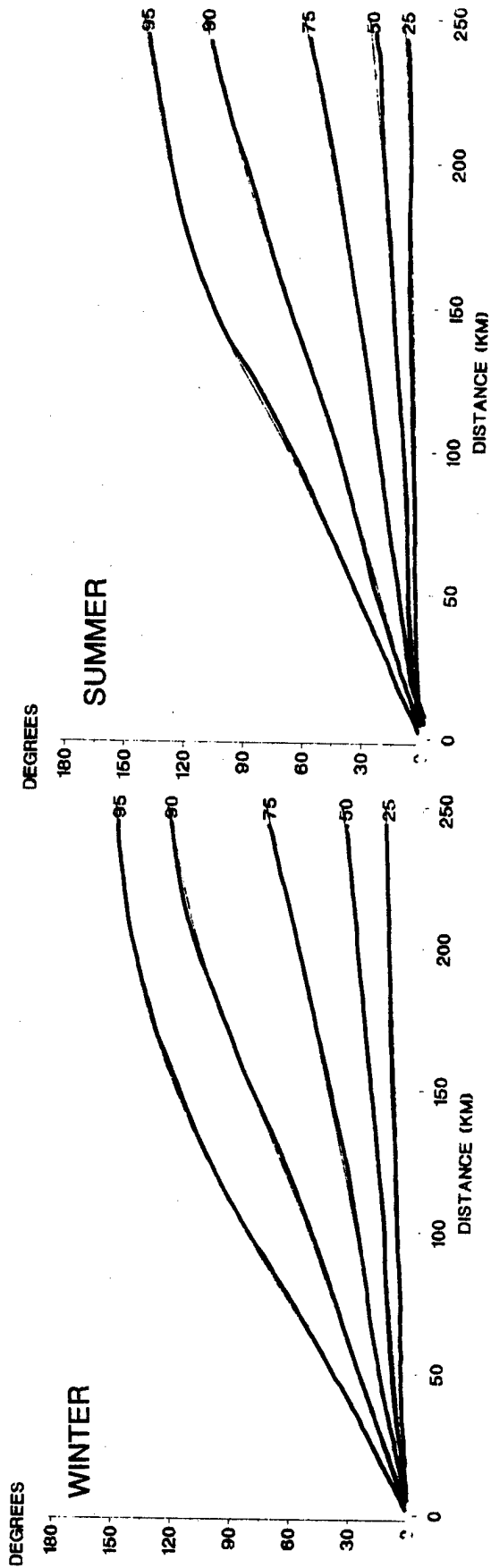
B-3 Spatial correlation of wind direction, continental climate, noon.



B-4 Spatial correlation of wind direction, arctic climate, midnight.

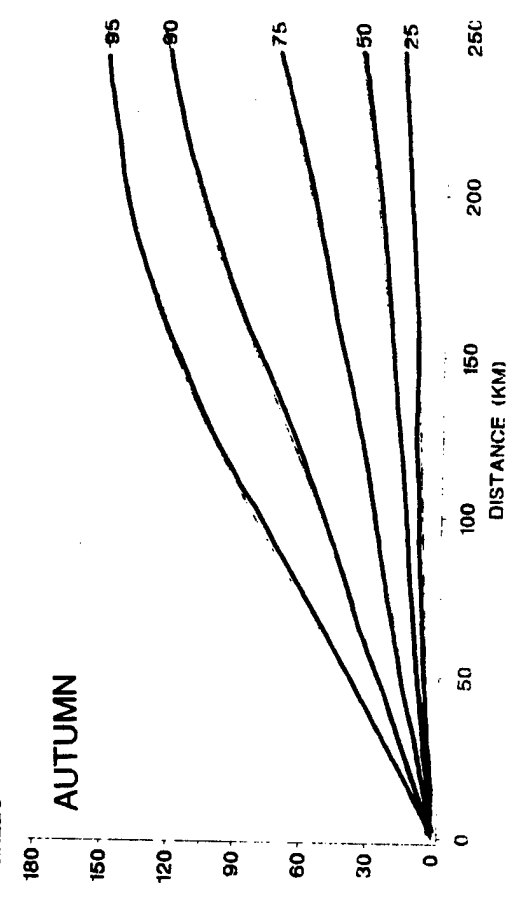


B-5 Spatial correlation of wind direction, arctic climate, sunrise.

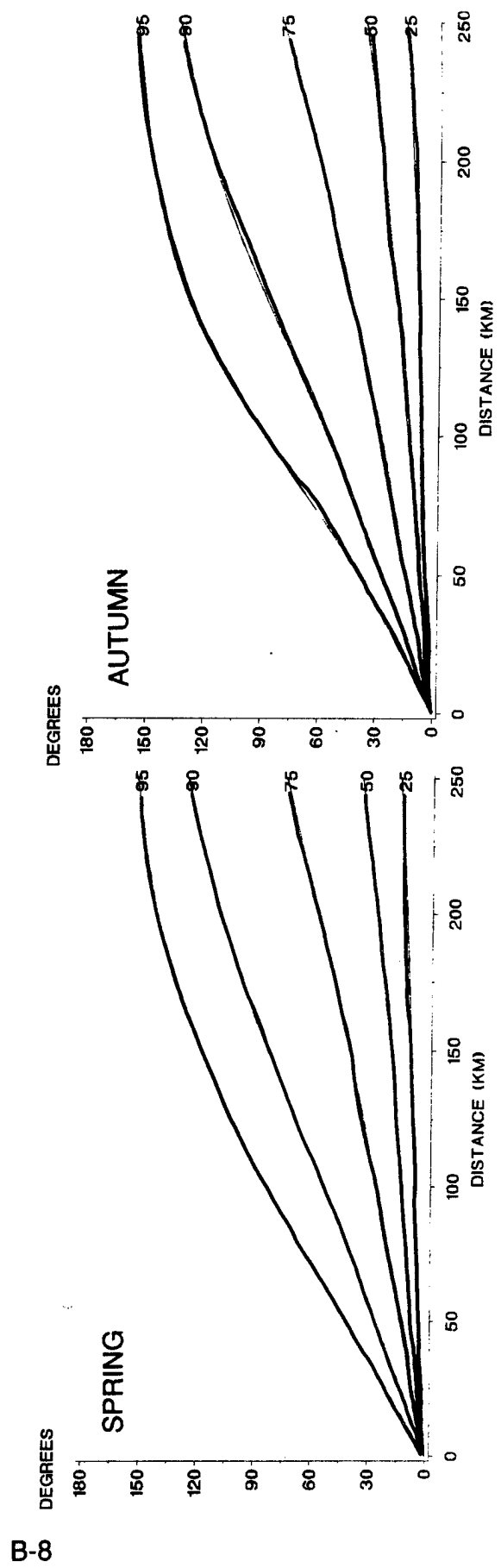
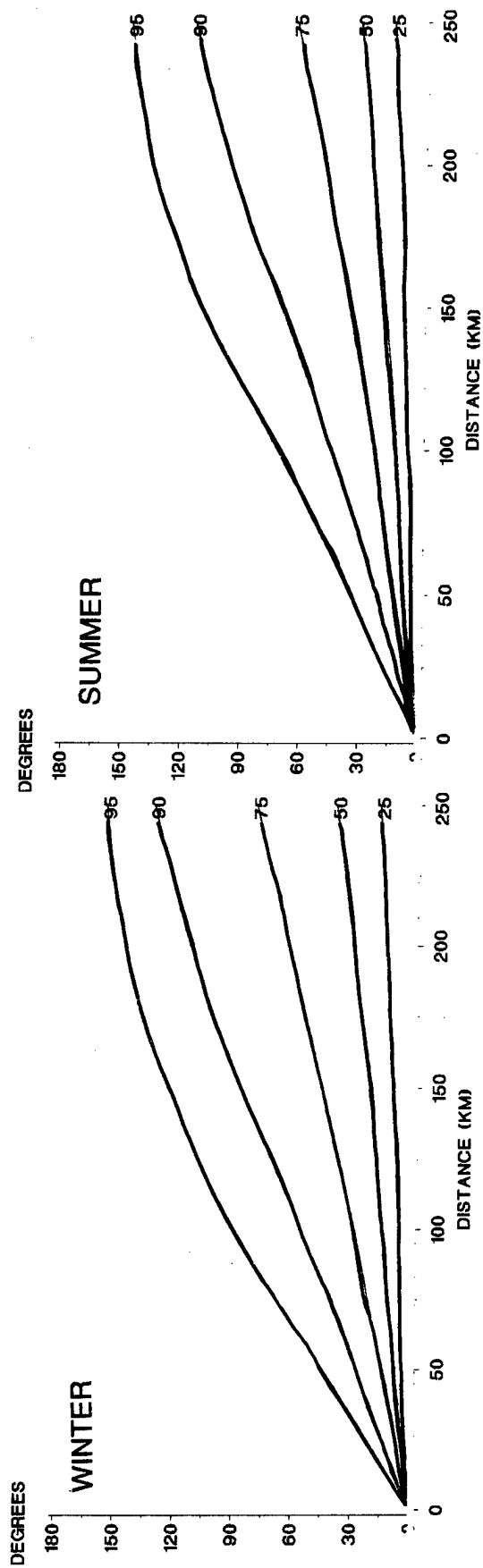


DEGREES

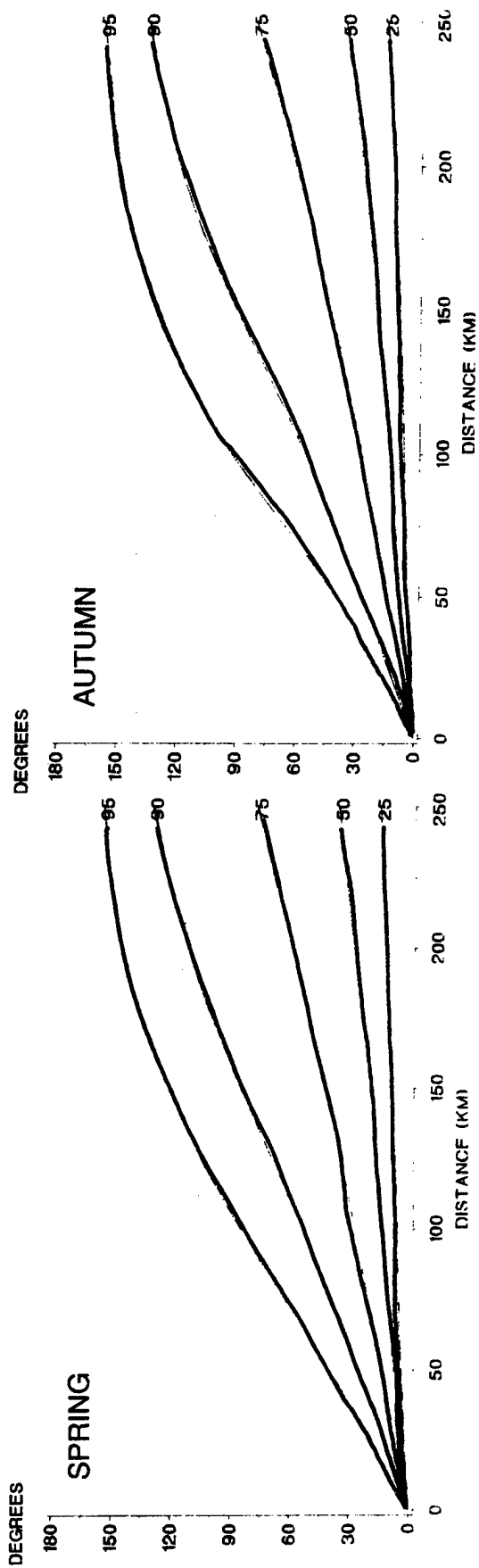
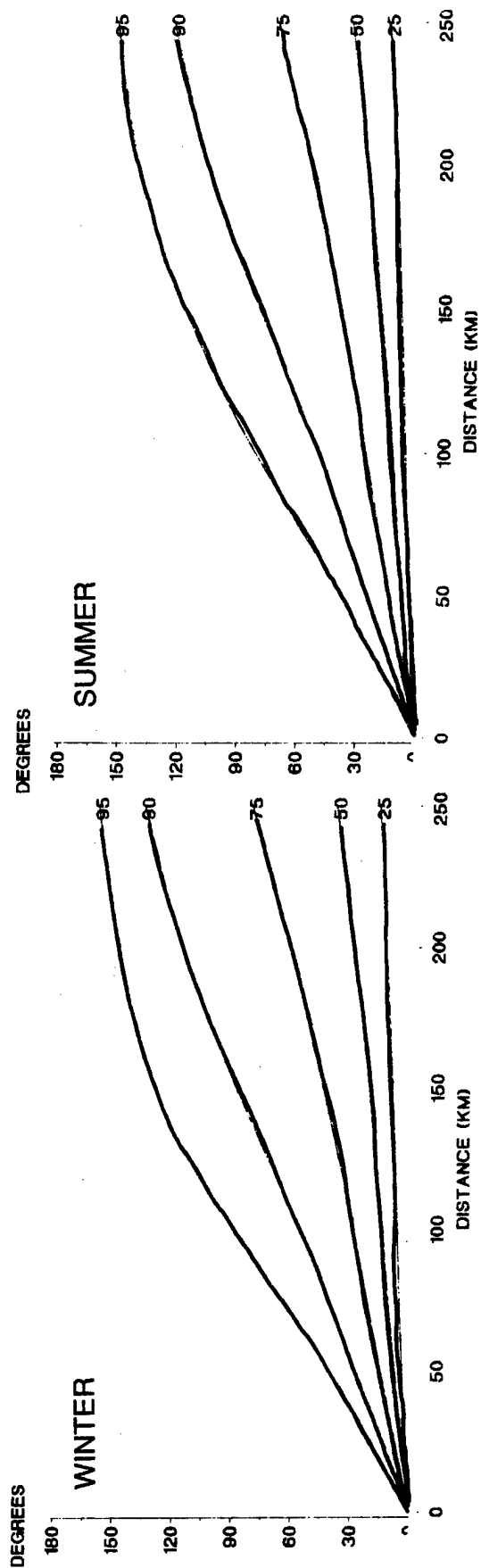
AUTUMN



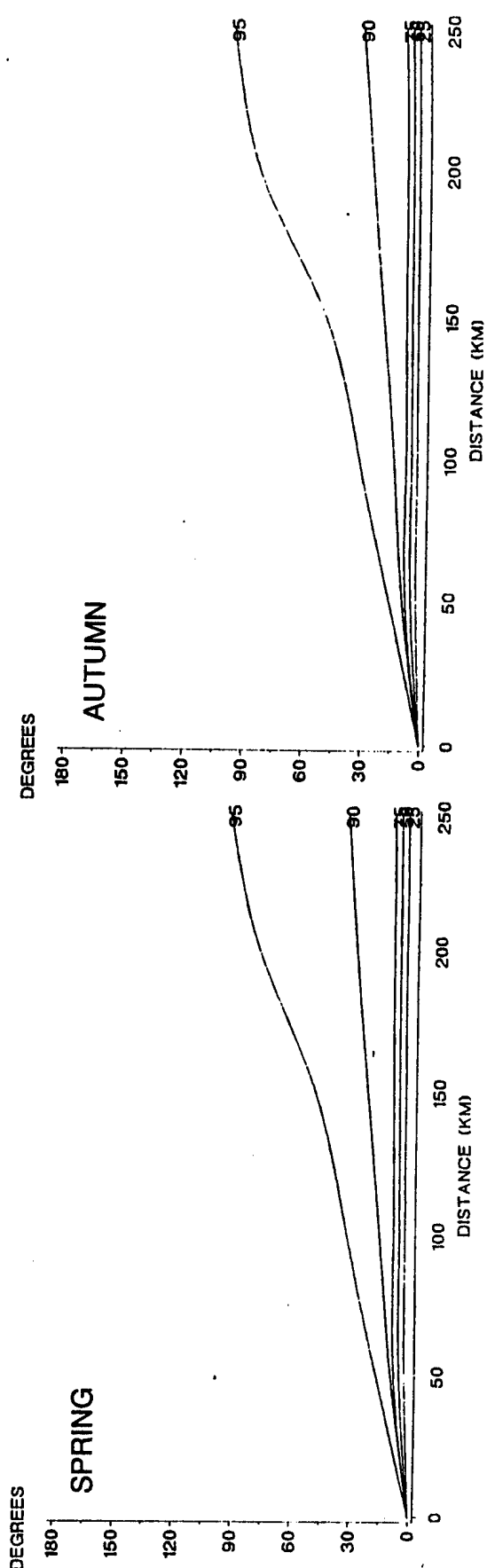
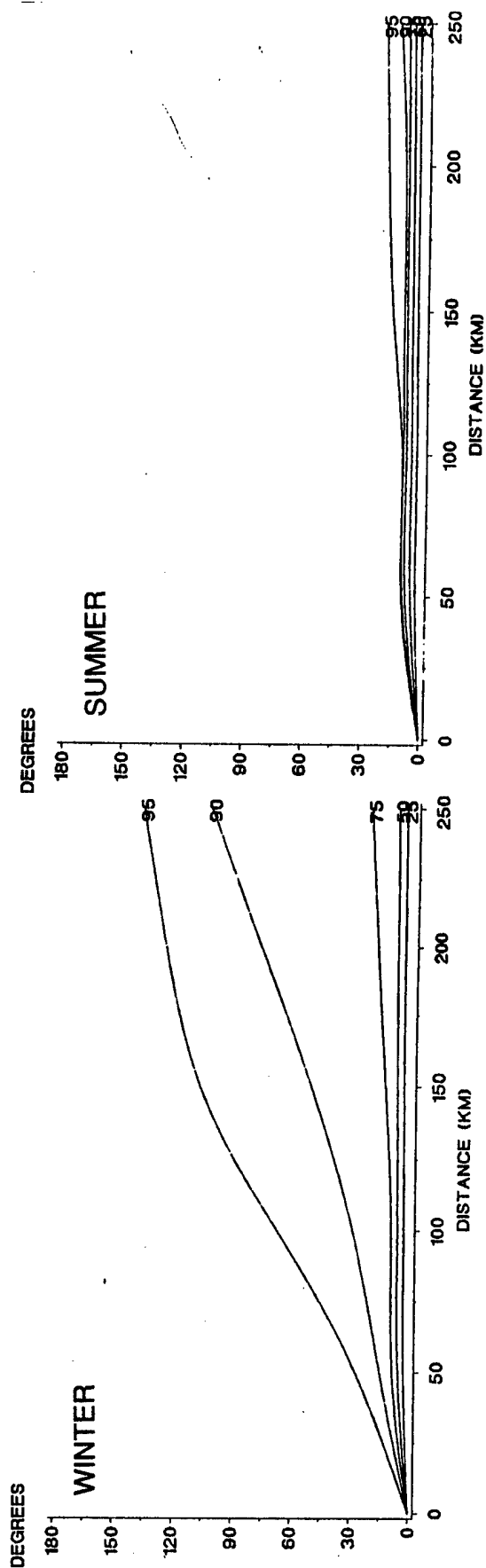
B-6 Spatial correlation of wind direction, arctic climate, noon.



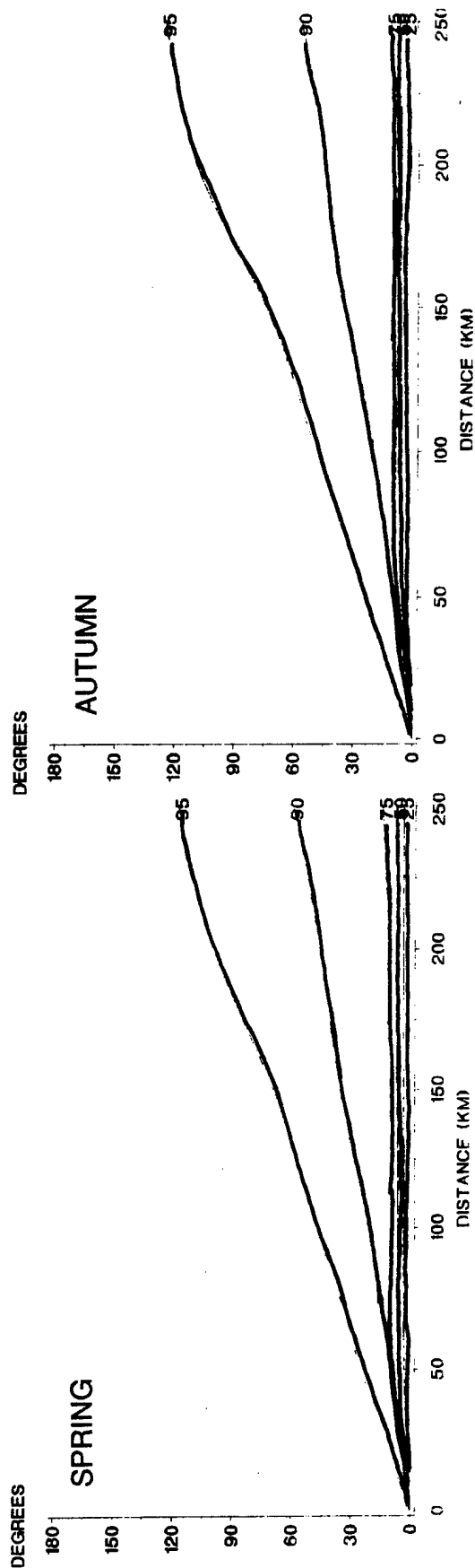
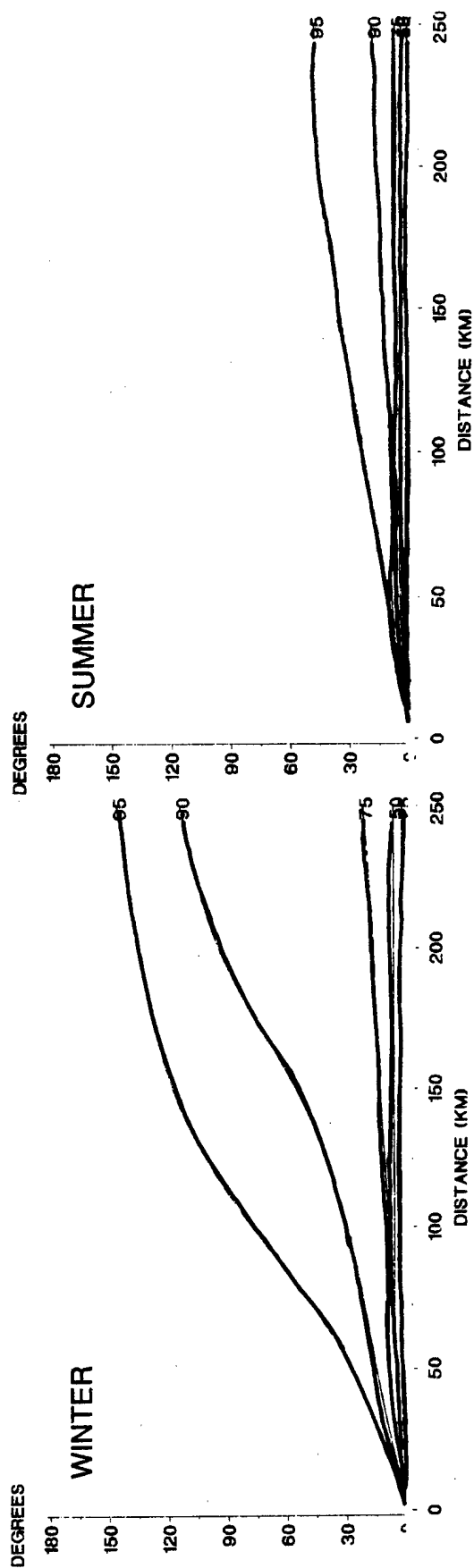
B-7 Spatial correlation of wind direction, desert climate, midnight.



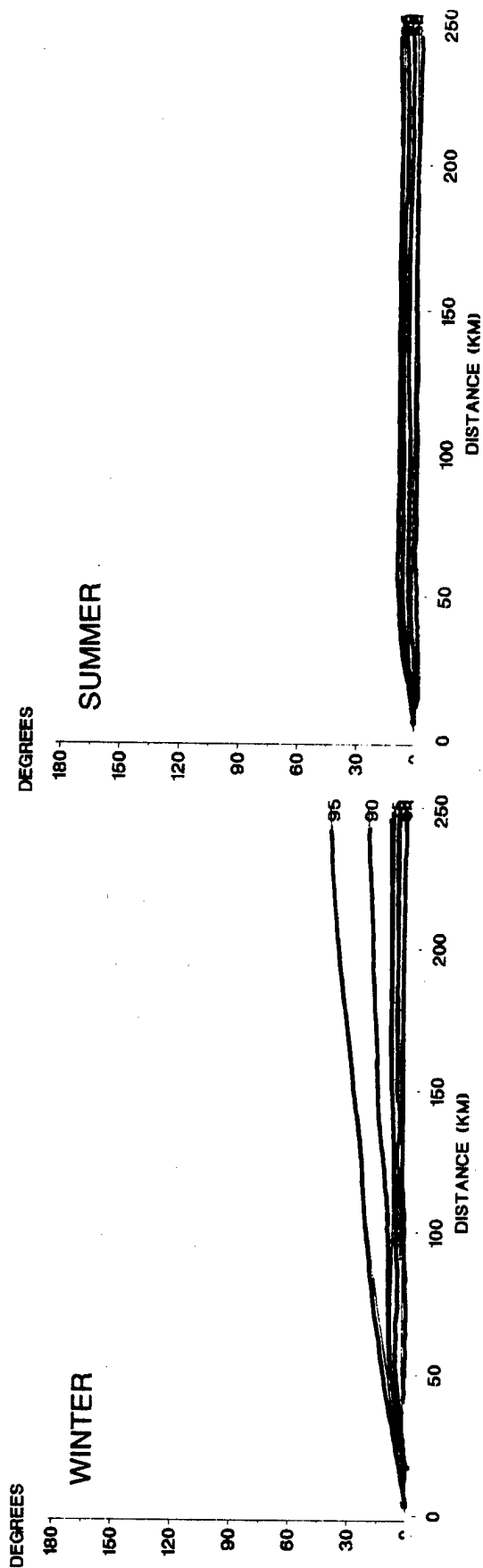
B-9 Spatial correlation of wind direction, desert climate, noon.



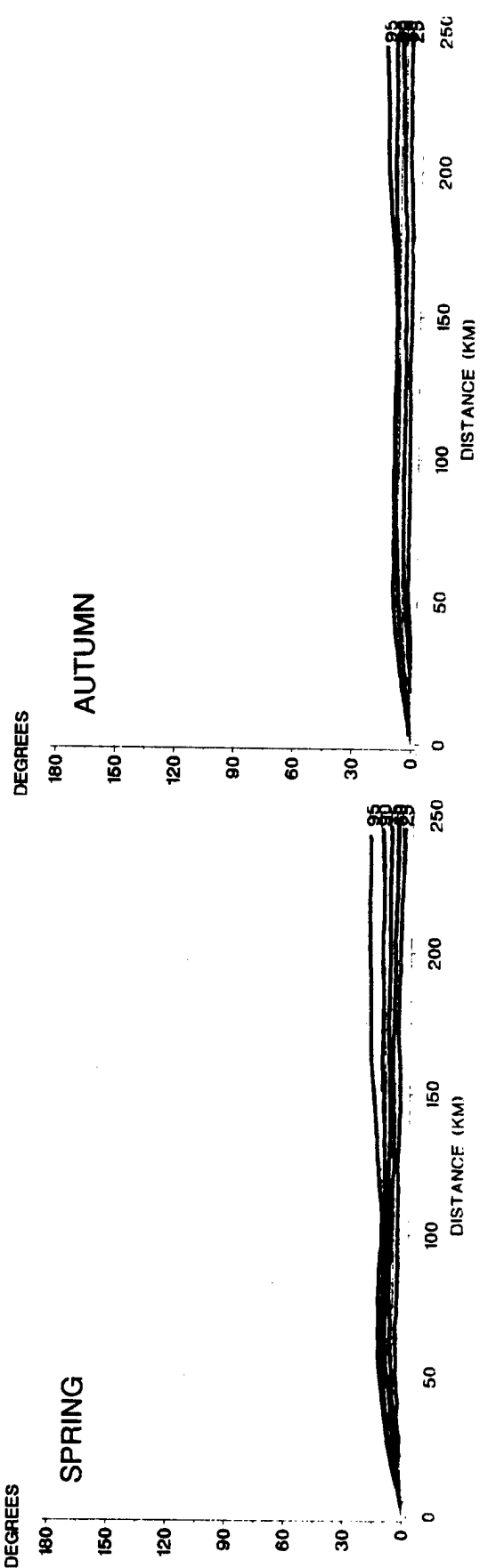
B-10 Spatial correlation of wind direction, maritime climate, midnight.



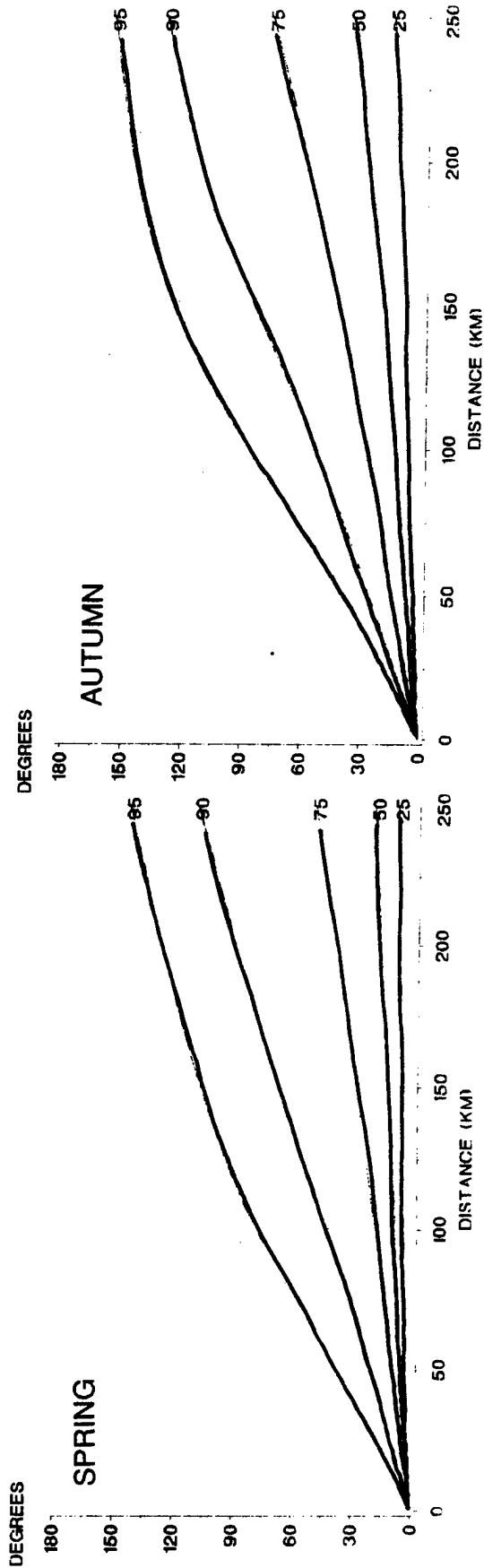
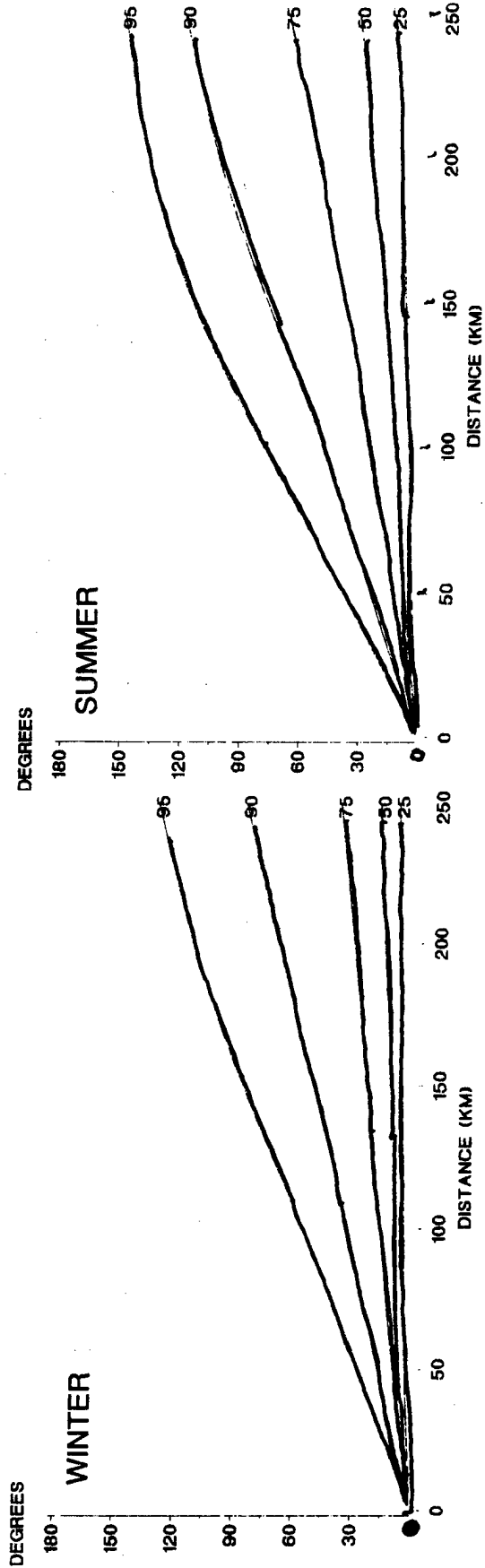
B-11 Spatial correlation of wind direction, maritime climate, sunrise.



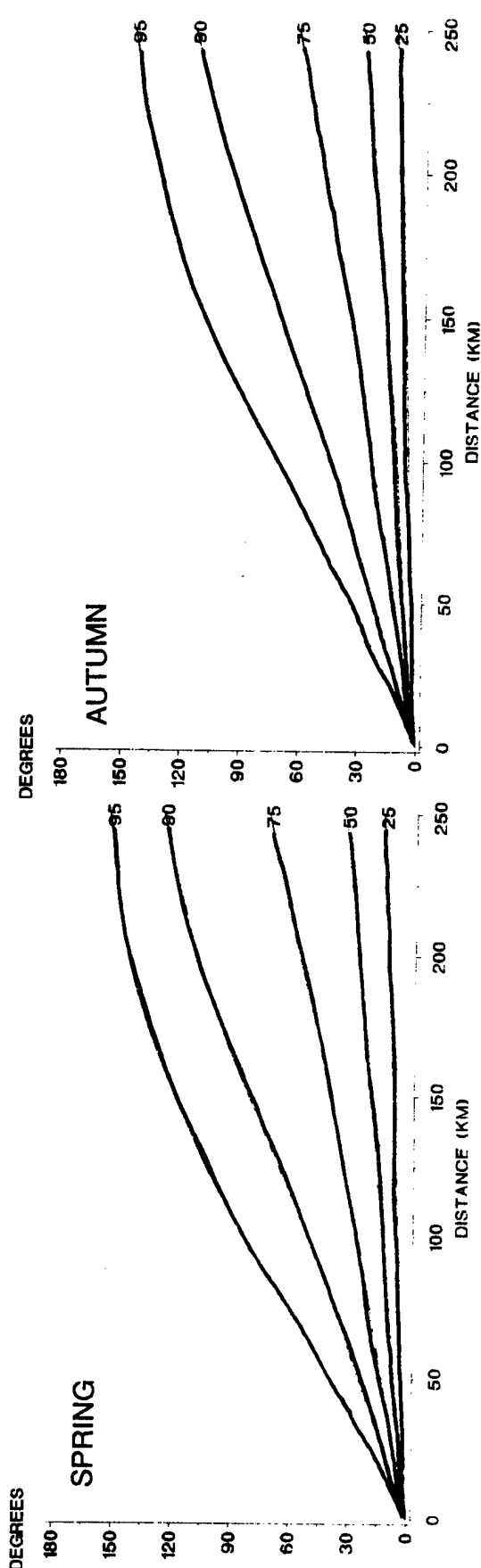
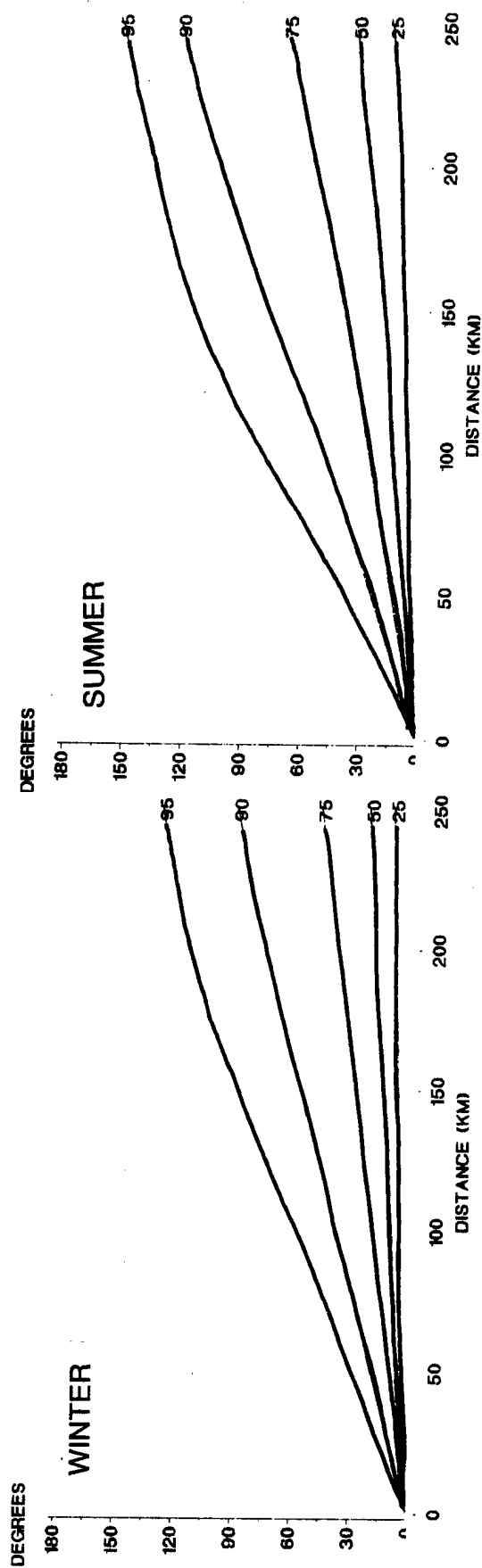
B-13



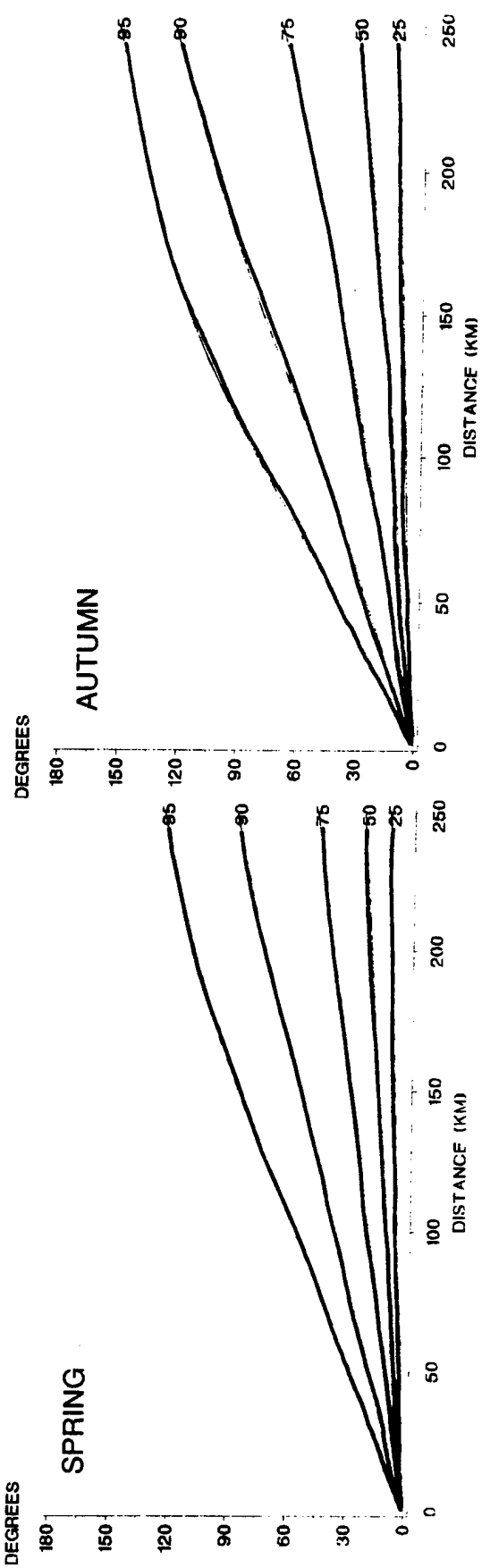
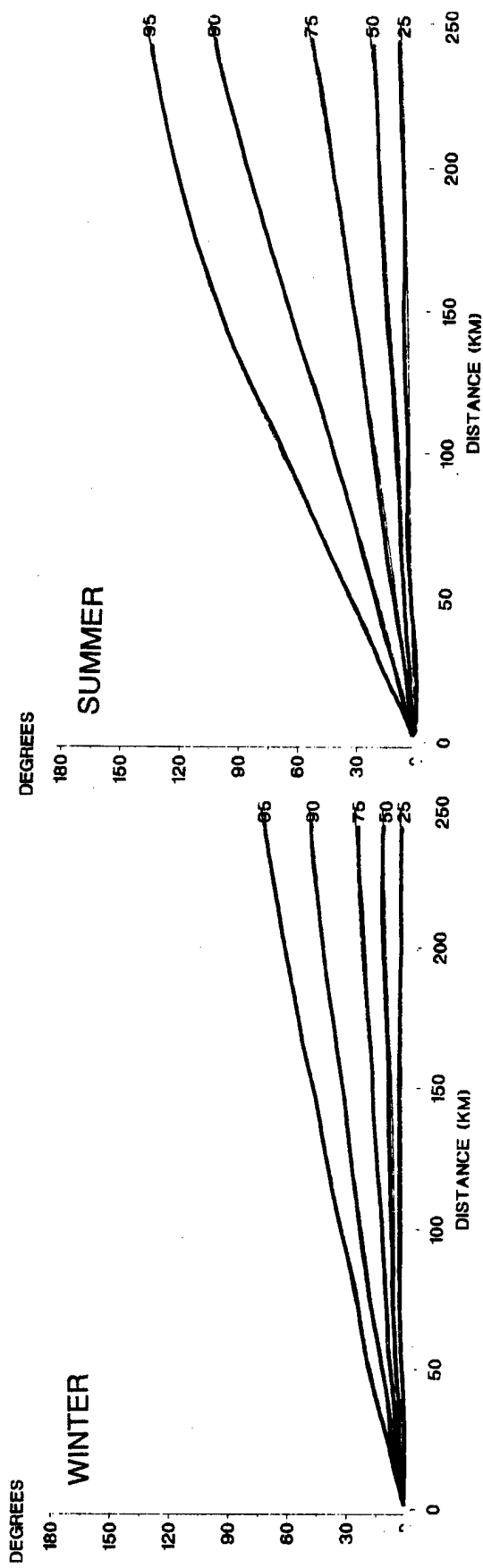
B-12 Spatial correlation of wind direction, maritime climate, noon.



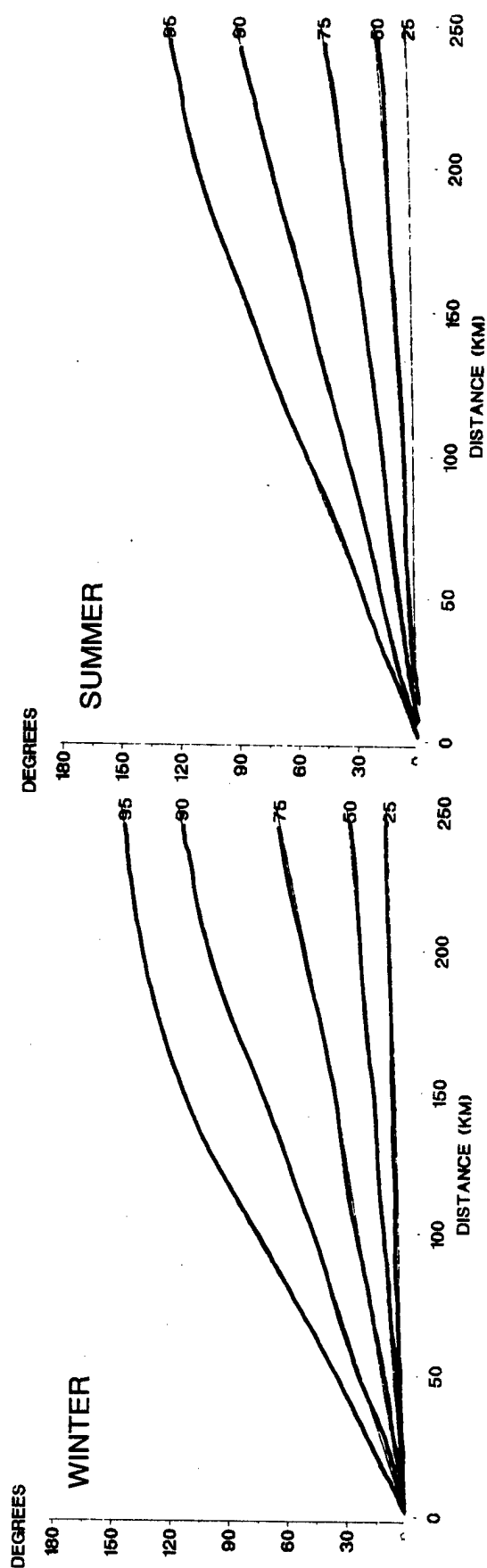
B-13 Spatial correlation of wind direction, tropical climate, midnight.



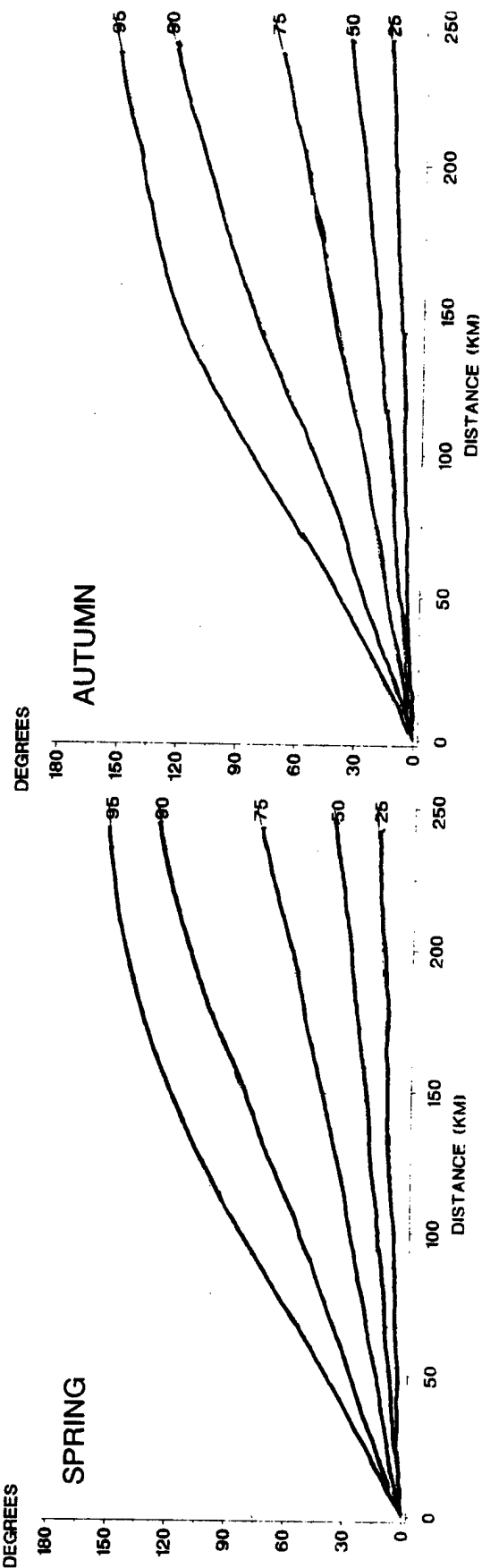
B-14 Spatial correlation of wind direction, tropical climate, sunrise.



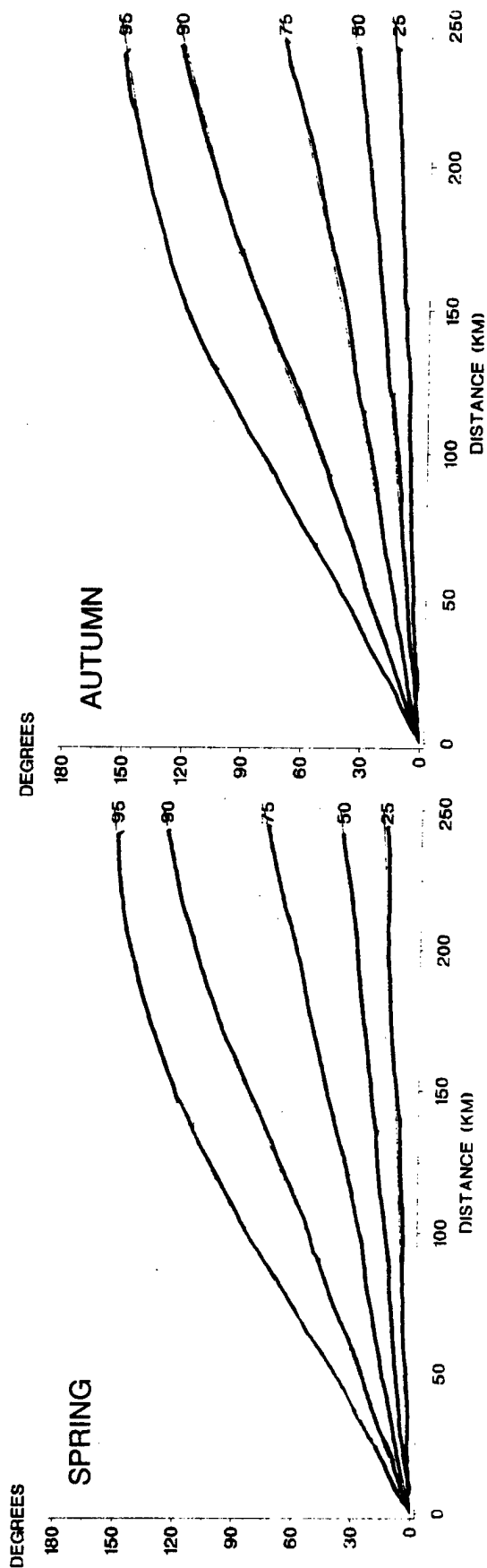
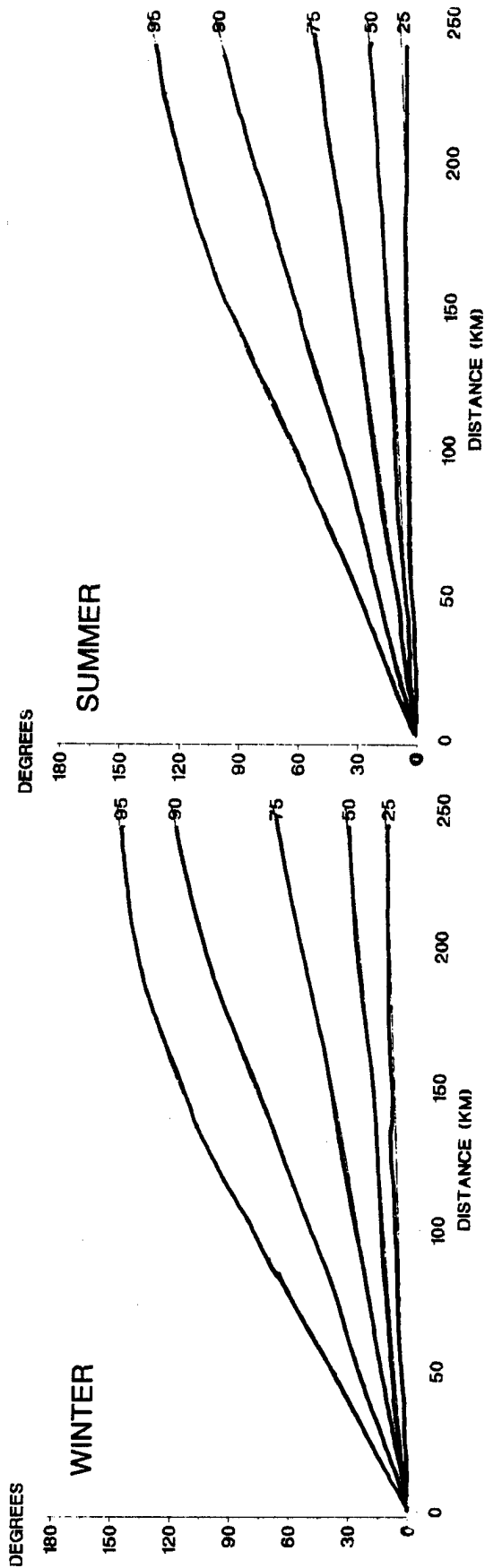
B-15 Spatial correlation of wind direction, tropical climate, noon.



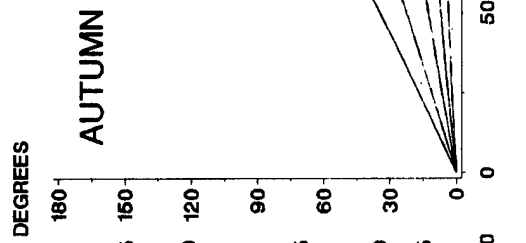
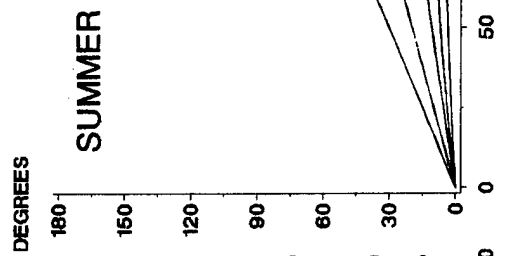
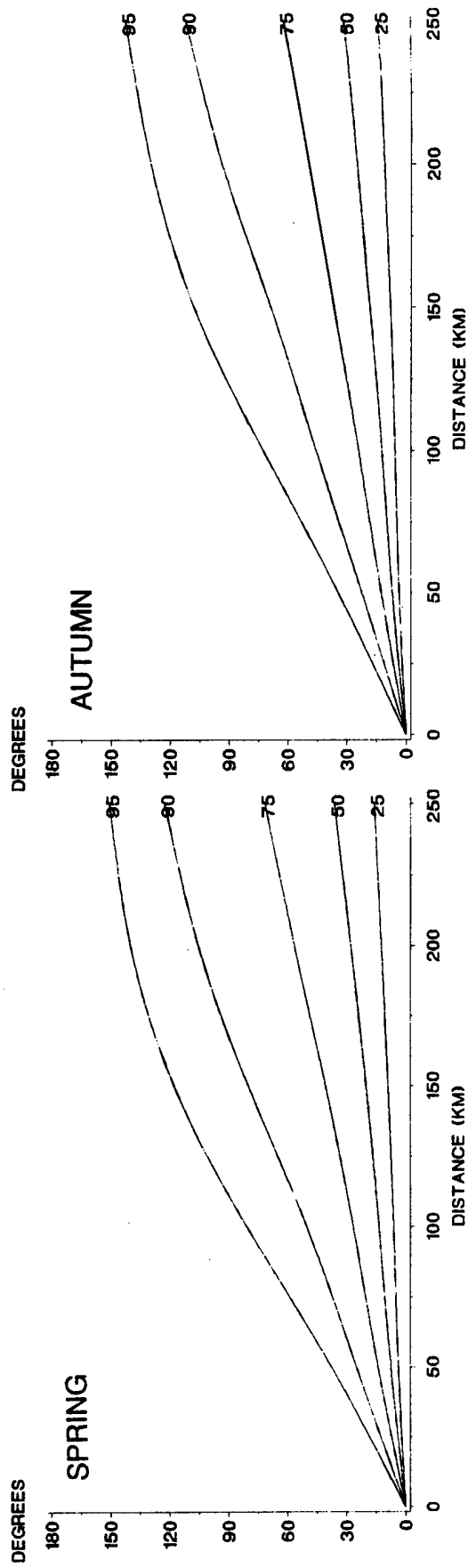
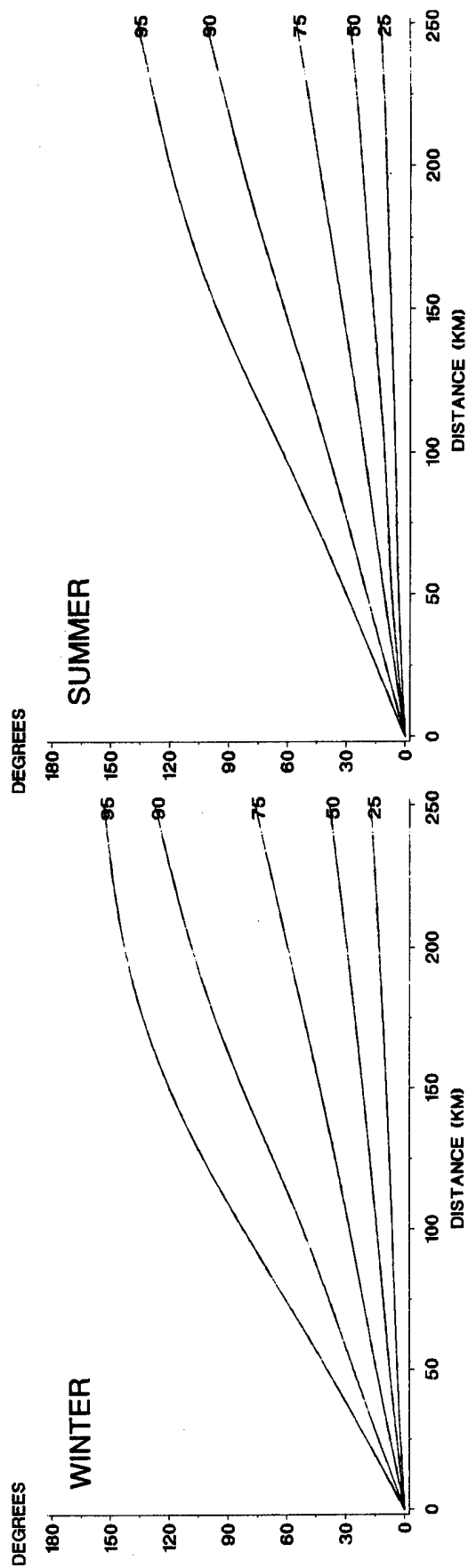
B-17



B-16 Spatial correlation of wind direction, coastal climate, midnight.



B-17 Spatial correlation of wind direction, coastal climate, sunrise.

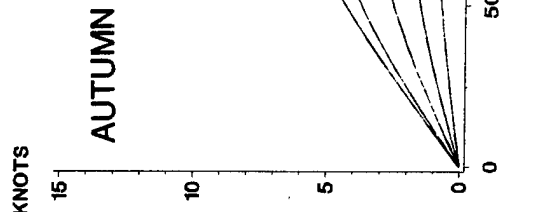
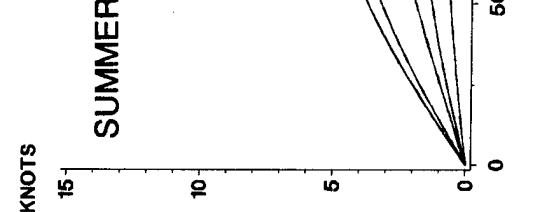
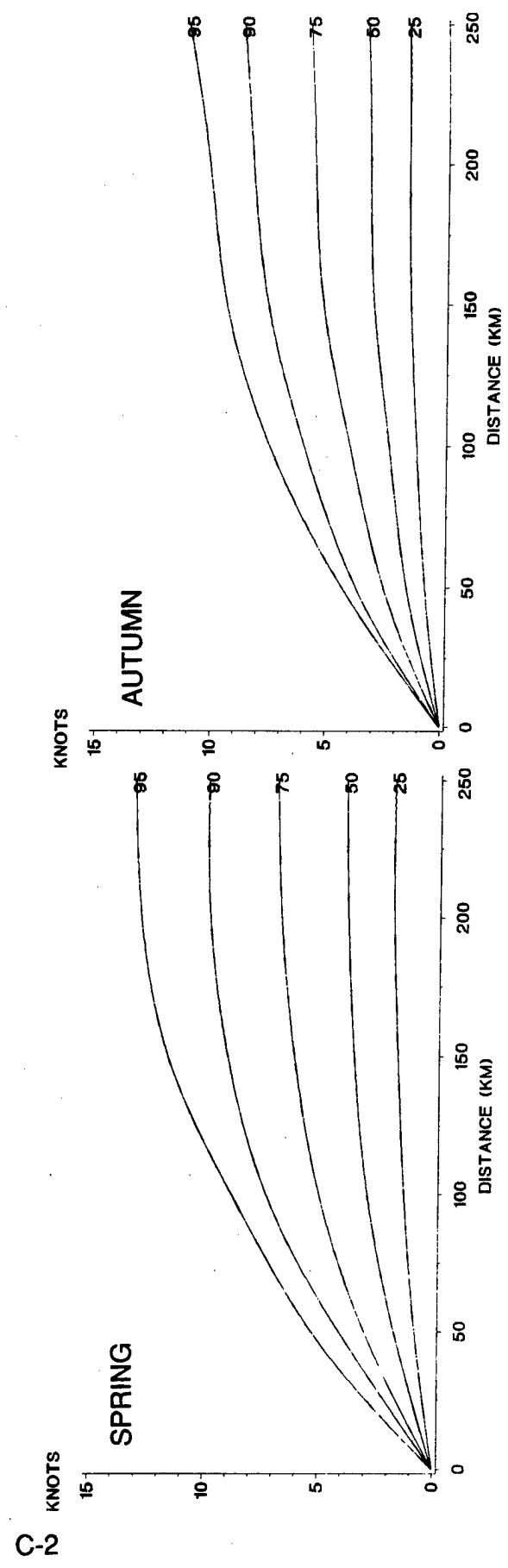
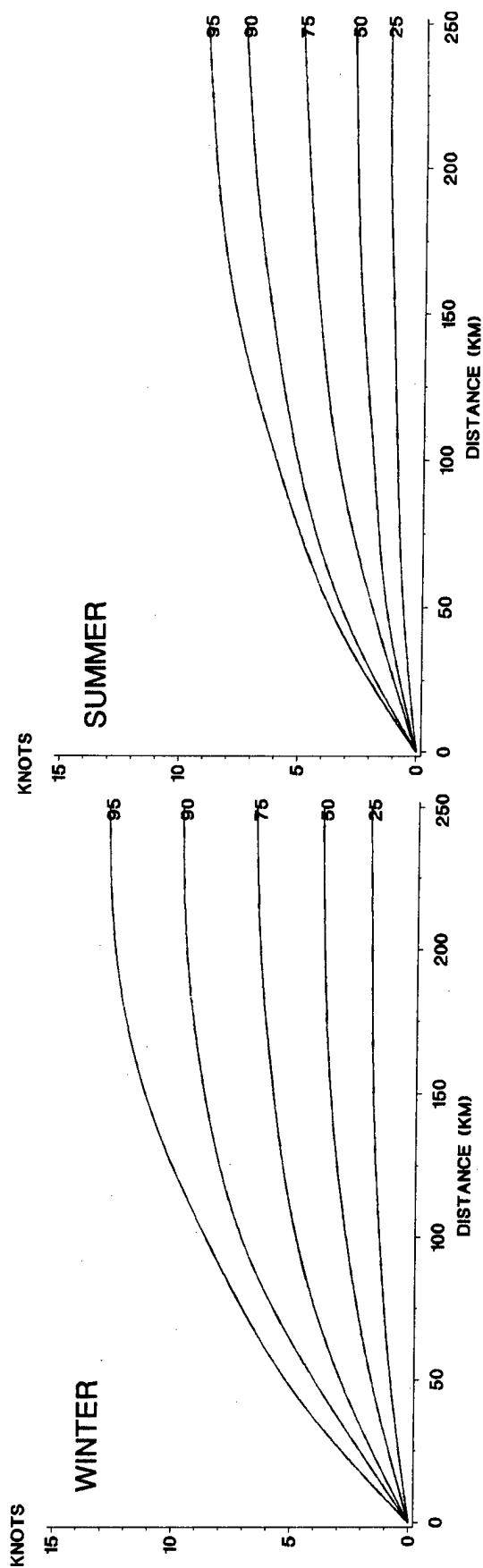


B-18 Spatial correlation of wind direction, coastal climate, noon.

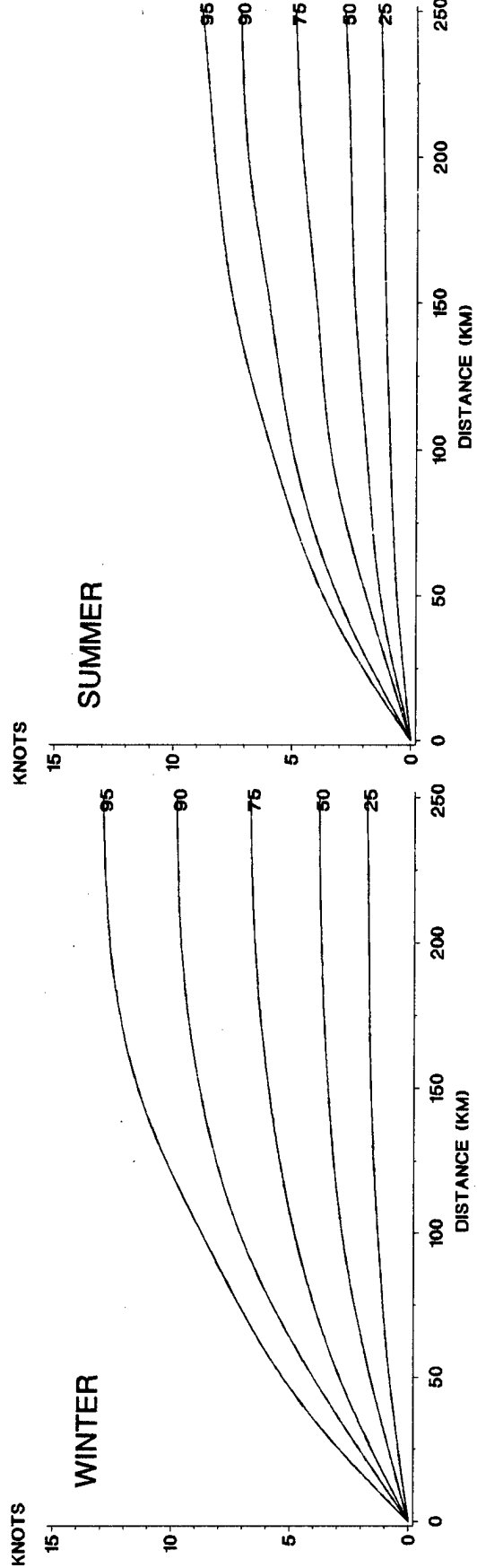
APPENDIX C

SPATIAL CORRELATION OF WIND SPEED

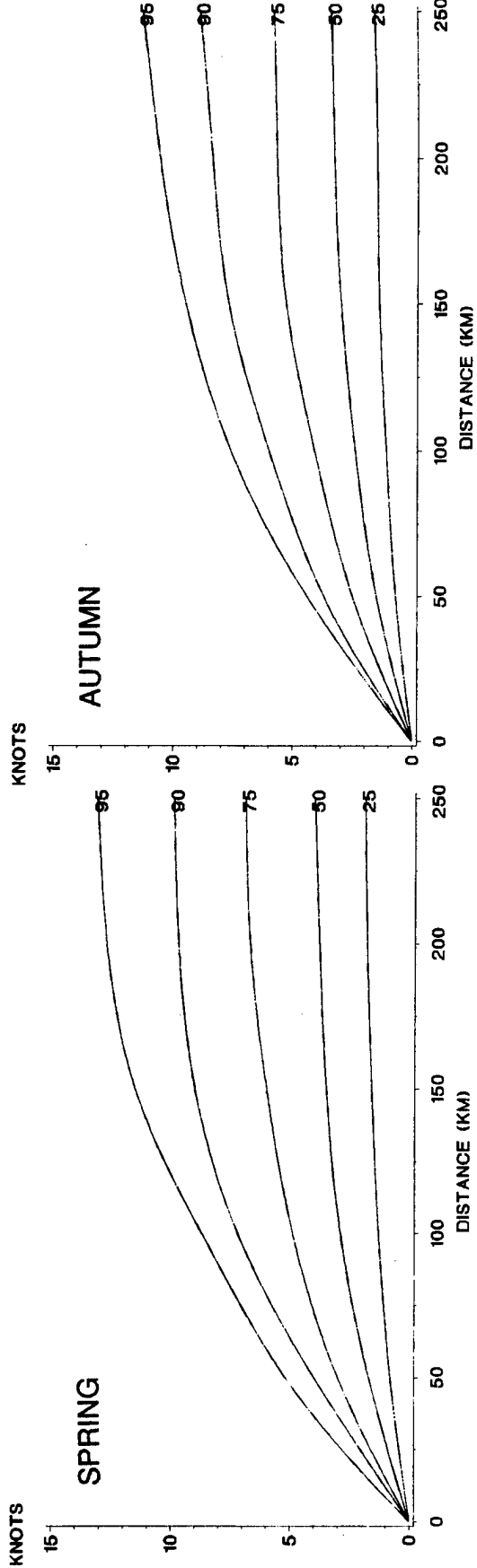
- C-1 Spatial correlation of wind speed, continental climate, midnight.
- C-2 Spatial correlation of wind speed, continental climate, sunrise.
- C-3 Spatial correlation of wind speed, continental climate, noon.
- C-4 Spatial correlation of wind speed, arctic climate, midnight.
- C-5 Spatial correlation of wind speed, arctic climate, sunrise.
- C-6 Spatial correlation of wind speed, arctic climate, noon.
- C-7 Spatial correlation of wind speed, desert climate, midnight.
- C-8 Spatial correlation of wind speed, desert climate, sunrise.
- C-9 Spatial correlation of wind speed, desert climate, noon.
- C-10 Spatial correlation of wind speed, maritime climate, midnight.
- C-11 Spatial correlation of wind speed, maritime climate, sunrise.
- C-12 Spatial correlation of wind speed, maritime climate, noon.
- C-13 Spatial correlation of wind speed, tropical climate, midnight.
- C-14 Spatial correlation of wind speed, tropical climate, sunrise.
- C-15 Spatial correlation of wind speed, tropical climate, noon.
- C-16 Spatial correlation of wind speed, coastal climate, midnight.
- C-17 Spatial correlation of wind speed, coastal climate, sunrise.
- C-18 Spatial correlation of wind speed, coastal climate, noon.



C-1 Spatial correlation of wind speed, continental climate, midnight.

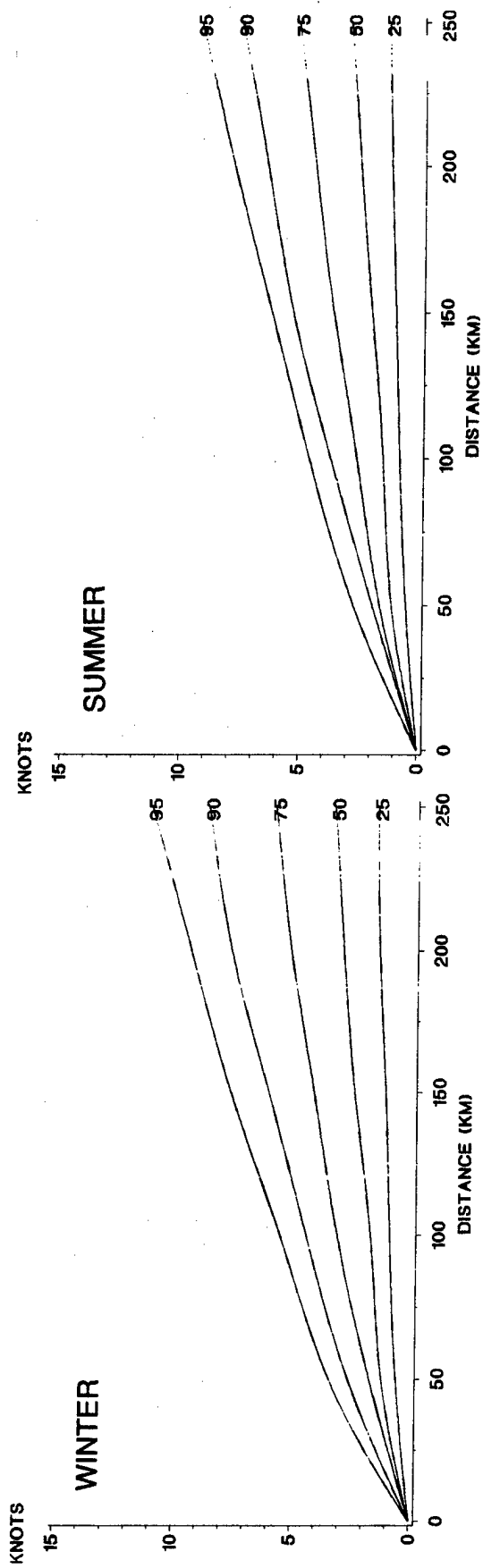


SUMMER

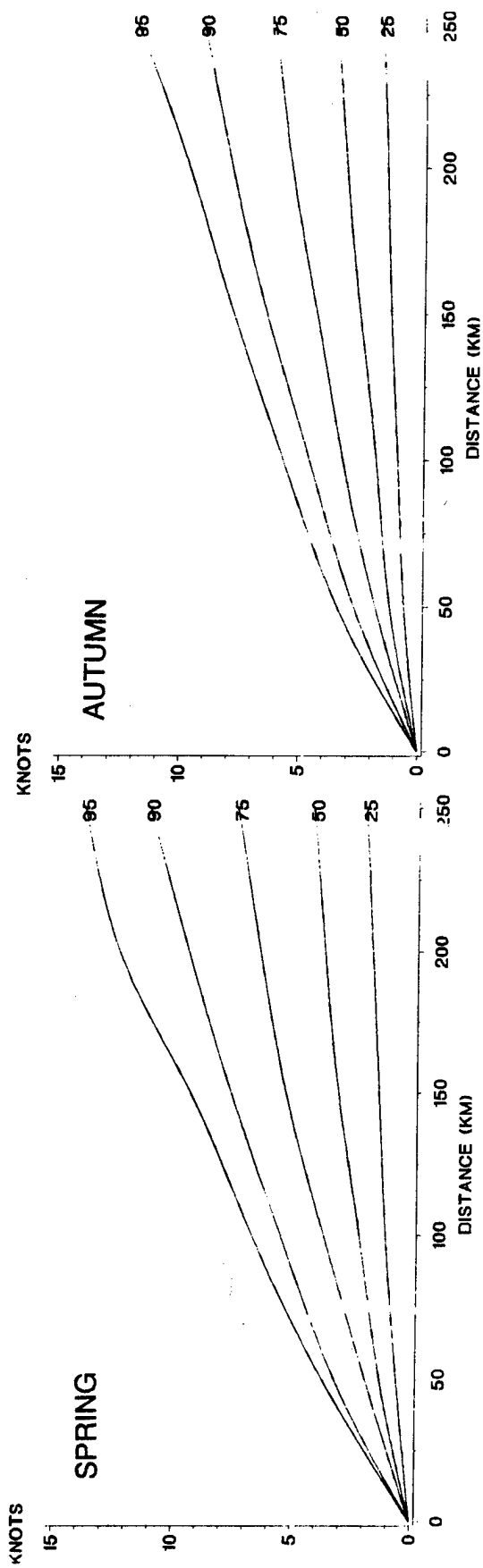


AUTUMN

C-2 Spatial correlation of wind speed, continental climate, sunrise.



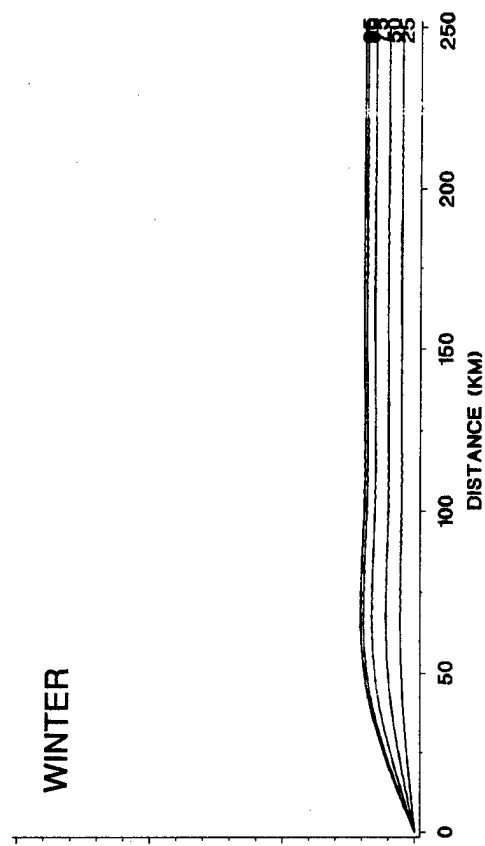
C-4



C-3 Spatial correlation of wind speed, continental climate, noon.

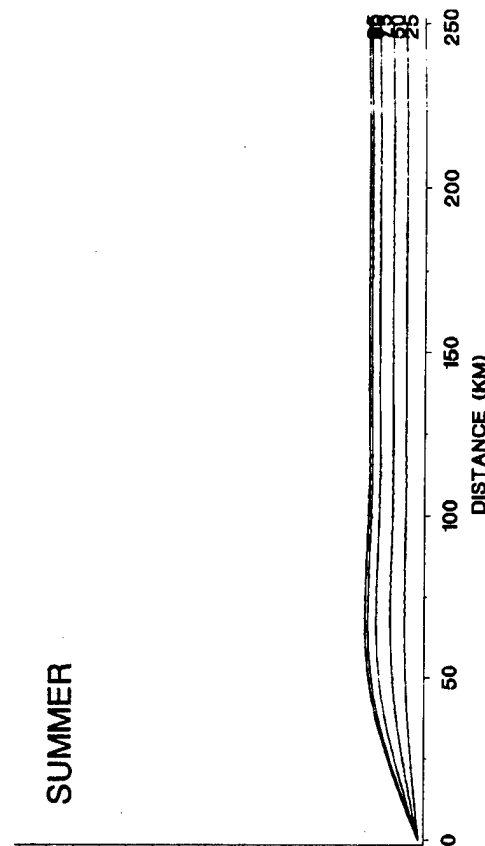
KNOTS

WINTER



KNOTS

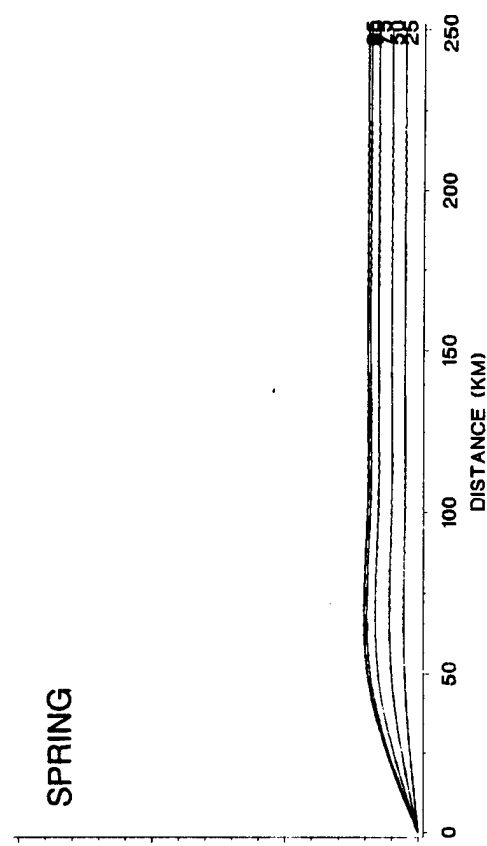
SUMMER



C-51

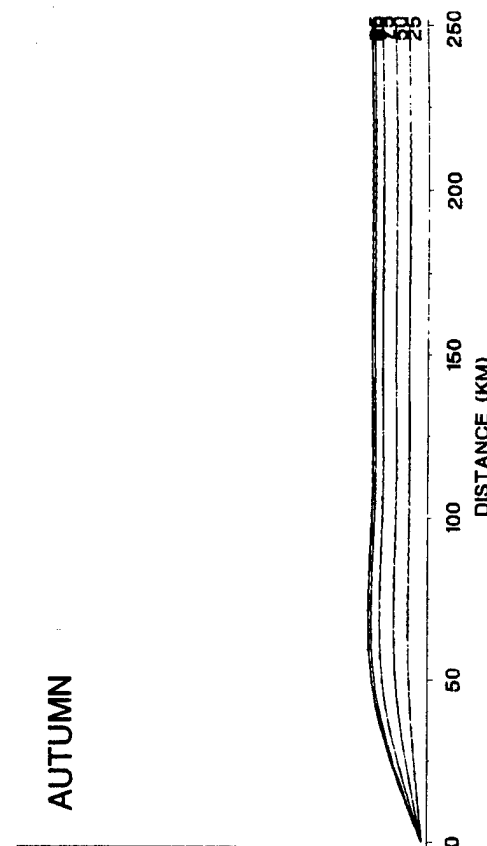
KNOTS

SPRING

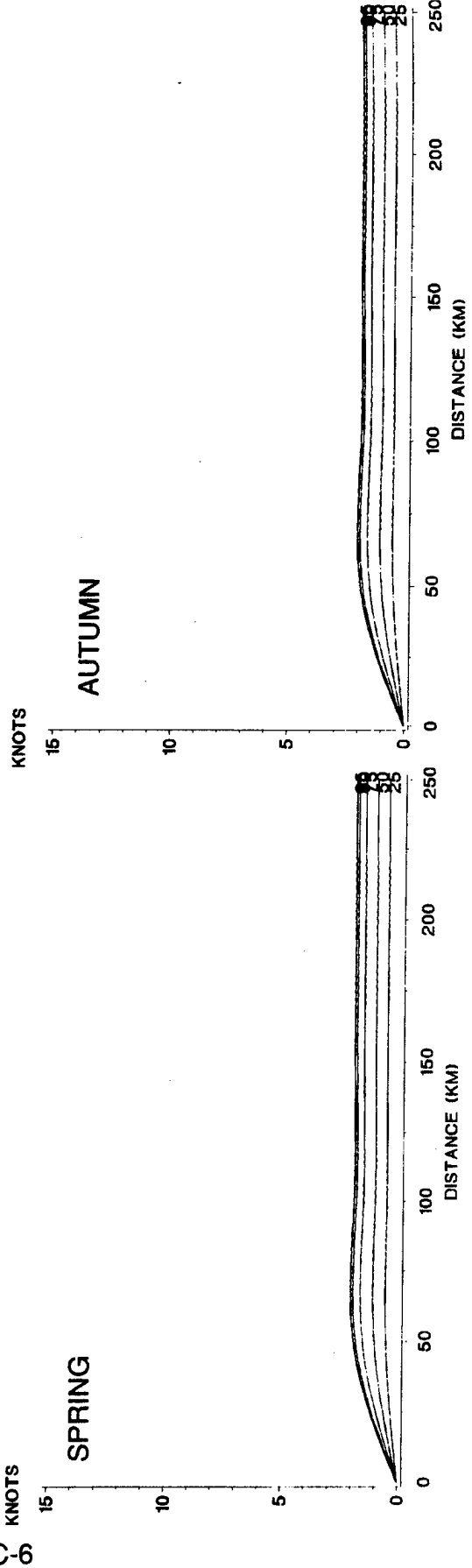
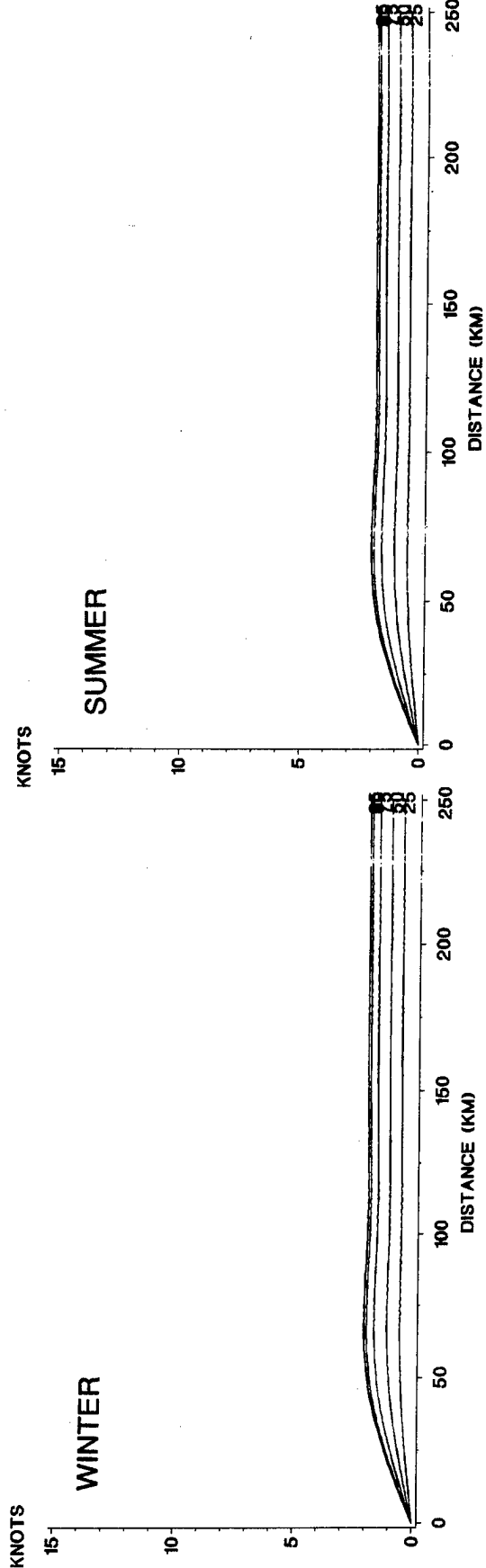


KNOTS

AUTUMN



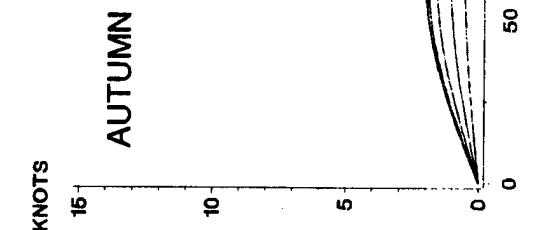
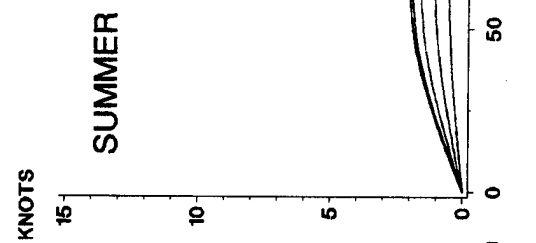
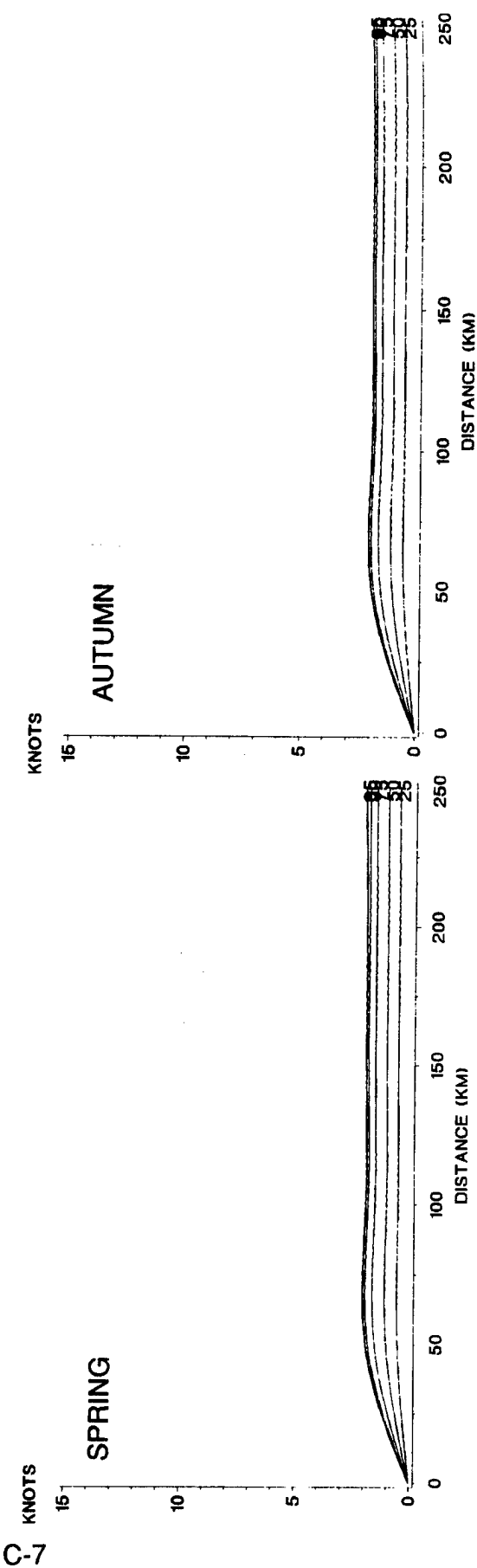
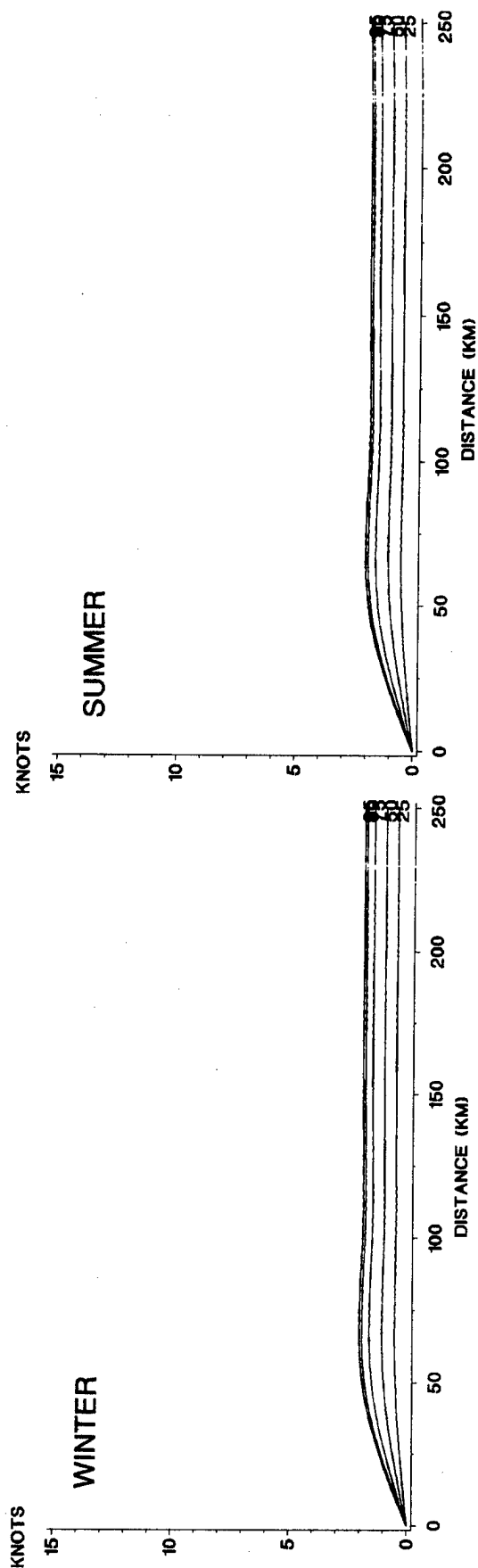
C-4 Spatial correlation of wind speed, arctic climate, midnight.



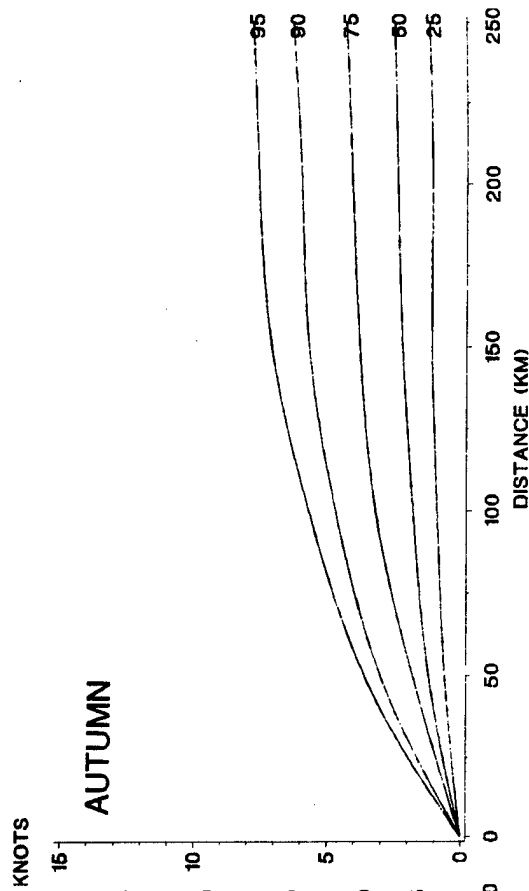
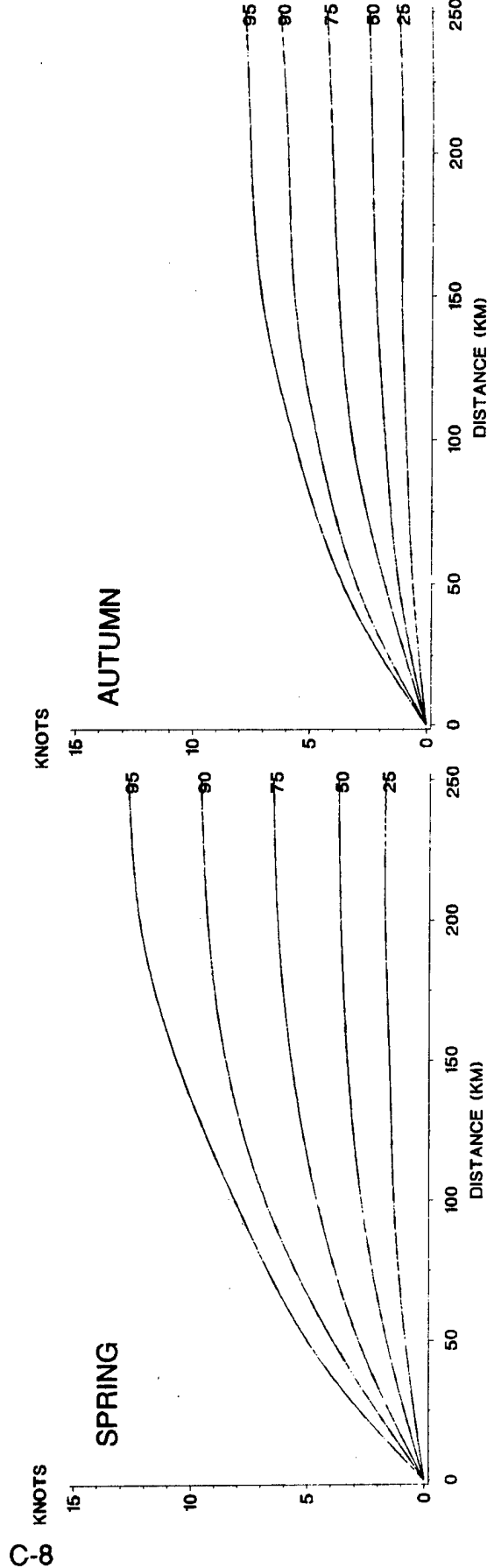
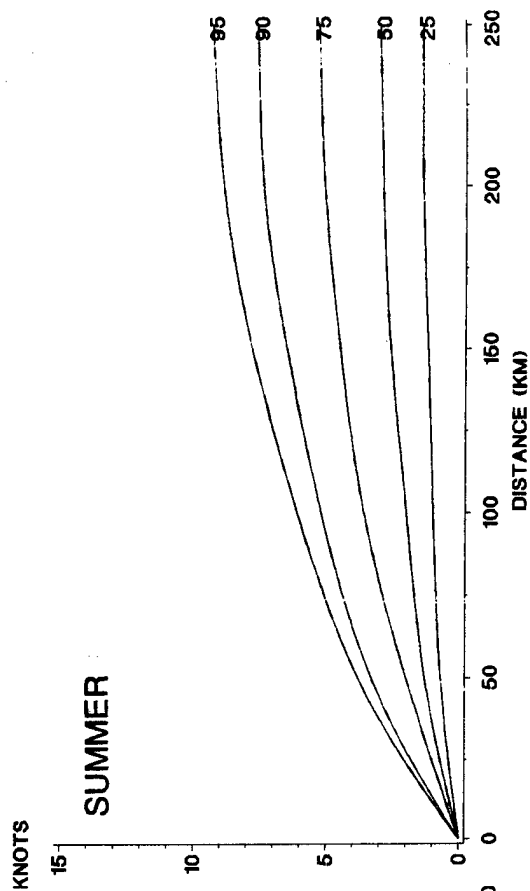
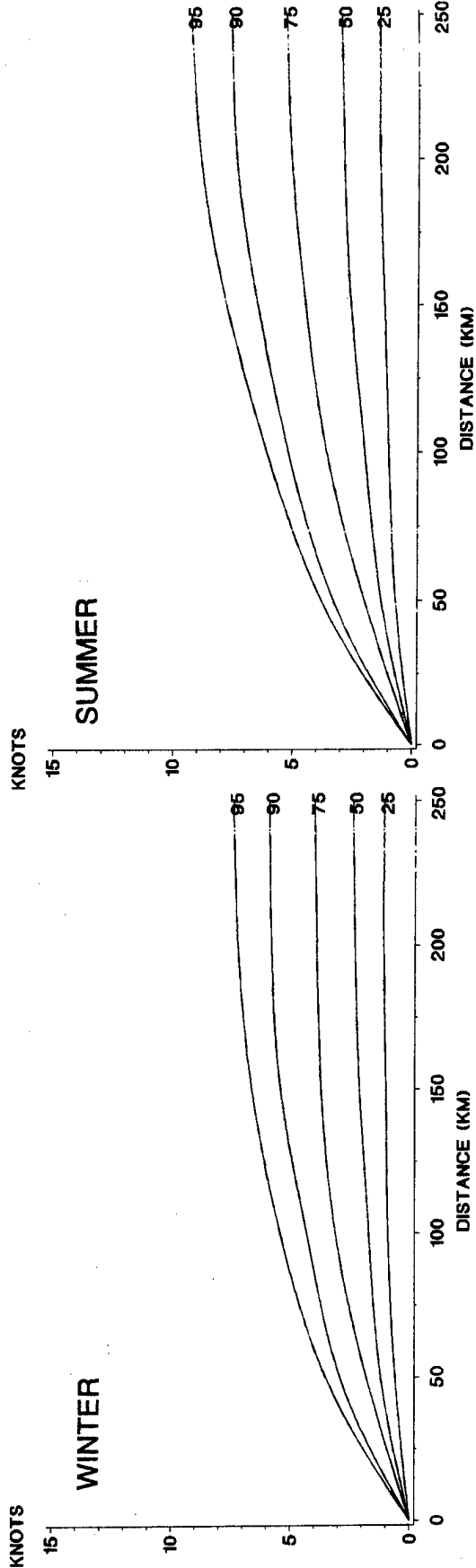
SUMMER

AUTUMN

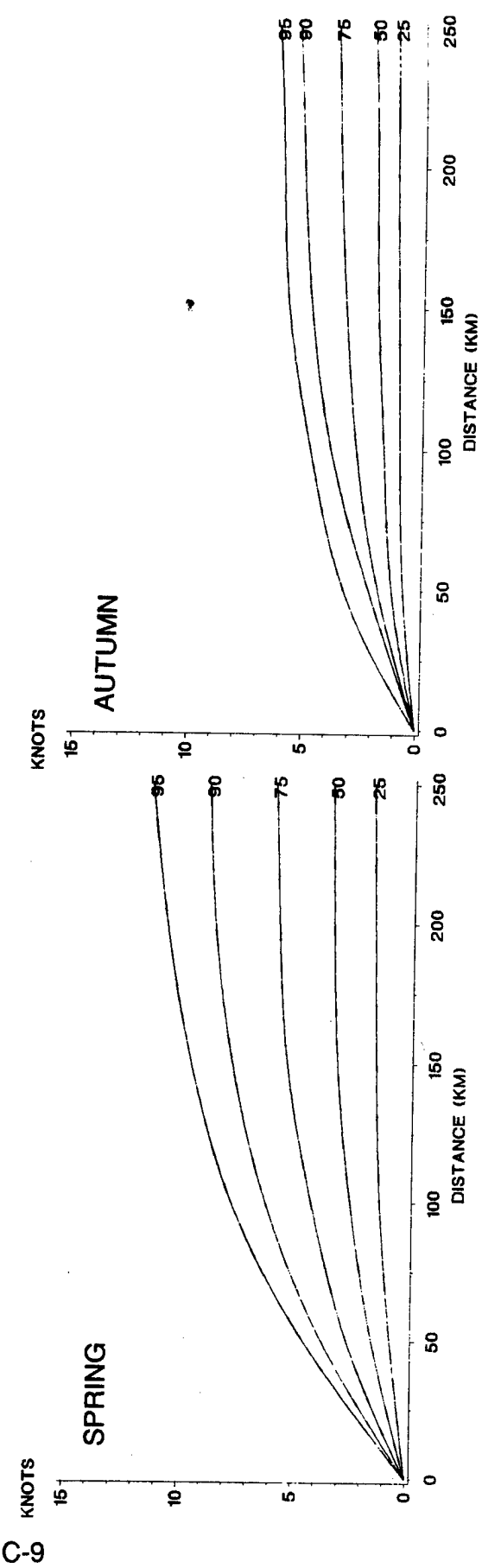
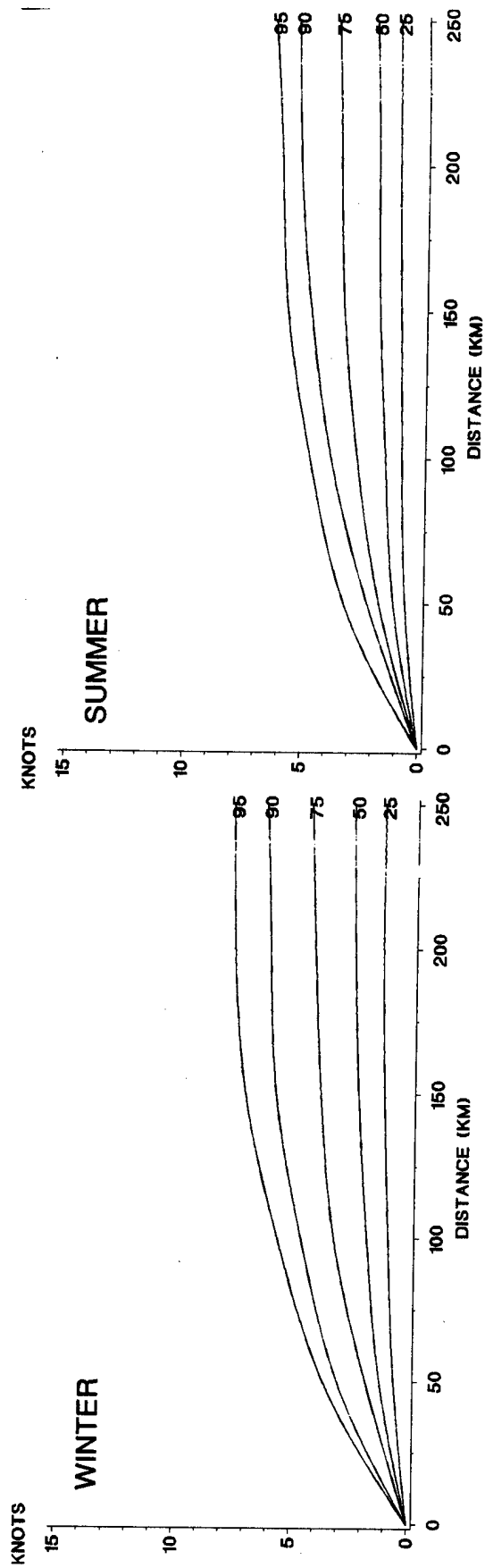
C-5 Spatial correlation of wind speed, arctic climate, sunrise.



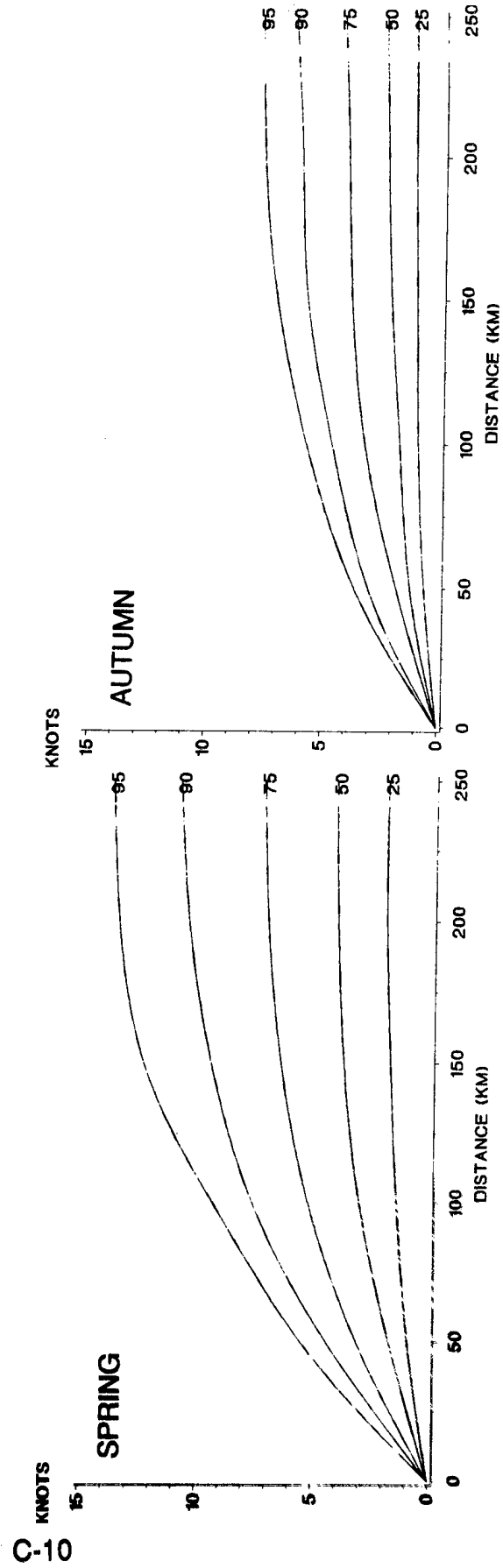
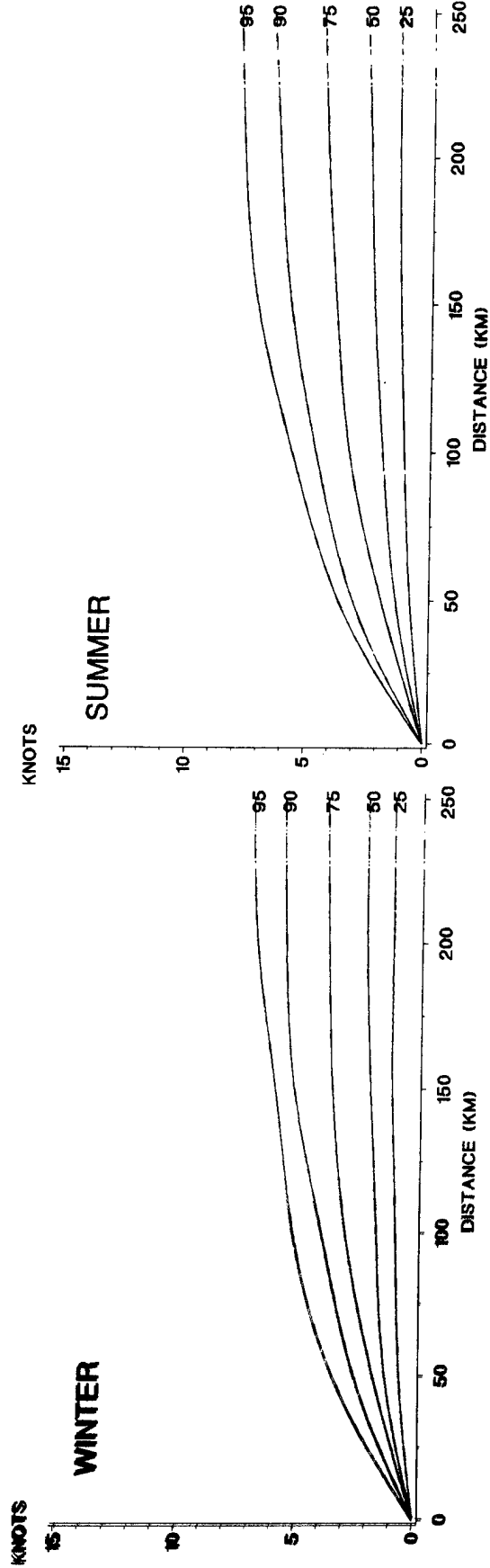
C-6 Spatial correlation of wind speed, arctic climate, noon.



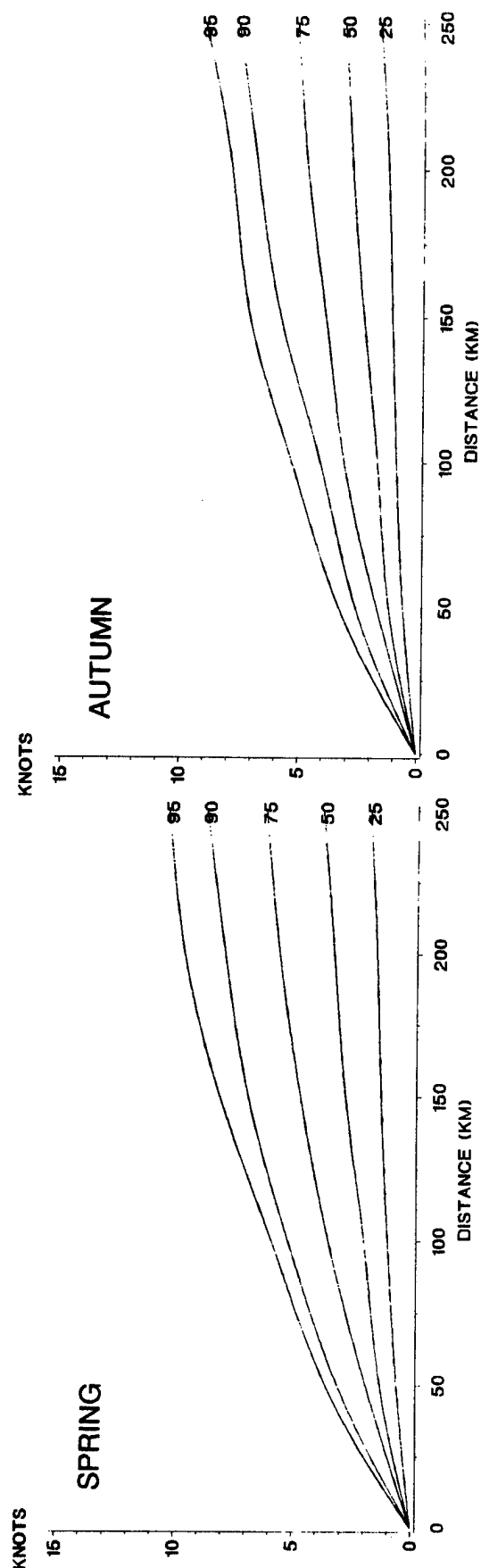
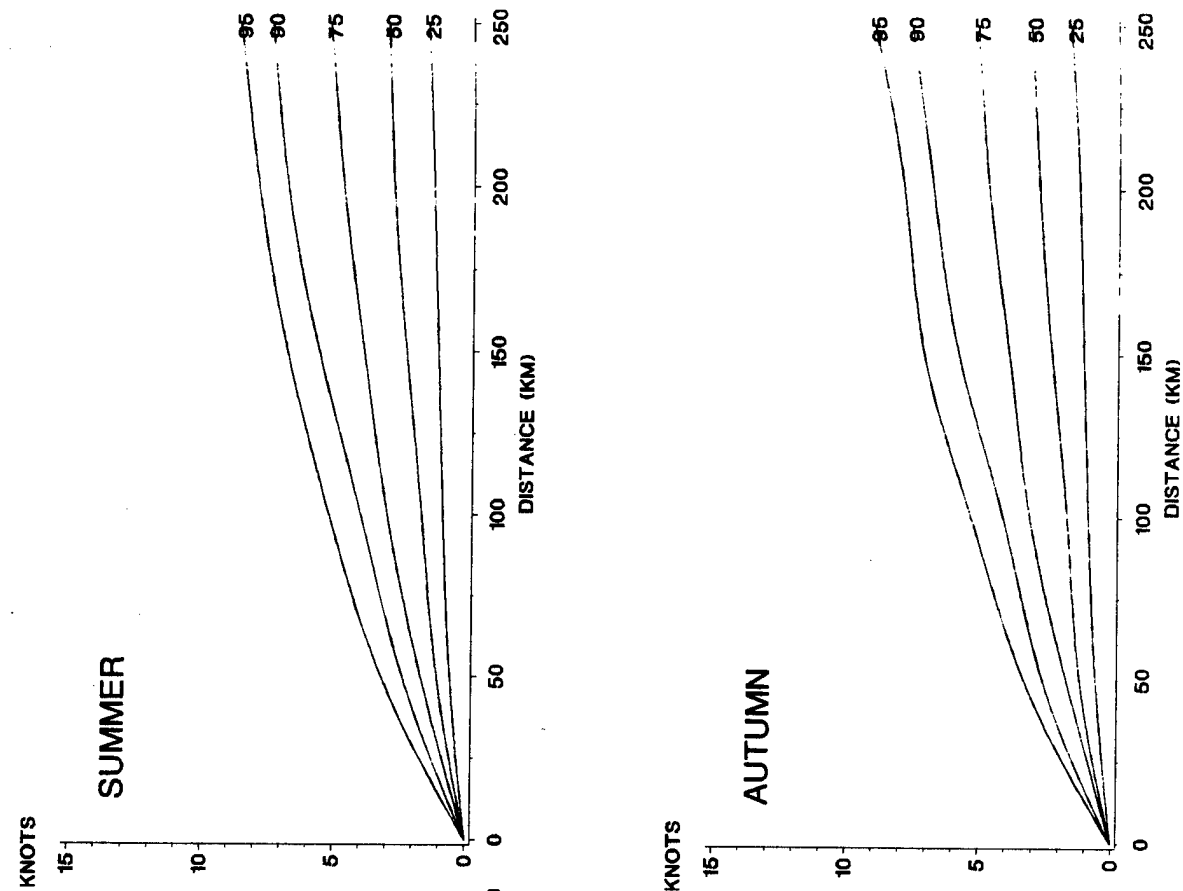
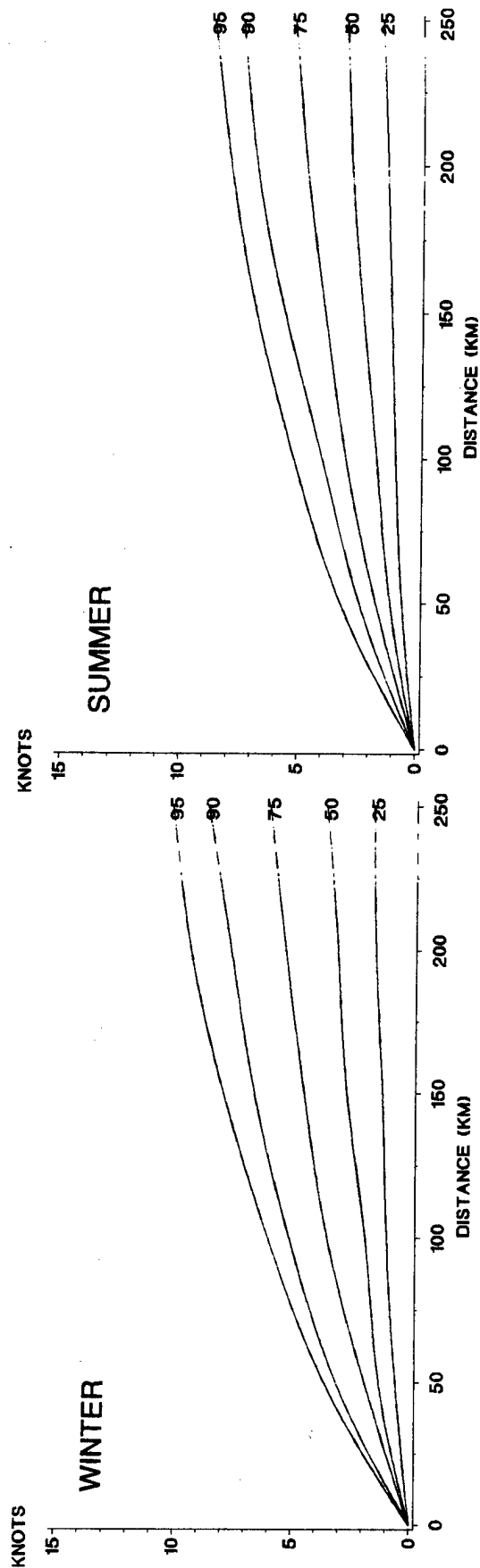
C-7 Spatial correlation of wind speed, desert climate, midnight.



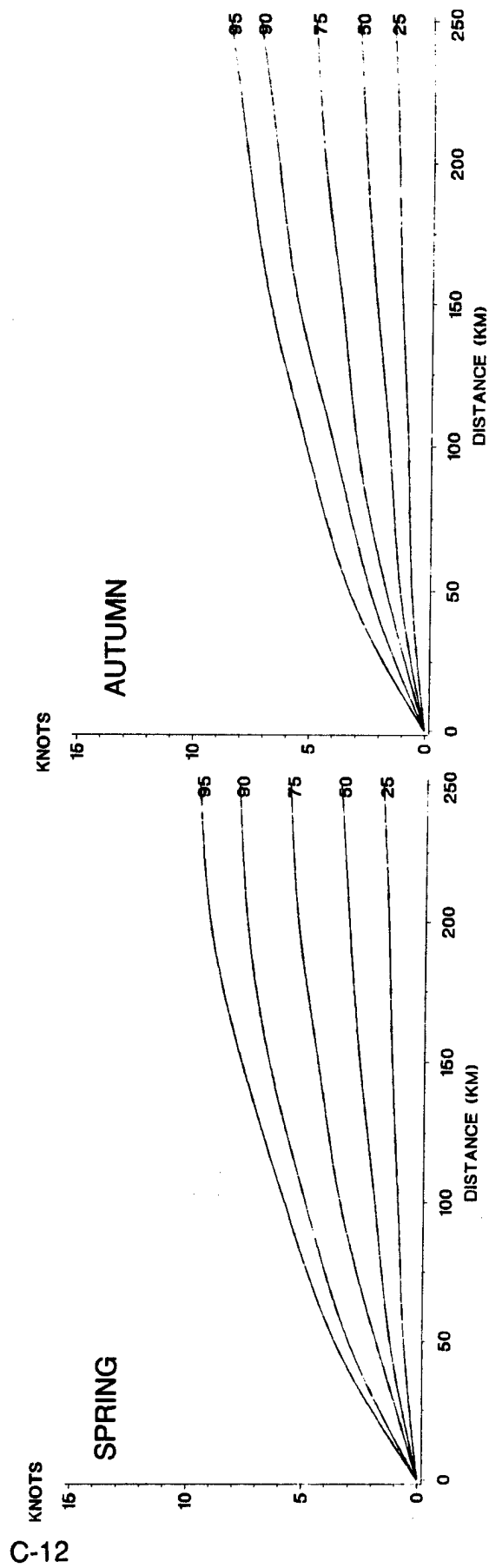
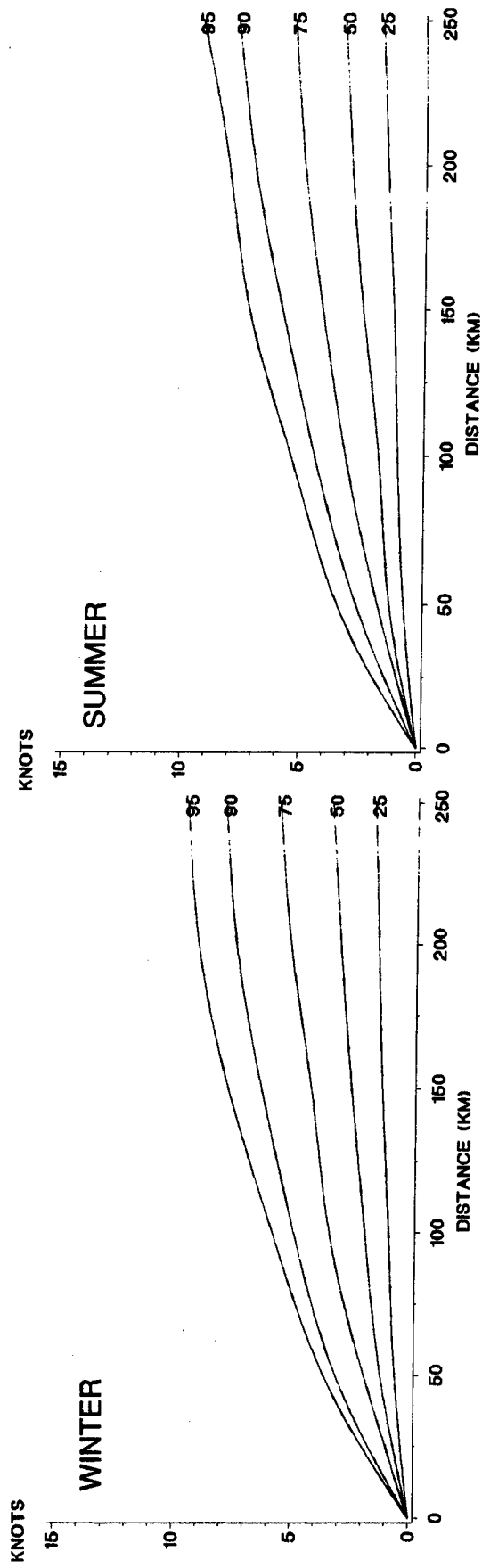
C-8 Spatial correlation of wind speed, desert climate, sunrise.



C-9 Spatial correlation of wind speed, desert climate, noon.



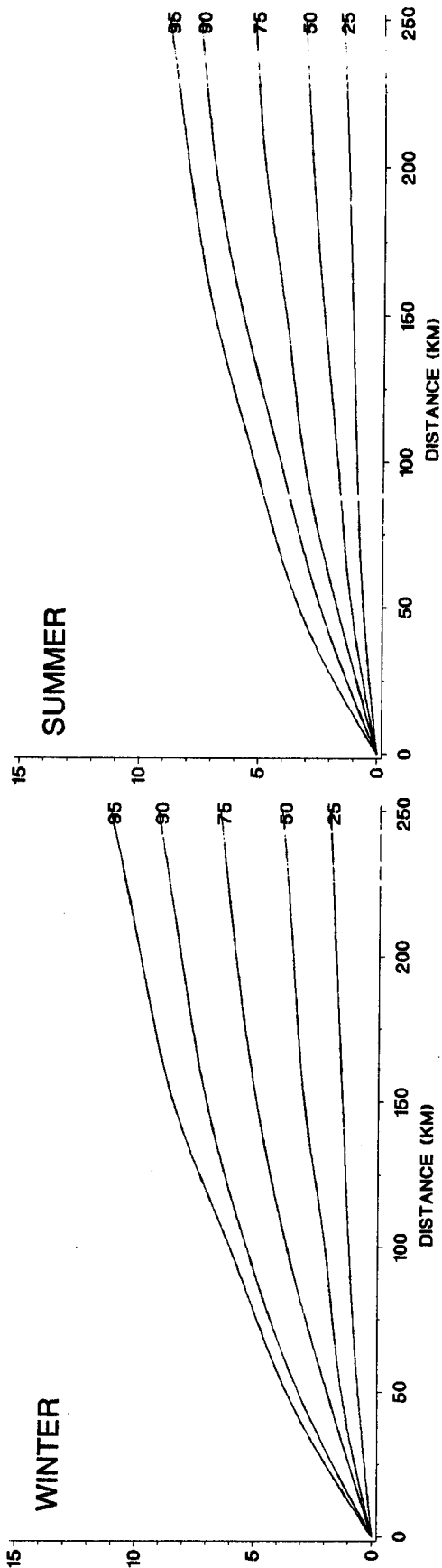
C-10 Spatial correlation of wind speed, maritime climate, midnight.



C-11 Spatial correlation of wind speed, maritime climate, sunrise.

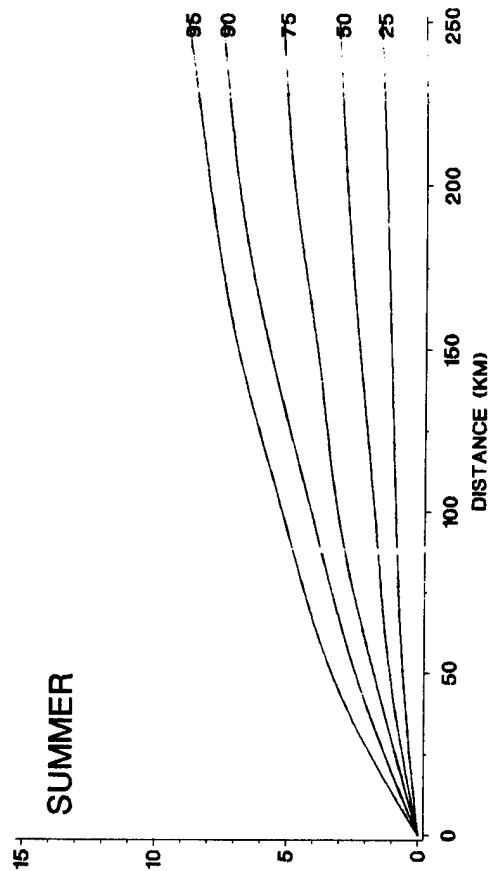
KNOTS

WINTER



KNOTS

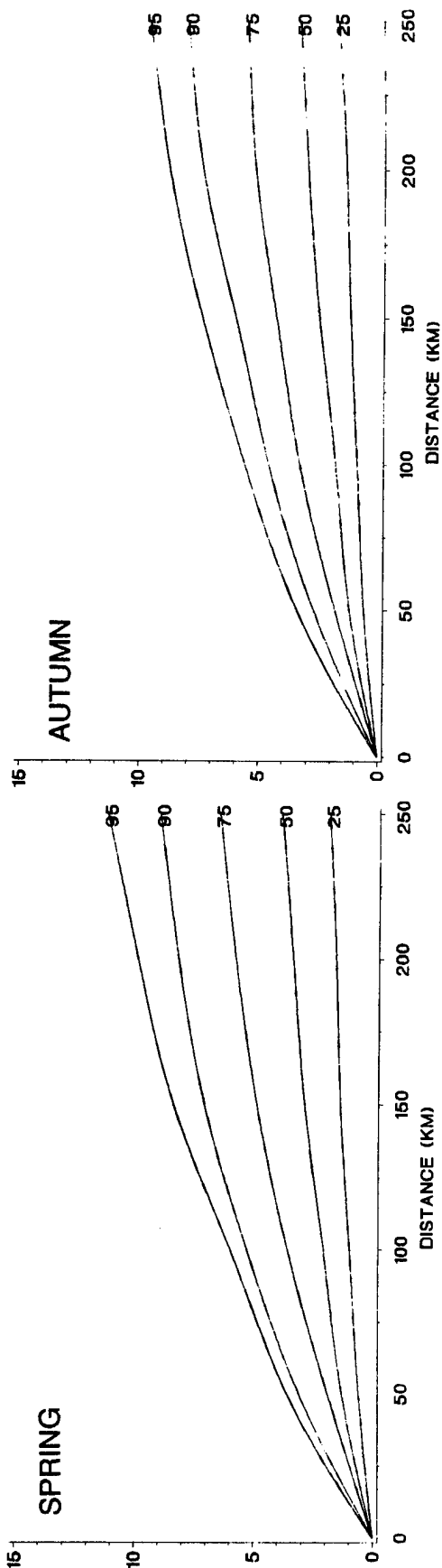
SUMMER



C-13

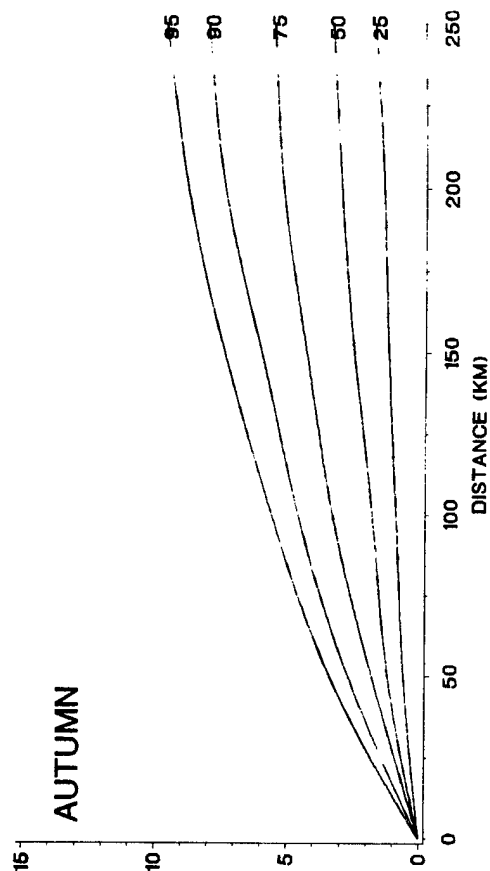
KNOTS

SPRING

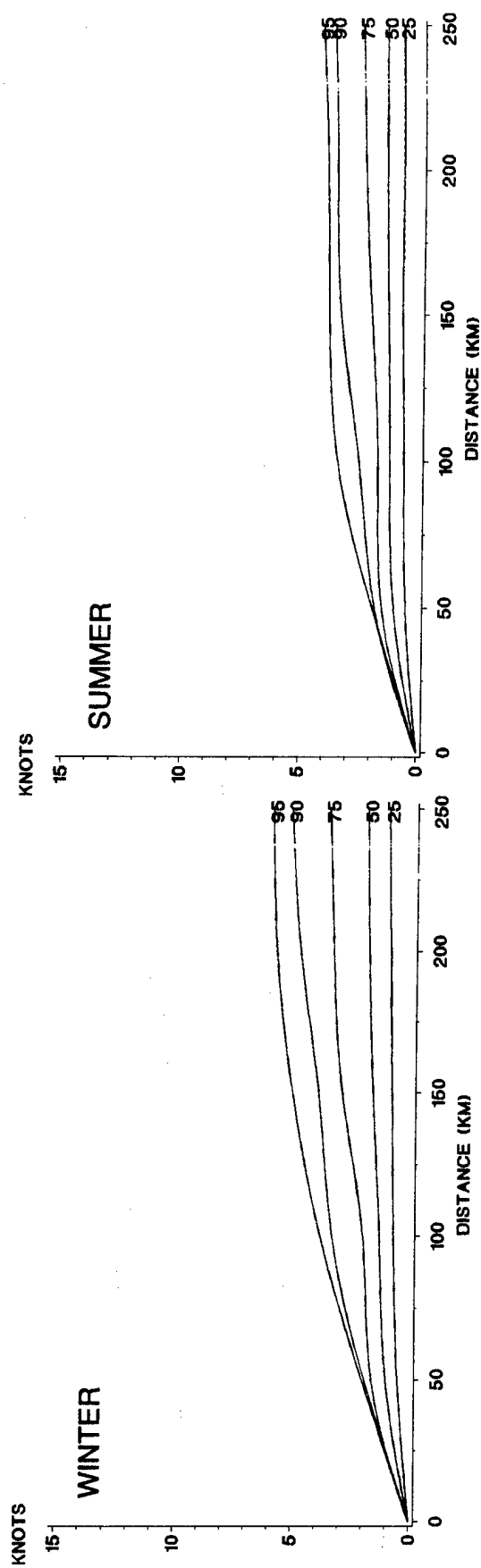


KNOTS

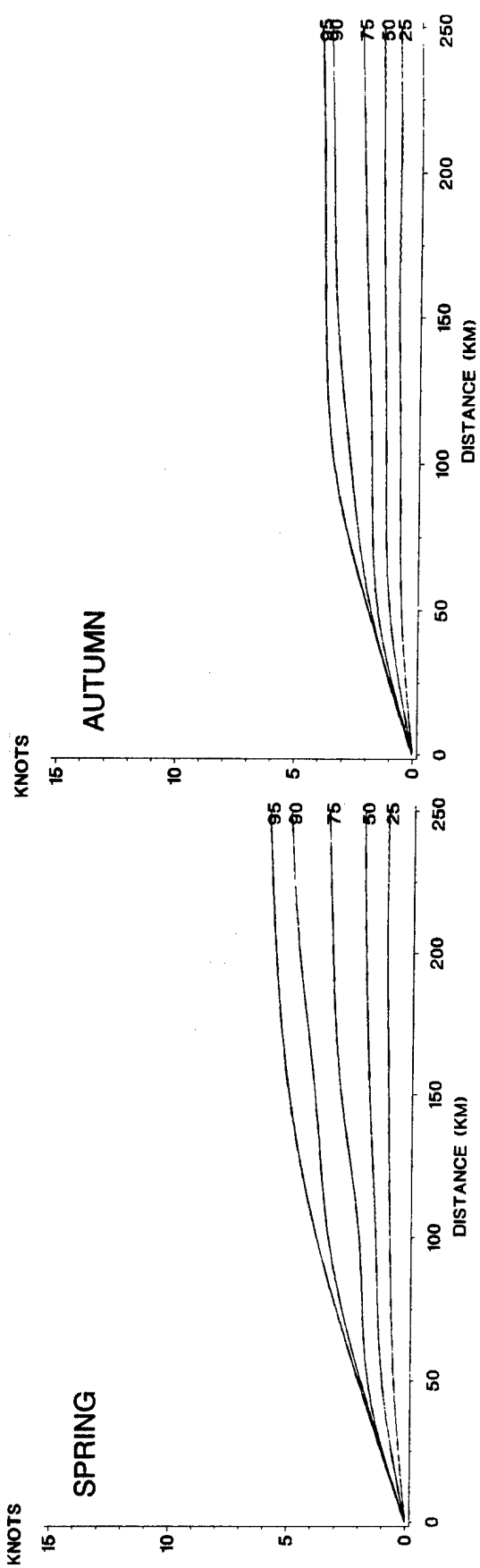
AUTUMN



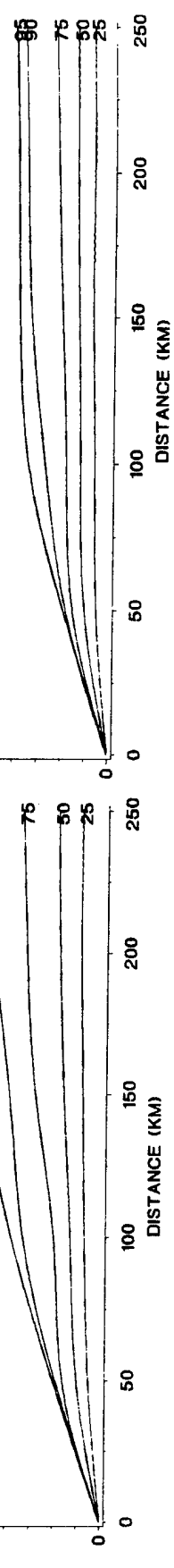
C-12 Spatial correlation of wind speed, maritime climate, noon.



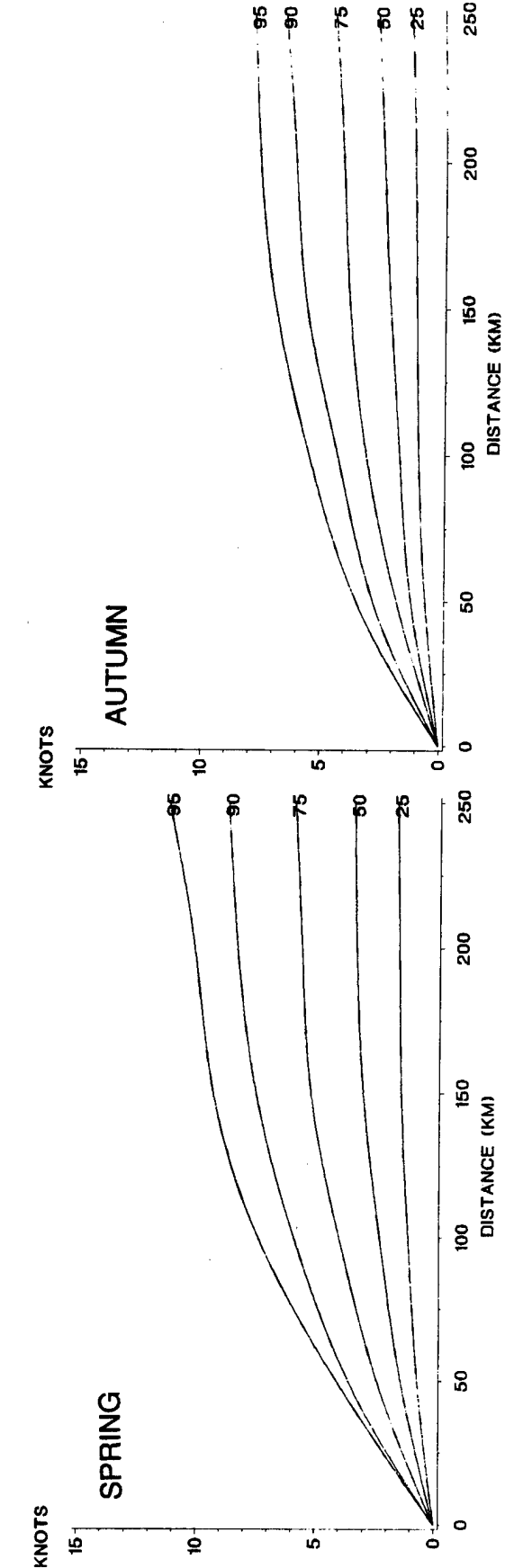
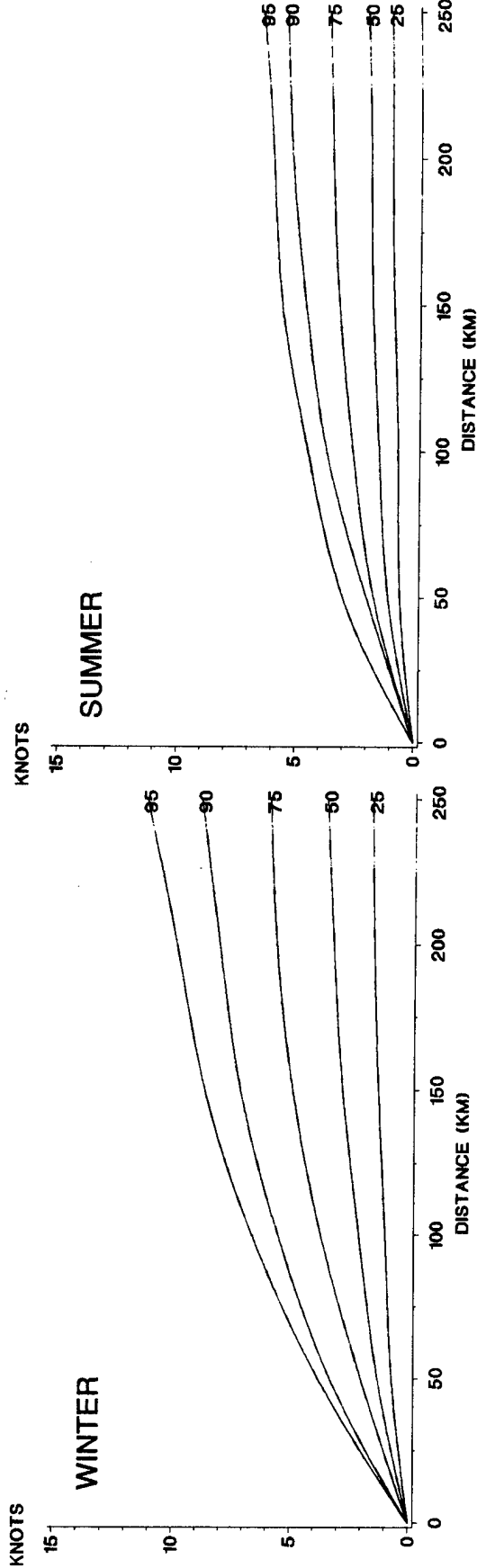
SUMMER



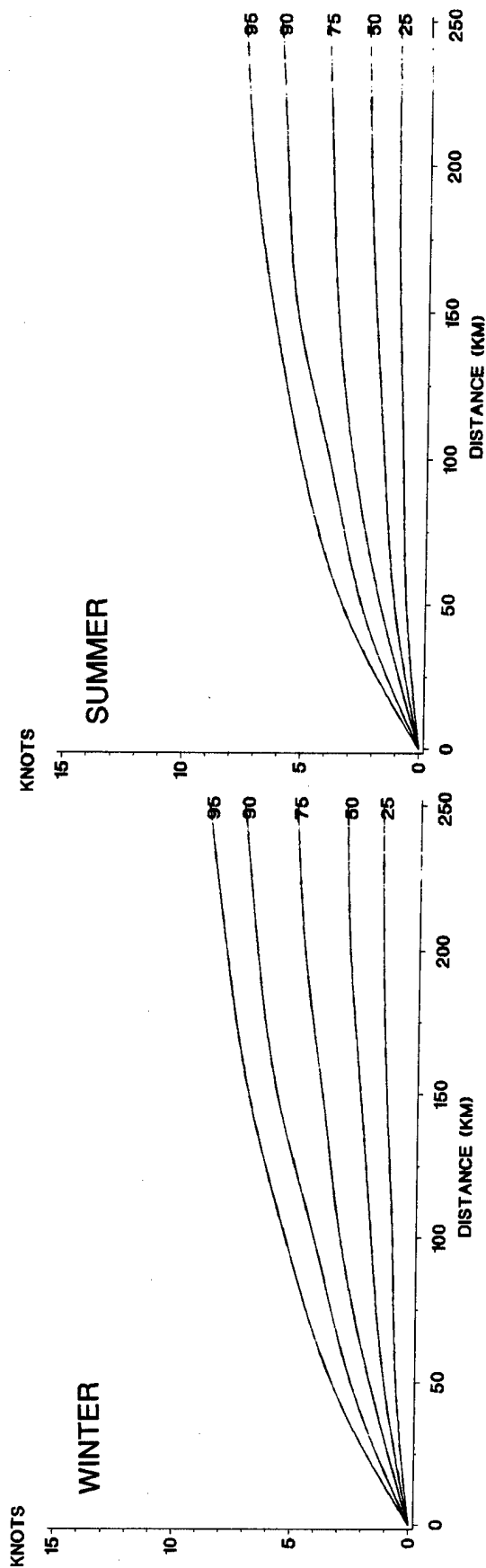
AUTUMN



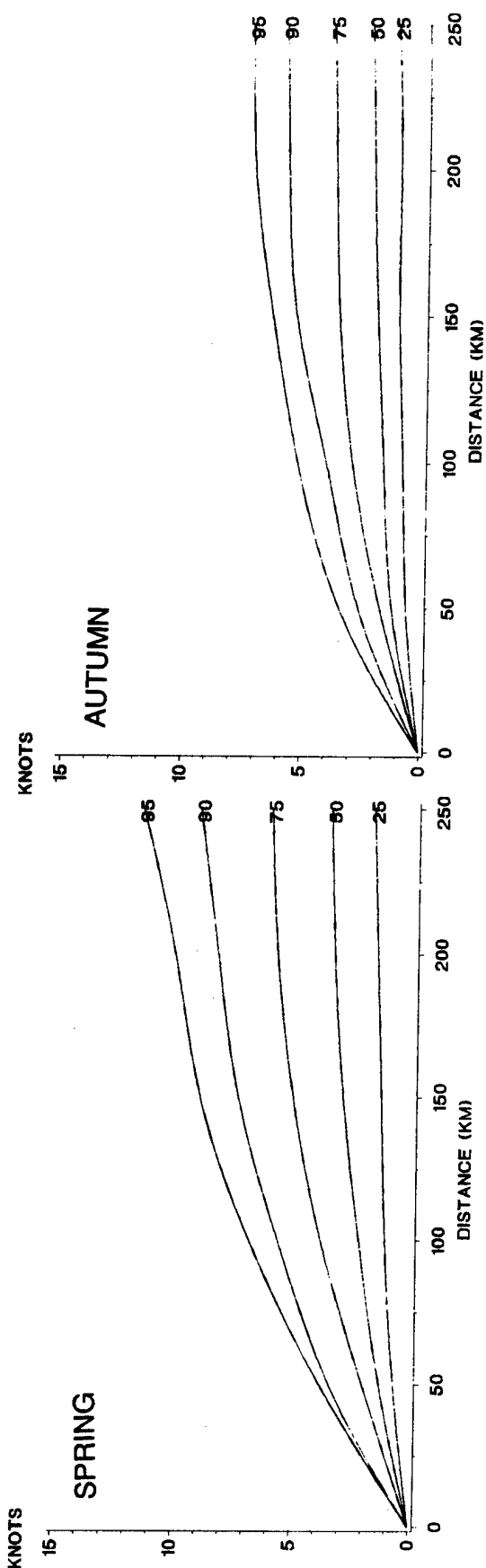
C-13 Spatial correlation of wind speed, tropical climate, midnight.



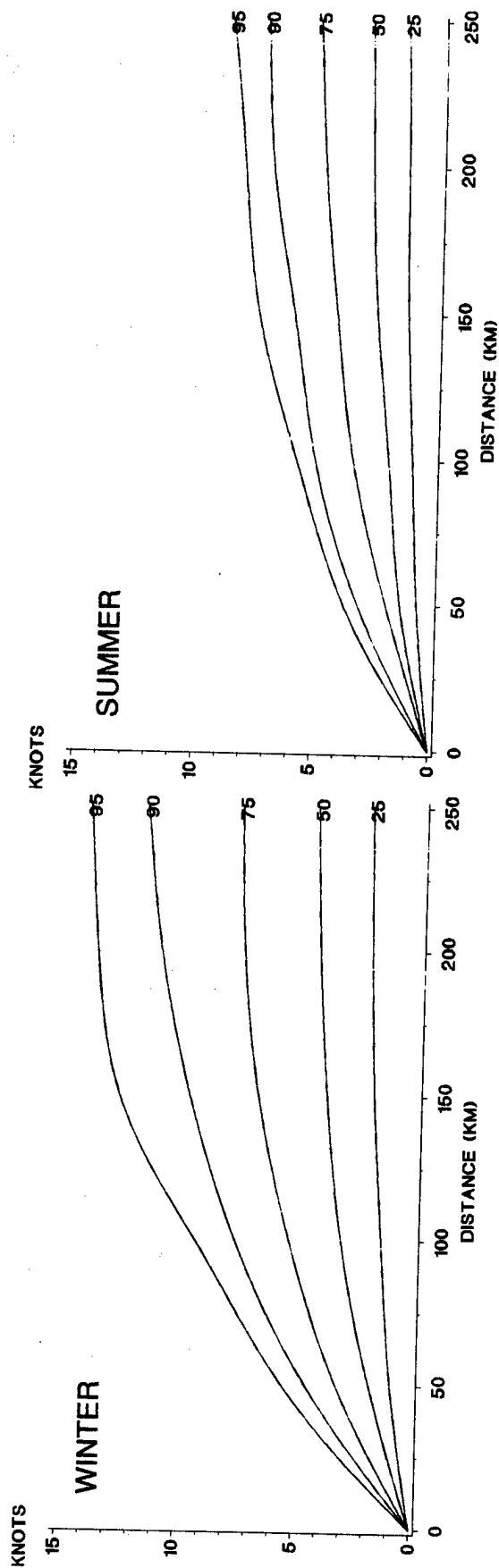
C-14 Spatial correlation of wind speed, tropical climate, sunrise.



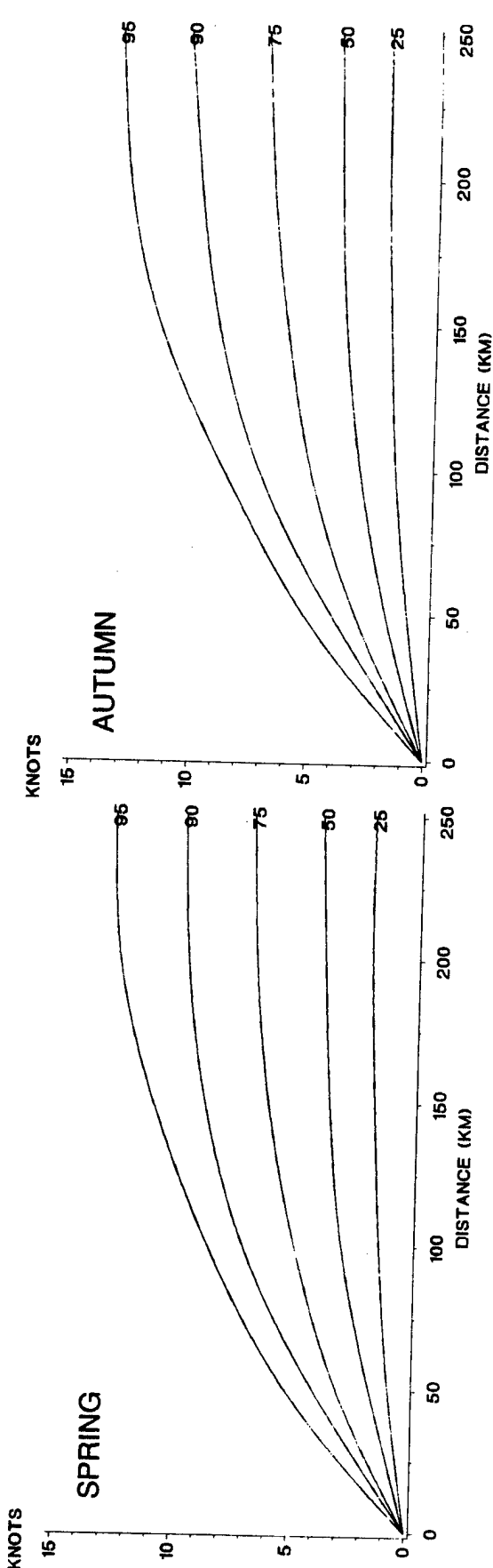
C-16



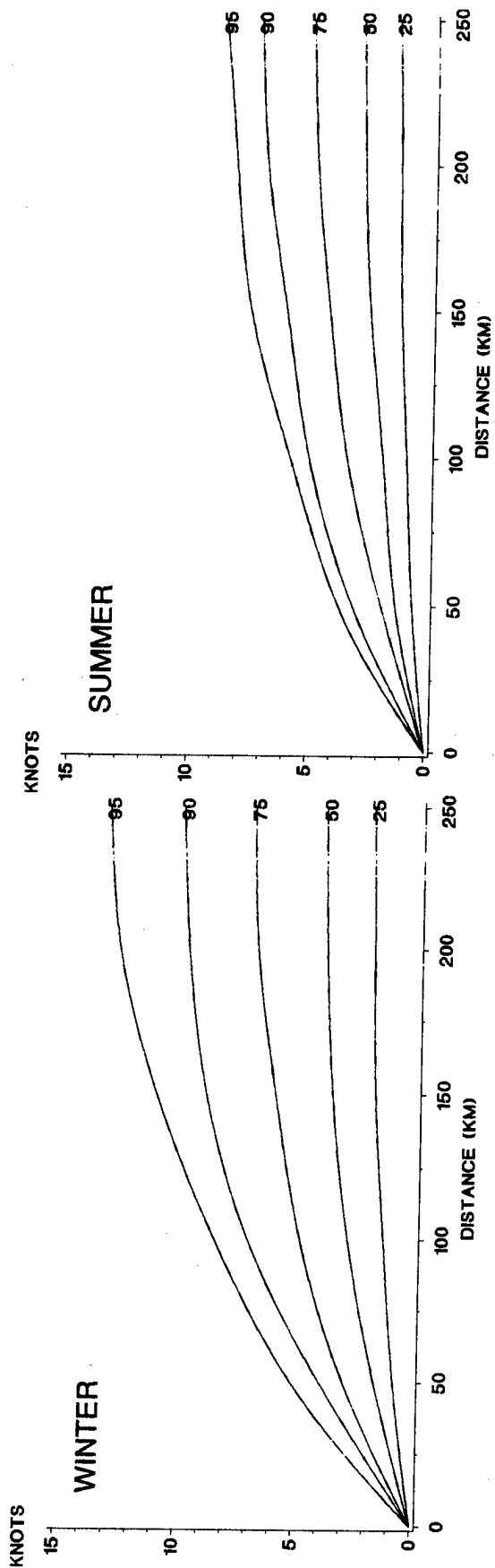
C-15 Spatial correlation of wind speed, tropical climate, noon.



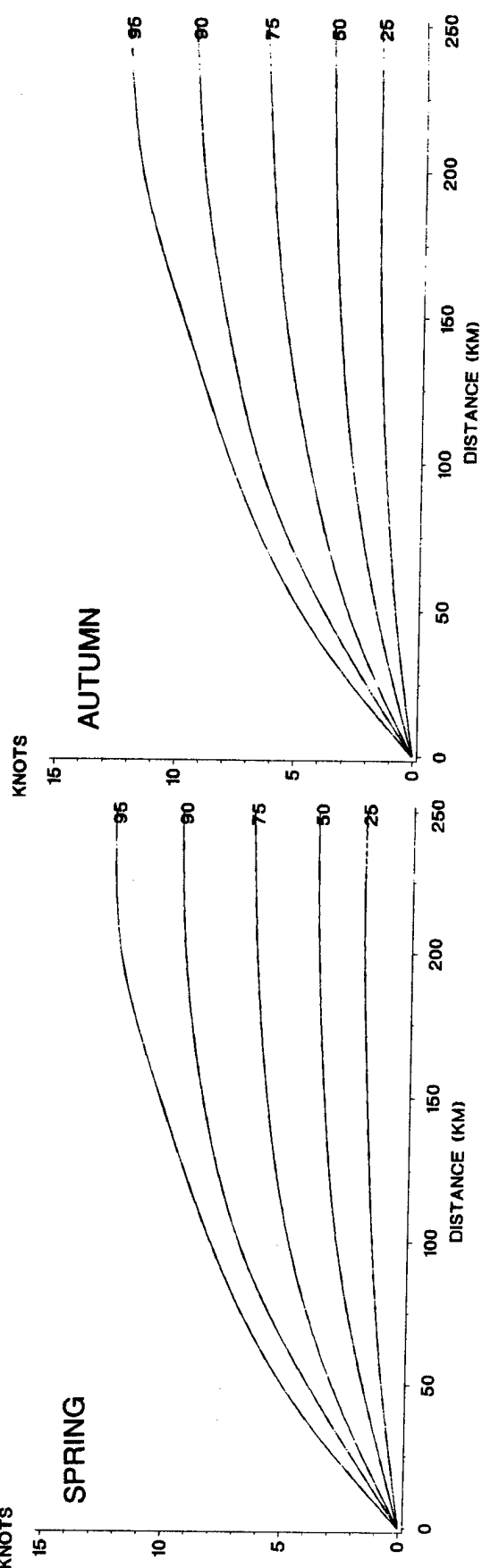
C-17



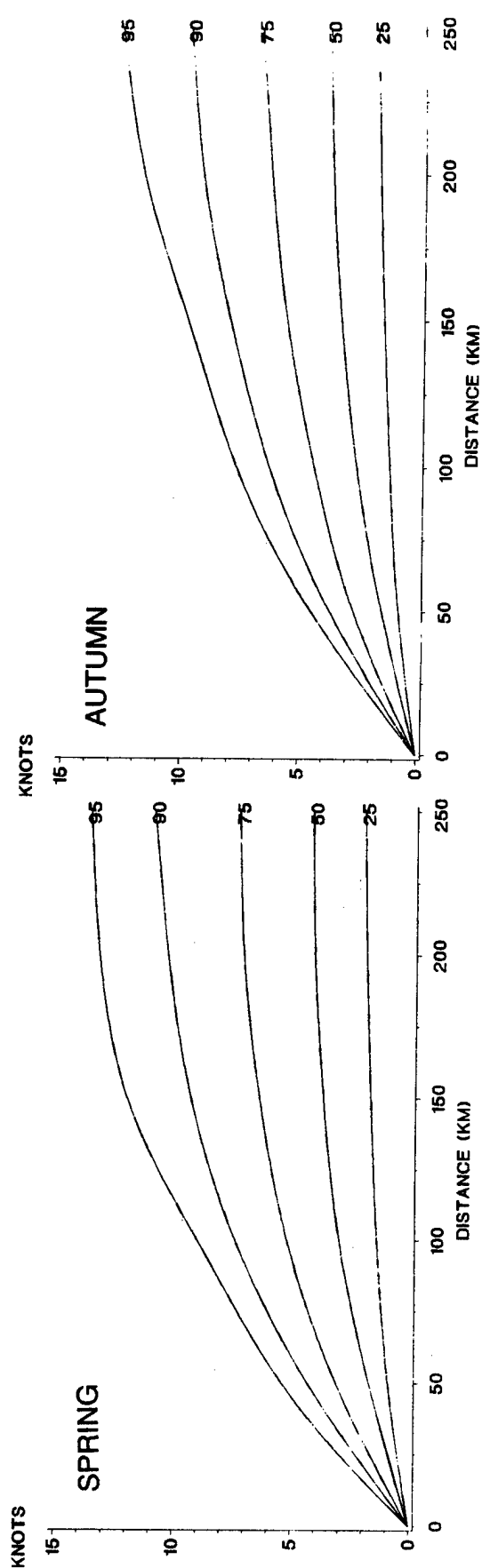
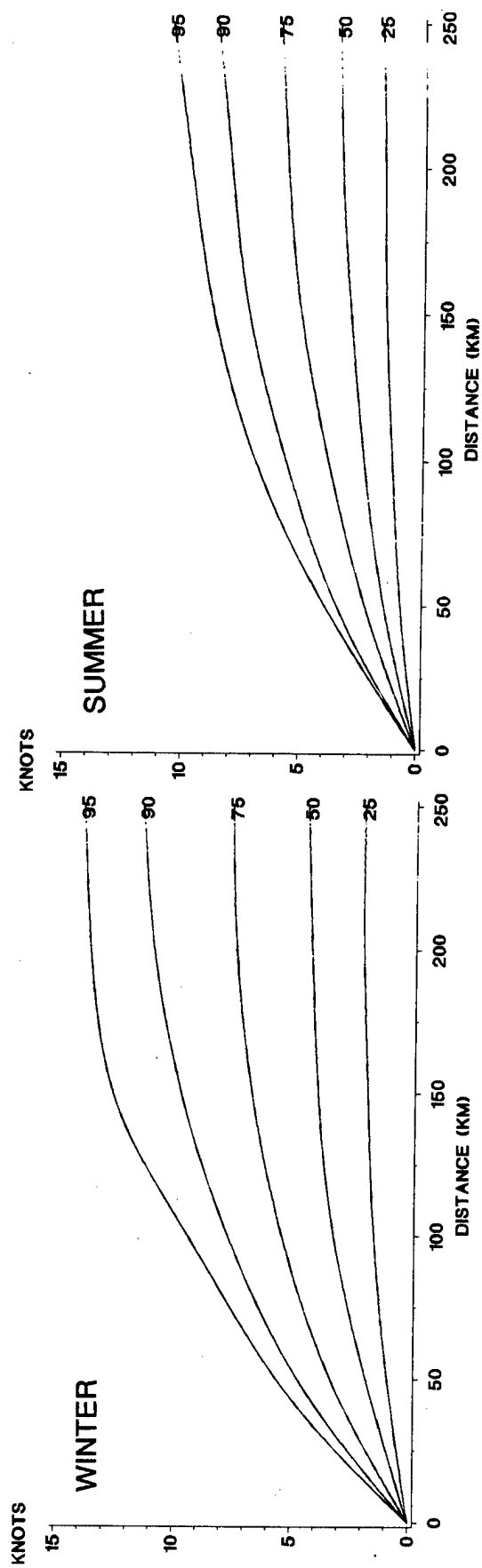
C-16 Spatial correlation of wind speed, coastal climate, midnight.



C-18



C-17 Spatial correlation of wind speed, coastal climate, sunrise.

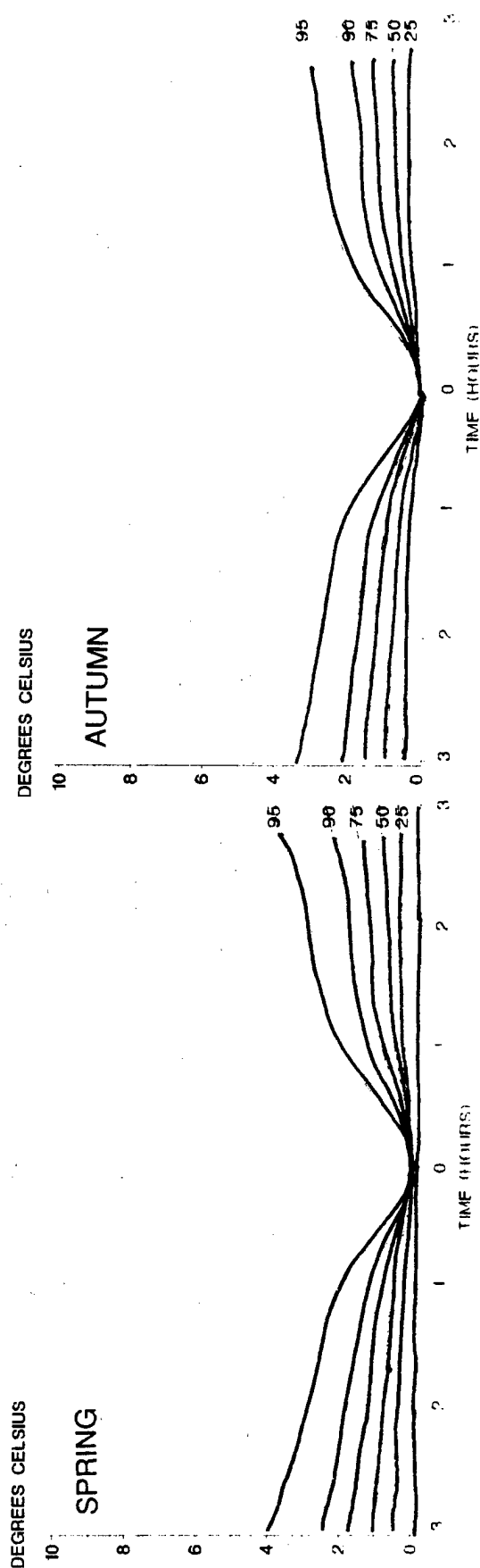
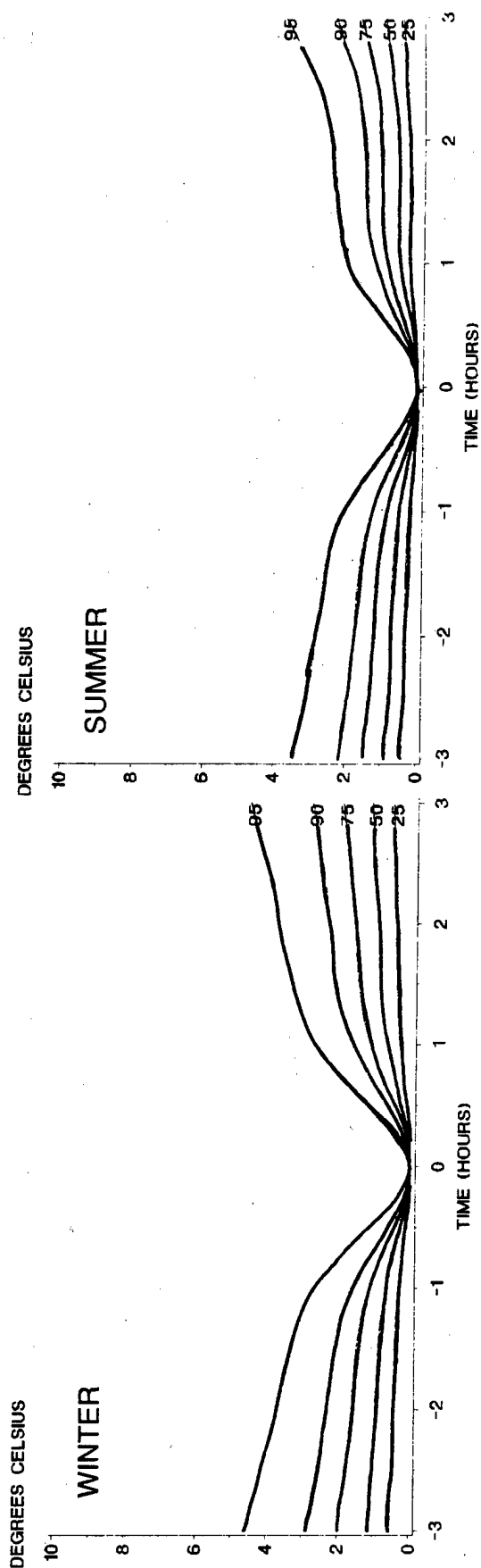


C-18 Spatial correlation of wind speed, coastal climate, noon.

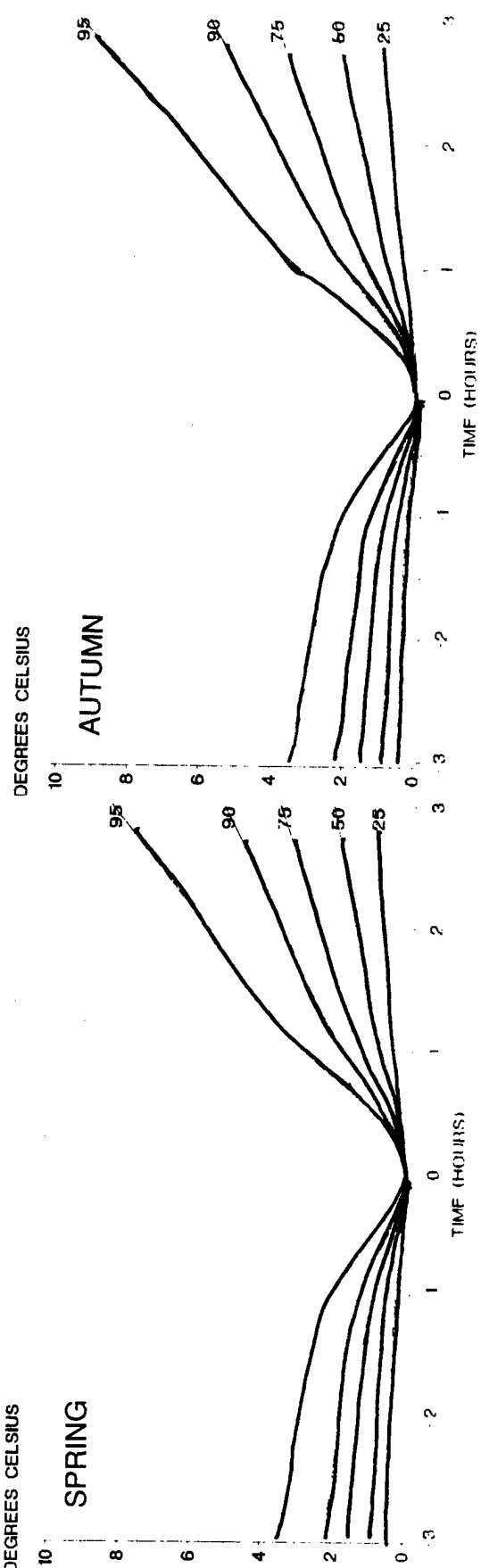
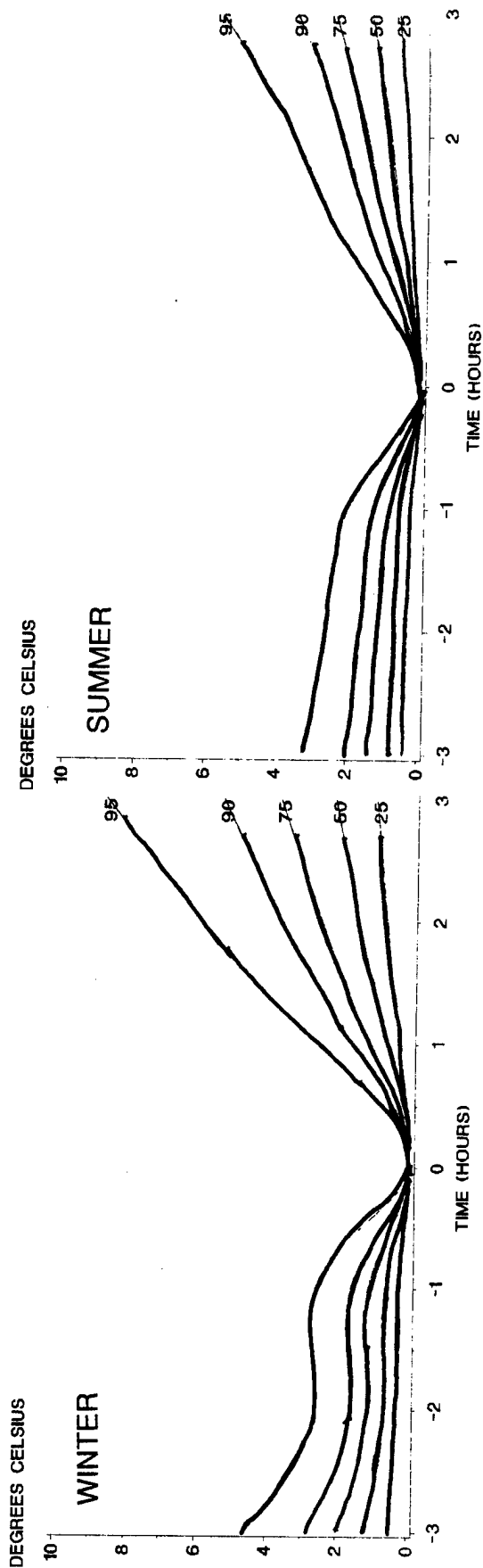
APPENDIX D

TEMPORAL CORRELATION OF TEMPERATURE

- D-1 Temporal correlation of temperature, continental climate, midnight.
- D-2 Temporal correlation of temperature, continental climate, sunrise.
- D-3 Temporal correlation of temperature, continental climate, noon.
- D-4 Temporal correlation of temperature, arctic climate, midnight.
- D-5 Temporal correlation of temperature, arctic climate, sunrise.
- D-6 Temporal correlation of temperature, arctic climate, noon.
- D-7 Temporal correlation of temperature, desert climate, midnight.
- D-8 Temporal correlation of temperature, desert climate, sunrise.
- D-9 Temporal correlation of temperature, desert climate, noon.
- D-10 Temporal correlation of temperature, maritime climate, midnight.
- D-11 Temporal correlation of temperature, maritime climate, sunrise.
- D-12 Temporal correlation of temperature, maritime climate, noon.
- D-13 Temporal correlation of temperature, tropical climate, midnight.
- D-14 Temporal correlation of temperature, tropical climate, sunrise.
- D-15 Temporal correlation of temperature, tropical climate, noon.
- D-16 Temporal correlation of temperature, coastal climate, midnight.
- D-17 Temporal correlation of temperature, coastal climate, sunrise.
- D-18 Temporal correlation of temperature, coastal climate, noon.



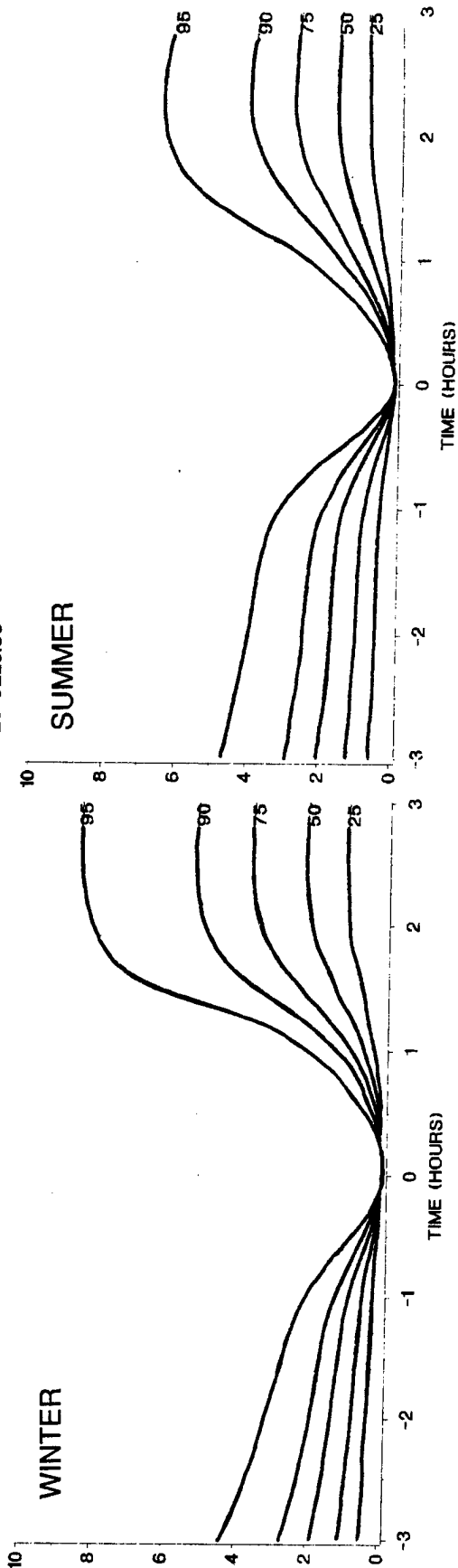
D-1 Temporal correlation of temperature, continental climate, midnight.



D-2 Temporal correlation of temperature, continental climate, sunrise.

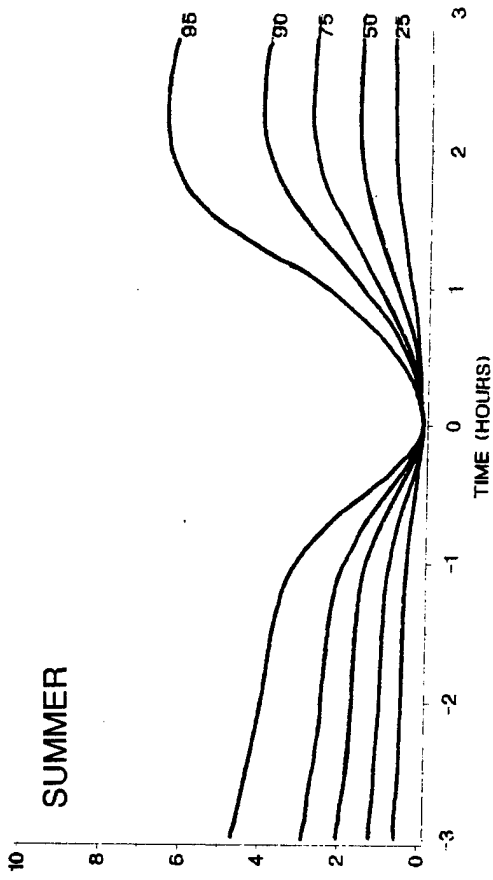
DEGREES CELSIUS

WINTER



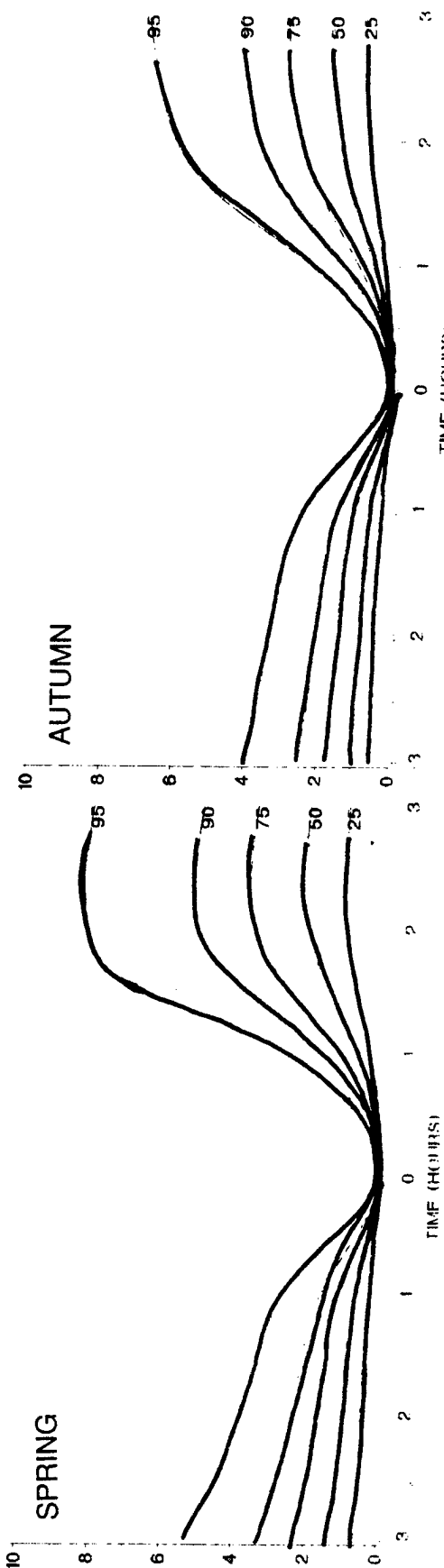
DEGREES CELSIUS

SUMMER



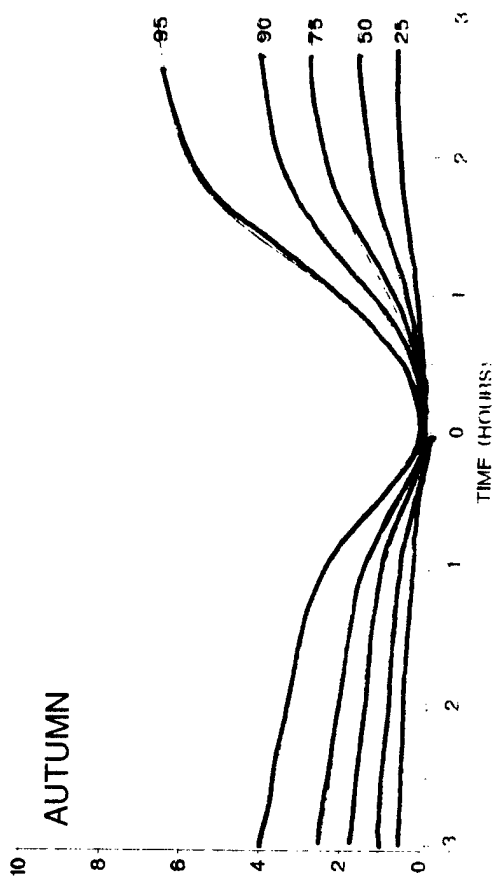
DEGREES CELSIUS

SPRING



DEGREES CELSIUS

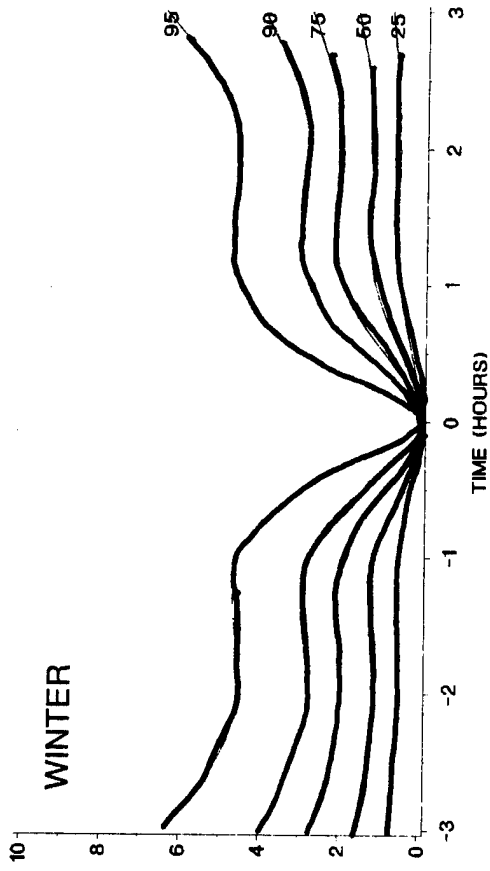
AUTUMN



D-3 Temporal correlation of temperature, continental climate, noon.

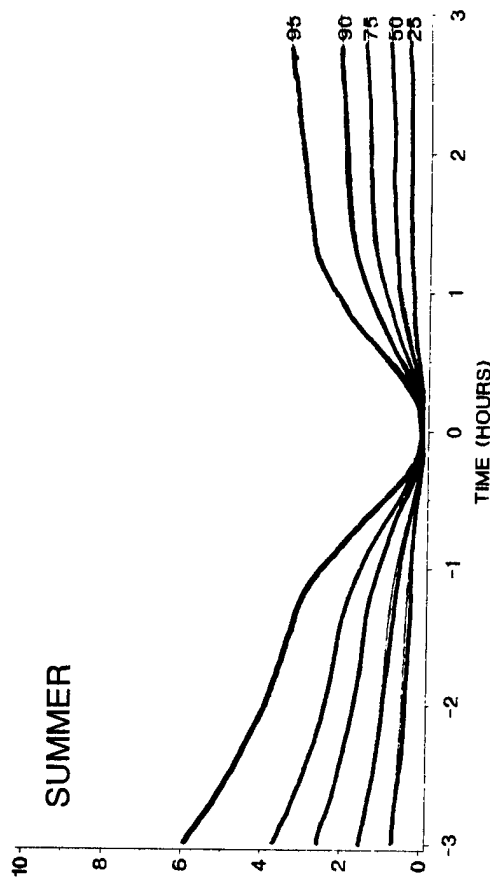
DEGREES CELSIUS

WINTER



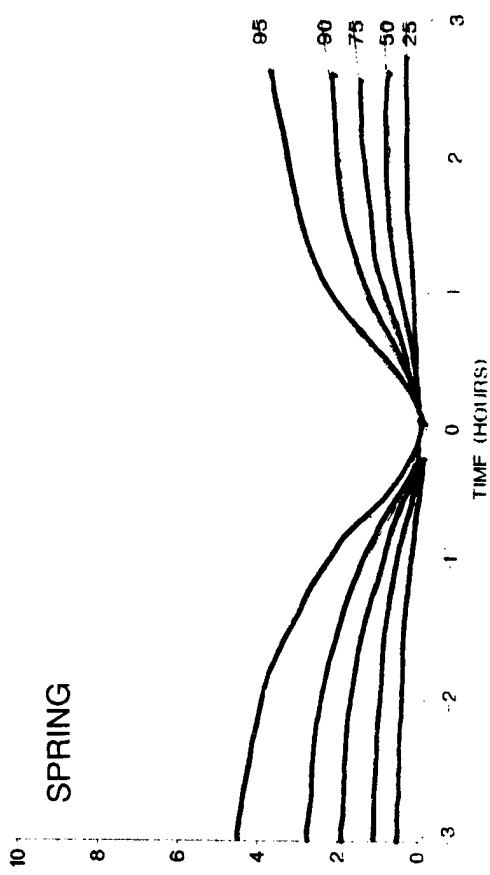
DEGREES CELSIUS

SUMMER



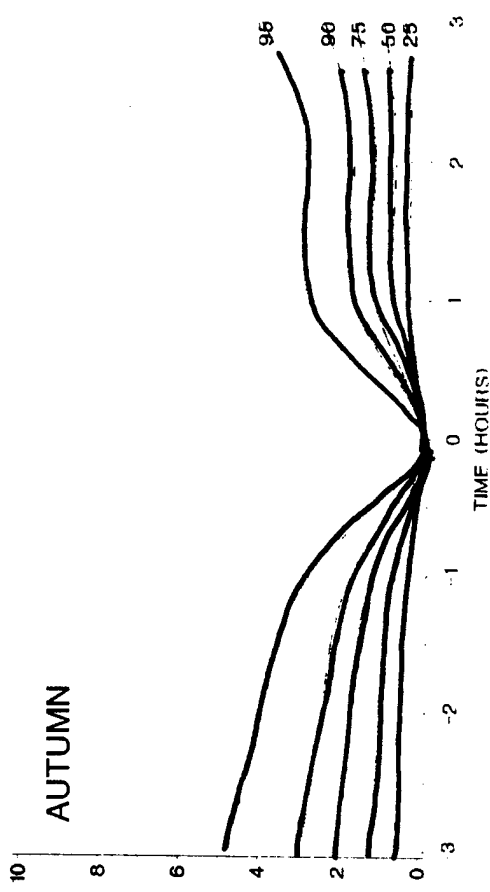
DEGREES CELSIUS

SPRING

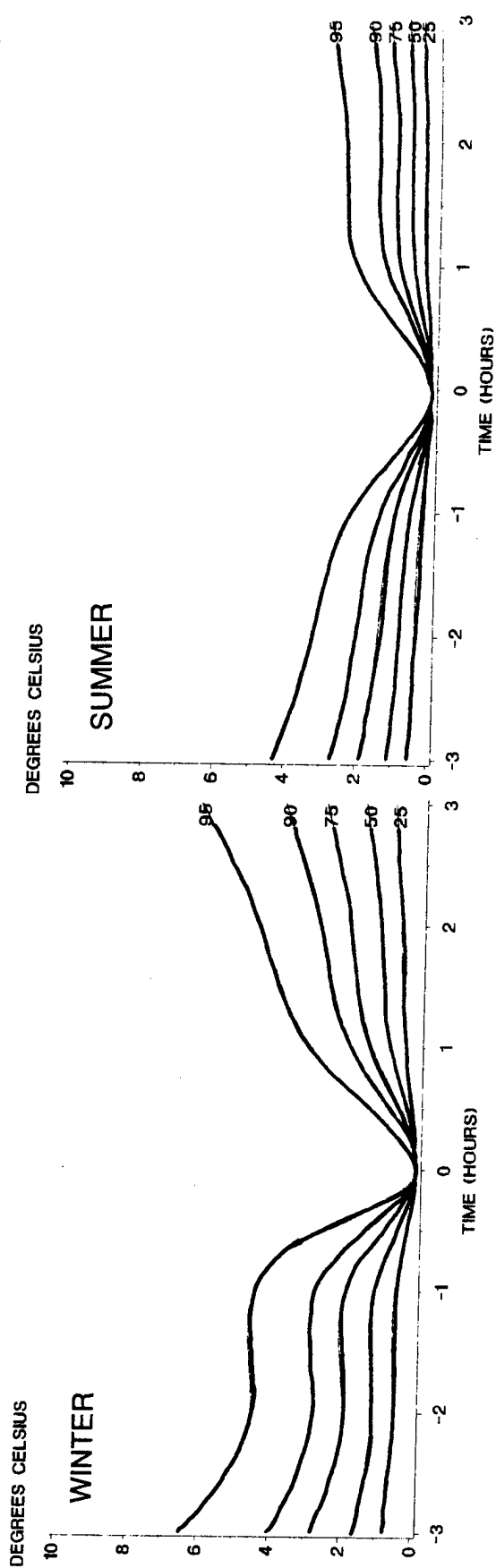


DEGREES CELSIUS

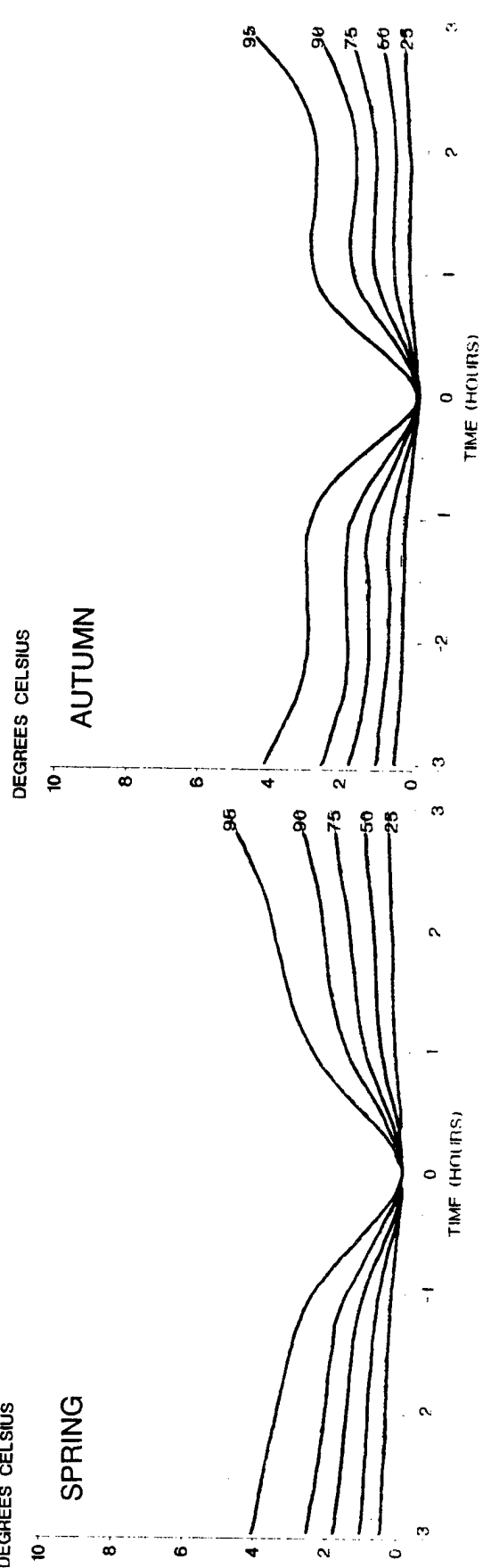
AUTUMN



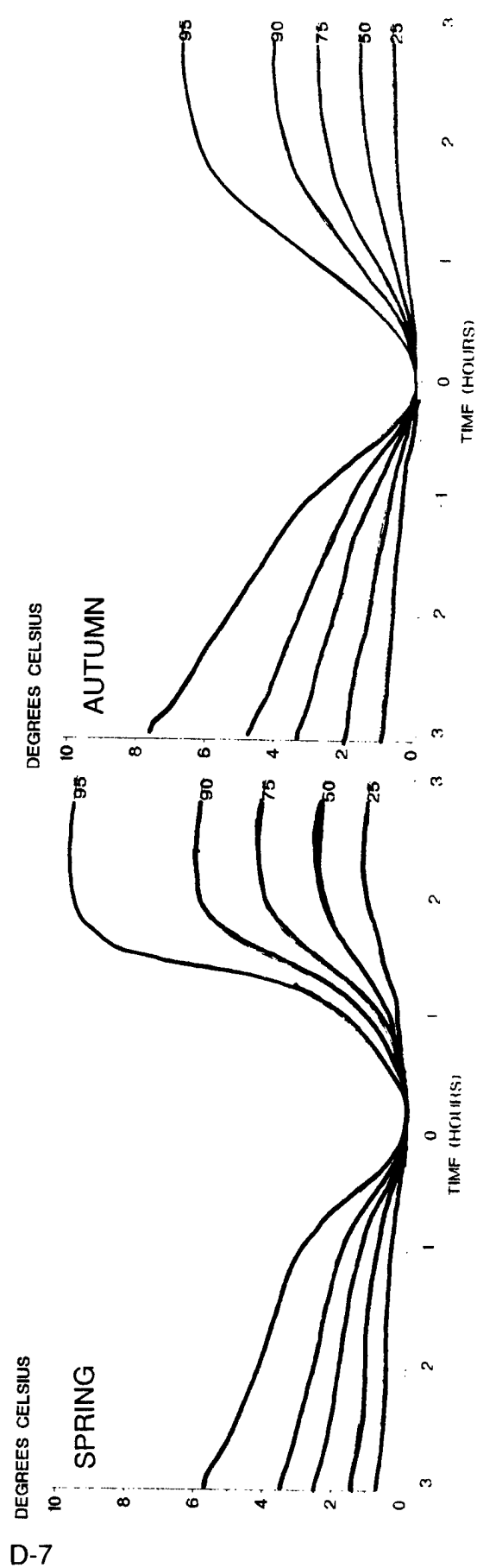
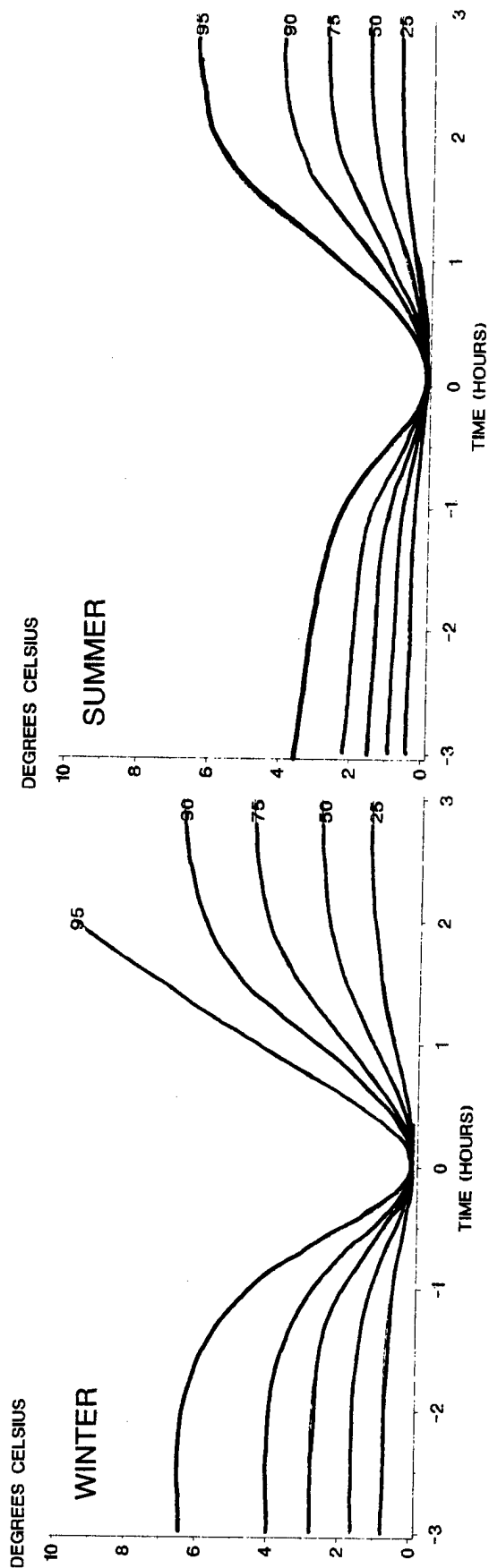
D-4 Temporal correlation of temperature, arctic climate, midnight.



D-5



D-5 Temporal correlation of temperature, arctic climate, sunrise.



D-6 Temporal correlation of temperature, arctic climate, noon.

DEGREES CELSIUS

WINTER

10

8

6

4

2

0

-3

-2

-1

0

1

2

3

TIME (HOURS)

DEGREES CELSIUS

SPRING

10

8

6

4

2

0

-3

-2

-1

0

1

2

3

TIME (HOURS)

DEGREES CELSIUS

SUMMER

10

8

6

4

2

0

-3

-2

-1

0

1

2

3

TIME (HOURS)

DEGREES CELSIUS

AUTUMN

10

8

6

4

2

0

-3

-2

-1

0

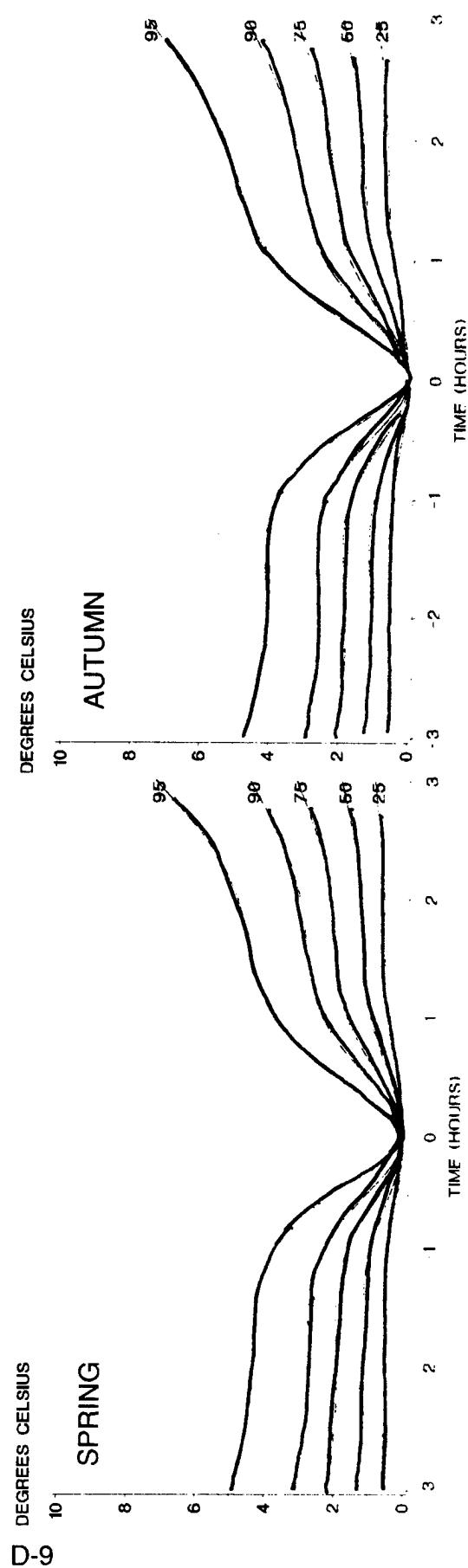
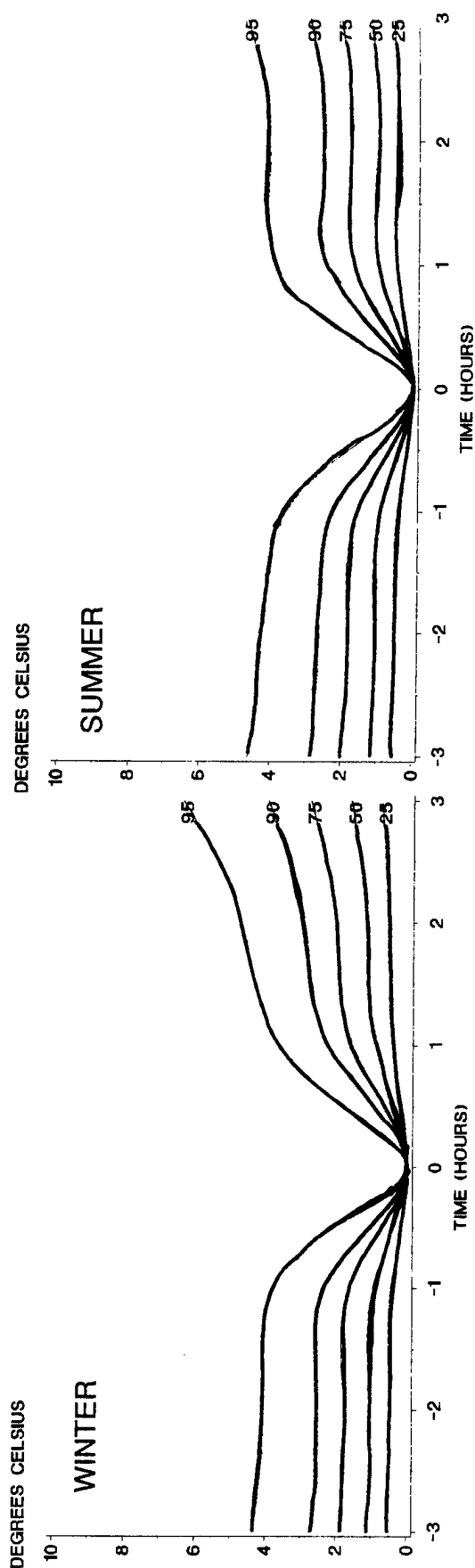
1

2

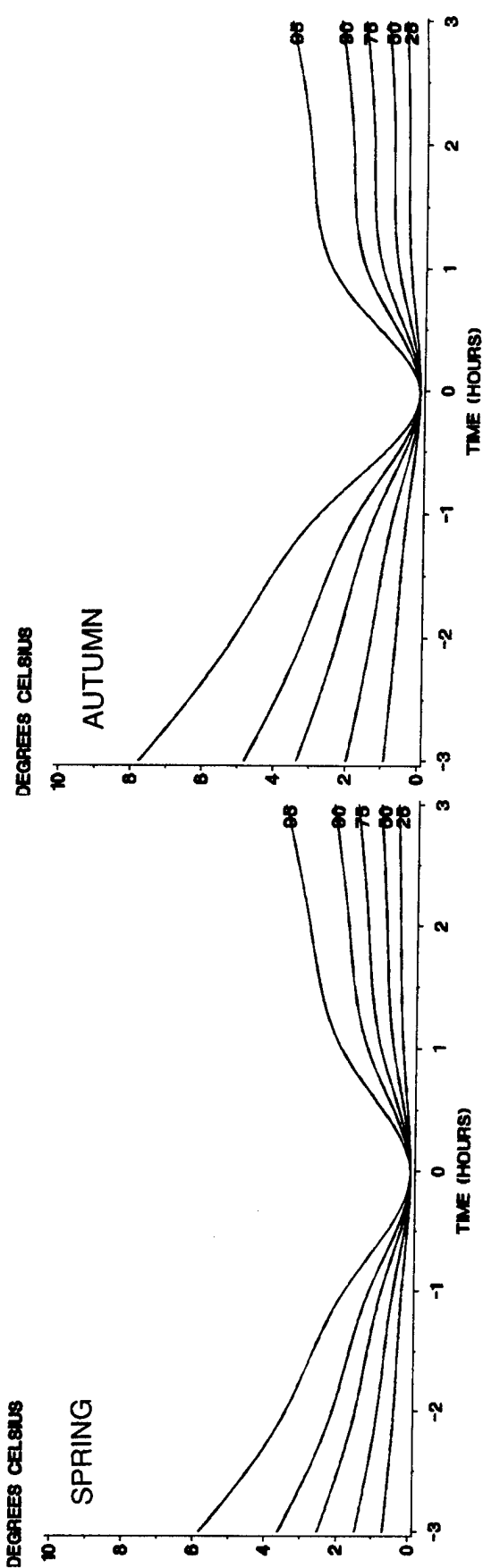
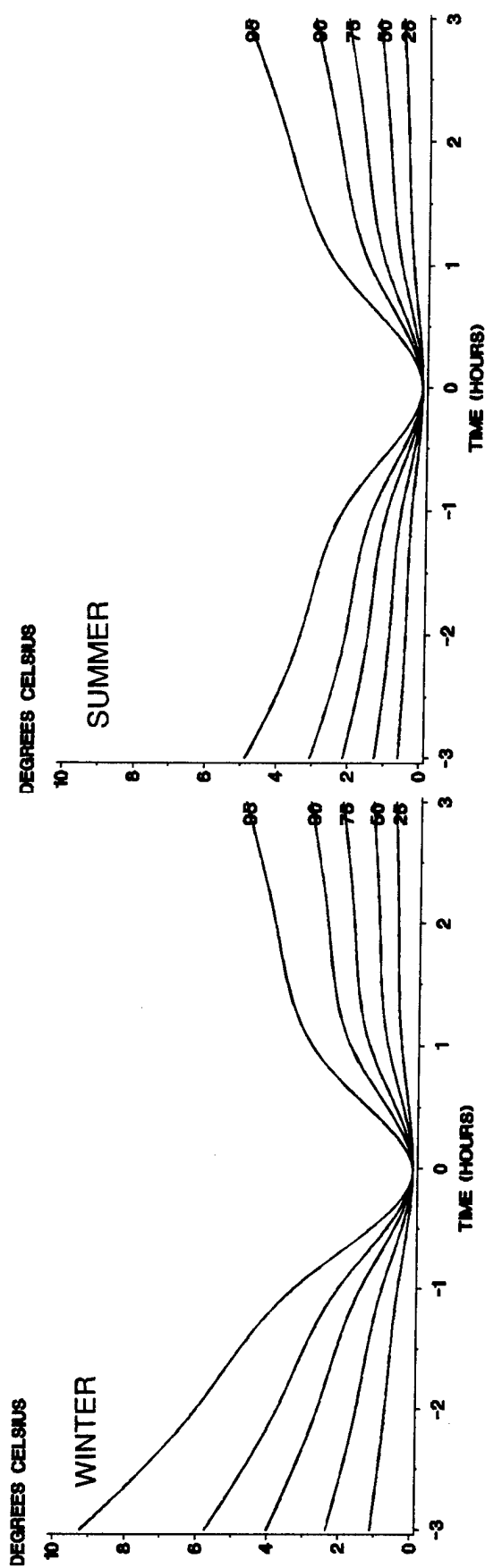
3

TIME (HOURS)

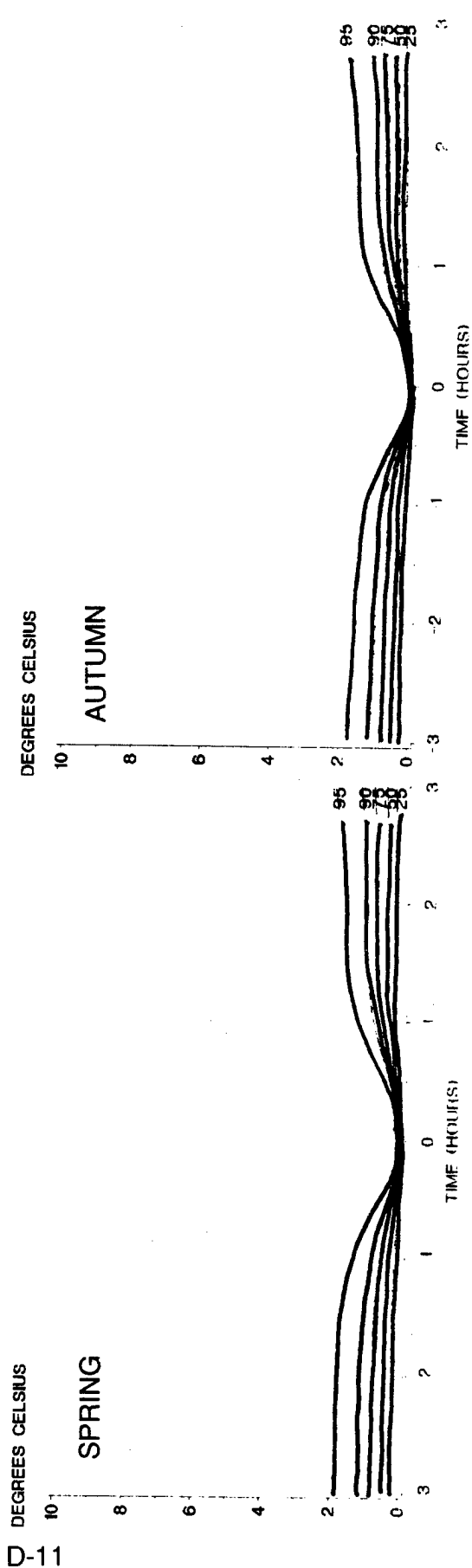
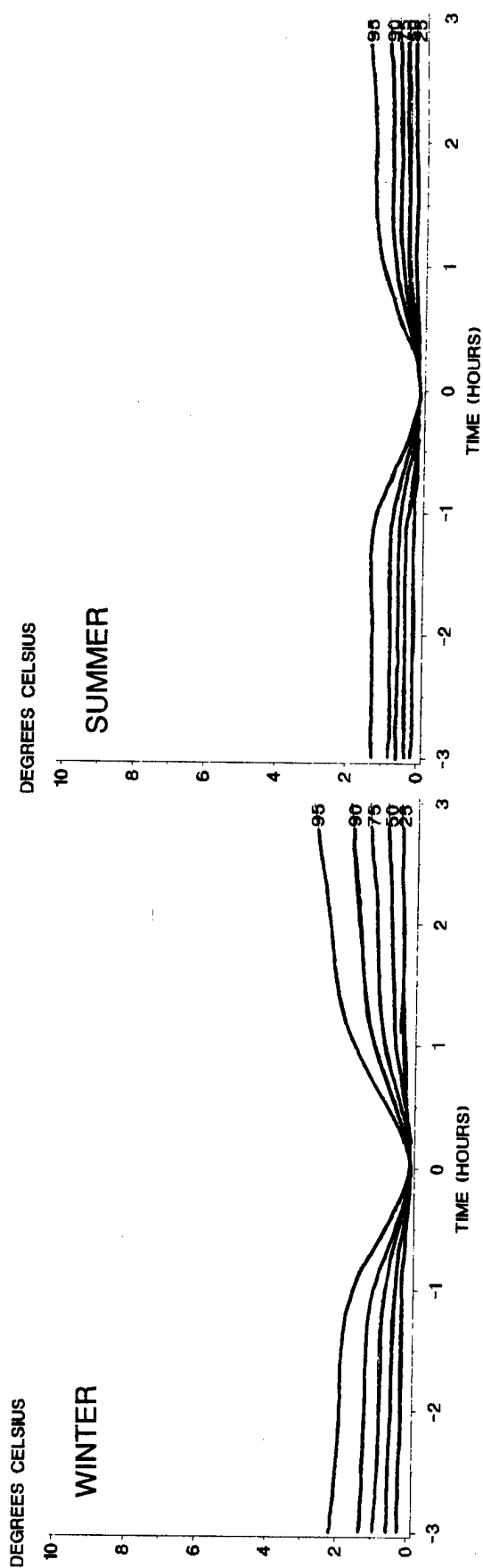
D-7 Temporal correlation of temperature, desert climate, midnight.



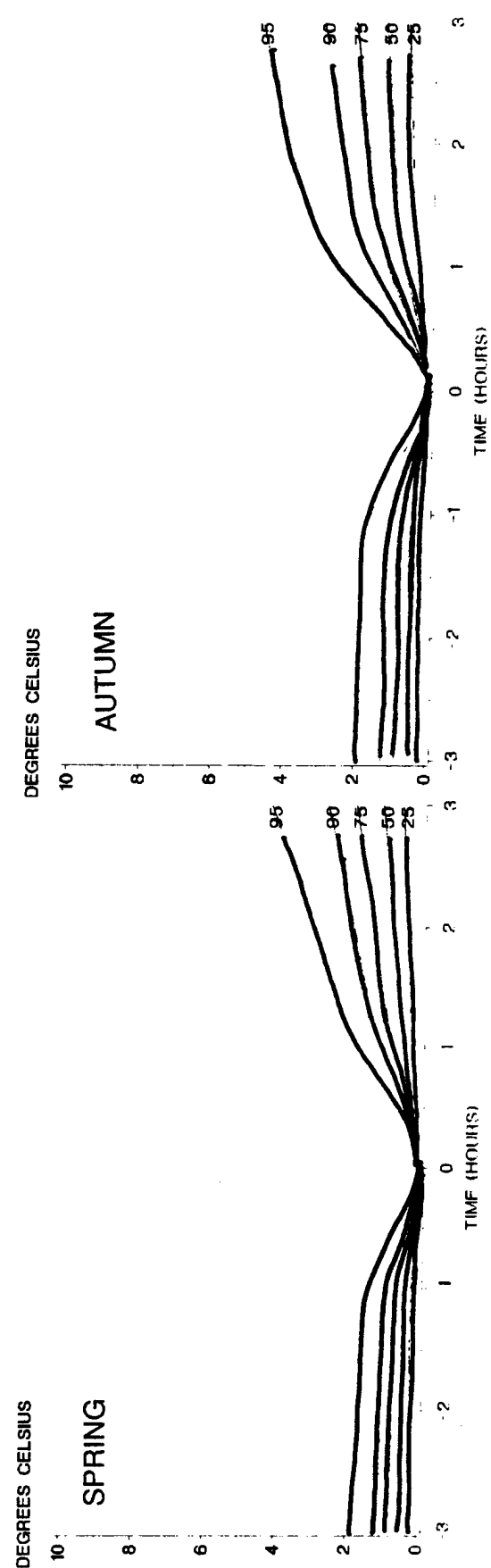
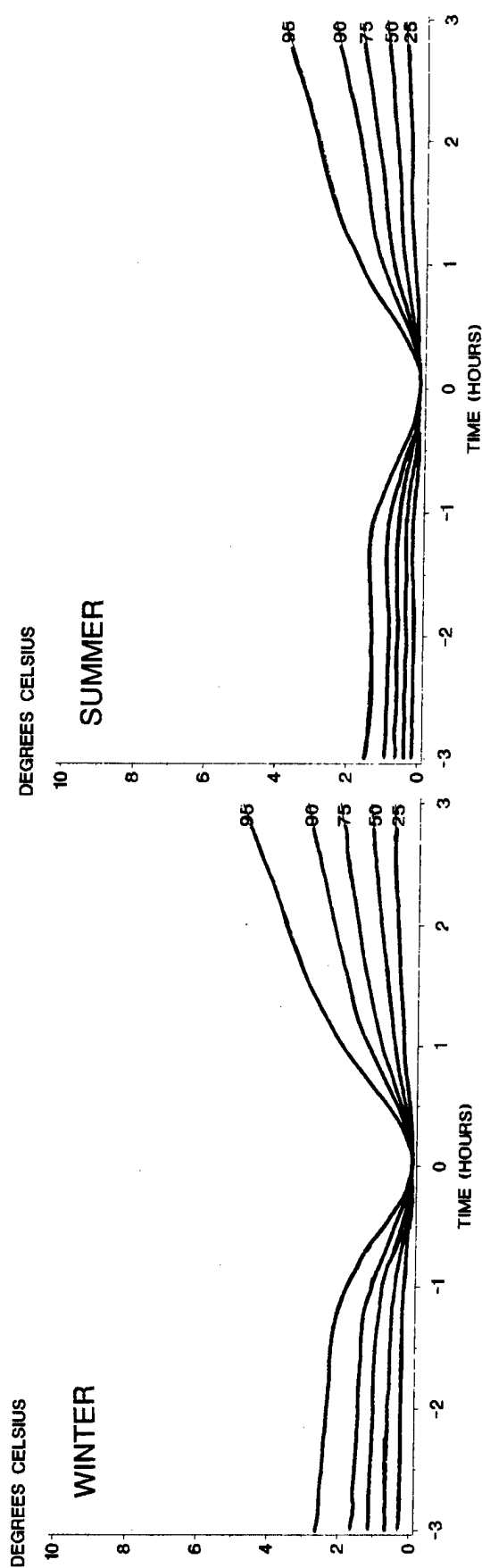
D-8 Temporal correlation of temperature, desert climate, sunrise.



D-9 Temporal correlation of temperature, desert climate, noon.



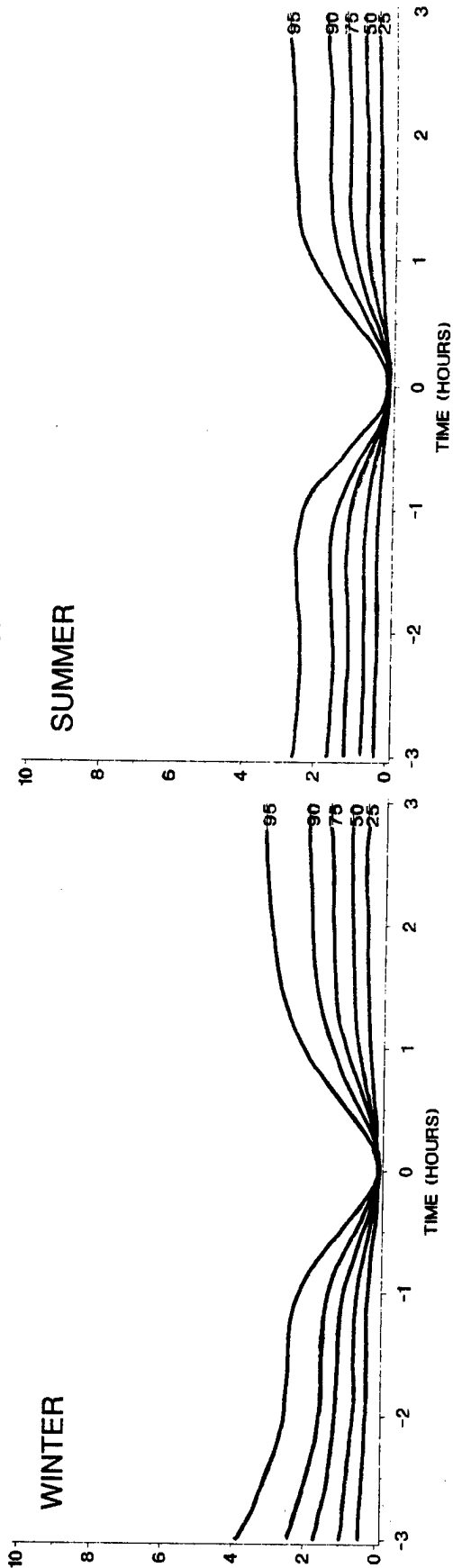
D-10 Temporal correlation of temperature, maritime climate, midnight.



D-11 Temporal correlation of temperature, maritime climate, sunrise.

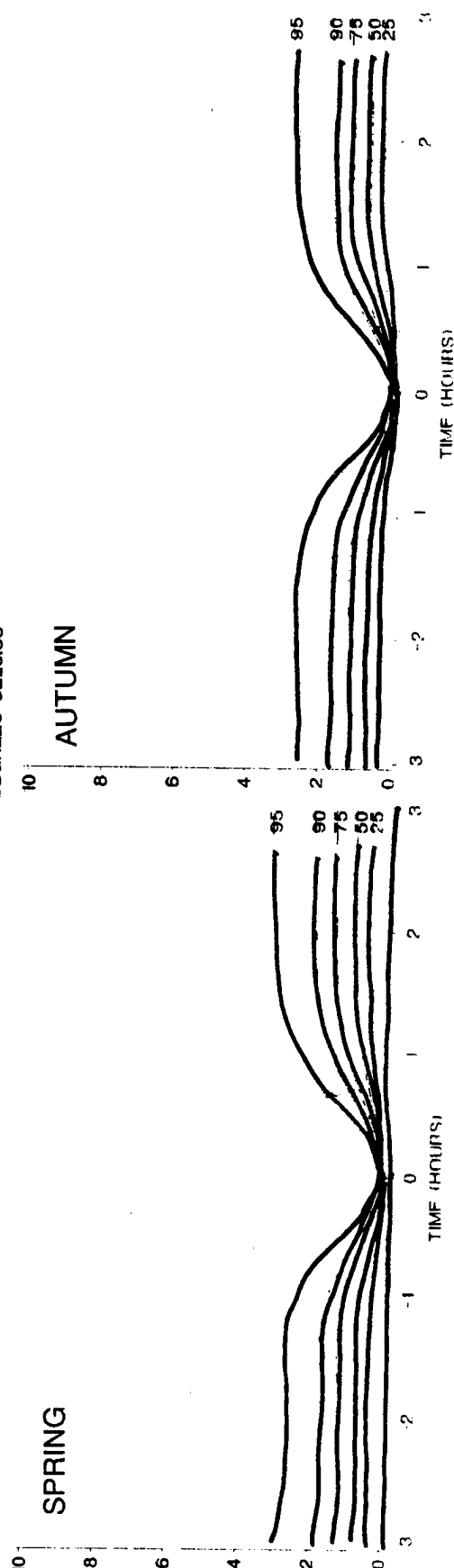
DEGREES CELSIUS

WINTER



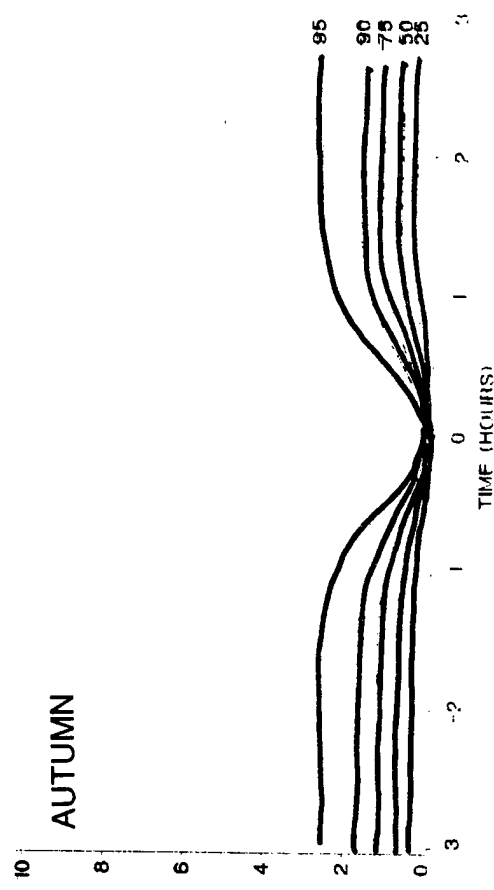
DEGREES CELSIUS

SPRING

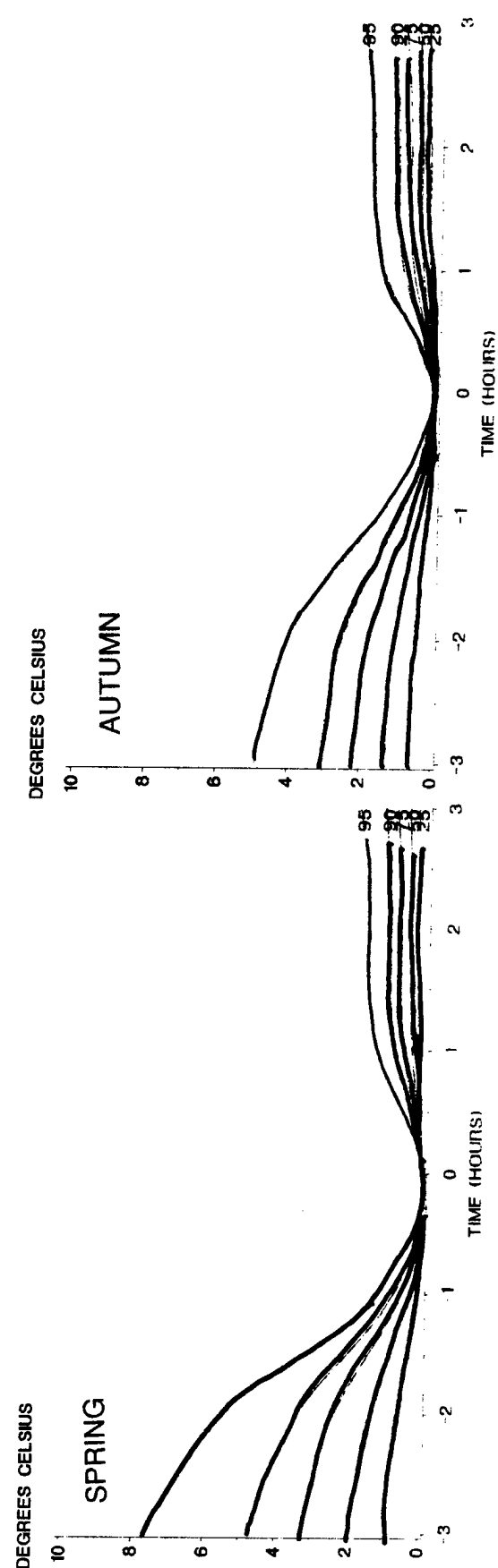
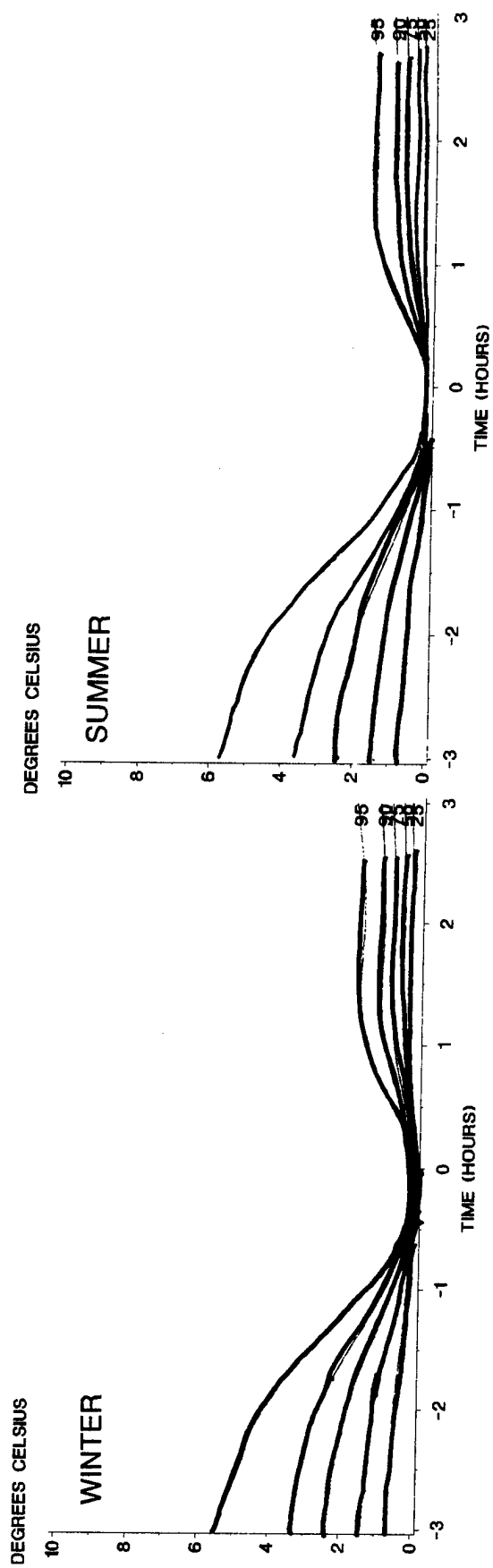


DEGREES CELSIUS

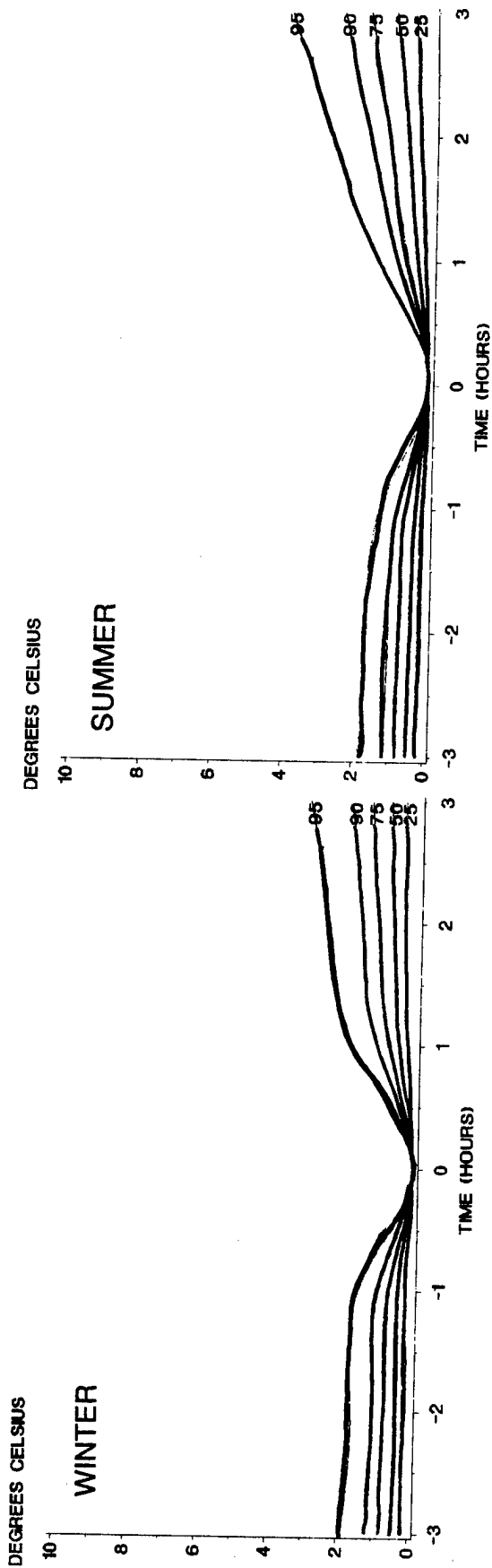
AUTUMN



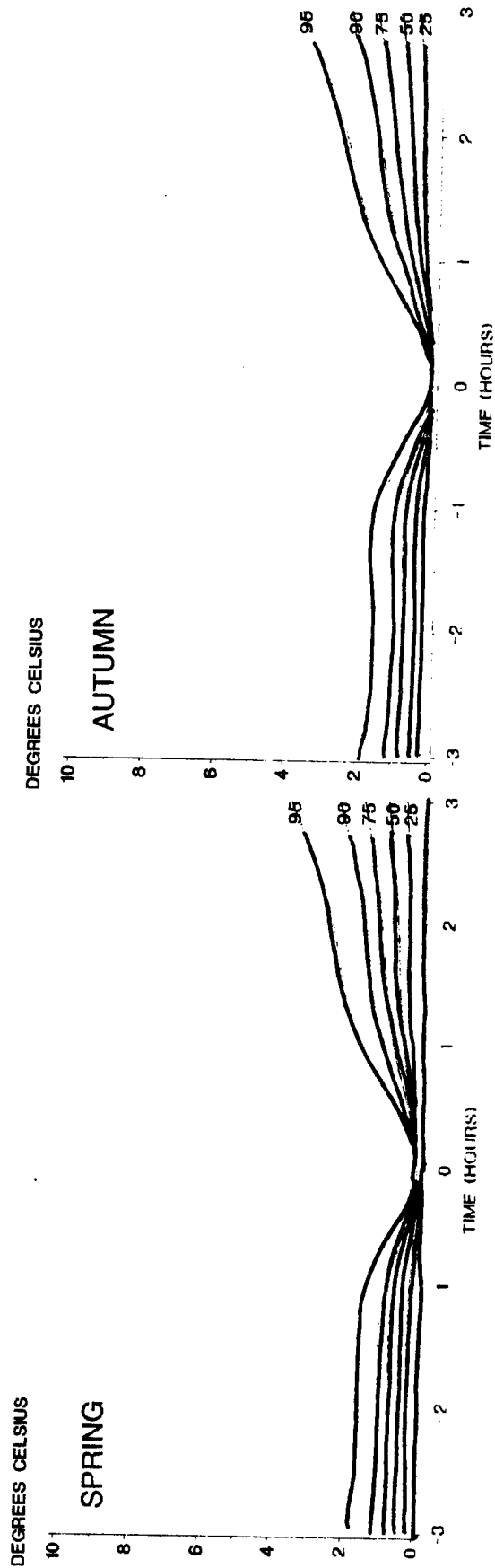
D-12 Temporal correlation of temperature, maritime climate, noon.



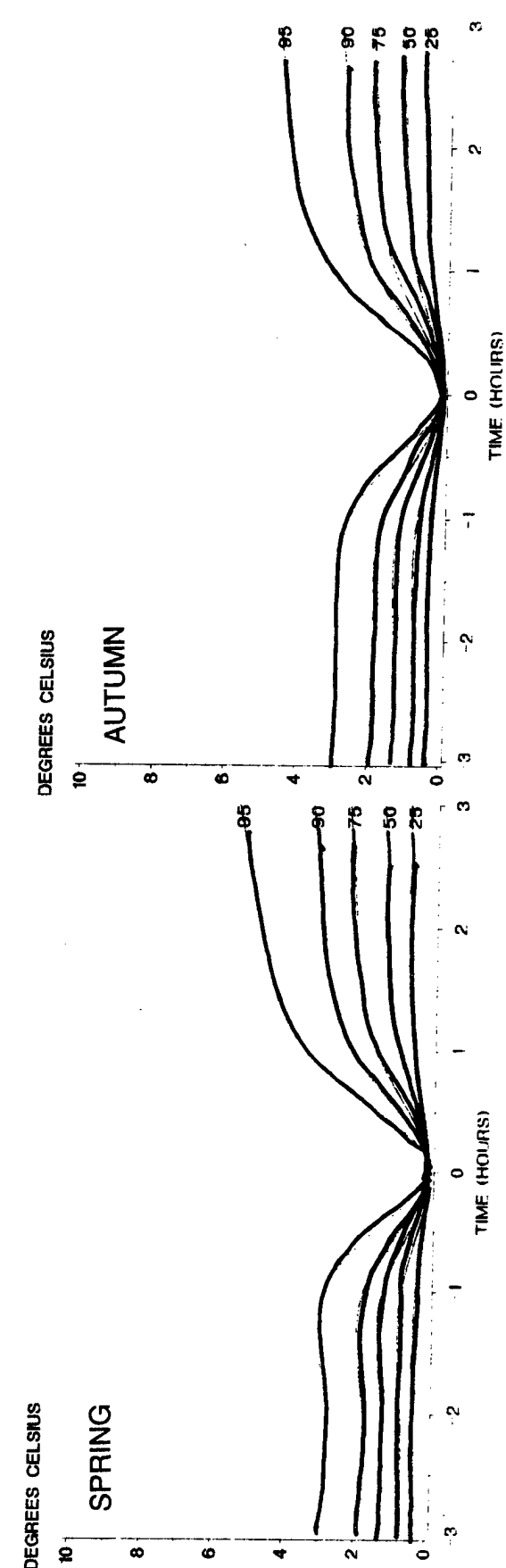
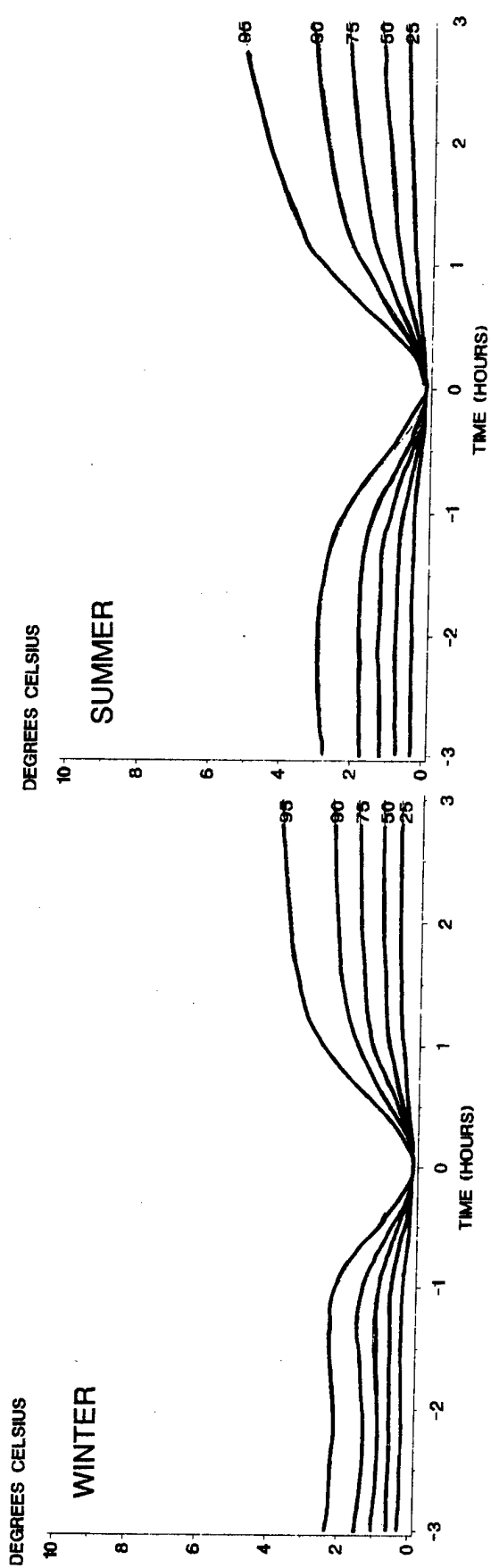
D-13 Temporal correlation of temperature, tropical climate, midnight.

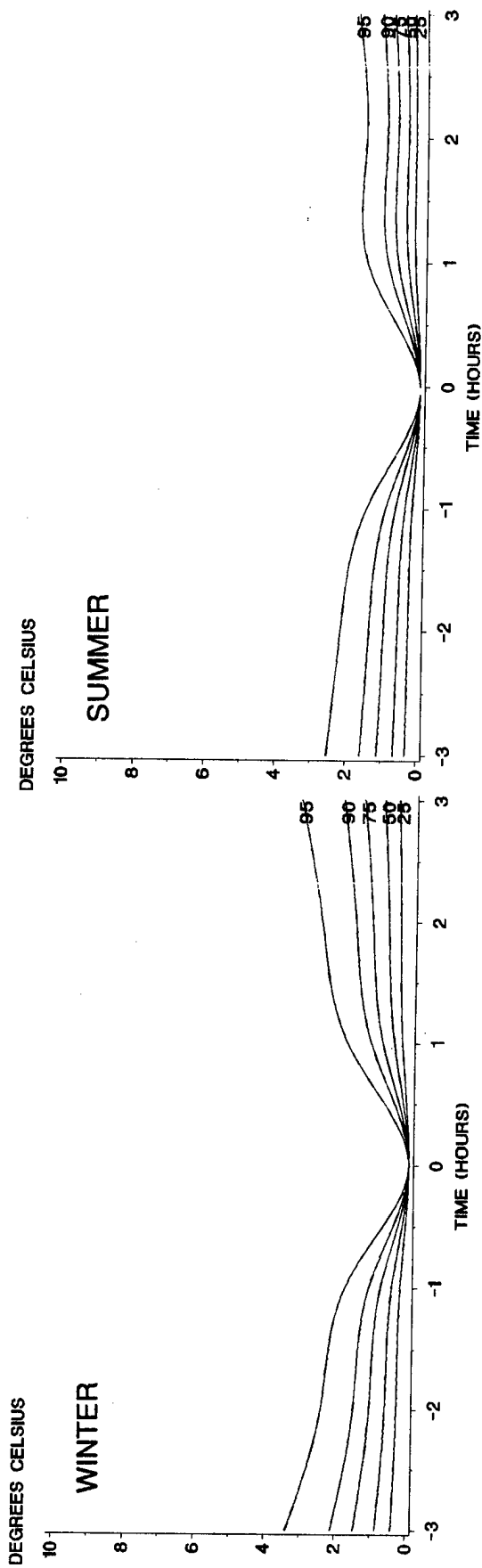


D-15

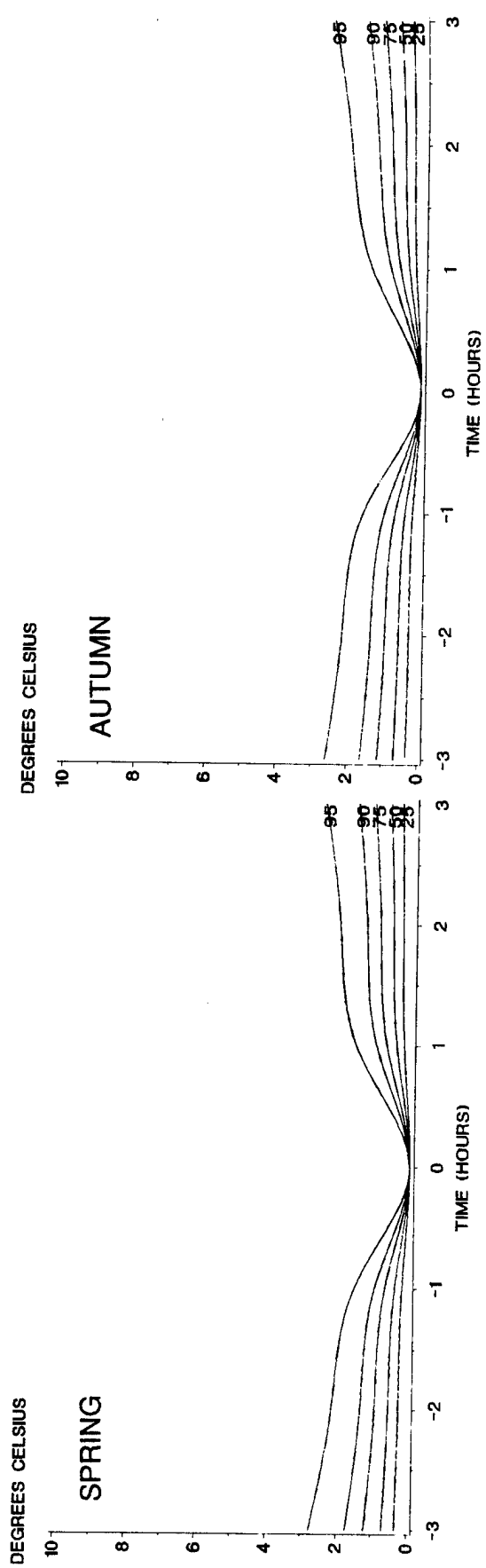


D-14 Temporal correlation of temperature, tropical climate, sunrise.

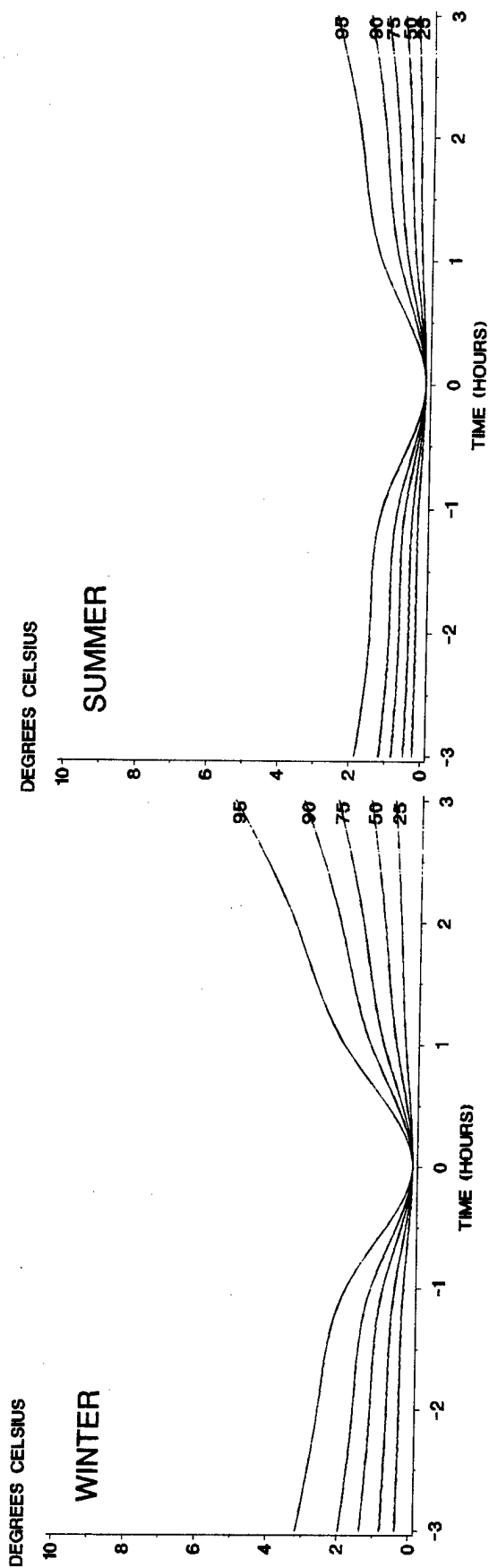




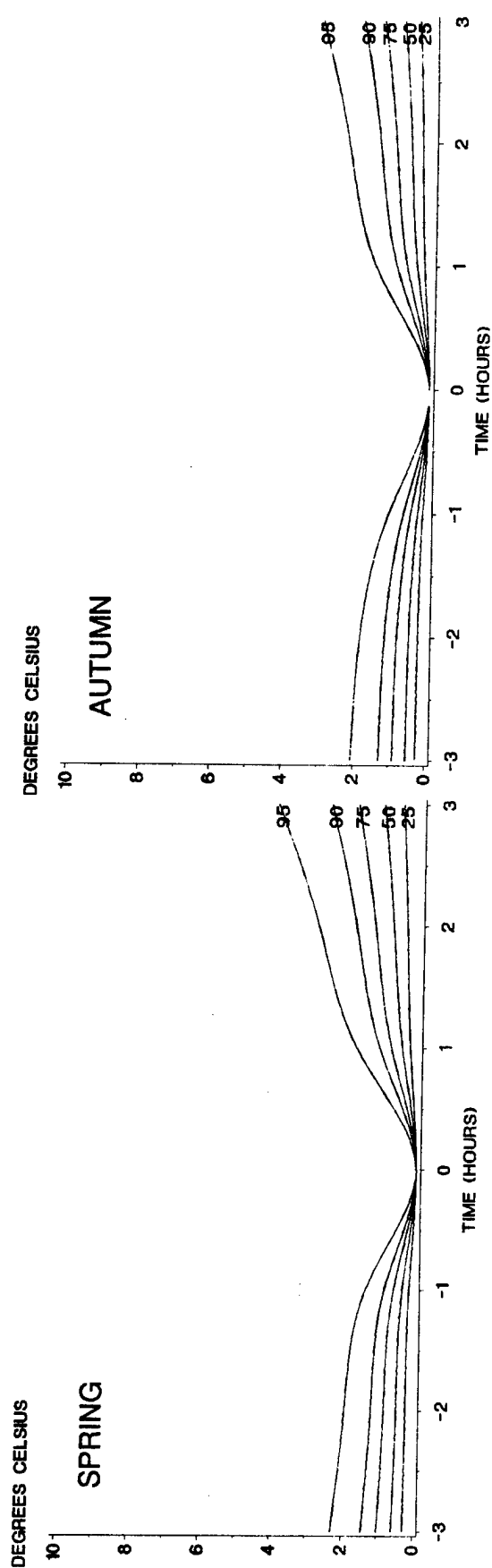
D-17



D-16 Temporal correlation of temperature, coastal climate, midnight.



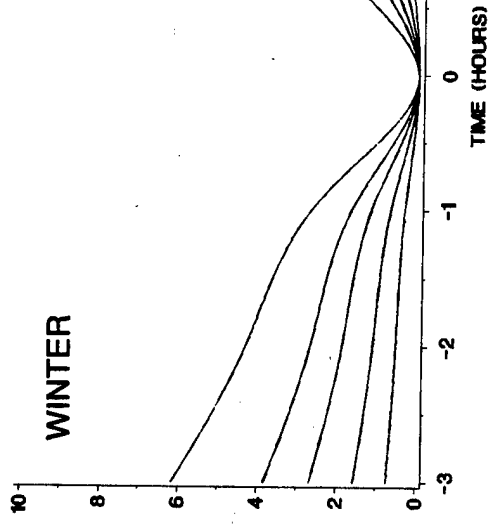
D-18



D-17 Temporal correlation of temperature, coastal climate, sunrise.

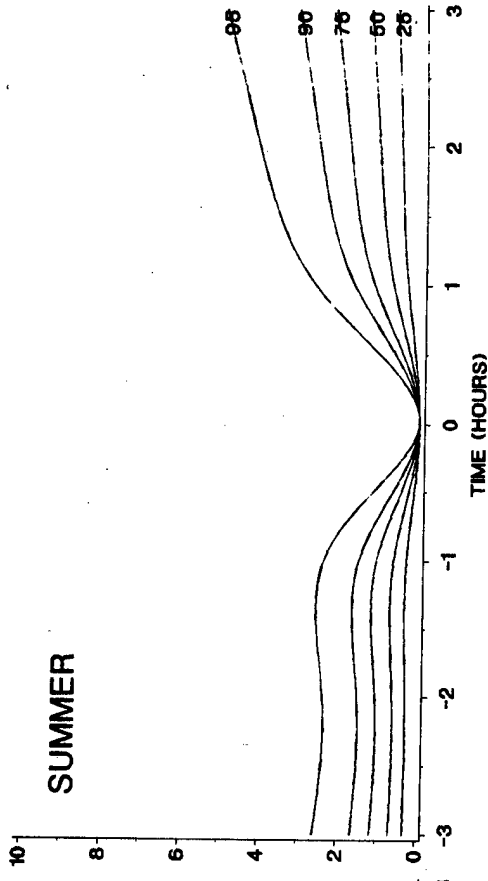
DEGREES CELSIUS

WINTER



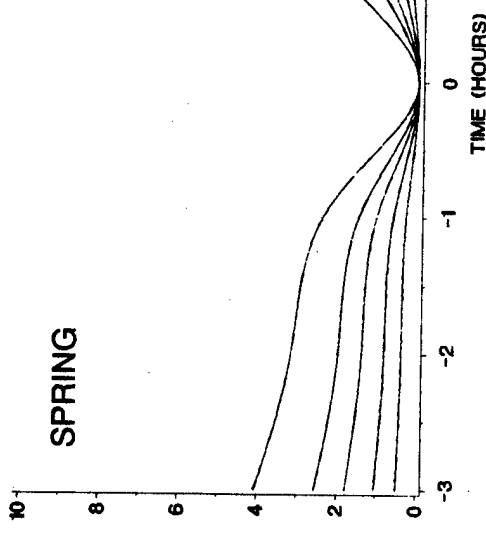
DEGREES CELSIUS

SUMMER



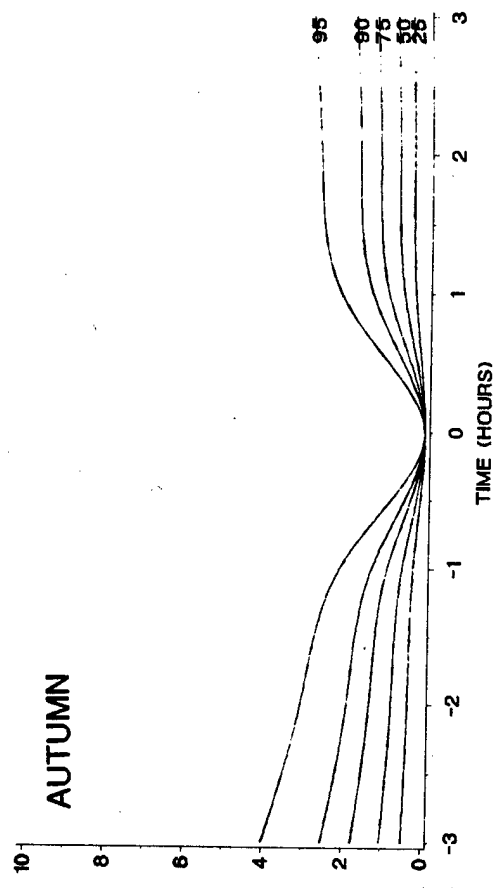
DEGREES CELSIUS

SPRING



DEGREES CELSIUS

AUTUMN

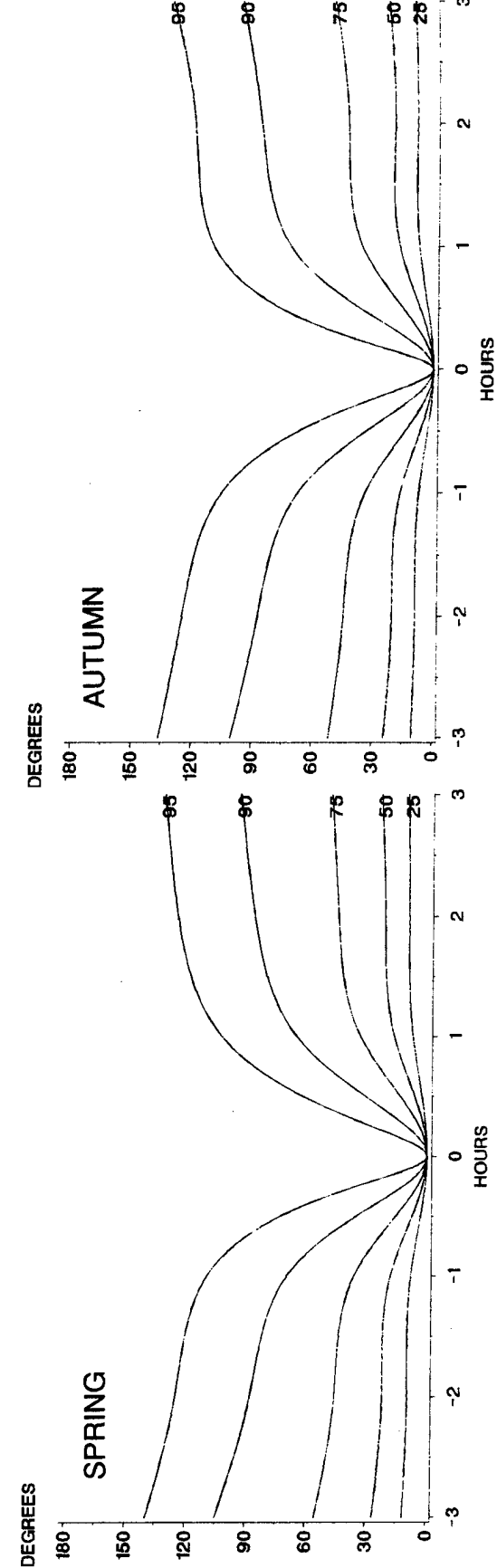
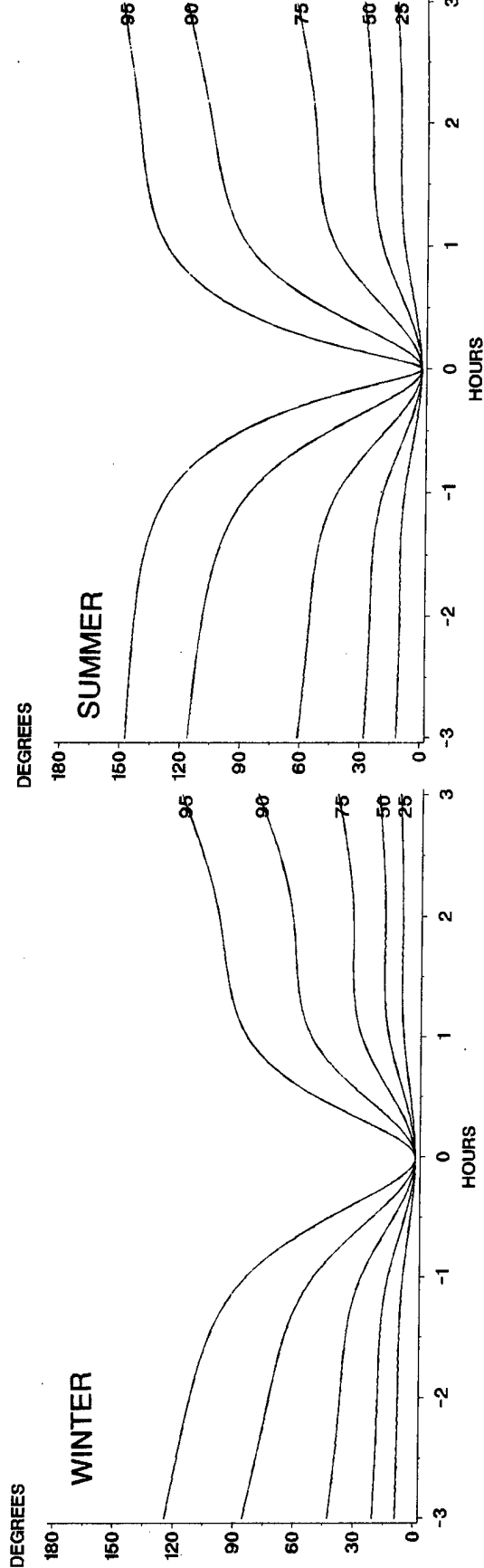


D-18 Temporal correlation of temperature, coastal climate, noon.

APPENDIX E

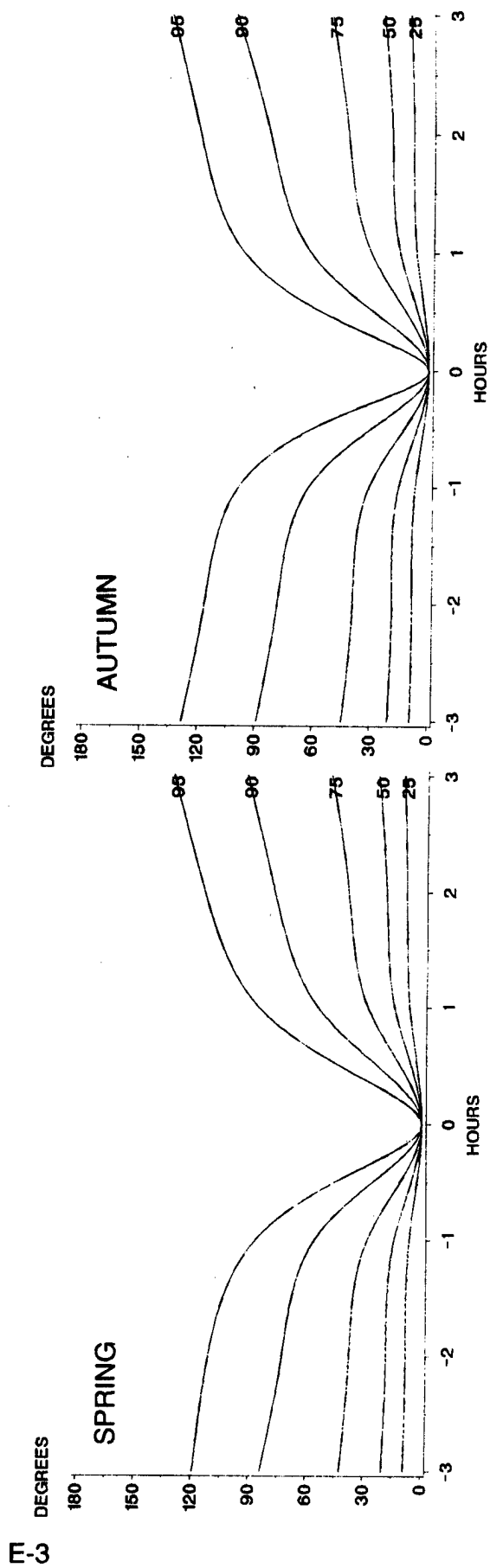
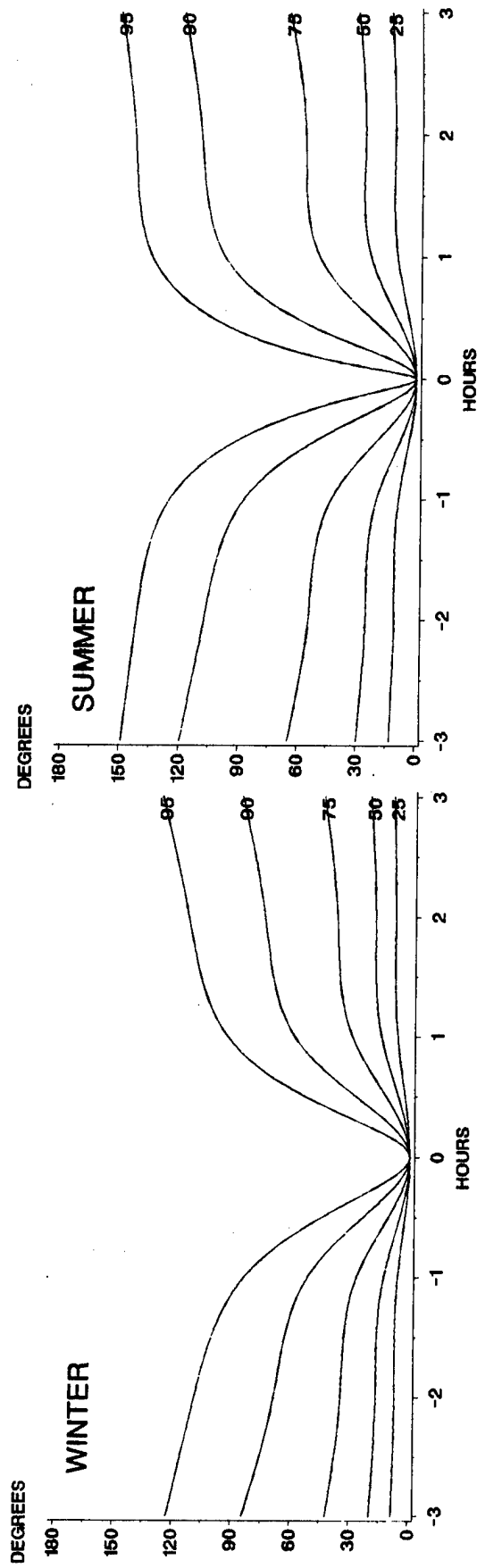
TEMPORAL CORRELATION OF WIND DIRECTION

- E-1 Temporal correlation of wind direction, continental climate, midnight.
- E-2 Temporal correlation of wind direction, continental climate, sunrise.
- E-3 Temporal correlation of wind direction, continental climate, noon.
- E-4 Temporal correlation of wind direction, arctic climate, midnight.
- E-5 Temporal correlation of wind direction, arctic climate, sunrise.
- E-6 Temporal correlation of wind direction, arctic climate, noon.
- E-7 Temporal correlation of wind direction, desert climate, midnight.
- E-8 Temporal correlation of wind direction, desert climate, sunrise.
- E-9 Temporal correlation of wind direction, desert climate, noon.
- E-10 Temporal correlation of wind direction, maritime climate, midnight.
- E-11 Temporal correlation of wind direction, maritime climate, sunrise.
- E-12 Temporal correlation of wind direction, maritime climate, noon.
- E-13 Temporal correlation of wind direction, tropical climate, midnight.
- E-14 Temporal correlation of wind direction, tropical climate, sunrise.
- E-15 Temporal correlation of wind direction, tropical climate, noon.
- E-16 Temporal correlation of wind direction, coastal climate, midnight.
- E-17 Temporal correlation of wind direction, coastal climate, sunrise.
- E-18 Temporal correlation of wind direction, coastal climate, noon.

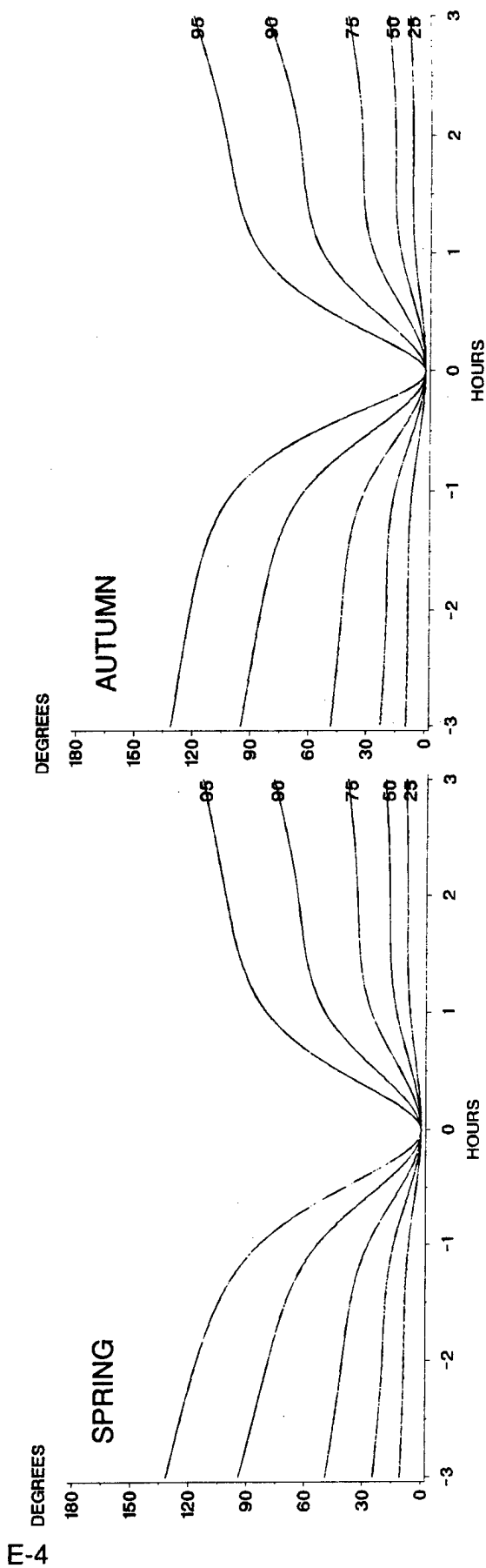
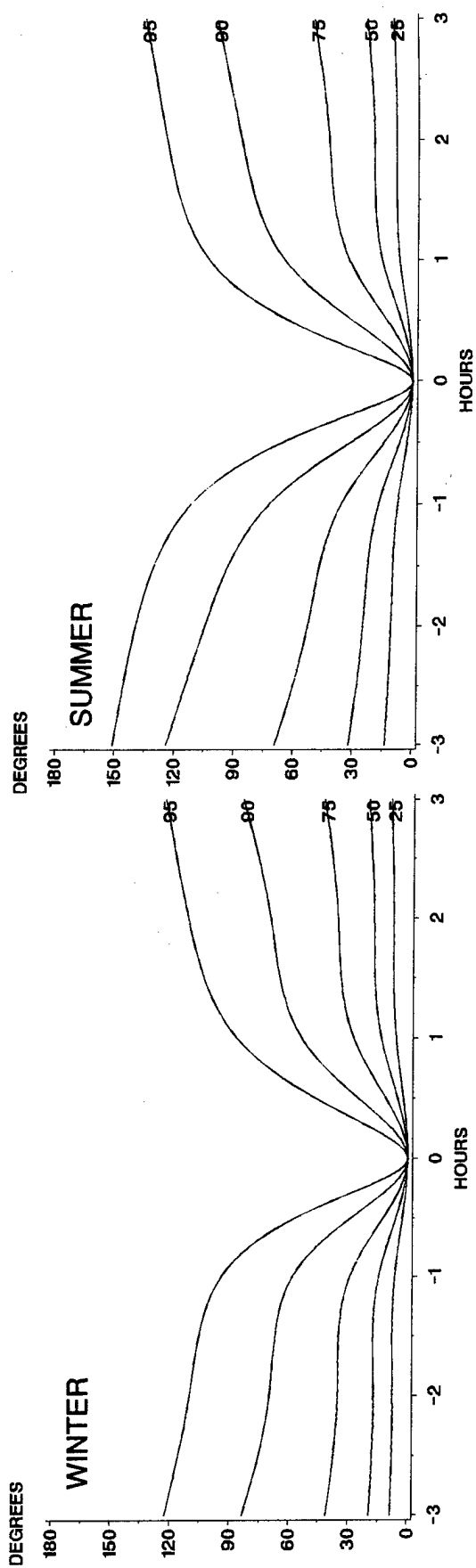


E-2

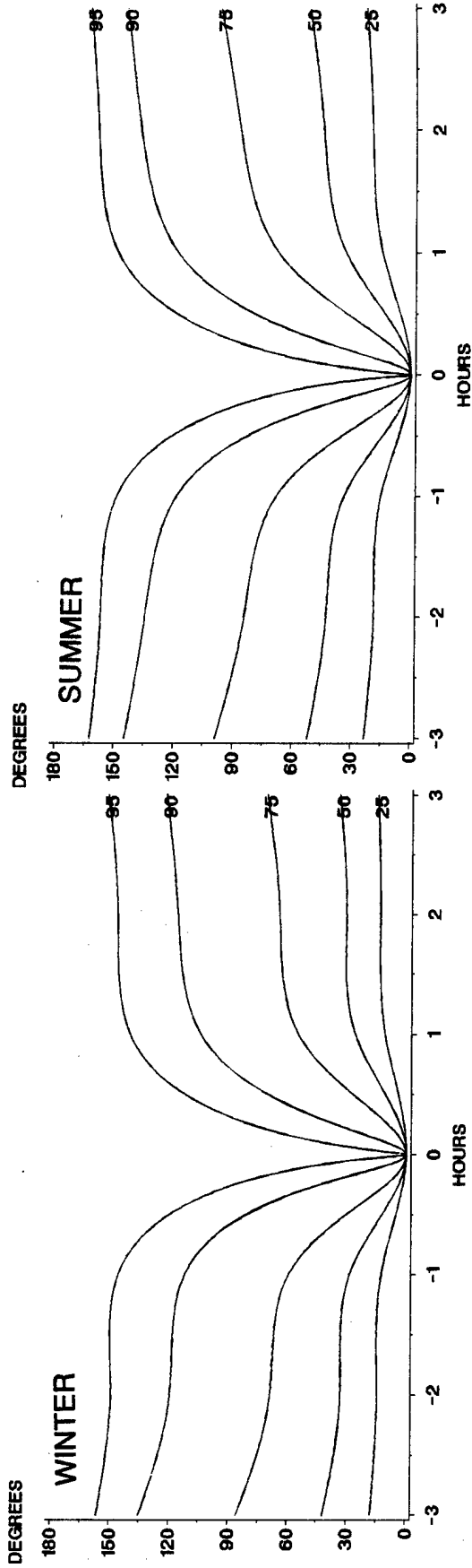
E-1 Temporal correlation of wind direction, continental climate, midnight.



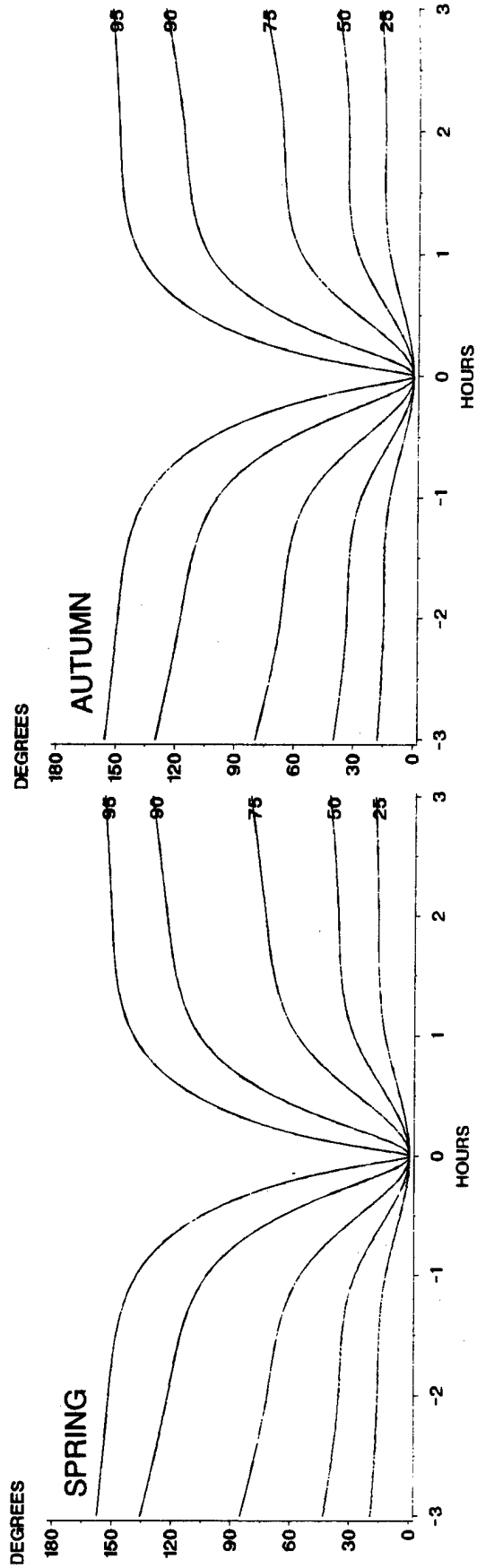
E-2 Temporal correlation of wind direction, continental climate, sunrise.



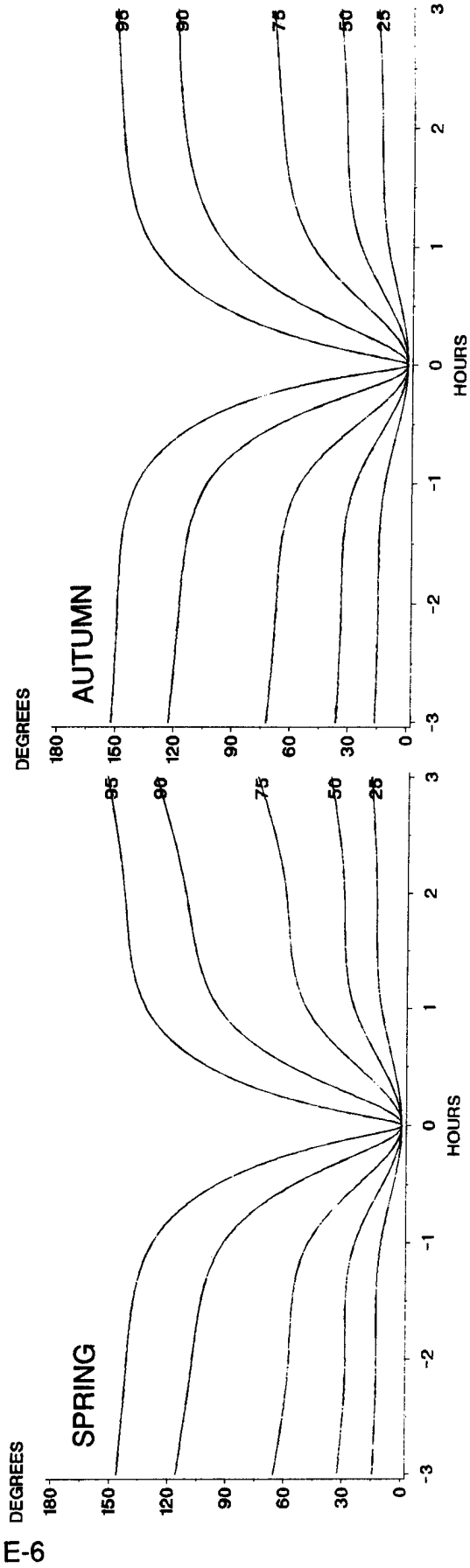
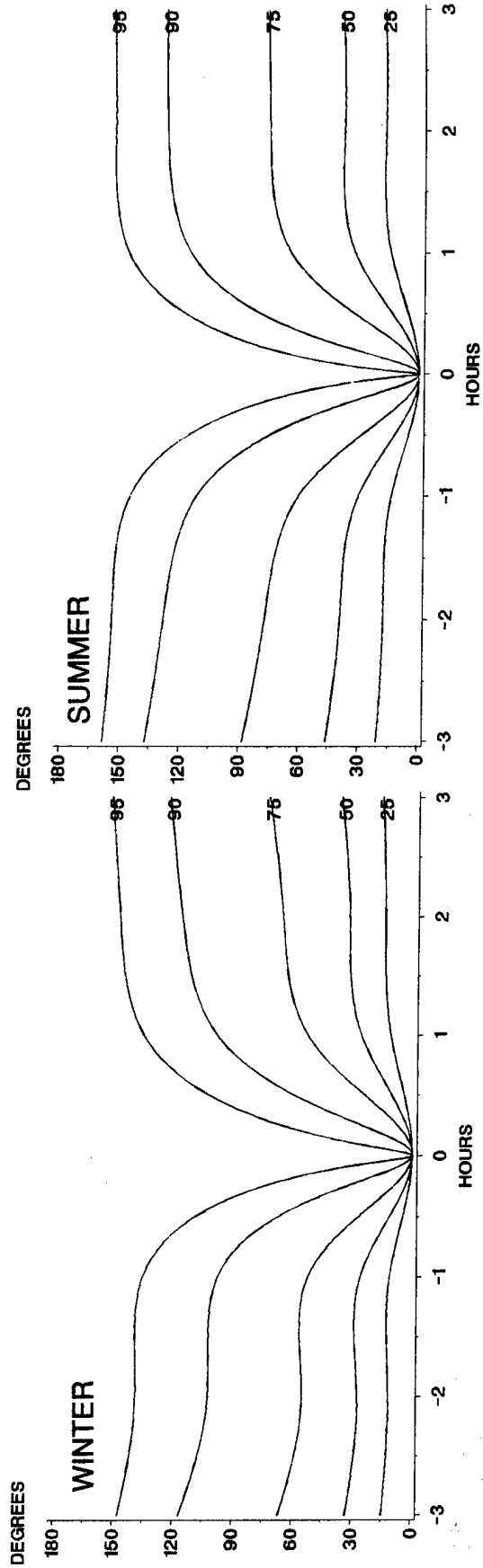
E-3 Temporal correlation of wind direction, continental climate, noon.



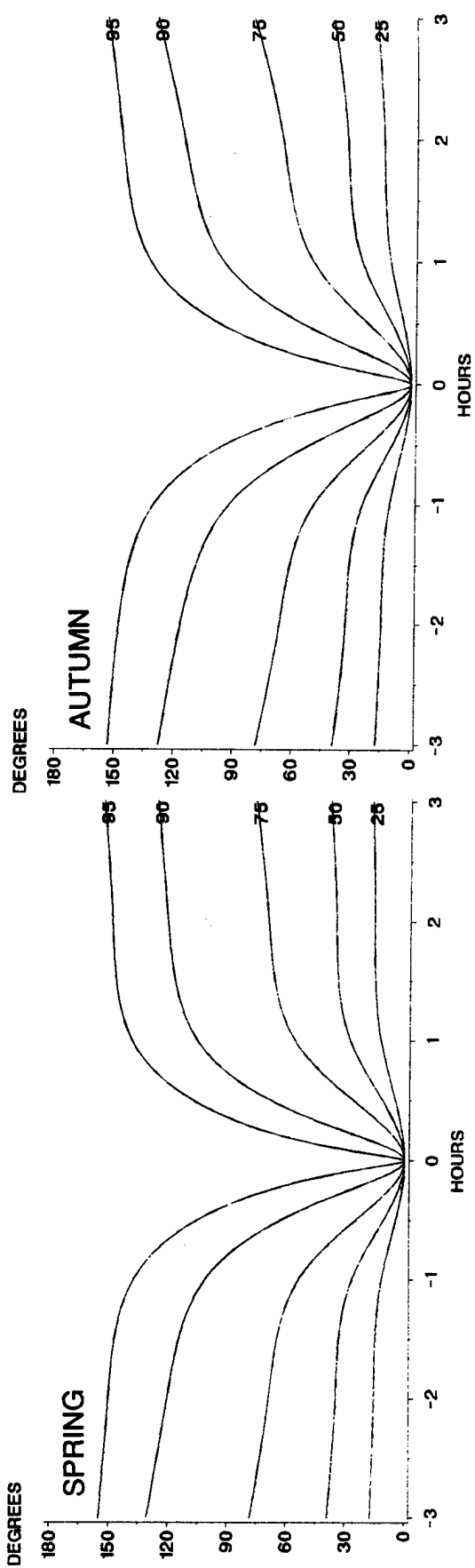
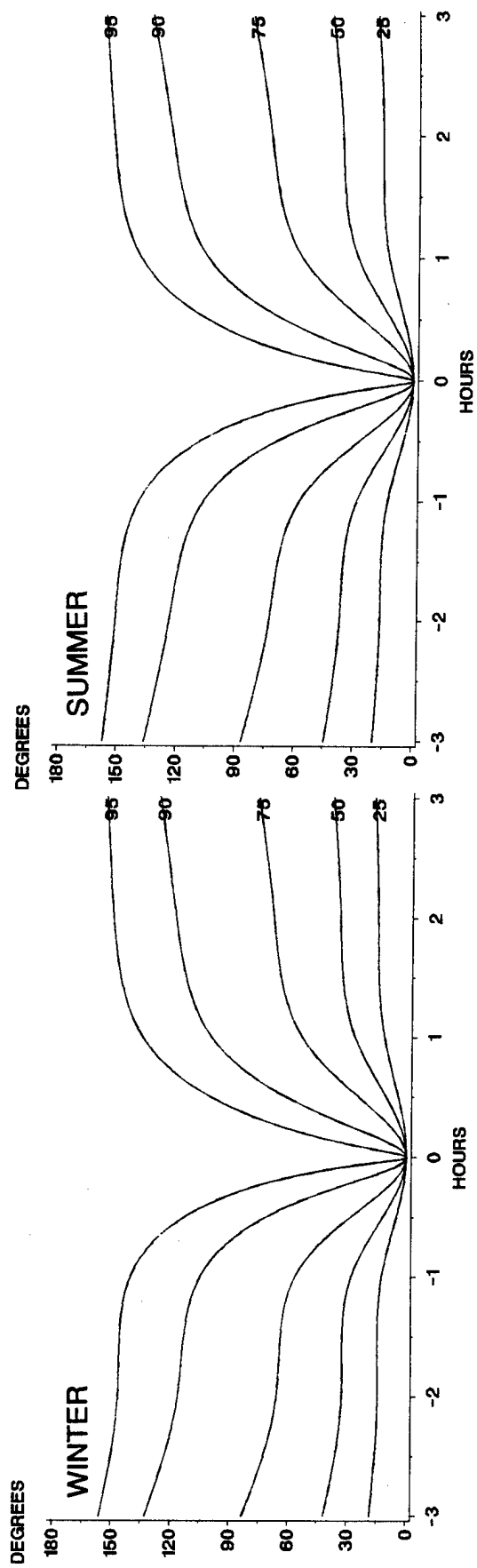
11-51



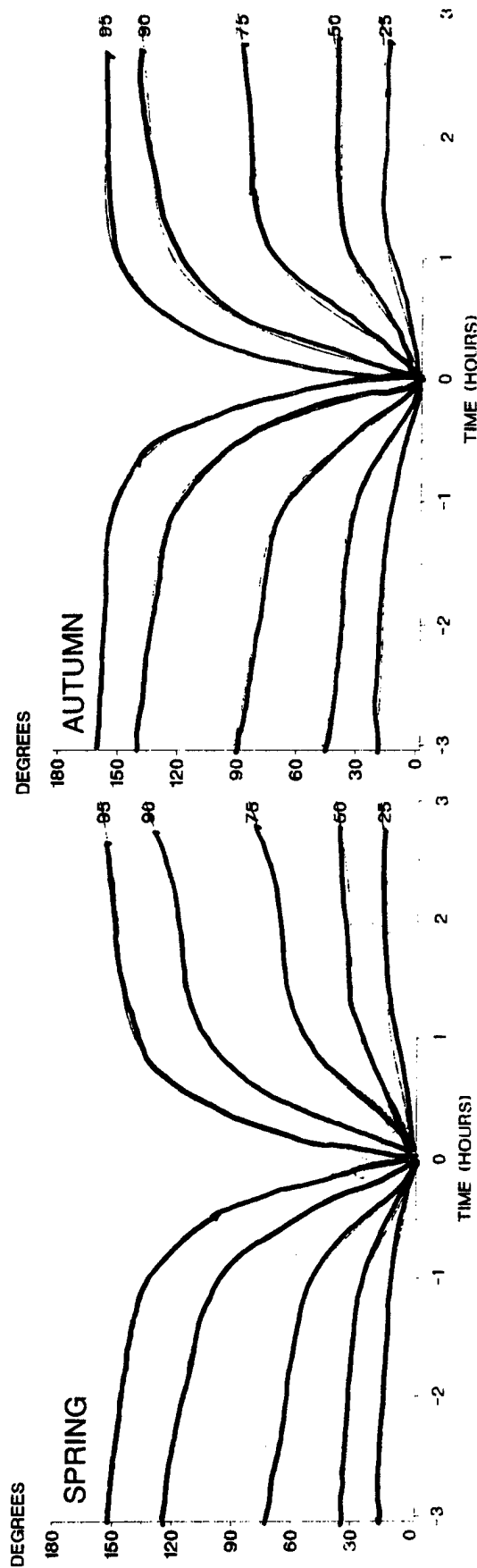
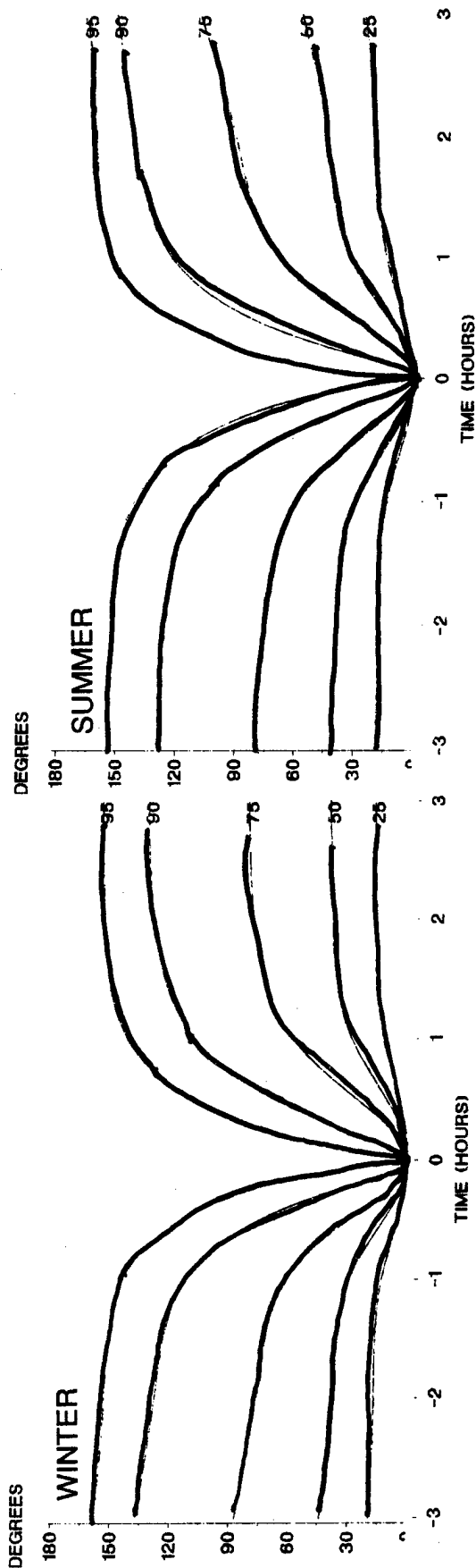
E-4 Temporal correlation of wind direction, arctic climate, midnight.



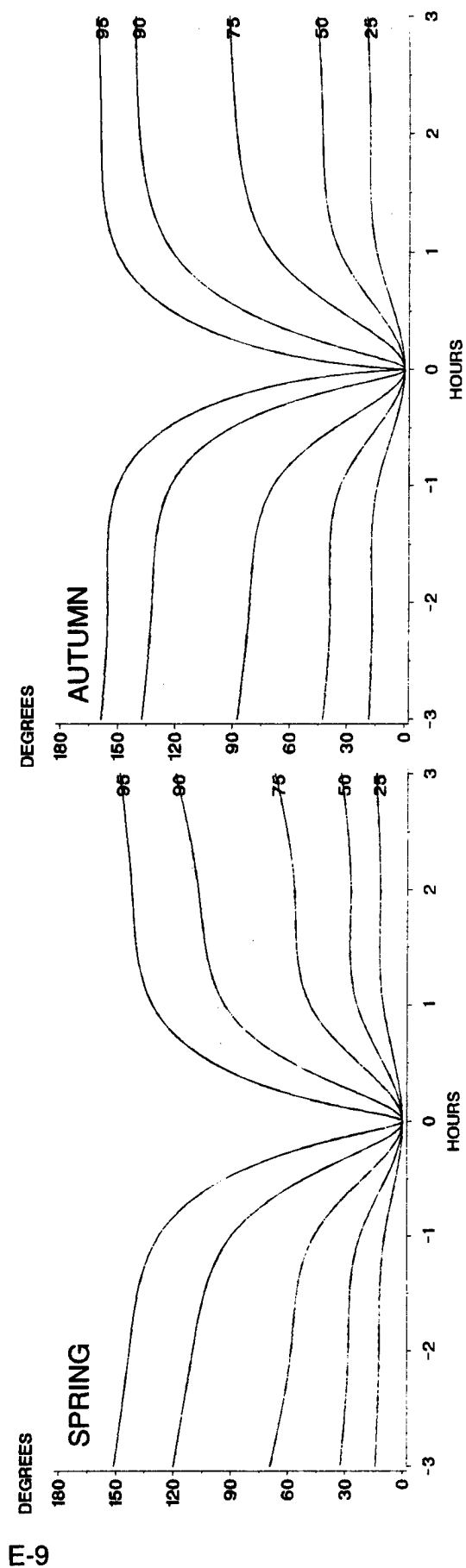
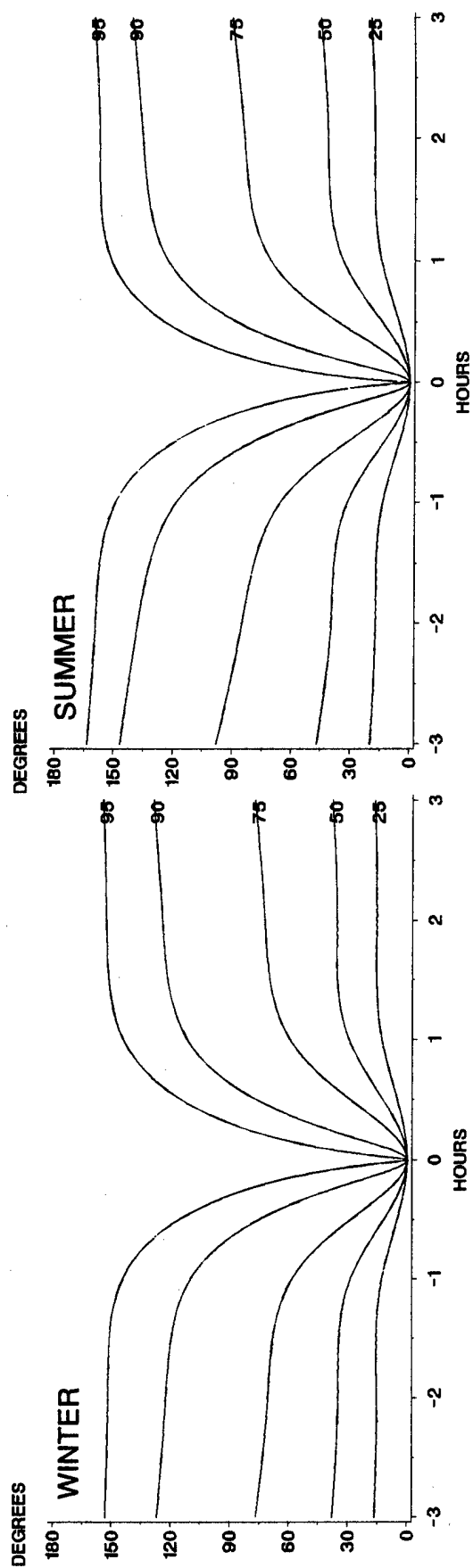
E-5 Temporal correlation of wind direction, arctic climate, sunrise.



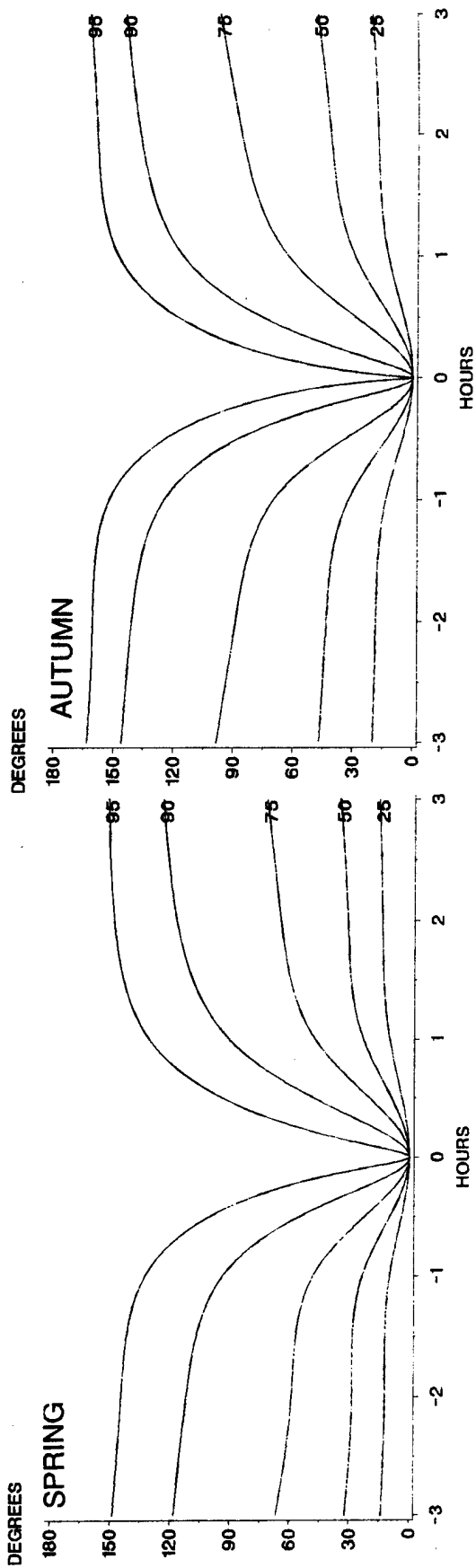
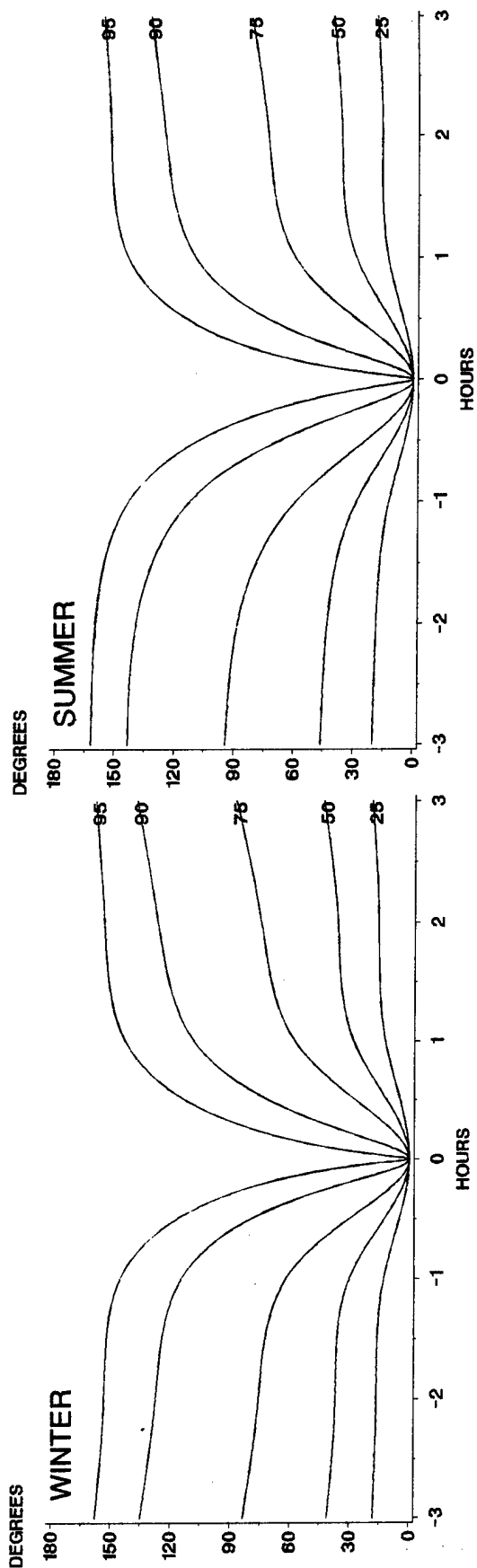
E-6 Temporal correlation of wind direction, arctic climate, noon.



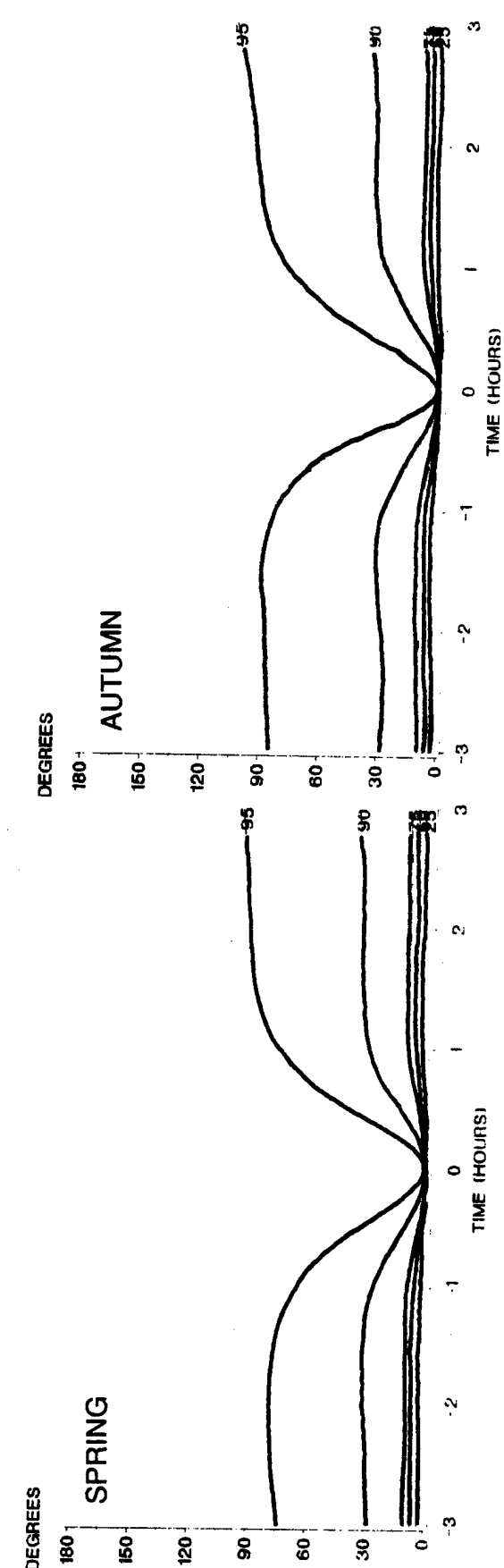
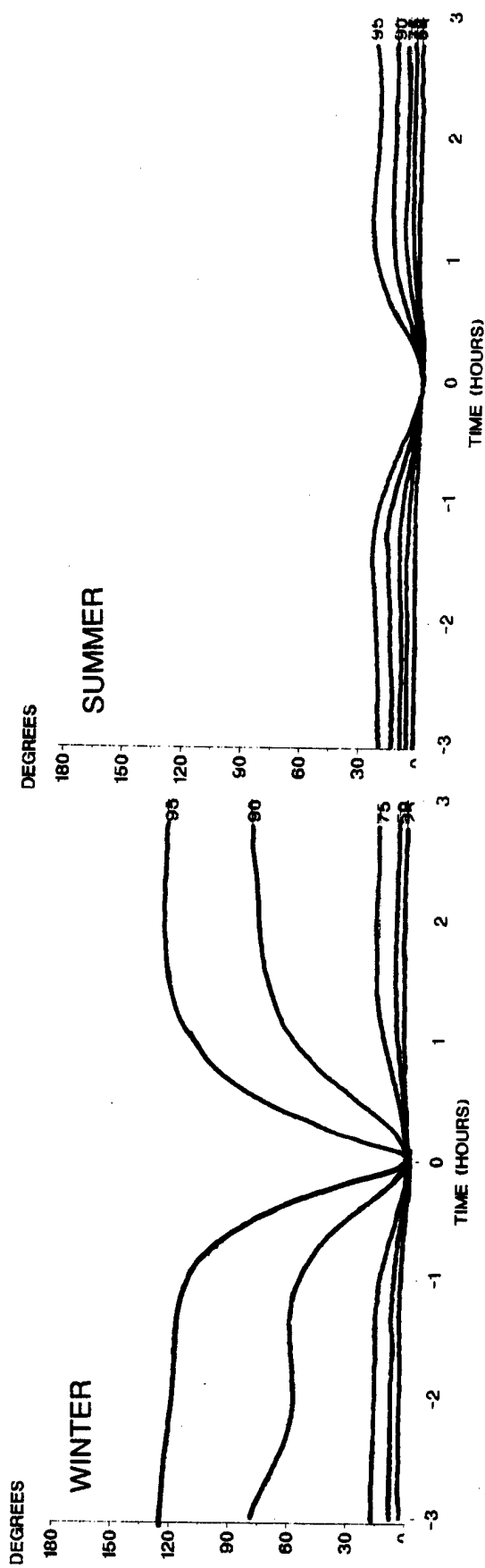
E-7 Temporal correlation of wind direction, desert climate, midnight.



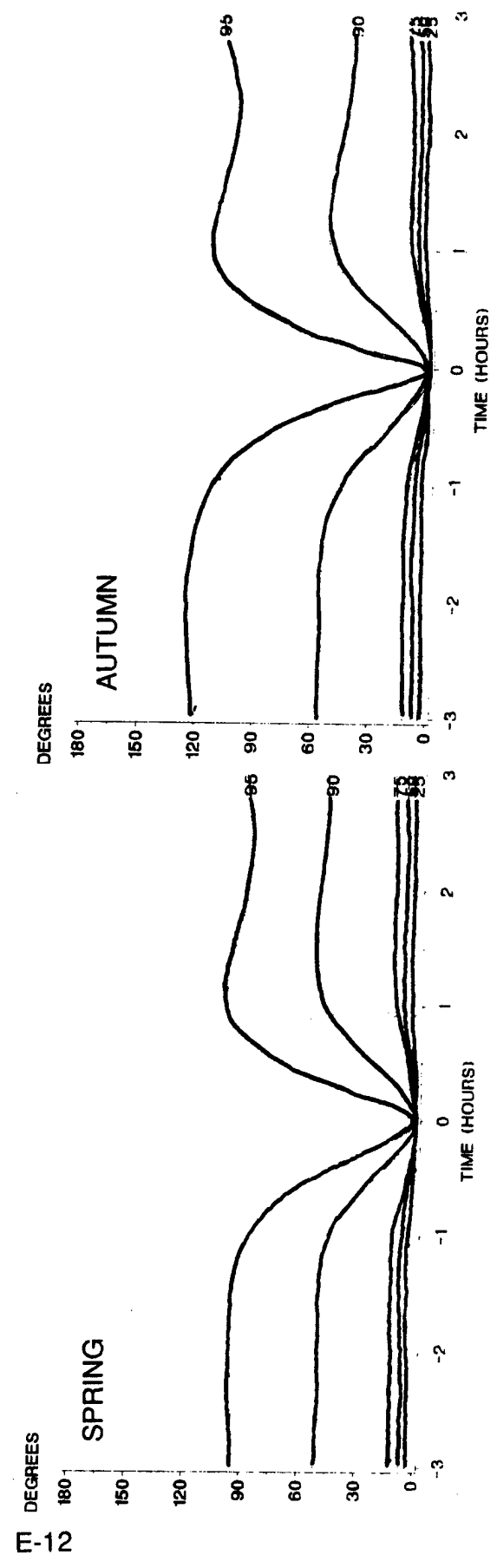
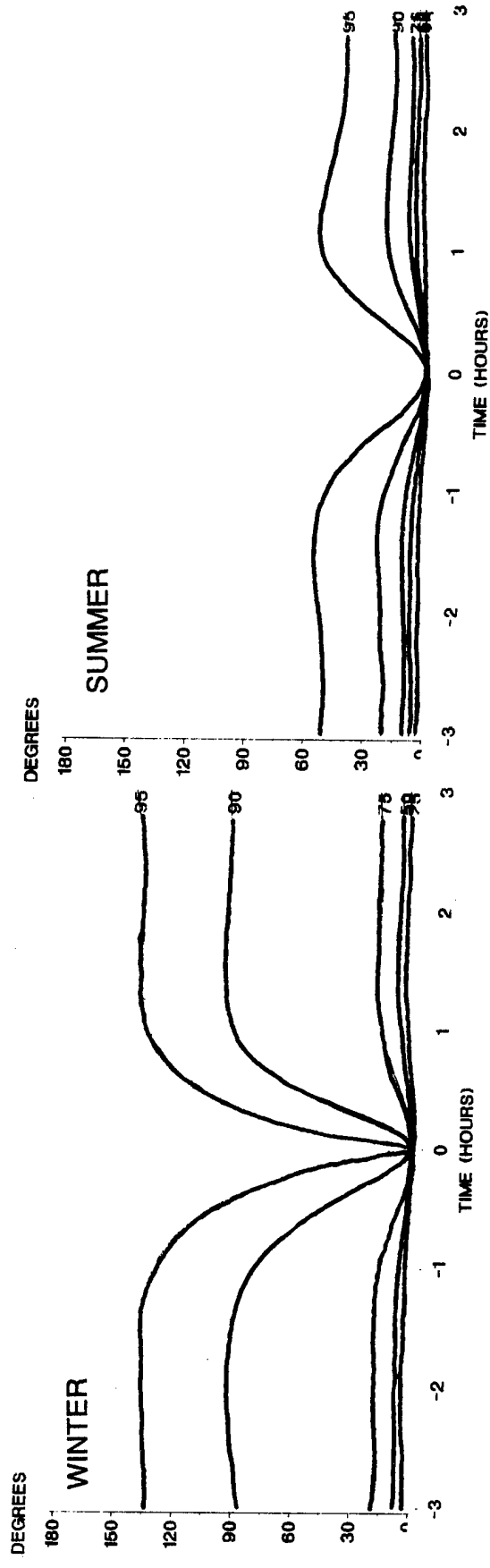
E-8 Temporal correlation of wind direction, desert climate, sunrise.



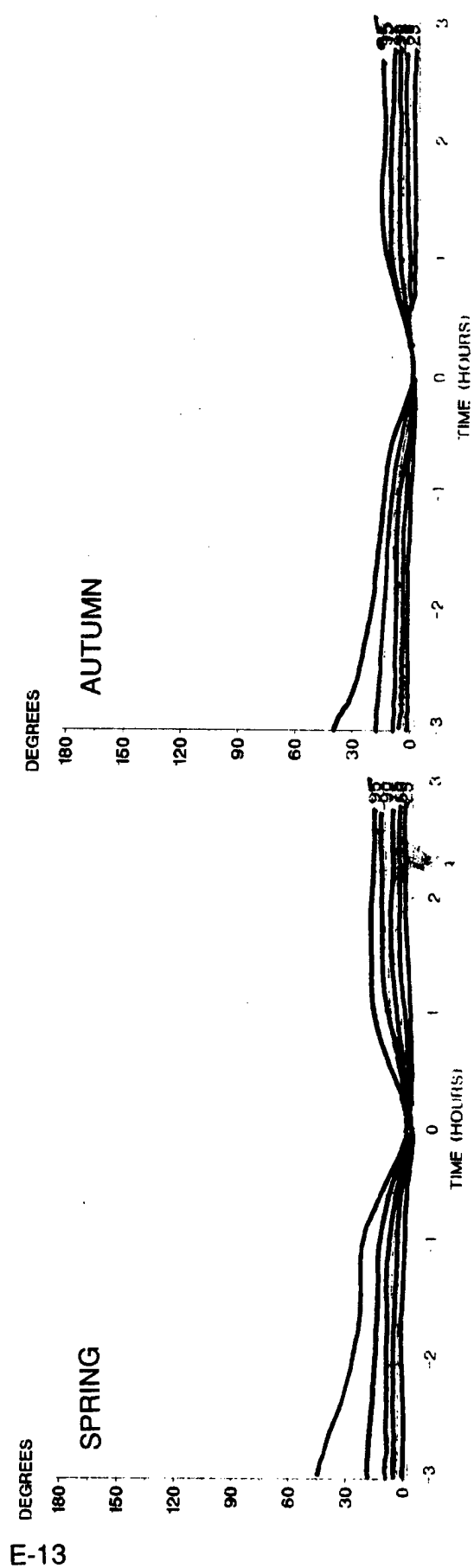
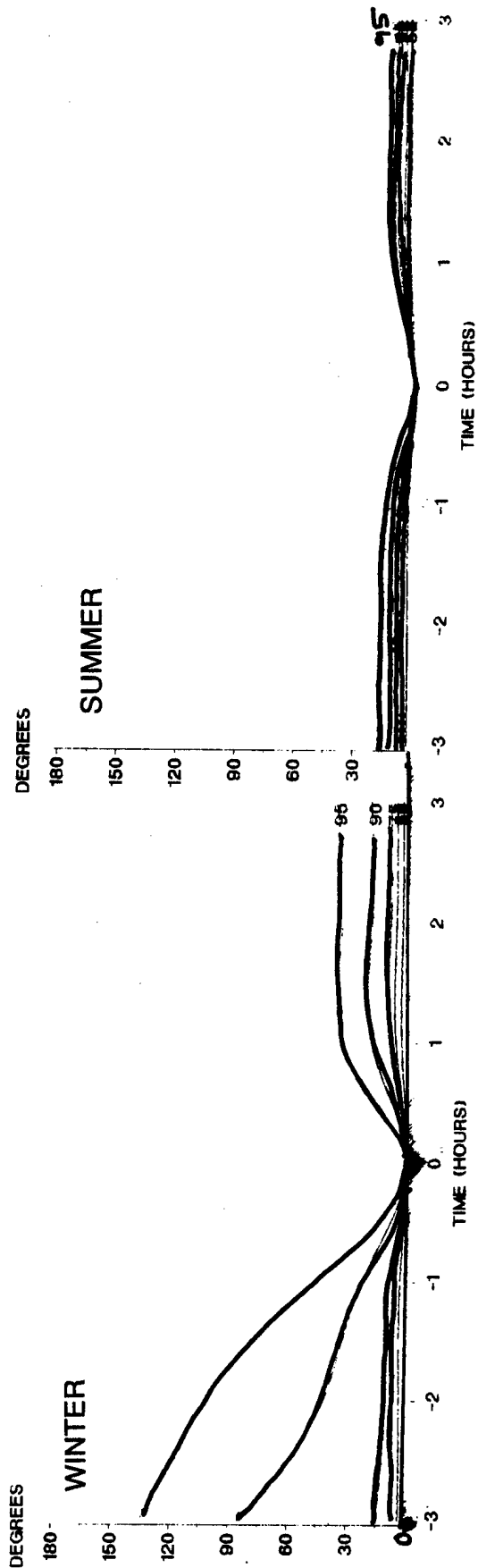
E-9 Temporal correlation of wind direction, desert climate, noon.



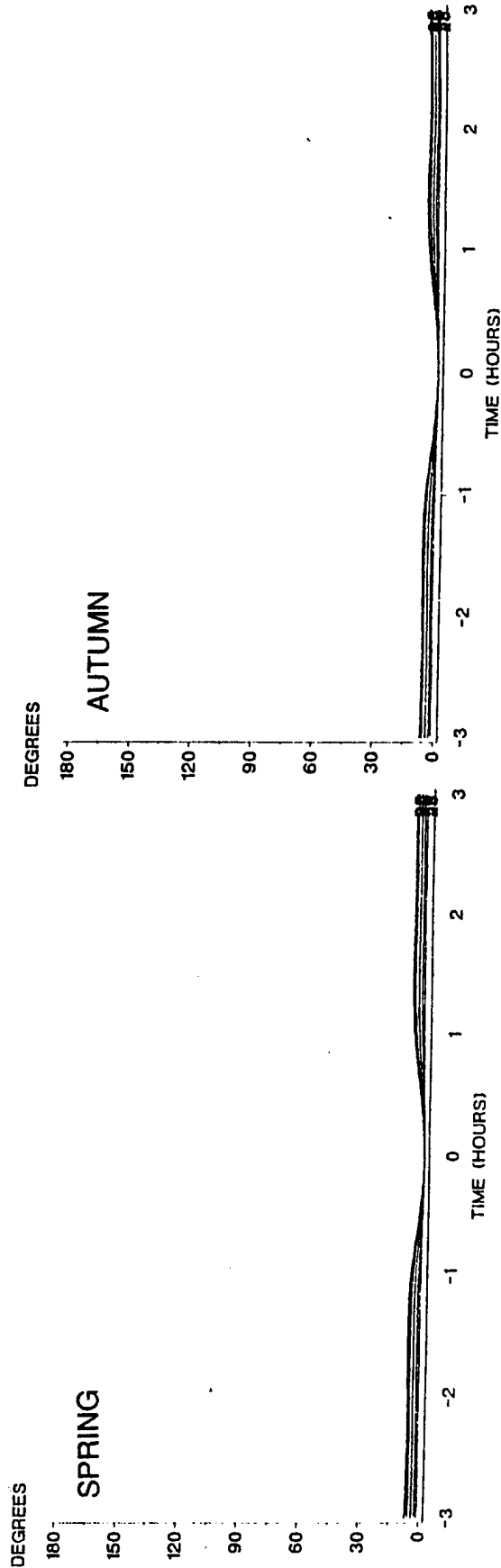
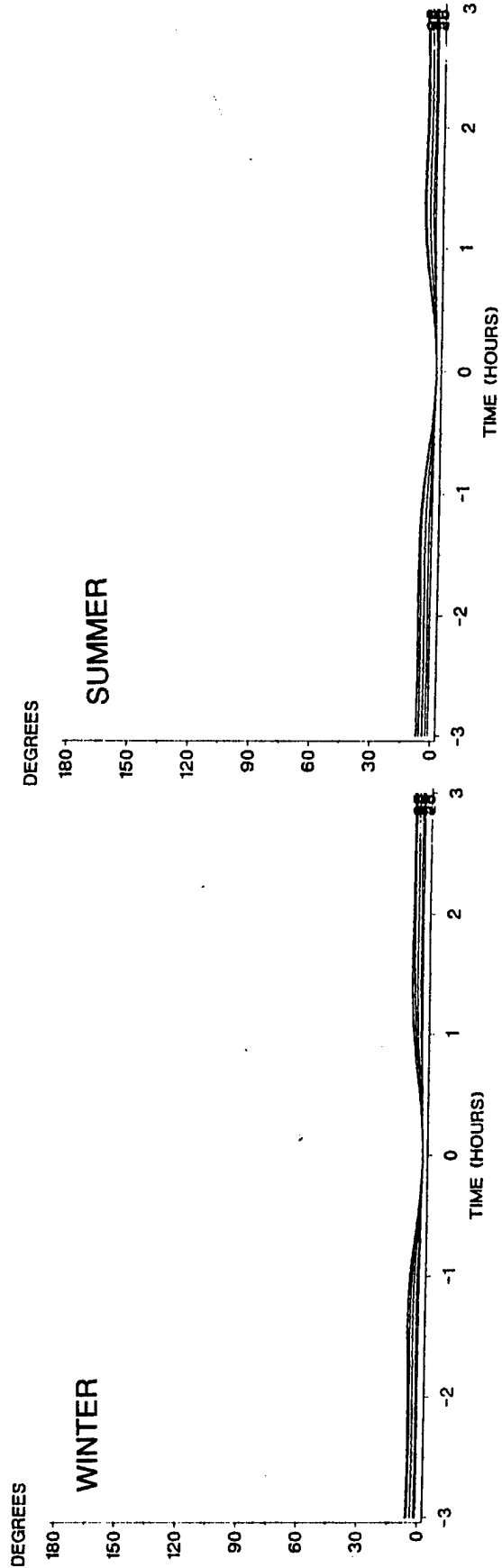
E-10 Temporal correlation of wind direction, maritime climate, midnight.



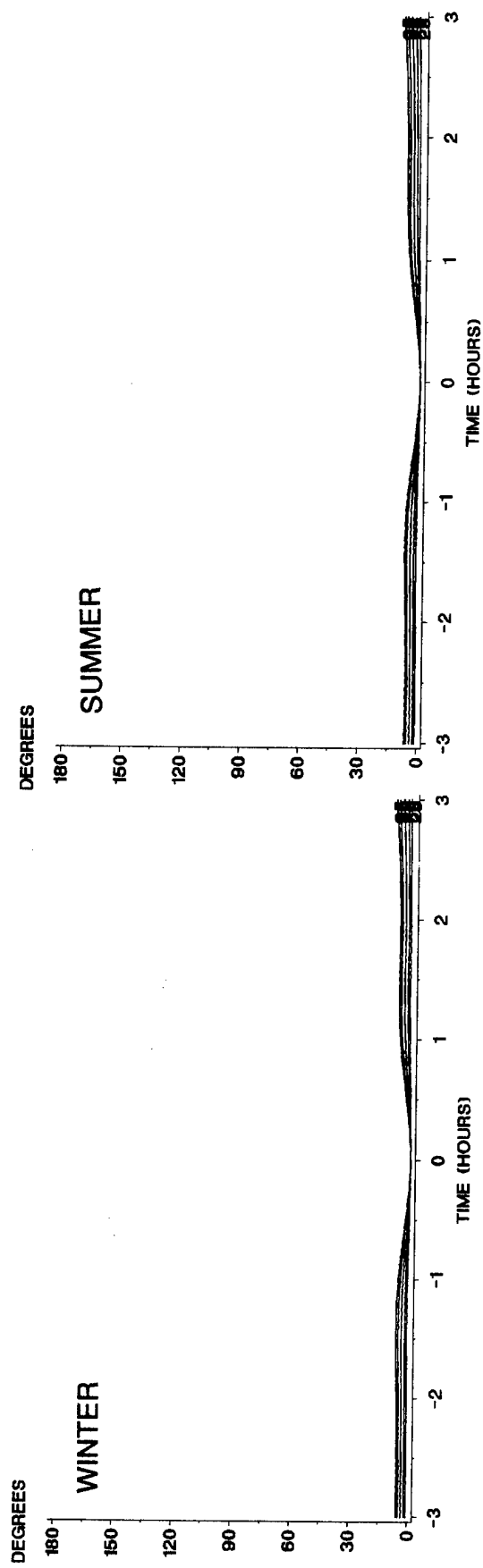
E-11 Temporal correlation of wind direction, maritime climate, sunrise.



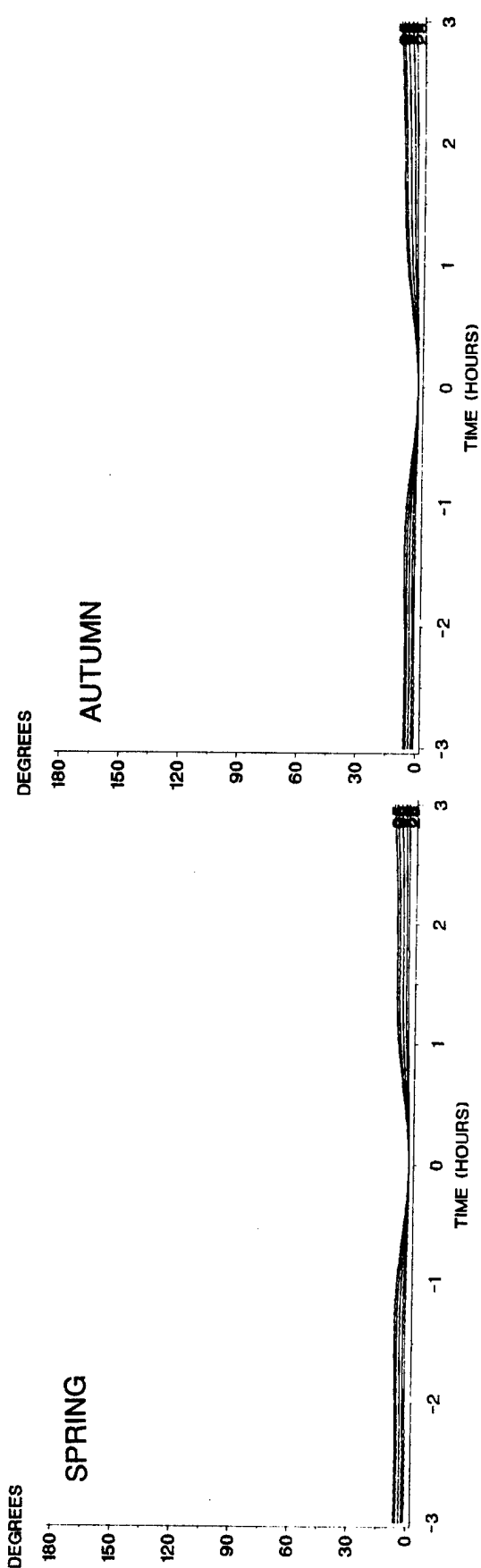
E-12 Temporal correlation of wind direction, maritime climate, noon.



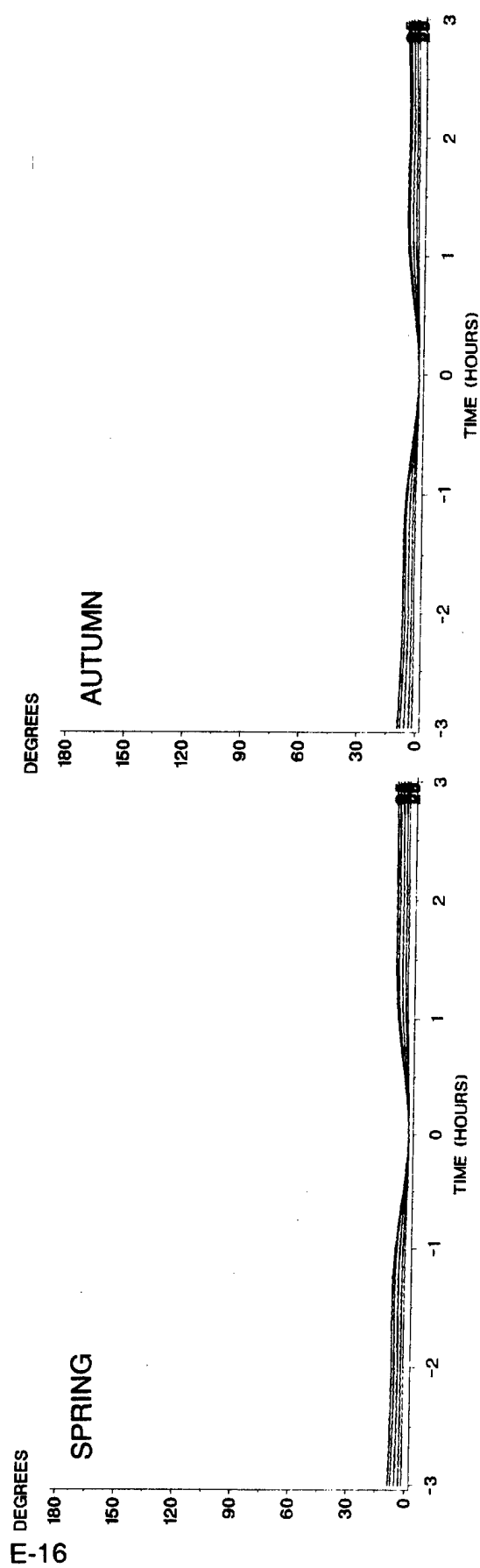
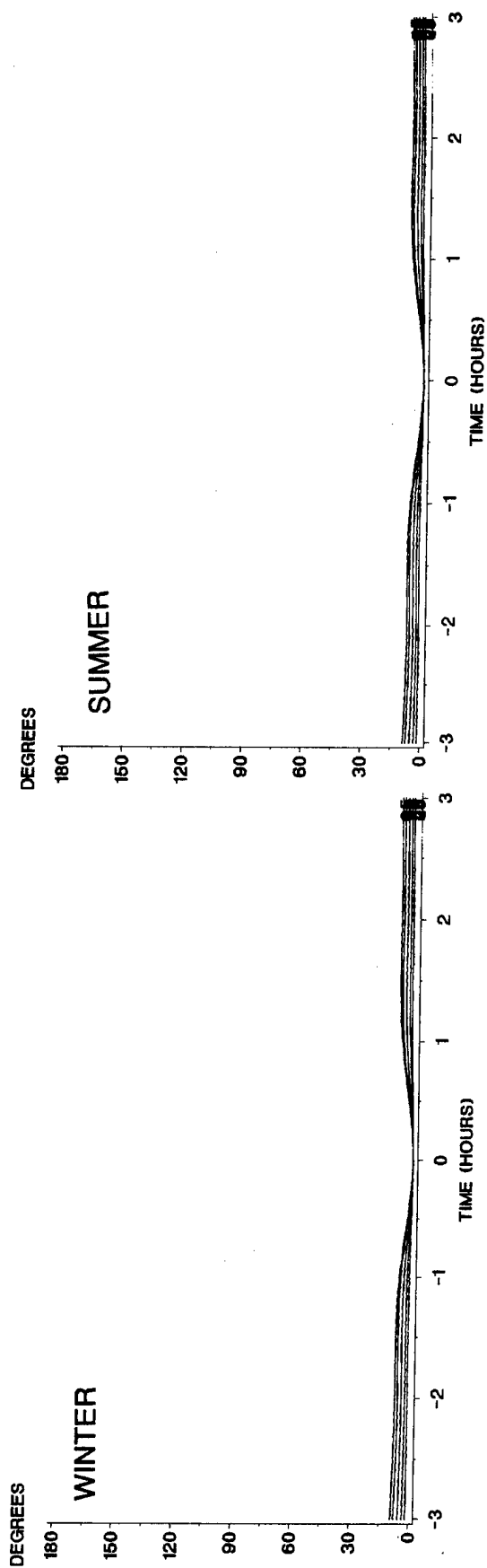
E-13 Temporal correlation of wind direction, tropical climate, midnight.



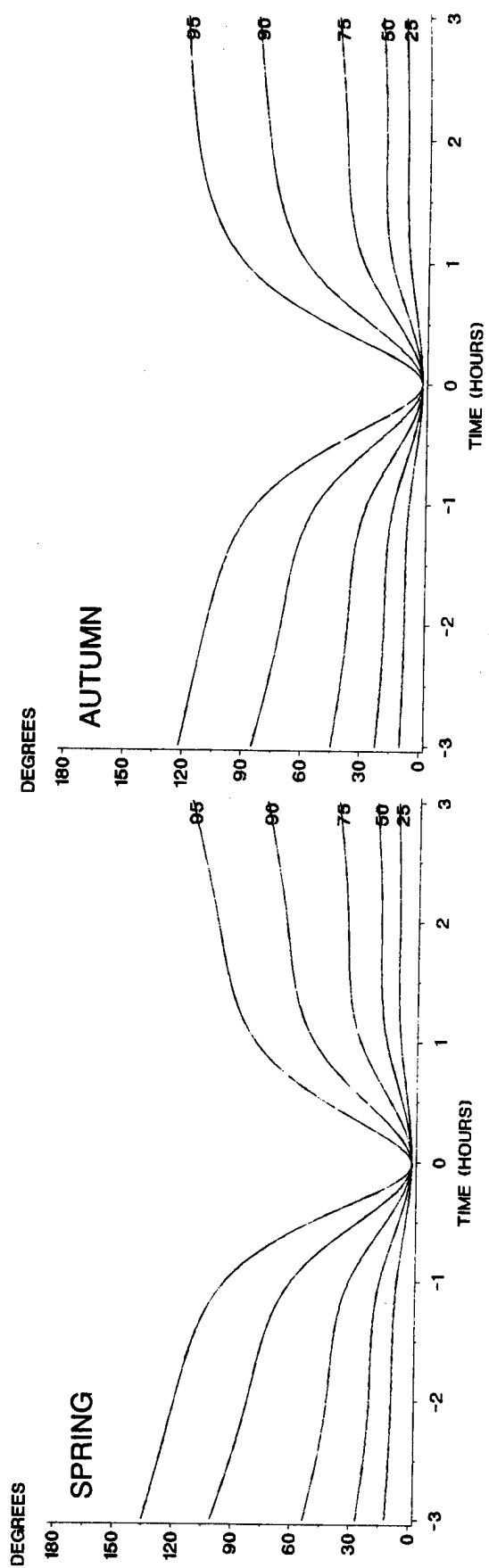
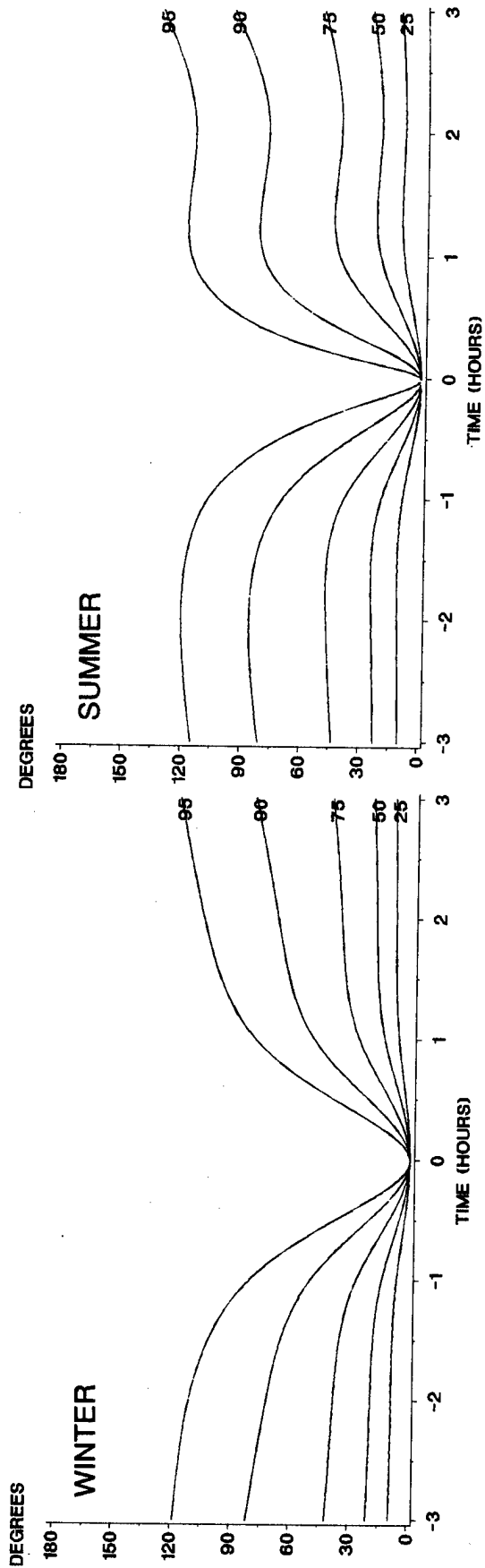
E-15



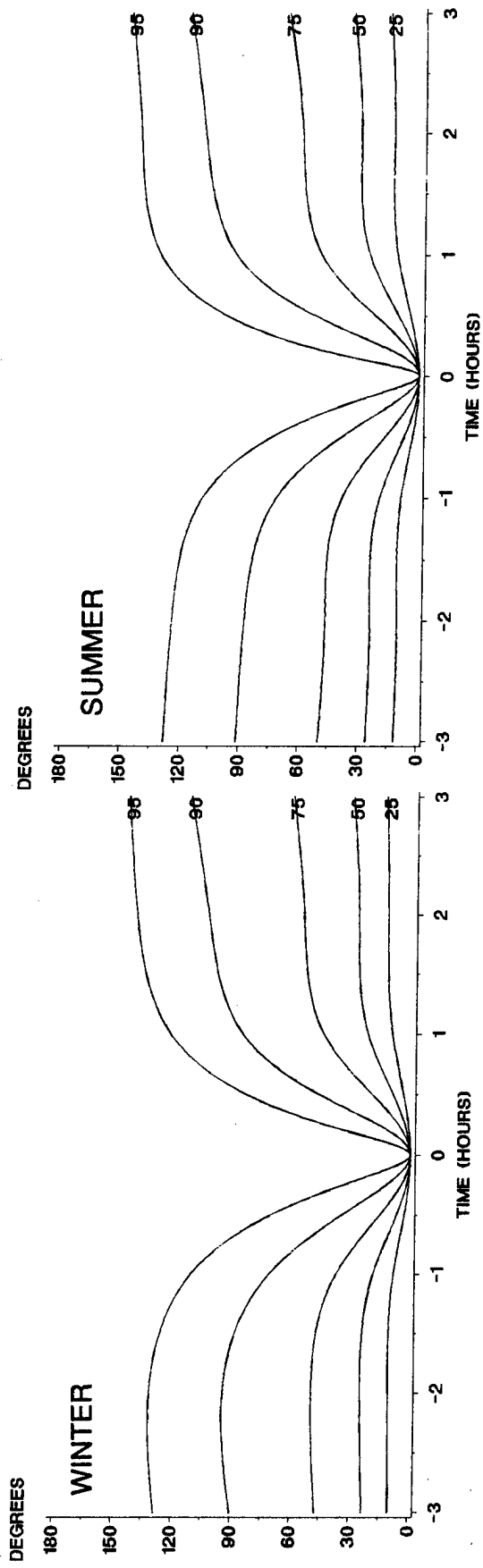
E-14 Temporal correlation of wind direction, tropical climate, sunrise.



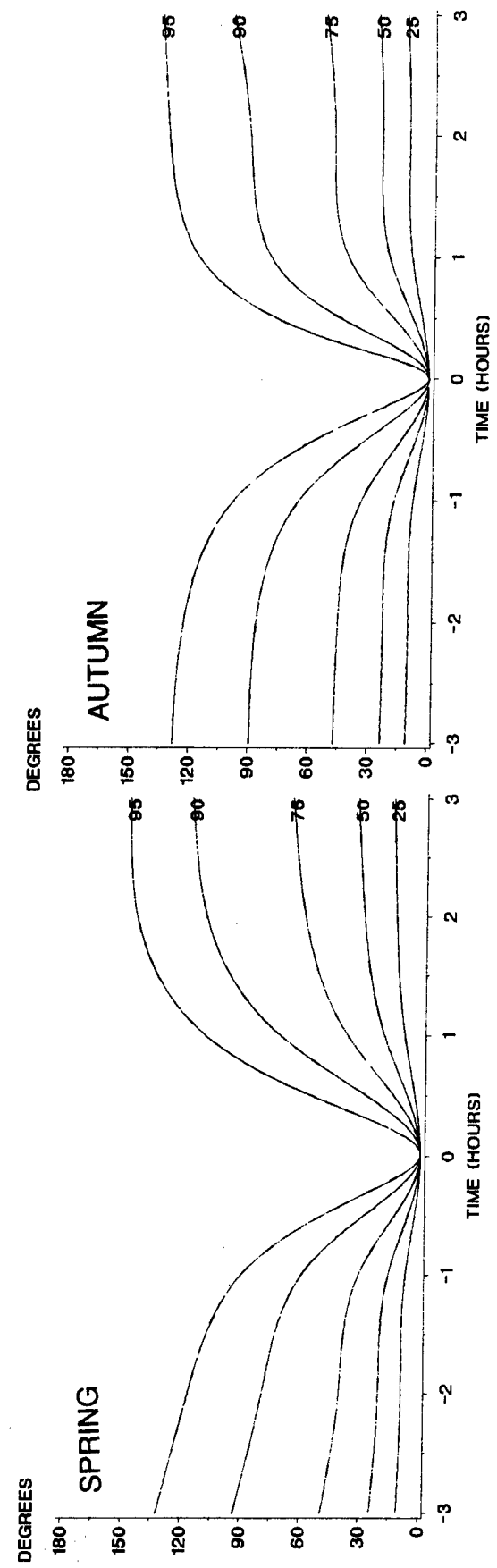
E-15 Temporal correlation of wind direction, tropical climate, noon.



E-16 Temporal correlation of wind direction, coastal climate, midnight.



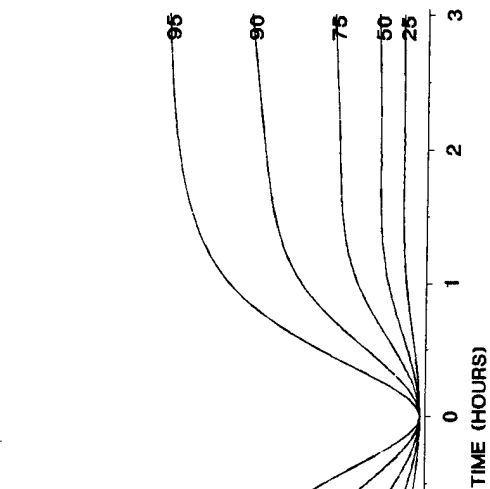
E-18



E-17 Temporal correlation of wind direction, coastal climate, sunrise.

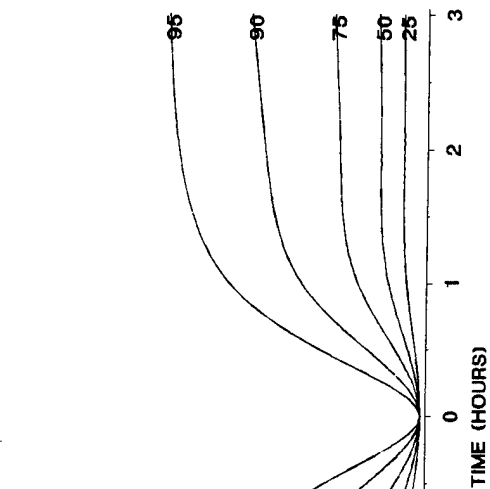
DEGREES

WINTER



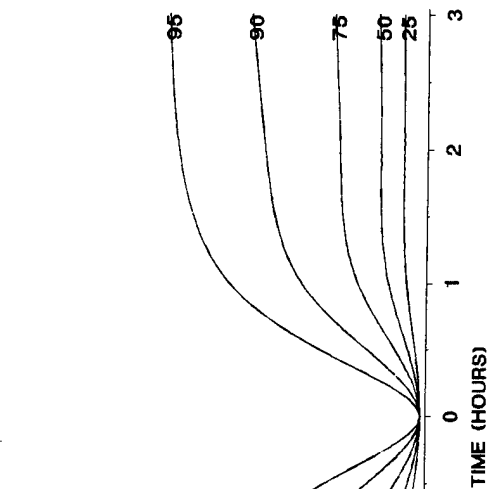
DEGREES

WINTER



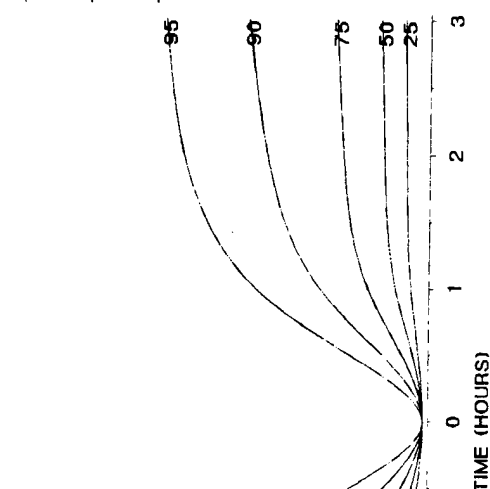
DEGREES

SUMMER



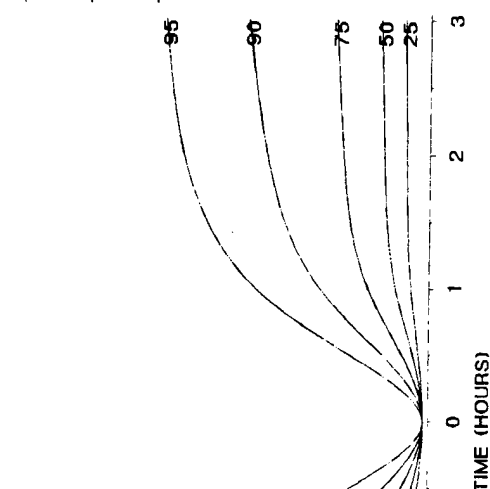
DEGREES

SPRING



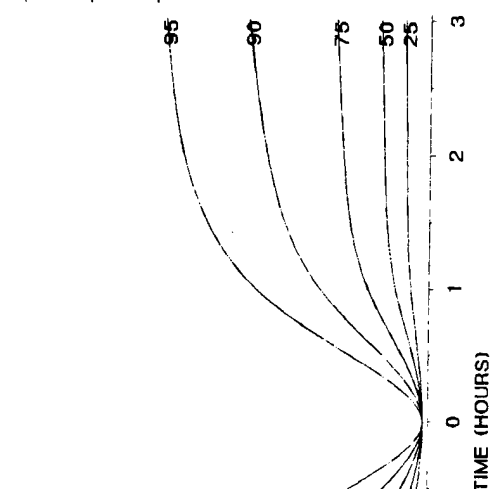
DEGREES

AUTUMN



DEGREES

SUMMER

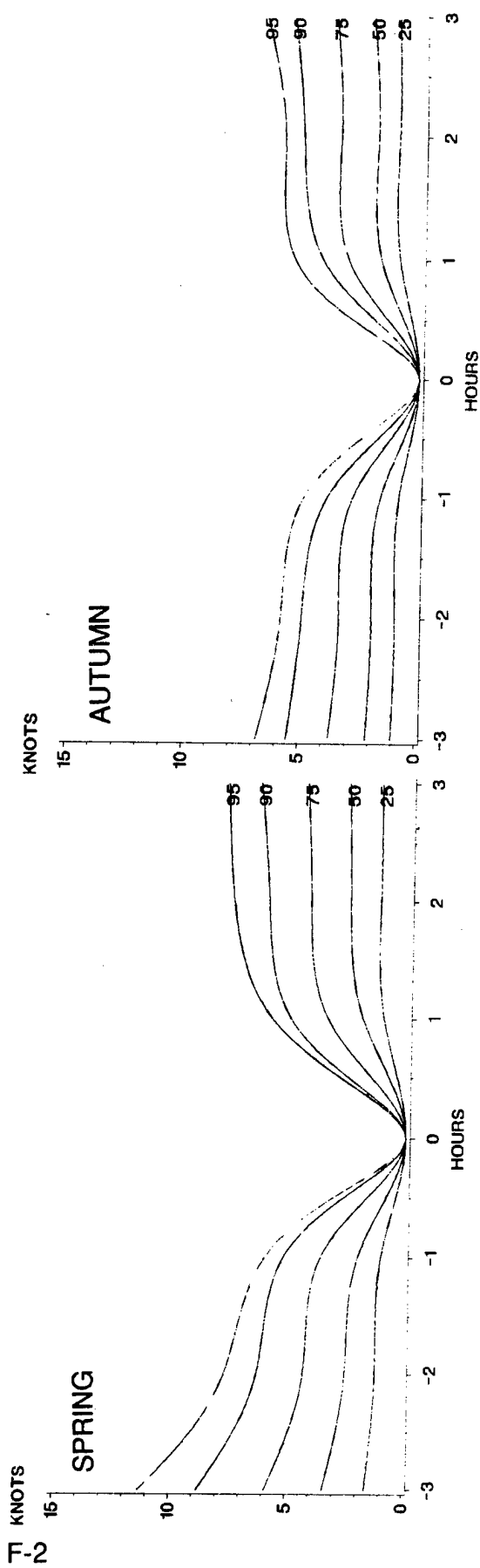
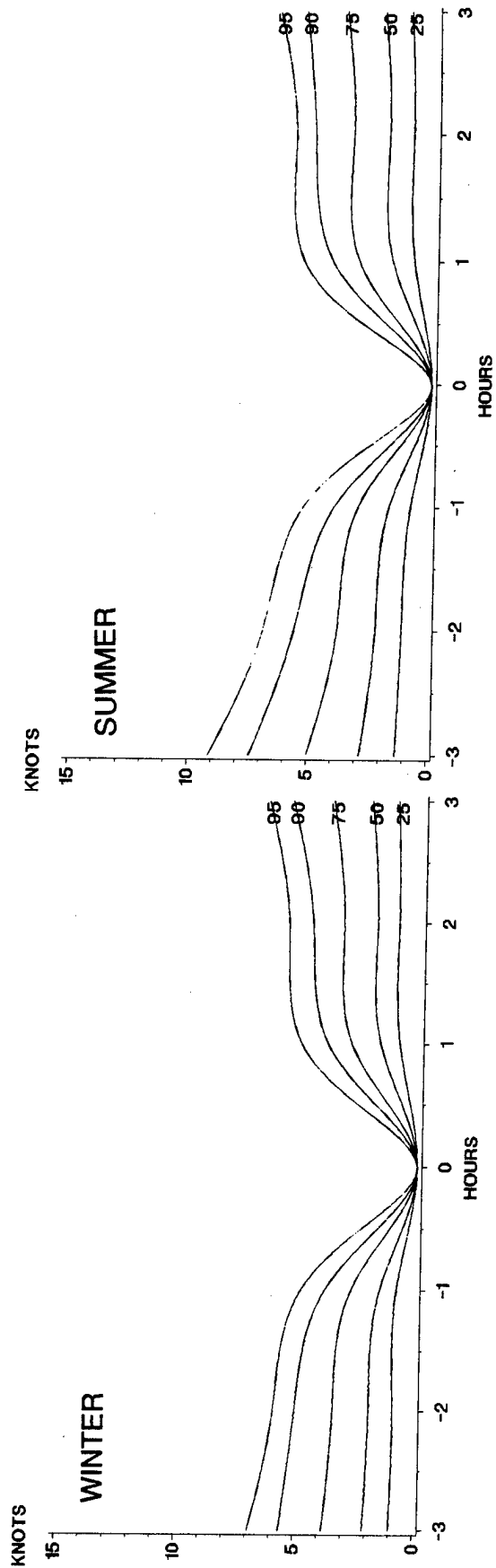


E-18 Temporal correlation of wind direction, coastal climate, noon.

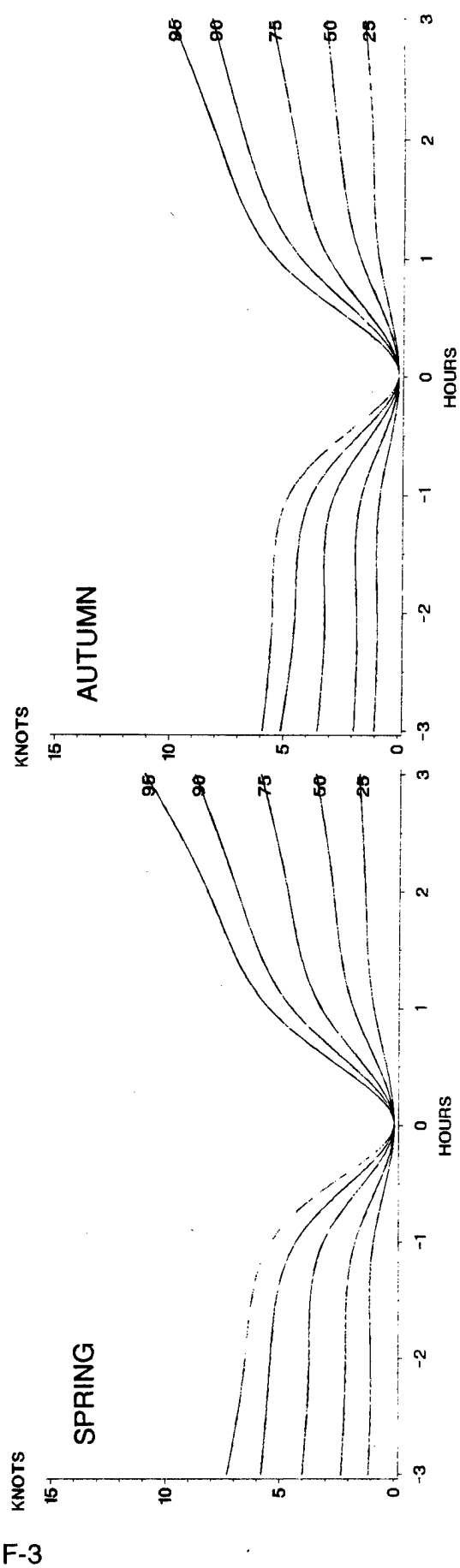
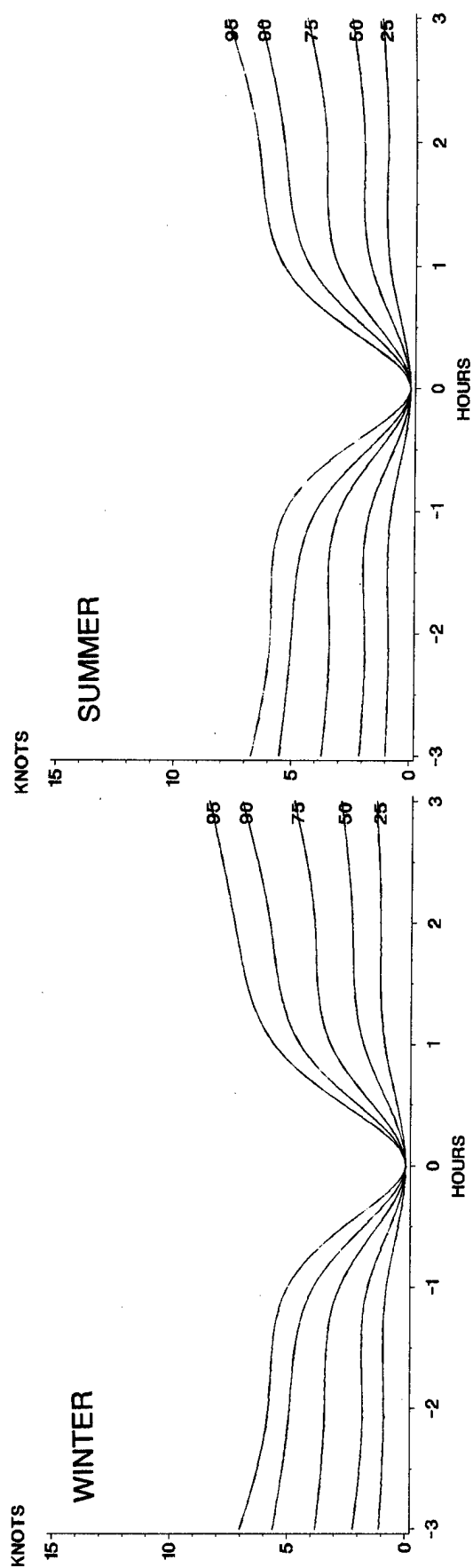
APPENDIX F

TEMPORAL CORRELATION OF WIND SPEED

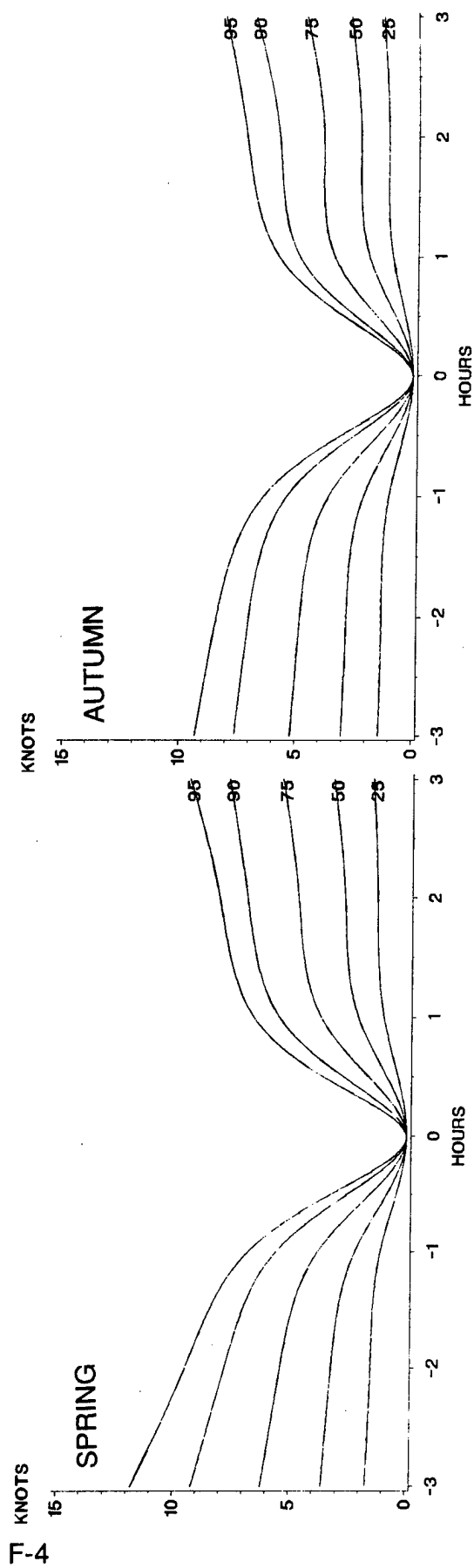
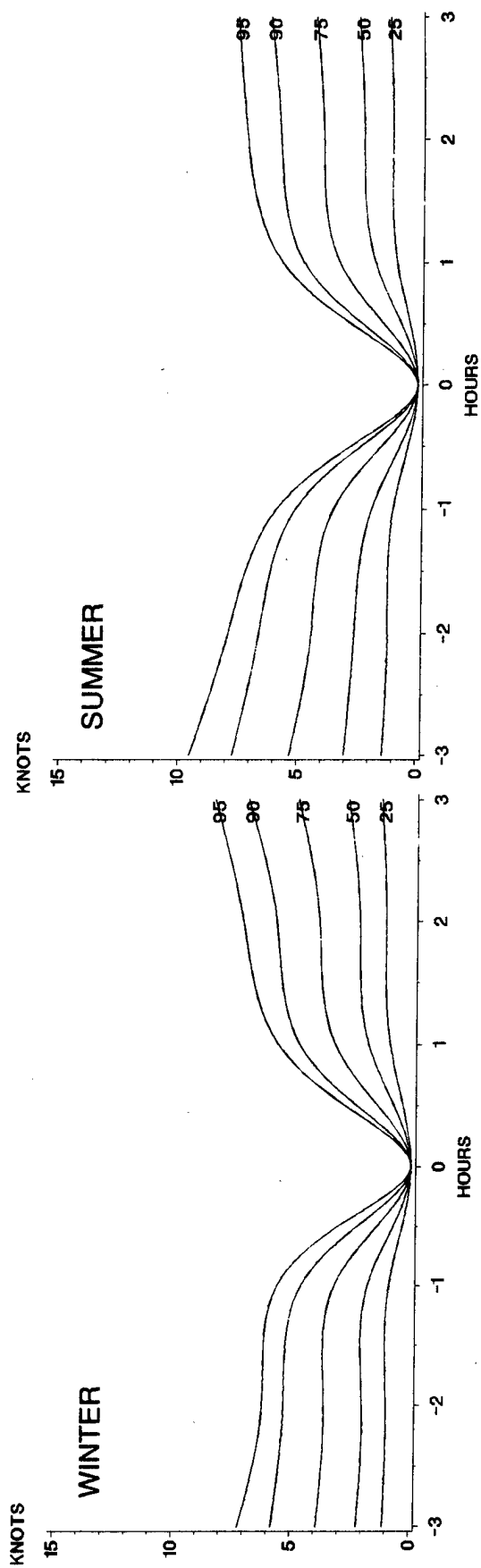
- F-1 Temporal correlation of wind speed, continental climate, midnight.
- F-2 Temporal correlation of wind speed, continental climate, sunrise.
- F-3 Temporal correlation of wind speed, continental climate, noon.
- F-4 Temporal correlation of wind speed, arctic climate, midnight.
- F-5 Temporal correlation of wind speed, arctic climate, sunrise.
- F-6 Temporal correlation of wind speed, arctic climate, noon.
- F-7 Temporal correlation of wind speed, desert climate, midnight.
- F-8 Temporal correlation of wind speed, desert climate, sunrise.
- F-9 Temporal correlation of wind speed, desert climate, noon.
- F-10 Temporal correlation of wind speed, maritime climate, midnight.
- F-11 Temporal correlation of wind speed, maritime climate, sunrise.
- F-12 Temporal correlation of wind speed, maritime climate, noon.
- F-13 Temporal correlation of wind speed, tropical climate, midnight.
- F-14 Temporal correlation of wind speed, tropical climate, sunrise.
- F-15 Temporal correlation of wind speed, tropical climate, noon.
- F-16 Temporal correlation of wind speed, coastal climate, midnight.
- F-17 Temporal correlation of wind speed, coastal climate, sunrise.
- F-18 Temporal correlation of wind speed, coastal climate, noon.



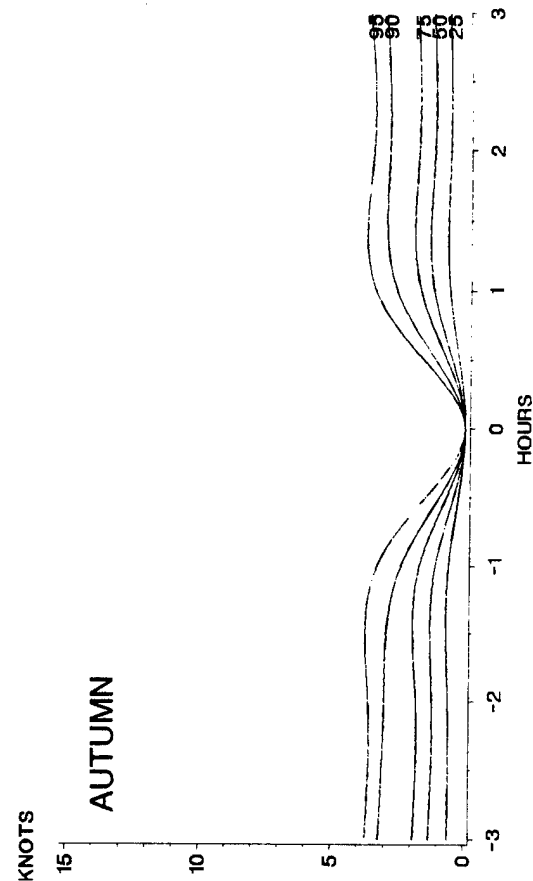
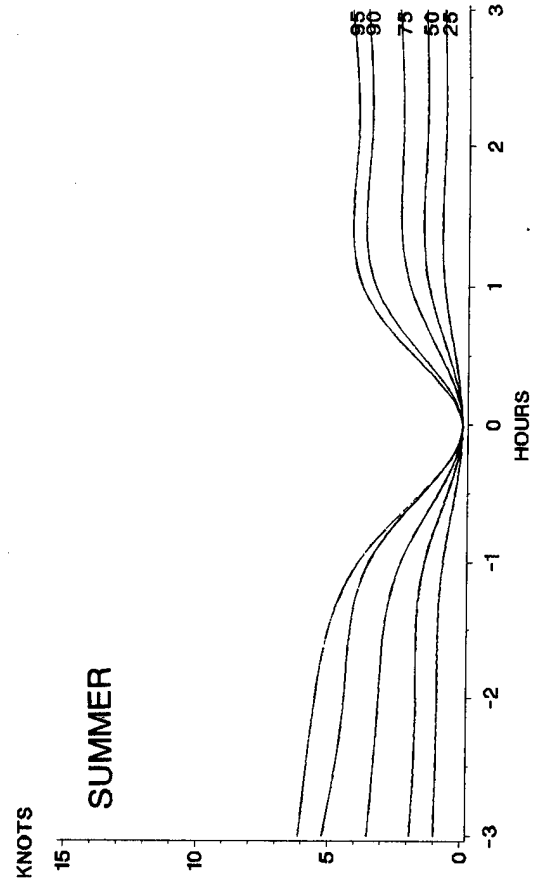
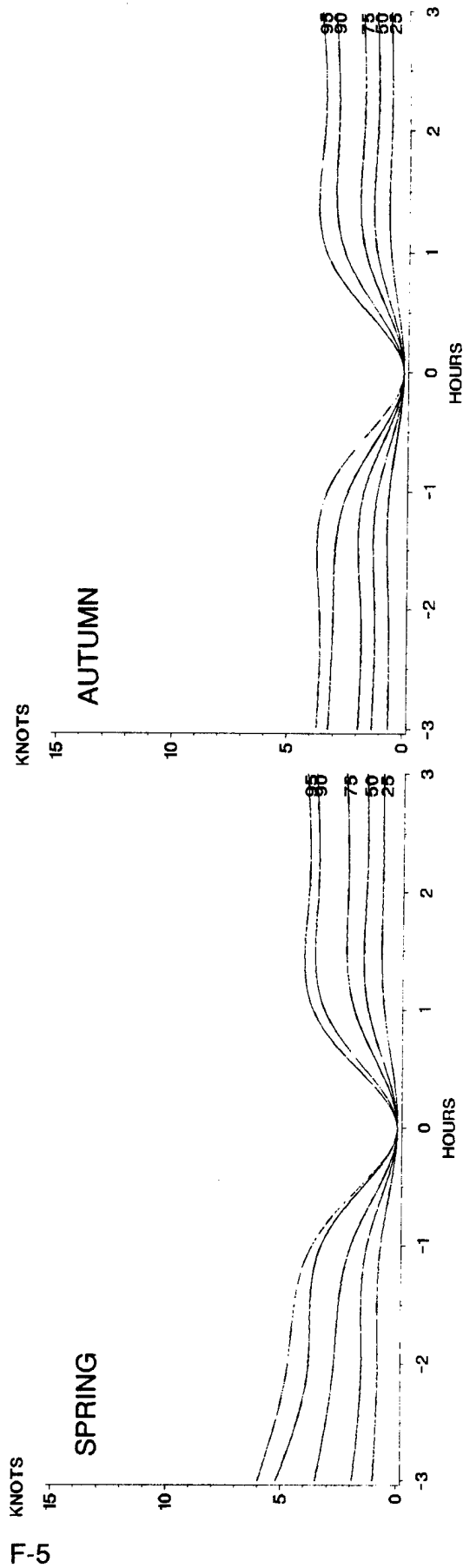
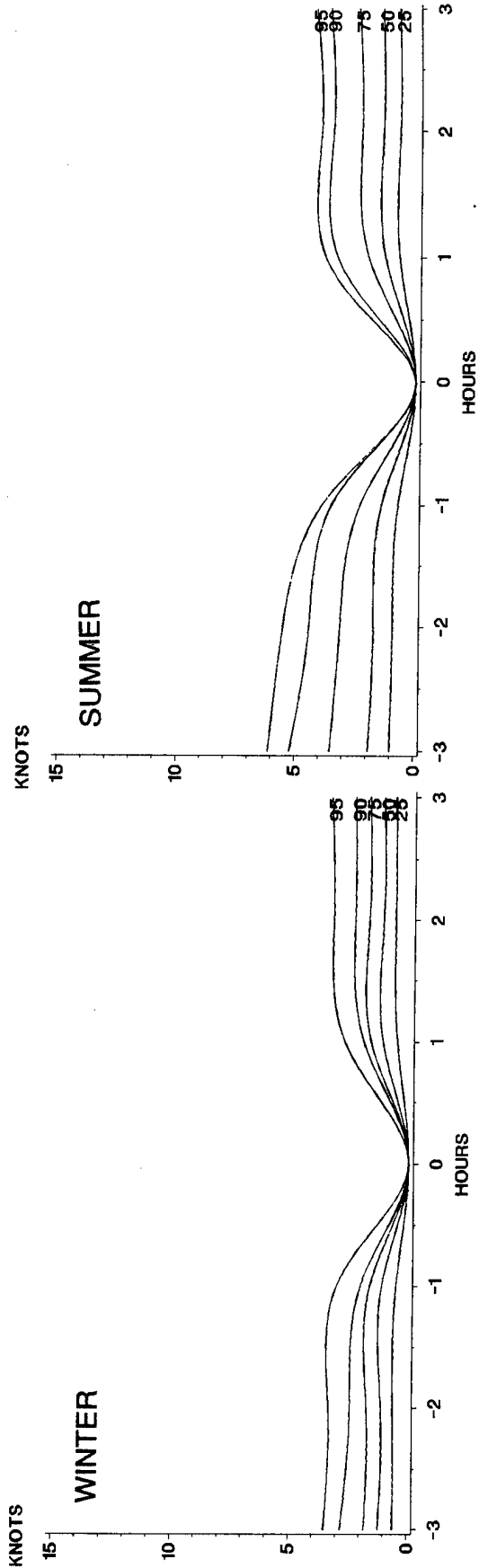
F-1 Temporal correlation of wind speed, continental climate, midnight.



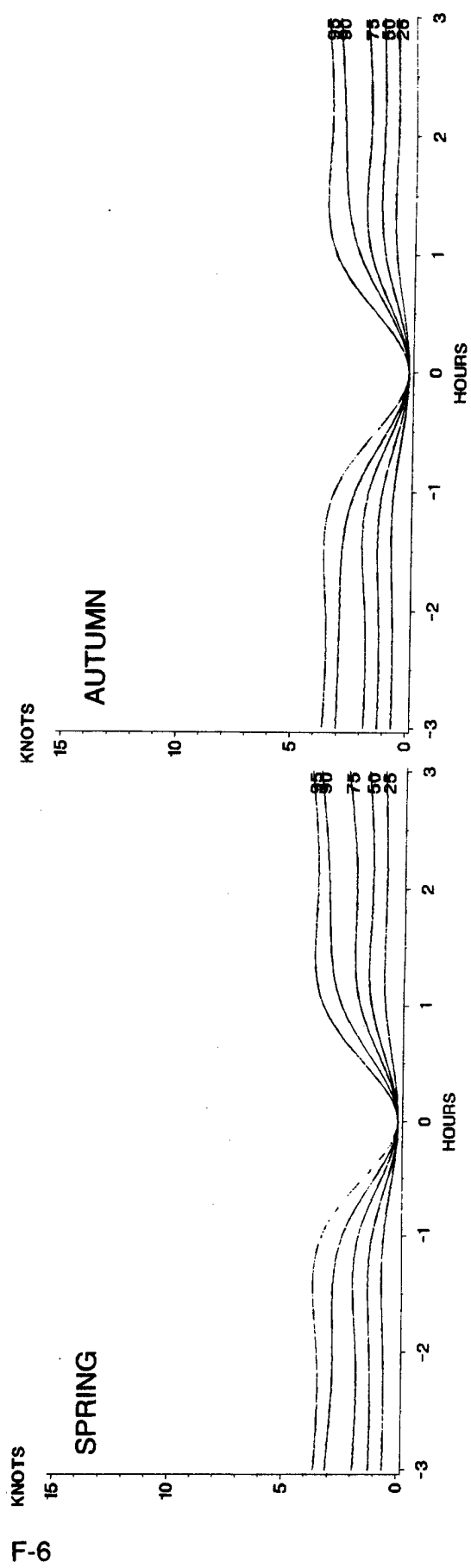
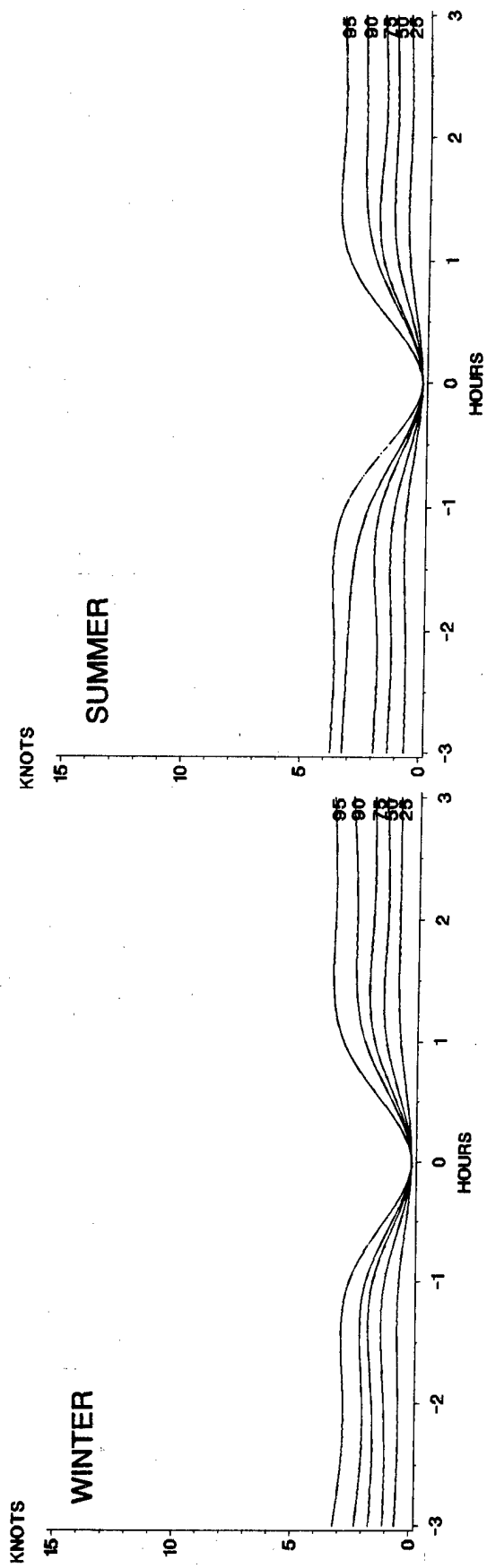
F-2 Temporal correlation of wind speed, continental climate, sunrise.



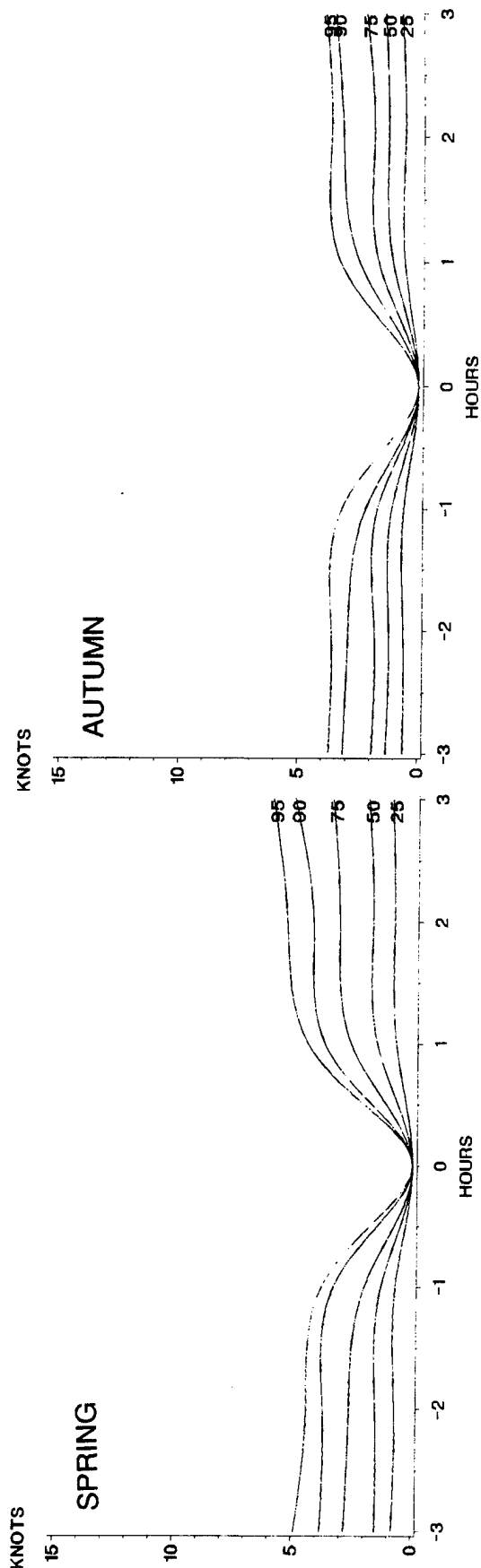
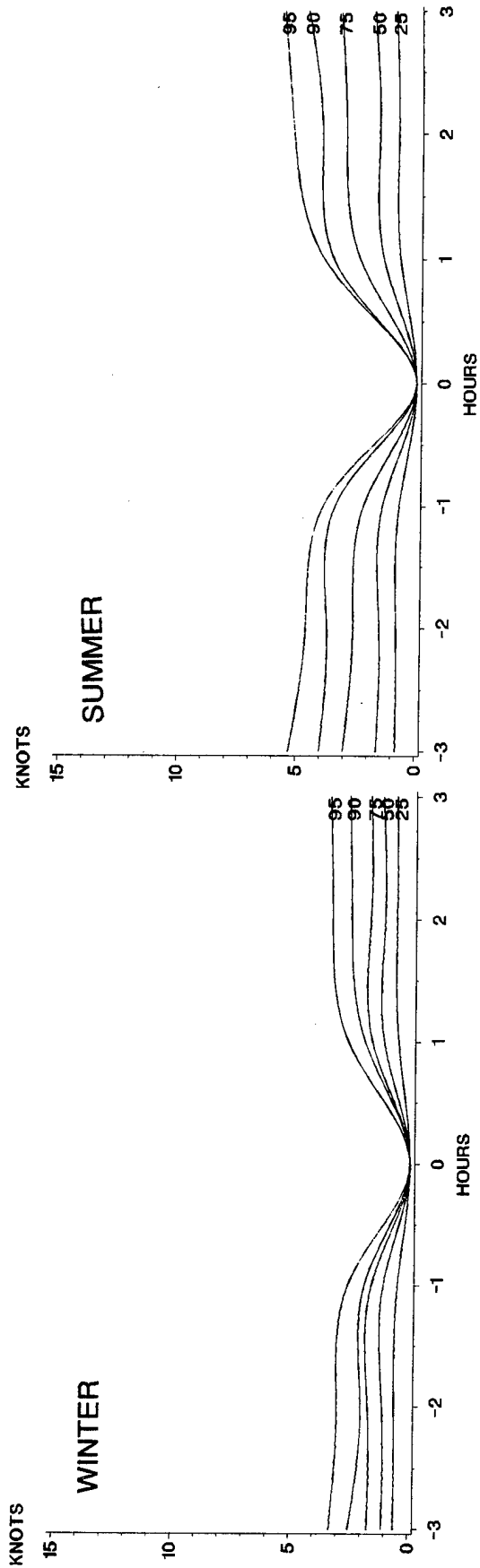
F-3 Temporal correlation of wind speed, continental climate, noon.



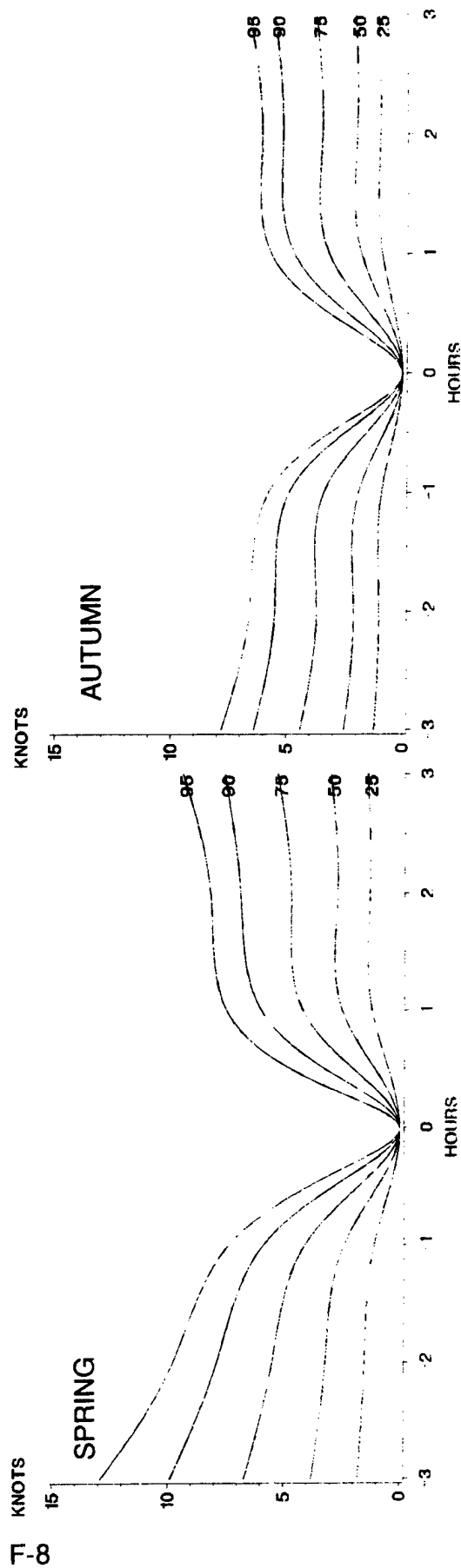
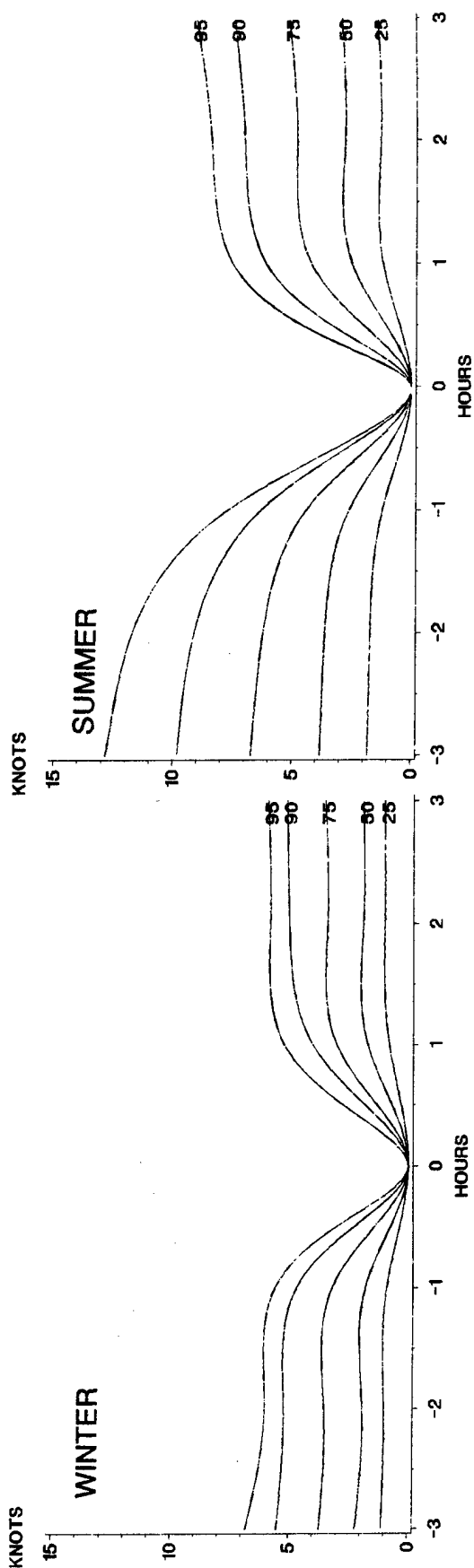
F-4 Temporal correlation of wind speed, arctic climate, midnight.



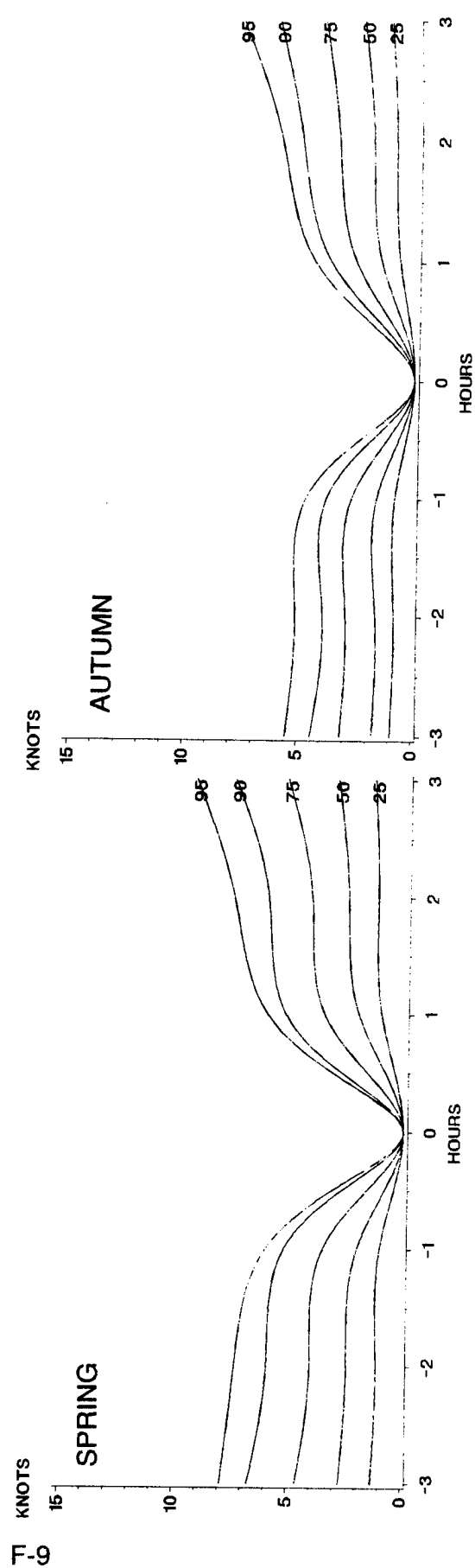
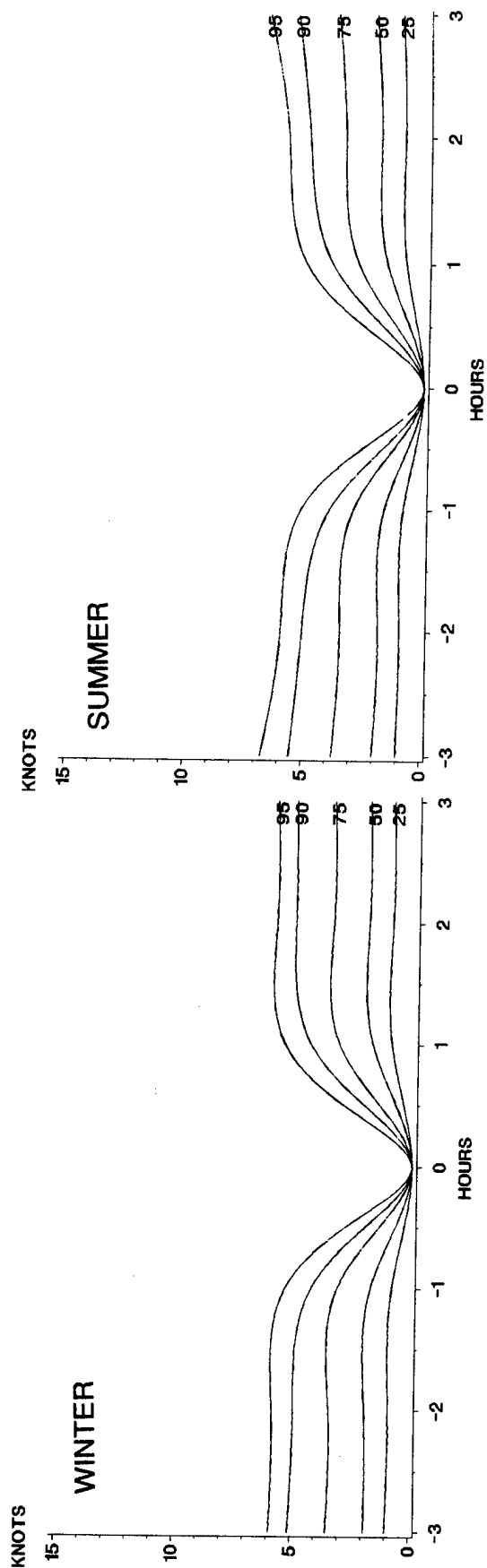
F-5 Temporal correlation of wind speed, arctic climate, sunrise.



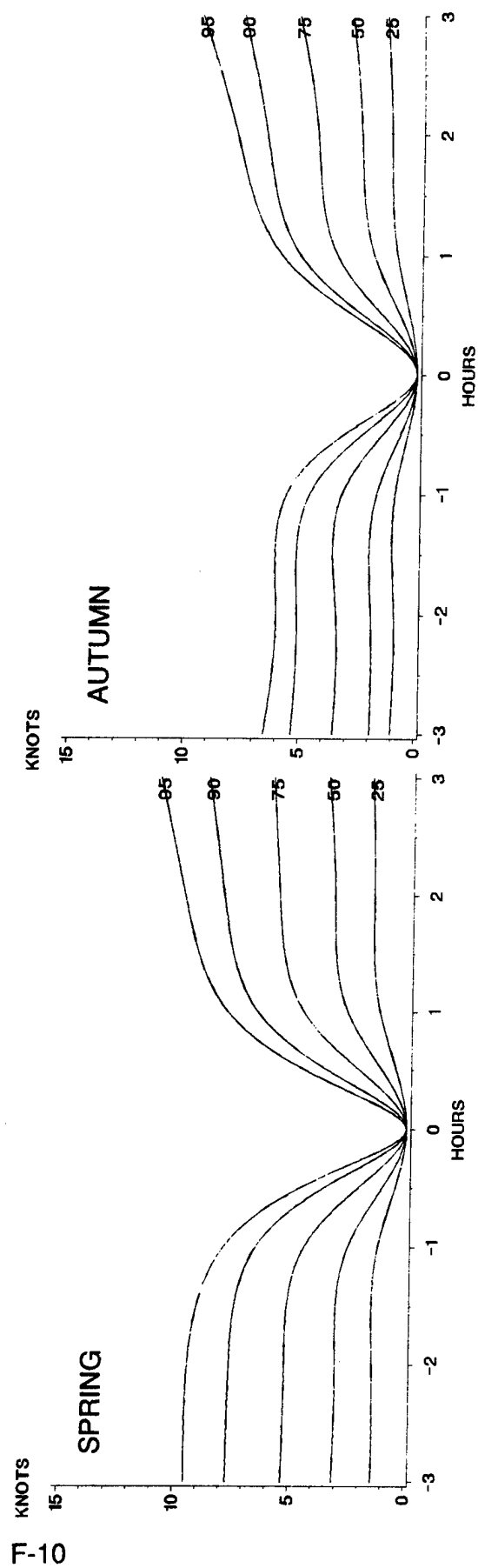
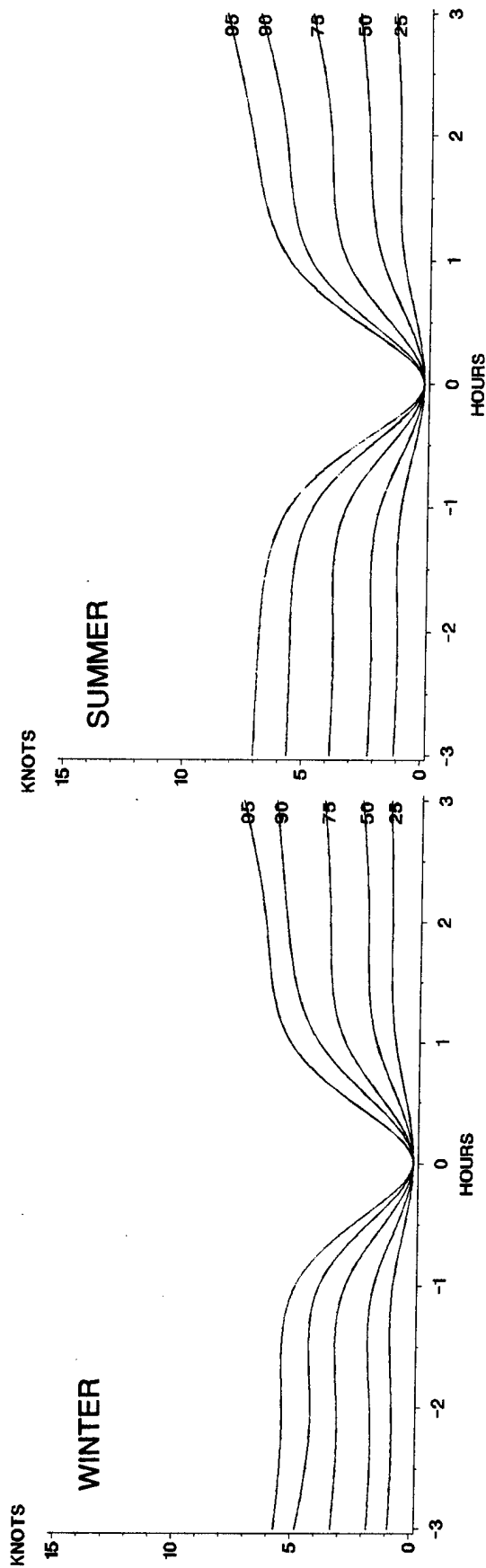
F-6 Temporal correlation of wind speed, arctic climate, noon.



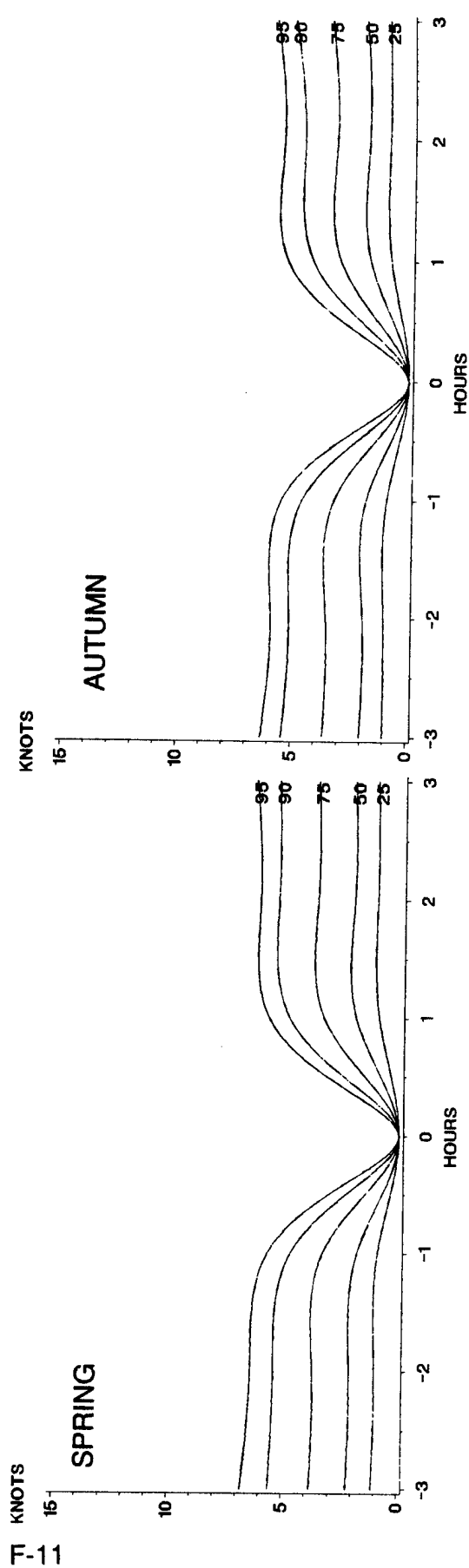
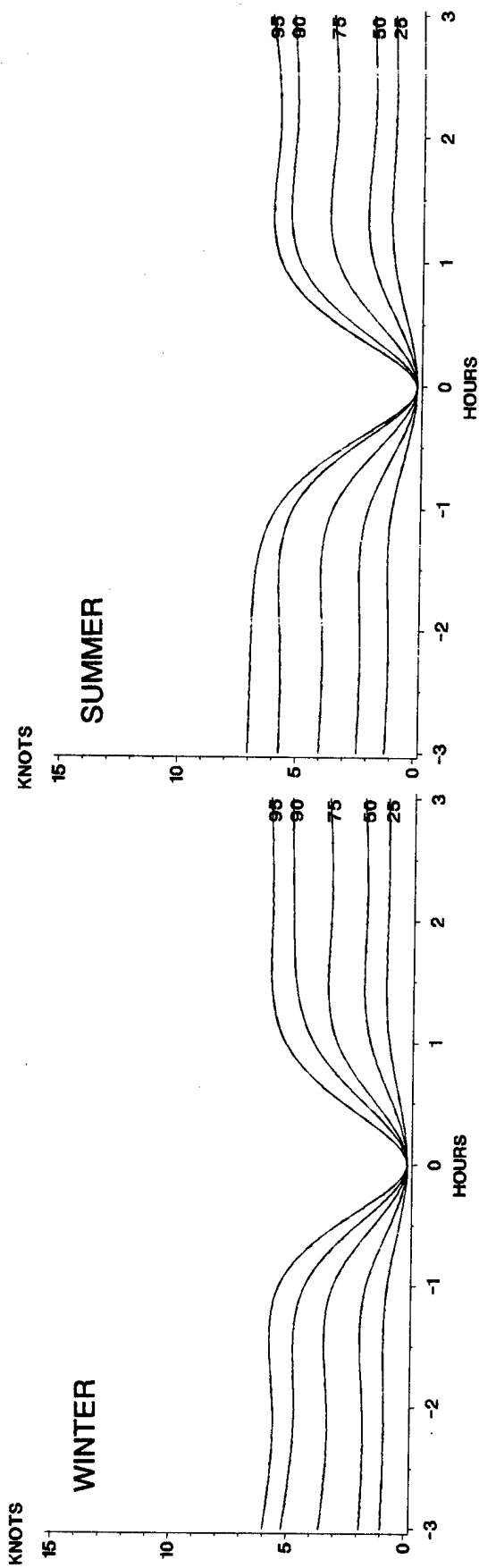
F-7 Temporal correlation of wind speed, desert climate, midnight.



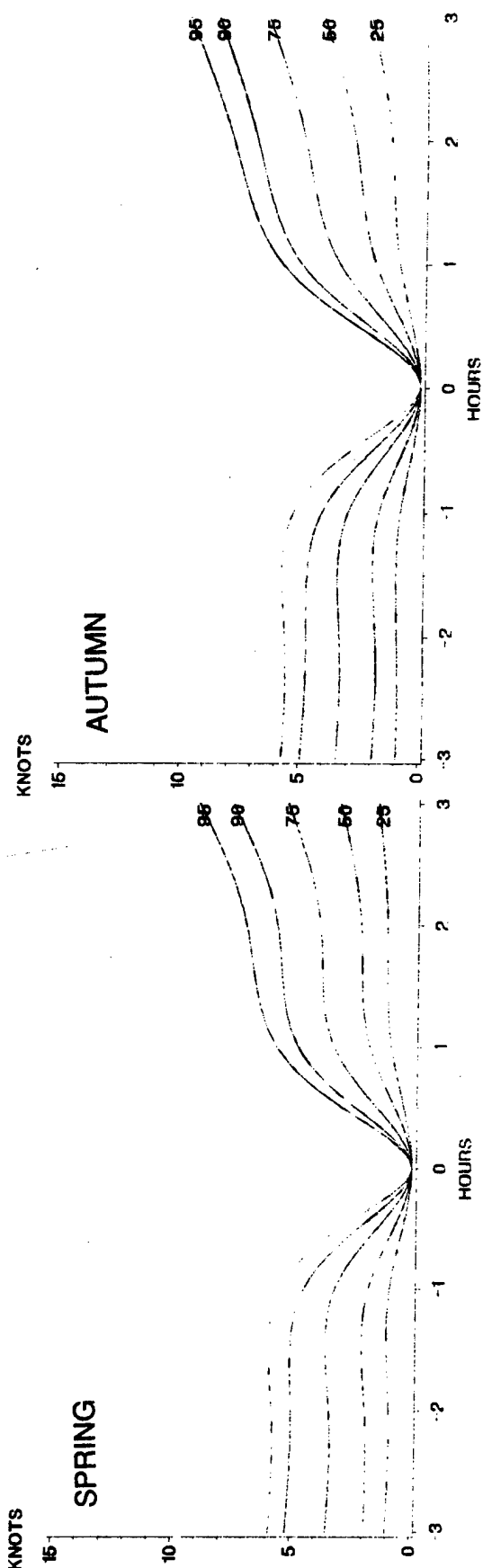
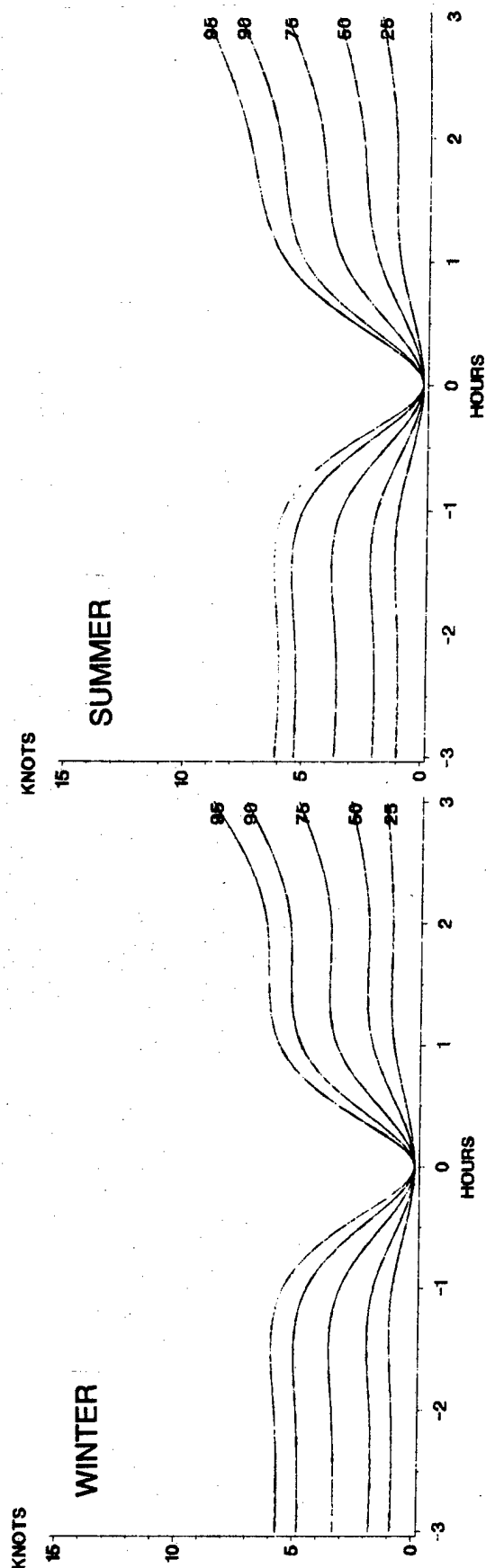
F-8 Temporal correlation of wind speed, desert climate, sunrise.



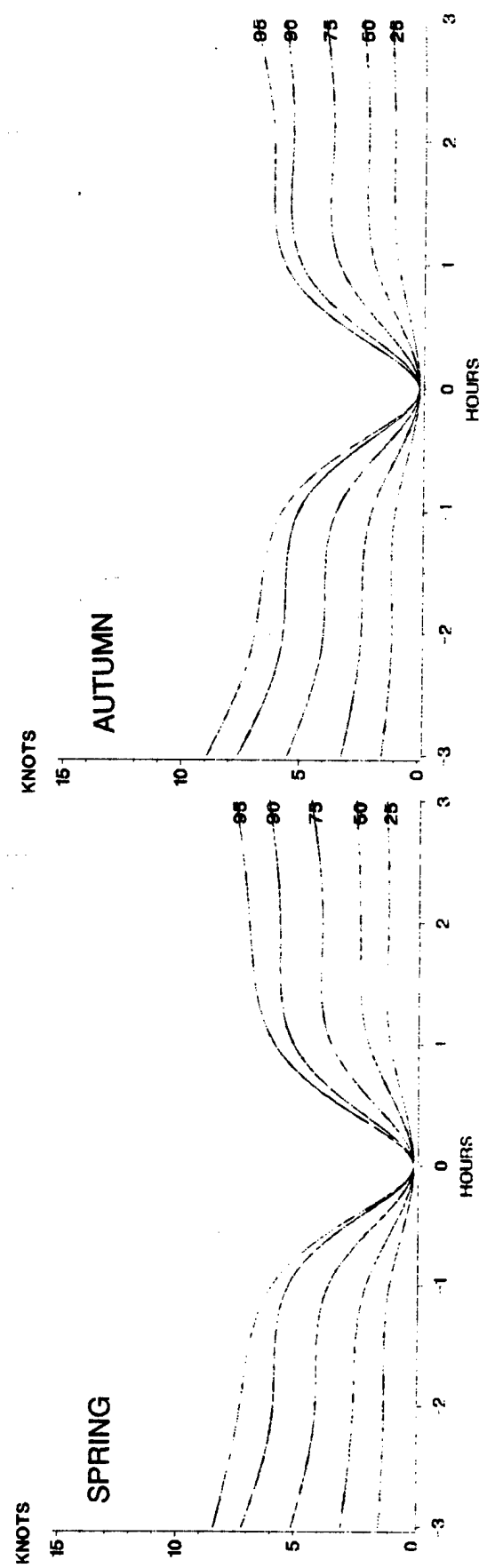
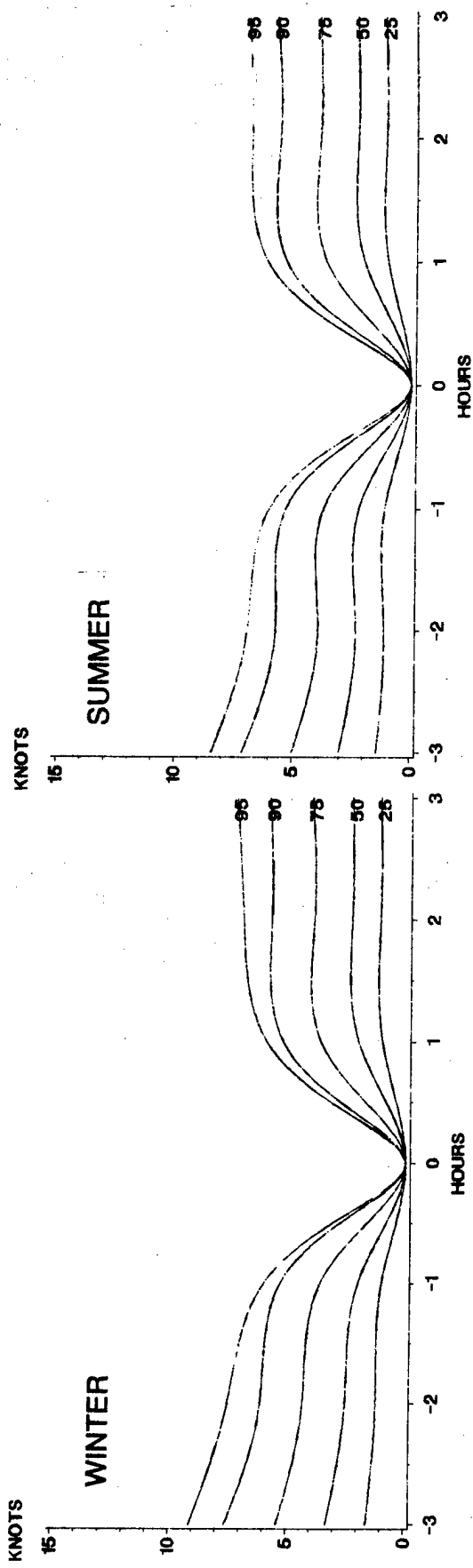
F-9 Temporal correlation of wind speed, desert climate, noon.



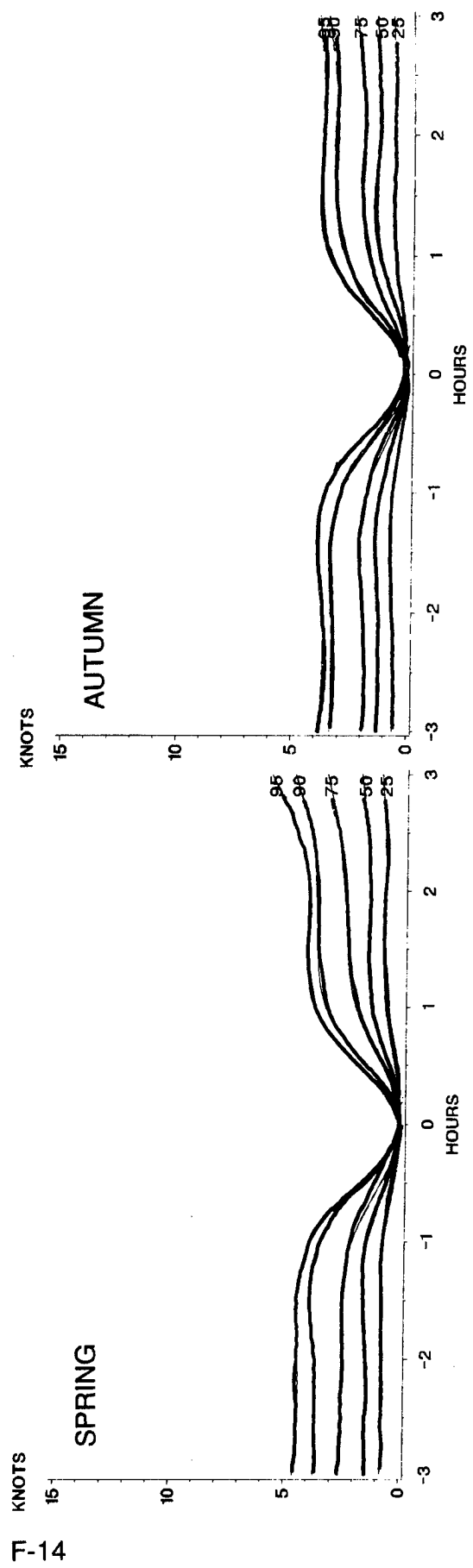
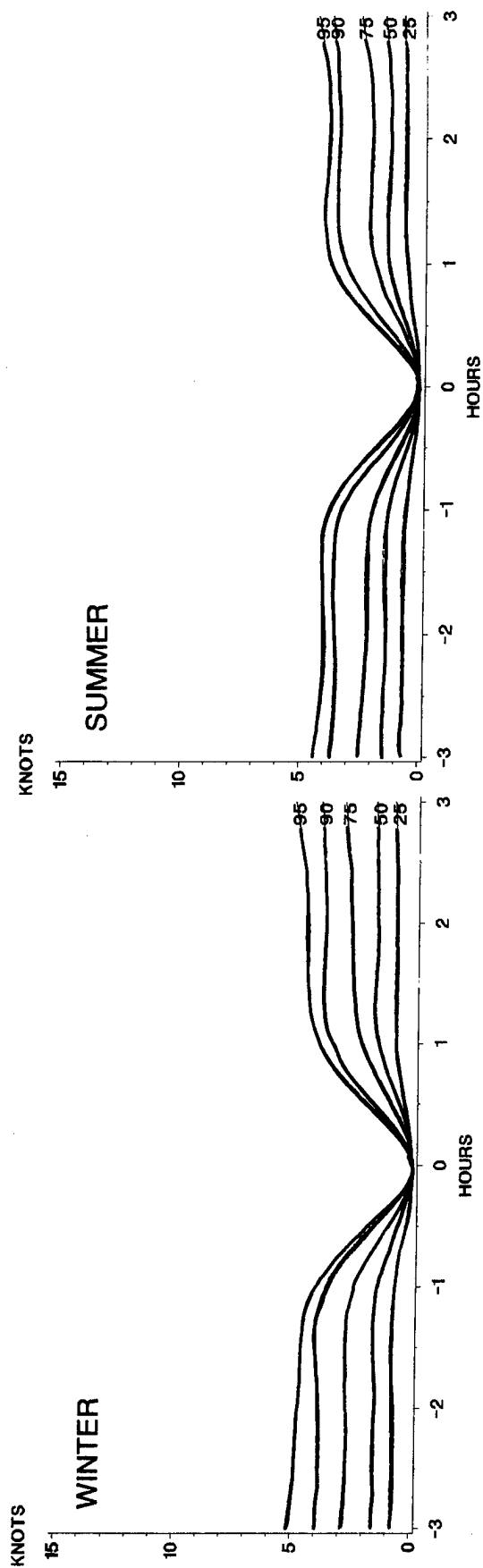
F-10 Temporal correlation of wind speed, maritime climate, midnight.



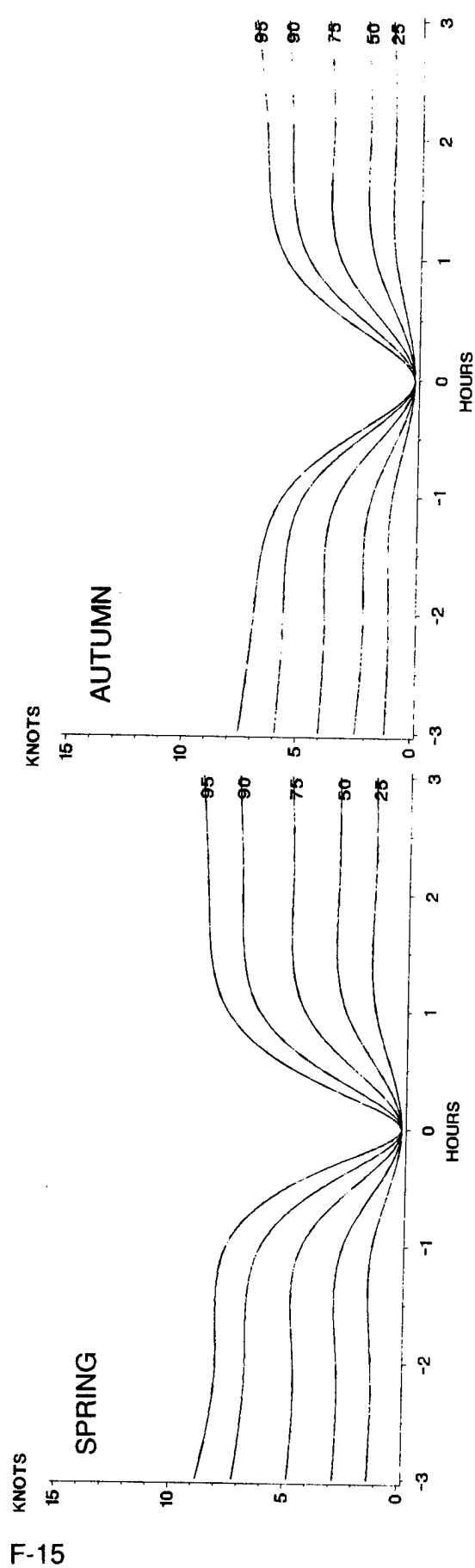
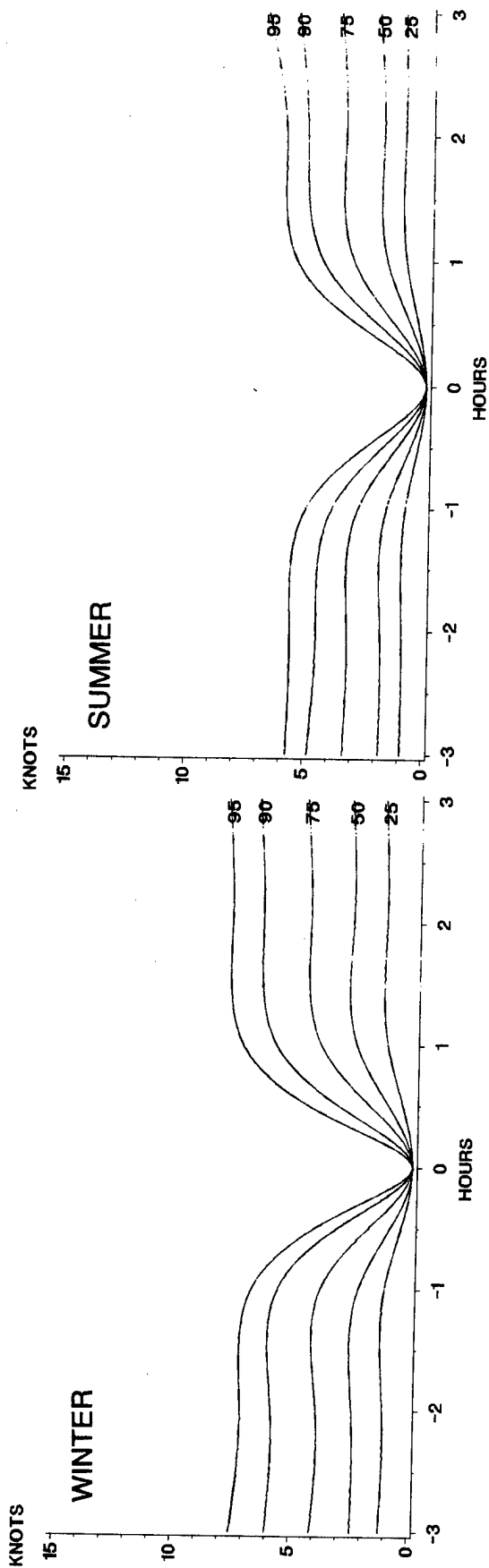
F-11 Temporal correlation of wind speed, maritime climate, sunrise.



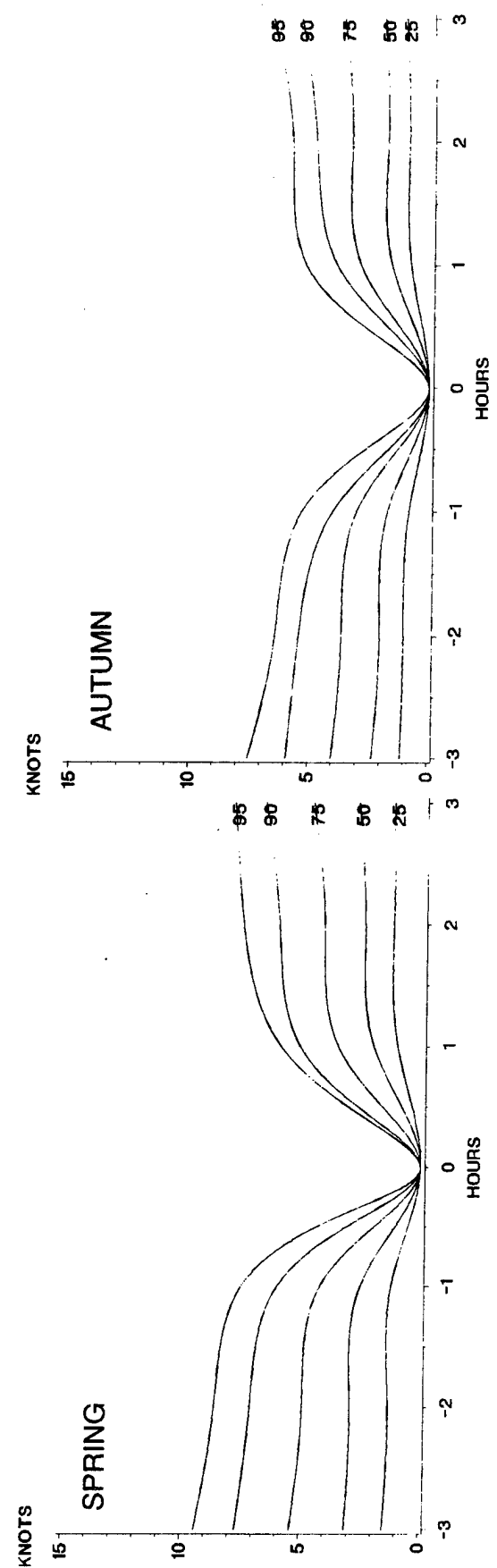
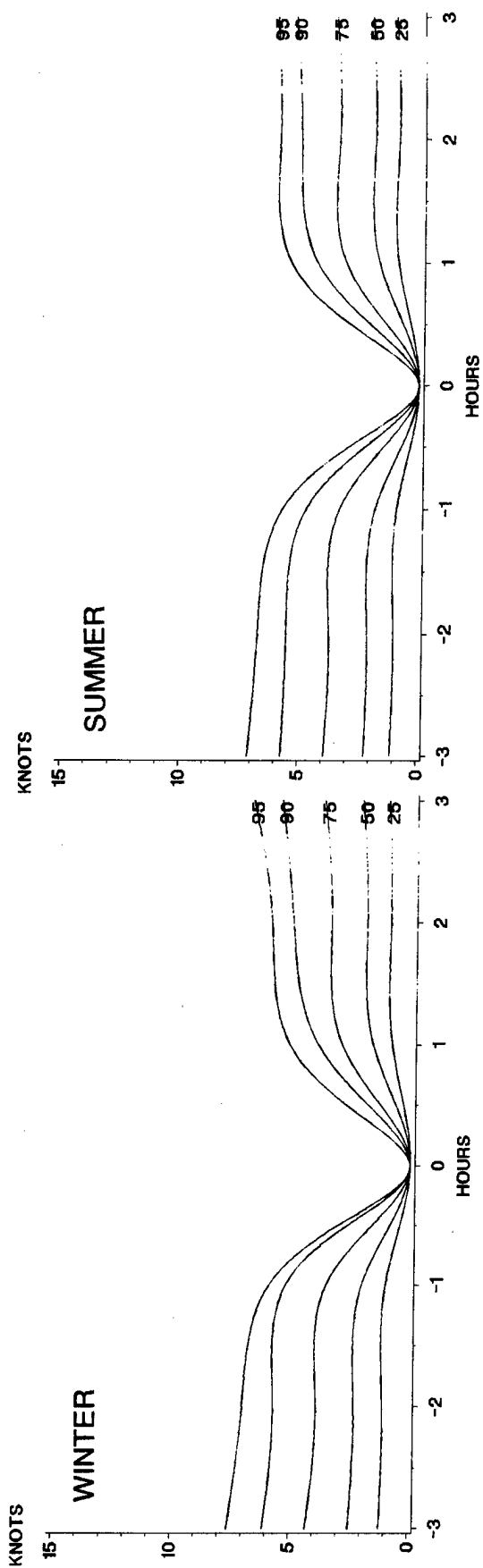
F-12 Temporal correlation of wind speed, maritime climate, noon.



F-13 Temporal correlation of wind speed, tropical climate, midnight.

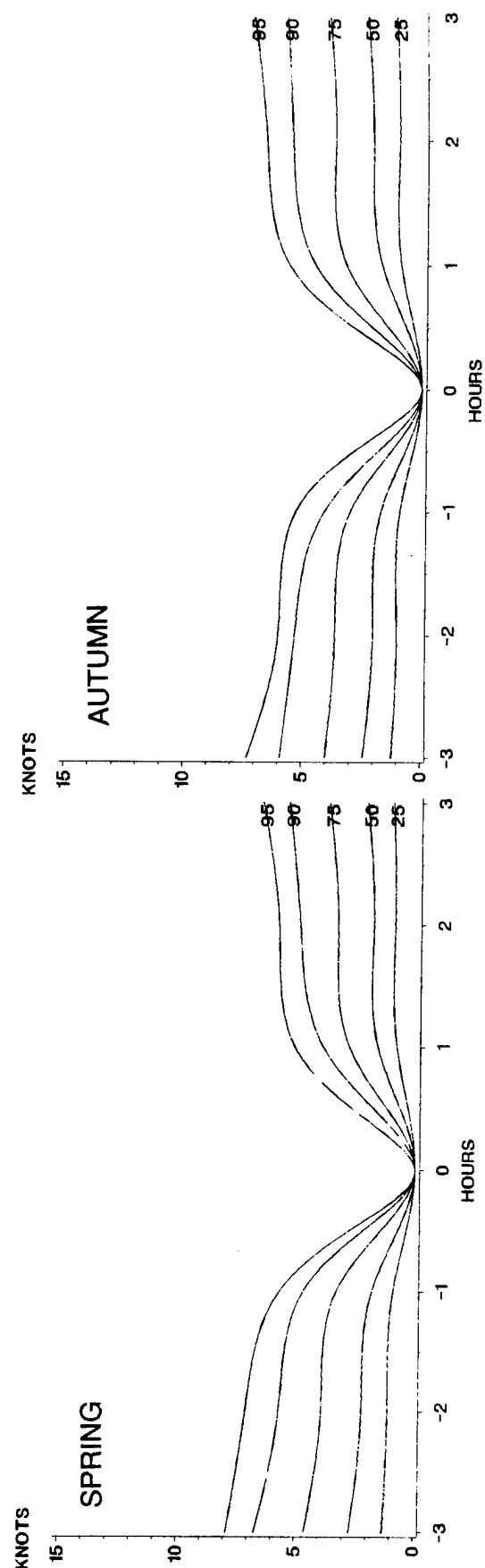
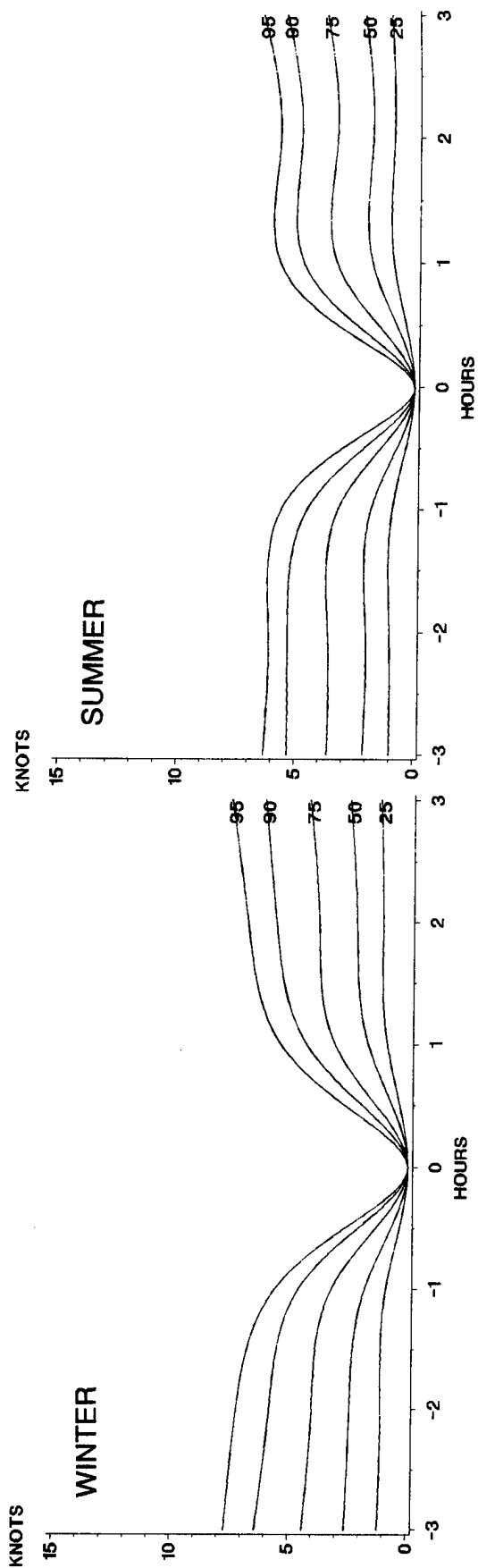


F-14 Temporal correlation of wind speed, tropical climate, sunrise.

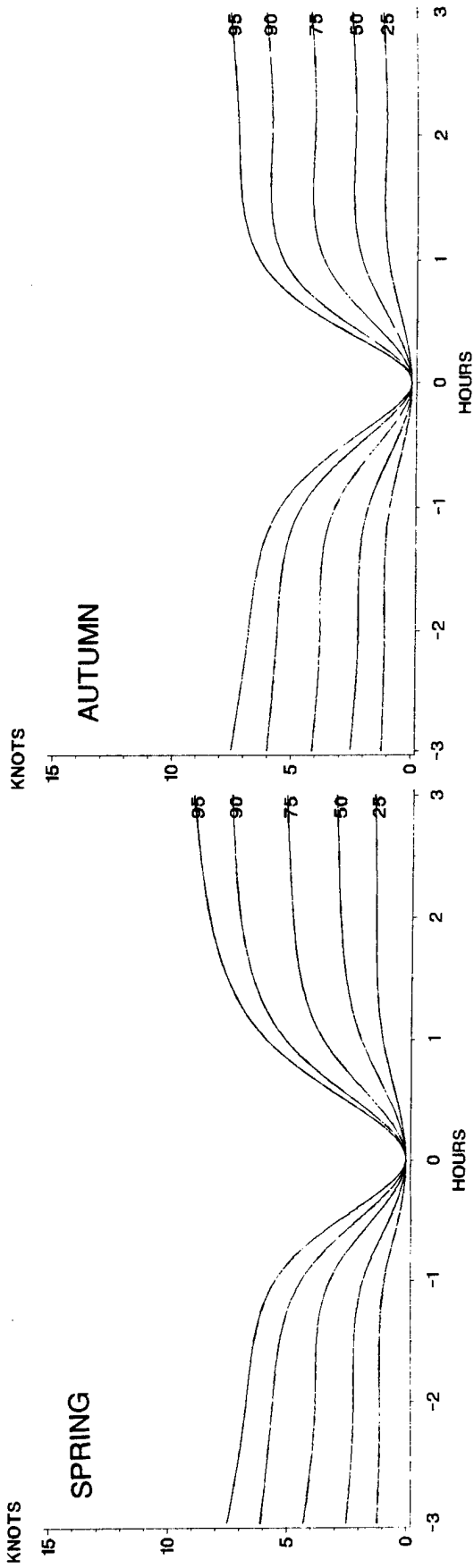
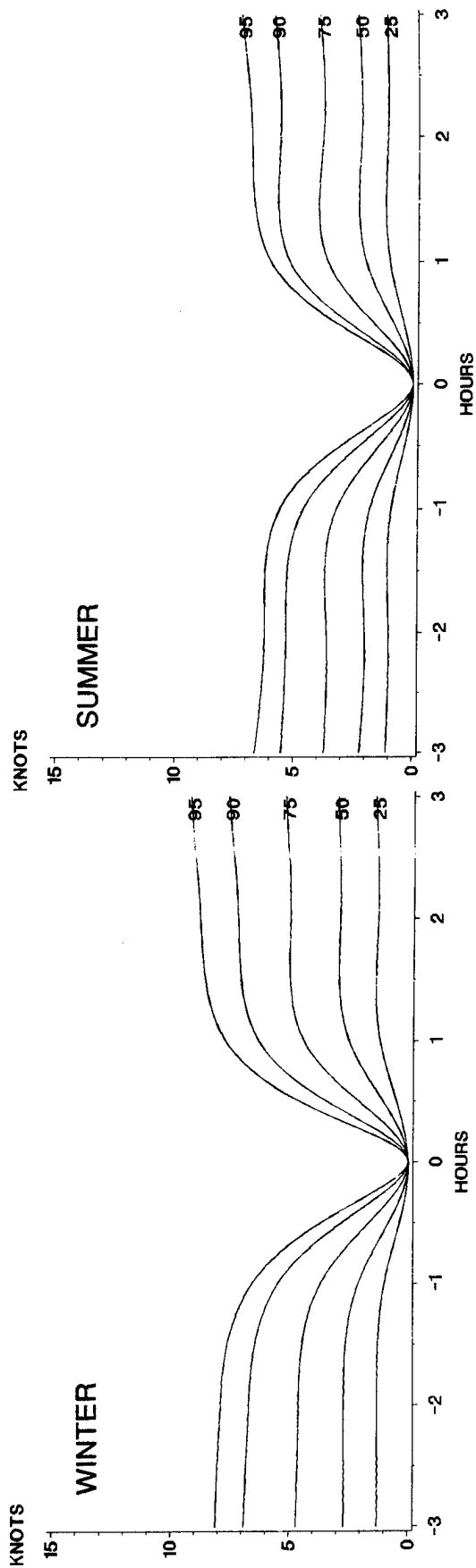


F-16

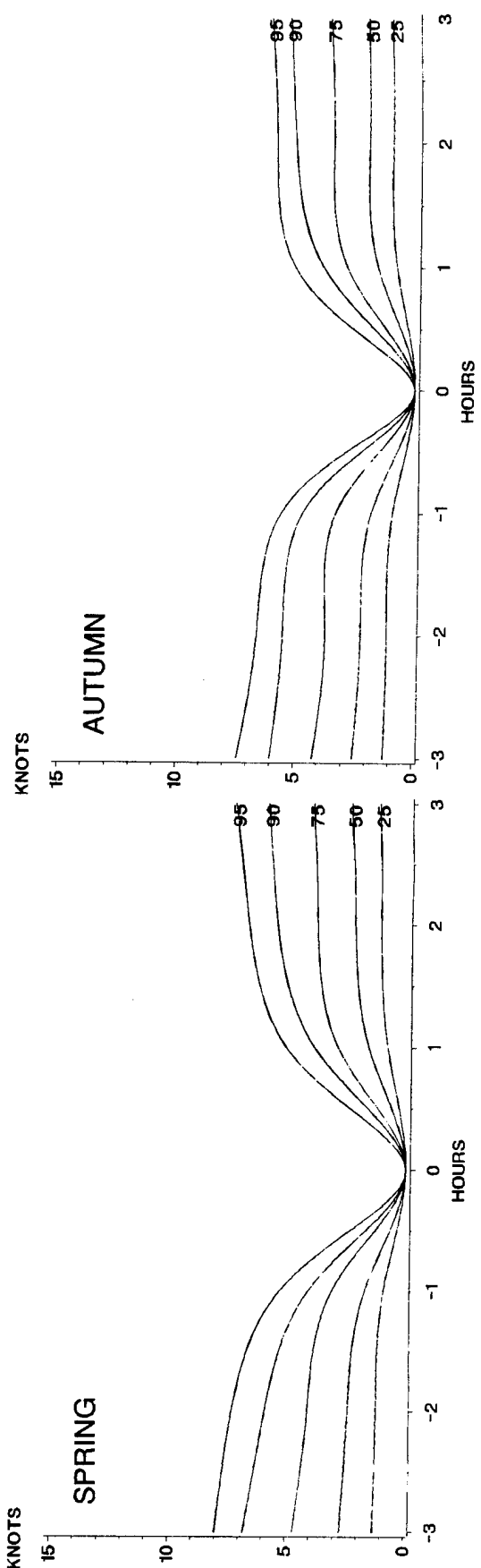
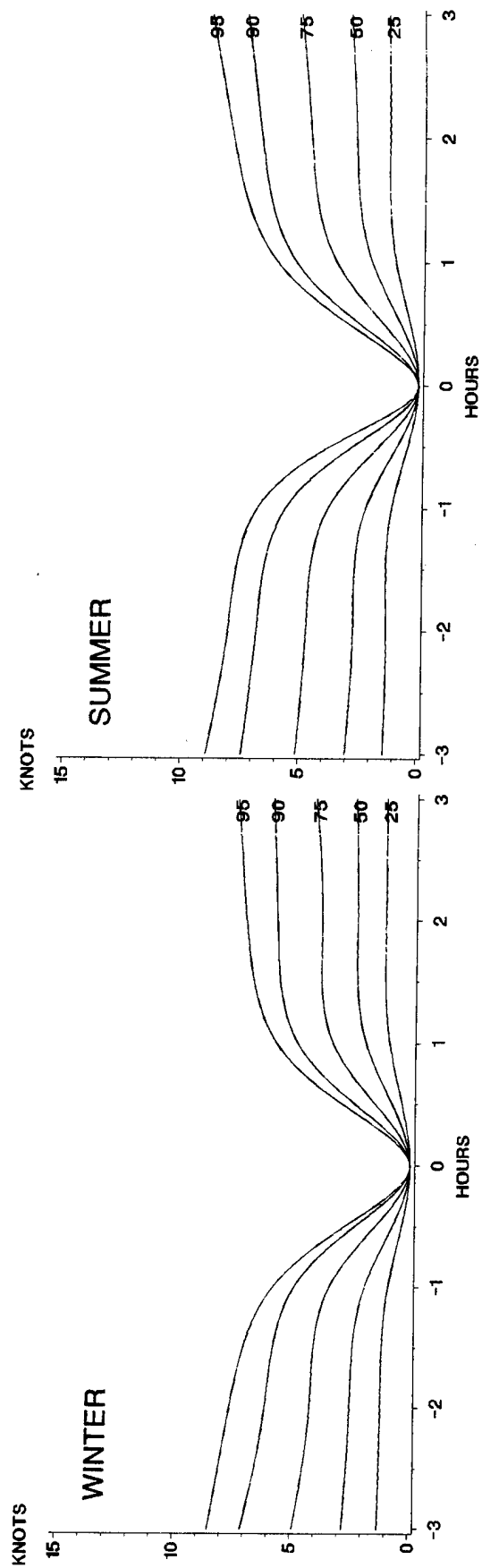
F-15 Temporal correlation of wind speed, tropical climate, noon.



F-16 Temporal correlation of wind speed, coastal climate, midnight.



F-17 Temporal correlation of wind speed, coastal climate, sunrise.



F-18 Temporal correlation of wind speed, coastal climate, noon.

DISTRIBUTION

HQ USAF/XOW, Washington DC 20330-5054	1
USTC J3/J4-OW, 62225-7001	1
AWS/CV/DO/RM/PM/SC/XT/IG/LN, Scott AFB, IL 62225-5008	1
AWS/XTX, Scott AFB, IL 62225-5008	3
OSAF SS, Rm 4C1052, Pentagon (Attn: Weather Staff) Wash DC 20330-6560	1
OL A, AFCOS, Ft Ritchie MD 21719-5010	1
CSTC/WE, PO Box 3430, Onizuka AFB, CA 94088-3430	1
OD-4/DX, Onizuka AFB, CA 94088-3430	1
Det 4, HQ AWS, Weather Warrior Center, Hurlburt Fld, FL 32544-5000	1
Det 5, HQ AWS, Wea Tng Material Devel Ctr, Keesler AFB, MS 39534-50001	1
Det 9, HQ AWS, PO Box 12297, Las Vegas, NV 89112-0297	1
1SSD/WE (Stop 77), Buckley ANG Base, Aurora, CO 80011-9599	1
OL-B, HQ AWS, Hanscom AFB, MA 01731-5000	1
OL-E, HQ AWS, Ft Leavenworth, KS 66027-5310	1
SSD/MWA, PO Box 92960, Los Angeles, CA 90009-2960	1
OL-H, HQ AWS, Ft Huachuca, AZ 85613-7000	1
OL-I, HQ AWS, Ft Monroe, VA 23651-5000	1
AFGWC/DO/SY, MBB39 106 PEACEKEEPER DR STE2N3 OFFUTT AFB, NE 68113-4039	1
AFGWC/SYSE MBB39 106 PEACEKEEPER DR STE2N3 OFFUTT AFB, NE 68113-4039	3
USAFETAC, Scott AFB, IL 62225-5438	5
PACAF/DOW, Hickam AFB, HI 96853-5000	1
USAFE/WE, Unit 3050, Box 15, APO AE 09094-5000	1
7WS/DON, APO AE 09403-5000	1
HQ SAC DOW, 901 SAC Blvd, Ste M138, Offutt AFB, NE 68113-5340	1
15AF/DOW, March AFB, CA 92518-5000	1
ATC/DOTW, Randolph AFB, TX 78150-5000	1
8AF/DOW, Barksdale AFB, LA 71110-5002	1
2AF/DOW, Beale AFB, CA 95903-5000	1
SPACECOM/DOW, Peterson AFB, CO 80914-5000	1
AFMC/DOW, Wright-Patterson AFB, OH 45433-5000	1
AFMC/DOW, Andrews AFB, MD 20334-5000	1
TAC/DOW, Langley AFB, VA 23665-5000	1
9AF/WE, Shaw AFB, SC 29152-5000	1
5WS/DON, Ft McPherson, GA 30330-5000	1
12AF/WE, Bergstrom AFB, TX 78743-5000	1
MAC/XOW, Scott AFB, IL 62225-5008	1
438MAW/WXF, McGuire AFB, NJ 08641-5002	1
60MAW/WXF, Travis AFB, CA 94535-5986	1
3350 TCHTG/TTGU-W, Stop 62, Chanute AFB, IL 61868-5000	2
3395 TCHTG/TTKO-W, Keesler AFB, MS 39534-5000	2
AFIT/CIR, Wright-Patterson AFB, OH 45433-6583	1
NAVOCEANCOMDET, Federal Building, Asheville, NC 28801-2723	1
NAVOCEANCOMDET, Patuxent River NAS, MD 20670-5103	1
NAVOCEANCOMFAC, NAS North Island, San Diego, CA 92135-5130	1
COMNAVOCEANCOM, Code N312, Stennis Space Ctr, MS 39529-5000	1
COMNAVOCEANCOM (Capt Brown, Code N332), Stennis Space Ctr, MS 39529-5001	1
NAVOCEANO (Rusty Russum), Stennis Space Ctr, MS 39522-5001	1
NAVOCEANO, Code 9220 (Tony Ortolano), Stennis Space Ctr, MS 39529-5001	1
Maury Oceanographic Library (NOC), Code XJL, Stennis Space Ctr, MS 39529-5001	1

NAVOCEANCOMDET, Patuxent River NAS, MD 20670-5103	1
NAVOCEANCOMFAC, NAS North Island, San Diego, CA 92135-5130	1
COMNAVOCEANCOM, Code N312, Stennis Space Ctr, MS 39529-5000.....	1
COMNAVOCEANCOM (Capt Brown, Code N332), Stennis Space Ctr, MS 39529-5001.....	1
NAVOCEANO (Rusty Russum), Stennis Space Ctr, MS 39522-5001.....	1
NAVOCEANO, Code 9220 (Tony Ortolano), Stennis Space Ctr, MS 39529-5001.....	1
Maury Oceanographic Library (NOC), Code XJL, Stennis Space Ctr, MS 39529-5001.....	1
FLENUMOCEANCEN, Monterey, CA 93943-5006.....	1
NOARL West, Monterey, CA 93943-5006.....	1
Naval Research Laboratory, Code 4323, Washington, DC 20375	1
Naval Postgraduate School, Chmn, Dept of Meteorology, Code 63, Monterey, CA 93943-5000.....	1
Naval Eastern Oceanography Ctr (Clim Section), U117 McCady Bldg, Norfolk NAS, Norfolk, VA 23511-5000.....	1
Naval Western Oceanography Ctr, Box 113, Attn: Tech Library, Pearl Harbor, HI 96860-5000	1
Naval Oceanography Command Ctr, COMNAVMAR Box 12, FPO San Francisco, CA 96630-5000	1
Naval Oceanography Command Ctr, Box 31, USNAVSTA FPO New York, NY 09540-3000.....	1
Pacific Missile Test Center, Geophysics Division, Code 3253, Pt Mugu, CA 93042-5000	1
HQ NATO Staff Meteorological Officer IMS/OPS APO AE 09724	1
NOAA/MASC Library MC5, 325 Broadway, Boulder, CO 80303-3328	2
OFCM, Suite 900, 6010 Executive Blvd, Rockville, MD 20852	1
NOAA Library-EOC4WSC4, Attn: ACQ, 6009 Executive Blvd, Rockville MD 20852	1
NOAA/NESDIS (Attn: Nancy Everson, E/RA22), World Weather Bldg, Rm 703, Washington, DC 20233	1
NOAA/NESDIS (Attn: Capt Pereira, E/SP1), FB #4, Rm 0308, Washington DC 20233-0001	1
NGDC, NOAA, Mail Code E/GC4, 325 Broadway, Boulder, CO 80303-3328	1
Armed Forces Medical Intelligence Agency, Info Svcs Div., Bldg 1607, Ft Detrick, Frederick, MD 21701-5004.....	1
PL OL-AA/SULLA, Hanscom AFB, MA 01731-5000.....	1
Atmospheric Sciences Laboratory (SLCAS-AT-AB), Aberdeen Proving Grounds, MD 21005-5001.....	1
Atmospheric Sciences Laboratory (SLCAS-AS-I 310-2c), White Sands Missile Range, NM 88002-5501.....	1
TECOM Atmos Sci Div, AMSTE-TC-AA (MacBlain), White Sands Missile Range, NM 88002-5504	1
White Sands Met Team, AMSTE-TC-AM (WS), White Sands Missile Range, NM 88002-5501	1
Army Missile Command, ATTN: AMSMI-RD-TE-F, Redstone Arsenal, AL 35898-5250.....	1
Army Test & Eval Cmd, ATTN: AMSTE-TC-AM (RE) TCOM Met Team, Redstone Arsenal, AL 35898-8052.....	1
Commander and Director, U.S. Army CEETL, Attn: GL-AE, Fort Belvoir, VA 22060-5546.....	1
6510 TESTW/TSTL, Edwards AFB, CA 93523-5000.....	1
RL/DOVL, Bldg 106, Griffiss AFB, NY 13441-5700	1
AFESC/RDXT, Bldg 1120, Stop 21, Tyndall AFB, FL 32403-5000	1
Technical Library, Dugway Proving Ground, Dugway, UT 84022-5000	1
NWS W/OSD, Bldg SSM C-2 East-West Hwy, Silver Spring, MD 20910.....	1
NCDC Library (D542X2), Federal Building, Asheville, NC 28801-2723.....	1
NIST Pubs Production, Rm A-405, Admin Bldg, Gaithersburg, MD 20899	1
NASA-MSFC-ES44, Attn: Dale Johnson, Huntsville, AL 35812-5000	1
DTIC-FDAC, Cameron Station, Alexandria, VA 22304-6145	2
AUL/LSE, Maxwell AFB, AL 36112-5564	1
AWSTL, Scott AFB, IL 62225-5438	35